UNIVERSITY OF SOUTHAMPTON

FACULTY OF ENGINEERING, SCIENCE AND MATHEMATICS

School of Chemistry

SYNTHESIS AND FUNCTIONALISATION OF PAMAM DENDRIMERS AS HISTONE REPLACEMENT MOLECULES

by

ALAN CHARLES JENKINS

Thesis for the degree of Doctor of Philosophy

November 2009

UNIVERSITY OF SOUTHAMPTON

ABSTRACT

FACULTY OF ENGINEERING, SCIENCE AND MATHEMATICS

SCHOOL OF CHEMISTRY

DOCTOR OF PHILOSOPHY

SYNTHESIS AND MODIFICATION OF PAMAM DENDRIMERS AS HISTONE REPLACEMENT MOLECULES

By Alan Charles Jenkins

The primary objective of this work was to synthesise and structurally modify a series of PAMAM dendrimers with a view to investigating and controlling their complexation with, and compaction of, DNA. The Introduction gives an overview to the origins of polymer and dendrimer science, and describes the synthetic approaches and resulting properties of dendrimers together with their impact on biological systems.

The preparation of poly(amidoamine) (PAMAM) dendrimers utilising a number of different core materials are reported and characterised in Chapter 2. The conformational motion of the dendritic branches has been studied using ^{1}H spin-lattice relaxation time experiments, and the results have been compared for the differently cored materials.

Chapter 3 examines the modification of the dendrimer surfaces with acetyl, poly(ethylene glycol) and fluorescent groups and reports the results of a study of how the degree of DNA condensation affects gene expression by analysing dendrimer-DNA compaction using linear dichroism, dynamic light scattering and competitive binding of ethidium. Experiments designed to investigate modified dendrimer-lipid interactions are also discussed and the results of these are compared to molecular dynamic simulations.

The synthesis of novel small molecules based around L-histidine and photo-responsive azobenzene, and the use of these to modify the surface of 4^{th} and 5^{th} generation PAMAM dendrimers is reported in Chapters 4 and 5 respectively.

There follows a final chapter containing detailed descriptions of the synthetic procedures and characterisation for each of the compounds studied and the experimental methods used for exploring their behaviour.

Acknowledgements

At heart I am a traveller. I've been to many wonderful places around the world but the most interesting journey has been that of my PhD. Though maybe not as beautiful as the Himalayas, it has had more than it's fair share of ups and downs. The journey began four years ago with Martin Grossel offering me a rather interesting project. He has guided and supported me throughout its entirety and for that I am eternally grateful.

As an old travelling proverb goes, "it is the journey, not the destination, that maters most". I firmly believe this, and know that I couldn't have gotten through my PhD without the people who travelled it with me, whether for a long or short time. I'd like to thank the members of the Grossel group, past and present, for their aid and understanding, and for putting up with my sometimes shocking innuendo. Bear with me as I now try to name them all… Polski, James, Dan, Alex, Georgie, Jon, Francesco, Alain, Andrew, Richard, Andrew (Jeff), Dom and Nick. I'd also like to thank the project students who have had the unfortunate pleasure of being supervised by me; Tim, Sarah, SMoore and Louise. Special mention must go to Polski and Dan. You have both taught me much in the way of chemistry, and through our many random and fact filled conversations have given me a vast understanding of 'stuff'.

John Langley and Julie Herniman (mass spectrometry), Joan Street and Neil Wells (NMR), Carl and the stores team, and the glass blowers, I thank you all for your help. Without you the department would cease to function.

Possibly the greatest influence during the last three years of my life has come from Aimee. You've given me so much and opened my eyes to a great many things, I can't thank you enough for our time together.

Last but by no means least I'd like to thank my family. You've supported me and kept me going, never doubting that I'd succeed. I feel I should also mention my faithful travel companion Bungee, who has bounced all around the world trying to keep me sane!

Contents

Table of Figures

Table of Tables

Abbreviations

Boc	*tert*-Butyloxycarbonyl
br	Broad
Cbz	Carbobenzyloxy
$CDCl_3$	Deuterated chloroform
d	Doublet
D_2O	Deuterated water
DCM	Dichloromethane
DIPEA	N,N-Diisopropylethylamine
DMF	N,N-dimethylformaldehyde
DMSO	Dimethylsulphoxide
DMSO-d_6	Deuterated dimethylsulphoxide
DNA	Deoxyribonucleic acid
E	Trans
EDA	Ethylene diamine
EDC	1-Ethyl-3-(3-dimethylaminopropyl)carboiimde
ES^+, ES^-	Electrospray positive or negative
EtOH	Ethanol
FITC	Fluorescein isothiocyanate isomer I
Fmoc	9*H*-fluoenylmethyloxycarbonyl
FTIR	Fourier transform infrared spectroscopy
Gx	(dendrimer) Generation
HBTU	O-Benzotriazole-N,N,N',N'-tetramethyl-uronium-hexafluoro-phosphate
His	Histidine
HOBt	Hydroxybenzotriazole

HRMS	High resolution mass spectrometry
m	Multiplet
MD	Molecular dynamics
MeOD	Deuterated methanol
MeOH	Methanol
mp	Melting point
NMR	Nuclear magnetic resonance
PAMAM	Poly(amidoamine)
PE	Polyethylene, polythene
PEG	Poly(ethylene glycol)
POPE	1-Palmitoyl-2-oleoylphosphaditylethanolamine
POPG	1-Palmitoy-2-oleoylphosphaditylglycerol
PPI	Poly(propylene imine)
PVC	Poly(vinyl chloride)
q	Quartet
qu	Quintet
RDF	Radial distribution function
RNA	Ribonucleic acid
RT	Room temperature
s	Singlet
t	Triplet
T_1	Spin-lattice relaxation time
TFA	Trifluoroacetic acid
Trt	Trityl, triphenylmethyl
UV/Vis	Ultraviolet-visible spectroscopy
Z	Cis

Chapter 1 Introduction

1.1 Histones

1.1.1 Background

Deoxyribonucleic acid (*DNA*) is one of the most important building blocks of life. It contains the genetic instructions needed to create *proteins* and ribonucleic acid (*RNA*), and also acts as a long-term storage of information.[1,2] Without it, we simply would not exist. Discovered in 1869 by the Swiss biochemist Johann Friedrich Miescher, DNA has since been shown to be a linear, unbranched polymer that is constructed from 4 simple molecules (*nucleotides*) and has a backbone made of phosphate and sugar groups joined by ester bonds.[1,3] In 1953, the ratios of each nucleotide (namely *Adenine* (A), *Cystosine* (C), *Guanine* (G) and *Thymine* (T)) helped to lead James Watson and Francis Crick (with the aid of X-ray diffraction patterns) to discover that in living cells two DNA chains are intertwined to form a double helix.[4] The two polymer strands are held together *via* hydrogen bonds formed between complimentary nucleotides (A with T, and C with G) and, for this reason, the pairs of nucleotides are often referred to as Watson-Crick base pairs.[1,2]

The sequence in which these nucleotides are arranged along the backbone determines the information that is stored. This information can then be read using the genetic code by copying part of the DNA into the related nucleic acid RNA in a process known as *transcription*.[5] This RNA can then go on to create proteins as specified by the DNA.

DNA is generally located in the cell nucleus and is usually stored as part of a *chromosome*, a large structure where no transcription takes place. This latter is made up of *chromatin*, and is where the double helix of DNA is coiled around a protein. A collection of chromosomes within a cell makes its *genome*.[1]

If the DNA contained within a human cell were laid out, it would stretch 4 metres in length. With the aid of proteins (known collectively as *histones*) that bind to, and become coiled around the DNA, this length is reduced to 180 mm within 30 nm diameter fibres (chromatin). This is then further condensed to 120 μm within the 700 nm diameter arms of mitotic chromosomes.[6]

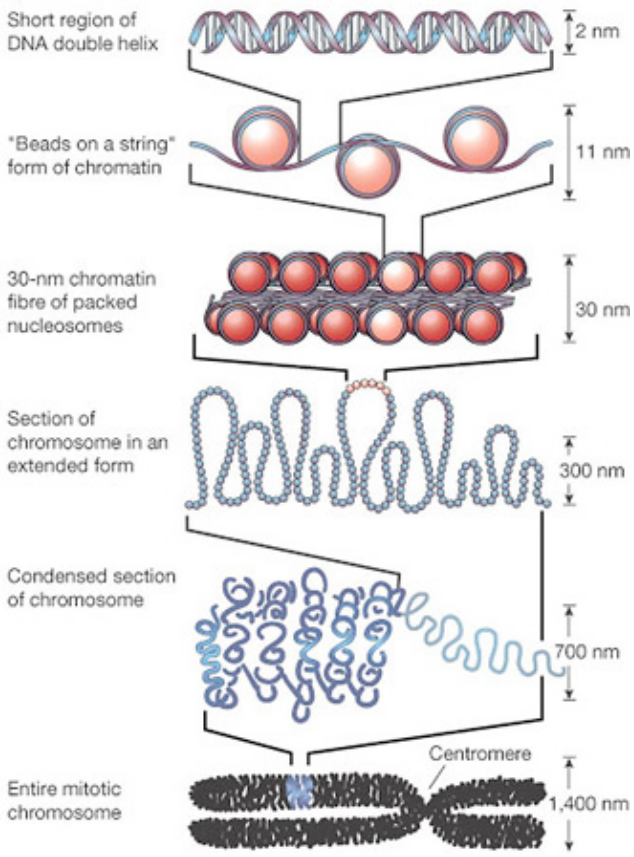

Figure 1. *The formation of a chromosome from DNA.*[7]

1.1.2 Structure of DNA – Histone Complexes

Histone proteins come in two classes, *core* histones and *linker* histones. There are four core histones, known as H2A, H2B, H3 and H4, and it is these that the DNA coils around. Initially, dimers are formed between two of these proteins e.g. between H3 and H4, or H2A and H2B (see **Figure 2**). Two of the same type of dimer then come together to form a tetramer. The two tetramers finally complex with each other to give rise to a *histone octamer*. Structural studies have shown that the core octamer forms a barrel shape when bound to DNA (forming a *nucleosome*); the DNA wrapping twice around the core.[1]

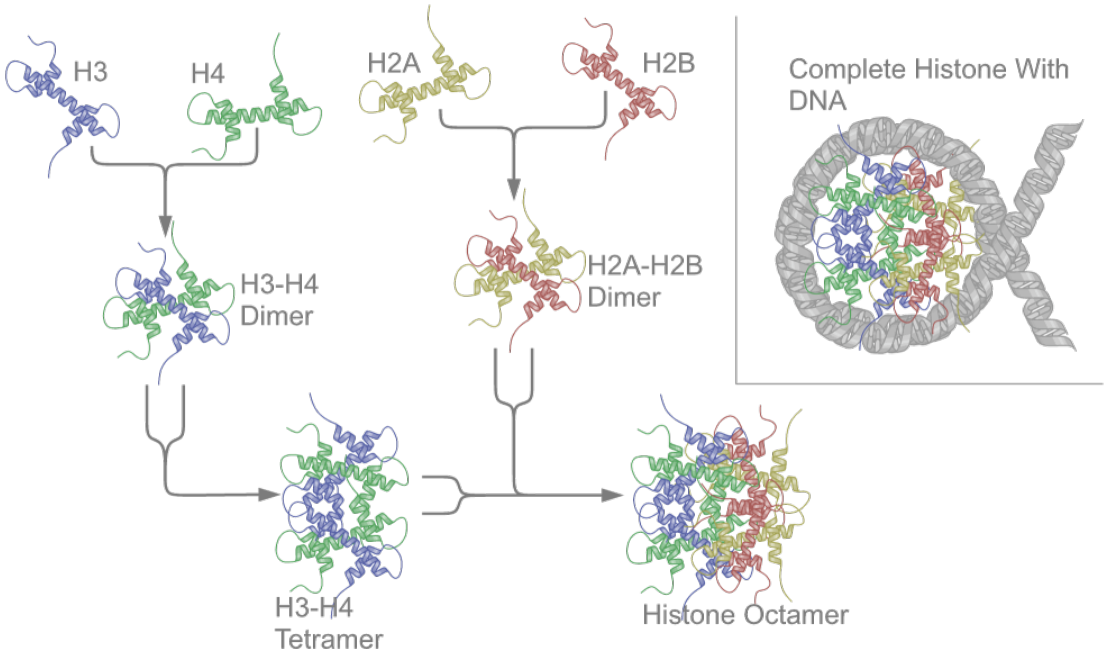

Figure 2. *Formation and structure of a histone core octamer, together with resulting nucleosome.*[8]

There are 5 main types of interaction between the core octamer and the DNA:[1,2]

- Electrostatic: dipoles generated by the protein form a net positive charge that is attracted to the negatively charged phosphate groups located on the DNA backbone. The basic nature of the histone also aids its solubility.

- Hydrogen bonds: these form between amide groups located on the protein and the DNA backbone.
- Salt links: these form between amino acids and the phosphate groups.
- Nonpolar and Van der Waals: these form between the DNA deoxyribose sugar groups and nonpolar components of the protein.

A linker histone, of which there are two classes (H1 and H5), then attaches itself to a nucleosome securing the DNA in place, though the exact position and nature of this attachment is unknown. There are two schools of thought for how the linker histones keep the DNA bound to the core octamer. In the first, the linker histone acts as a clamp, preventing the coiled DNA from unravelling (this theory is backed by structural studies[9,10]). The second suggests that the linker histone is located between the DNA and the core octamer, holding them together.[11,12] Whichever theory is correct, the end result is the same; DNA is securely bound to the histone core in what is known as a 10 nm fibre or '*beads-on-a-string*' structure. In comparison with an unbound histone octamer (~110 Å) the size of the nucleosome is much smaller (85 x 67 Å), suggesting that there is much free space within the histones' structure.[13]

Figure 1 shows a representation of an unpacked form of chromatin, that is to say, a collection of chromatosomes (a series of nucleosomes). These fibres have a diameter of ~ 10 nm and can become condensed into what is known as the '*30 nm fibre*'. The exact structure of this condensed fibre is again not known, though it is believed that the individual nucleosomes are held together either by linker-linker or core-core histone interactions.[5] This would then give rise to the most widespread and accepted solenoid representation of the structure (**Figure 3**), these 30 nm fibres can then 'super coil' to make the densely packed chromosomes which, at the time of cell division, resemble the characteristic X structure (**Figure 1**).

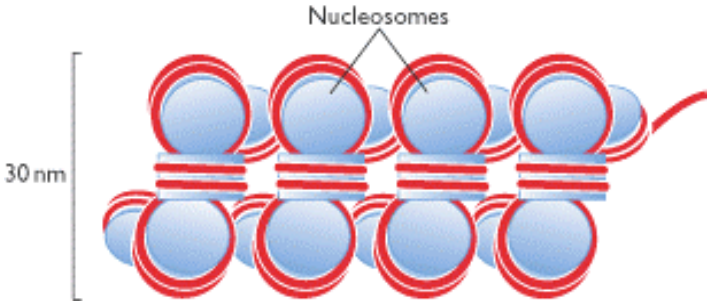

Figure 3. *Schematic representation of a 30 nm fibre.*[1]

1.1.3 Nature of DNA – Histone Binding

As stated above, there are a number of factors that affect the binding of DNA to a histone octamer. When the DNA is coiled up as part of the chromatin in a *eukaryotic cell* (a cell that contains a nucleus) its accessibility is greatly reduced, meaning that transcription is unlikely to occur. In order to make the DNA easier to reach, the compressed chromatin structure must first be unravelled, a process that is achieved through modification of the histones. These chemical modifications include acetylation, methylation and phosphorylation, all of which change the strength of the histones' interaction with the DNA.[14,15] It is very important to note that a strand of DNA is never completely unbound from the histone octamer; merely that part of the DNA helix becomes exposed to the transcription agents.

The most studied of these modifications is that of histone acetylation i.e. the addition of an acetyl group onto the amine groups of the amino acid lysine located in the *N*-terminal regions of the core octamer.[14] These *N*-terminal regions form tails that stick out from the nucleosome and their acetylation decreases the histones affinity for the DNA. It is also believed to disrupt the interactions holding the 30 nm fibres together.[2,14] The process of histone acetylation is accomplished by *histone acetyltransferases* (HATs), first identified by Pennisi in 1997[16] and is believed to neutralize the charge on the lysine. It is also possible that the acetylated group interacts with a binding site located on the histone (such as the bromodomain)[17,18] which could lead to chromatin

remodelling i.e. the structure of the histone is changed, weakening its contact with the DNA. In order to silence the transfection process, the acetyl groups must be removed, something that is achieved by *histone deacetylases* (HDACs), as first demonstrated by Taunton *et al*. in 1996.[19]

1.2 Polymers

It is known that a histone is approximately 110 Å in diameter when not bound to DNA, and that it uses a multitude of interactions, primarily electrostatic, to coil and compress the DNA around it.[1,13] If we are to synthesise a replacement for these histones it needs to be of suitable size, have the capability to be compressed (i.e. contains free space), be water soluble, and possess the ability to bind and unbind DNA through electrostatic interactions. The fact that such a large molecule is required alludes to the possibility of using a polymer, as these can be fine-tuned to achieve the desired properties.

1.2.1 Origins

The word *polymer* was first used by the Swedish chemist Jöns Jakob Berzelius in 1833.[20,21] It stems from the Greek words *poly*, meaning many, and *mer*, meaning part. Berzelius originally used the term to describe compounds that had the same empirical formula but differed in molecular weight e.g. hexene would be called a polymer of the smaller ethene molecule.[20,22] Nowadays, the term polymer is used to describe molecules of high molecular weight that are made from smaller units known as *monomers* by a process known as polymerisation.

During the nineteenth century a number of polymers were discovered, but with no understanding of their structures. Polymers such as polystyrene and nitrated cellulose (also known as nitrocellulose) were reported as early as 1839,[23] whilst the synthesis of poly(ethylene glycol)[24] and poly(ethylene succinate)[25] were published in the 1860s. Nitrated cellulose became a commercial success as 'gun cotton' after its preparation by Christian Schönbein in 1846 because of its explosive properties.[26] Its solubility and ability to be moulded led to products with many applications such as Parkesine

(Alexander Parkes, 1862) and Celluloid (John and Isaiah Hyatt, 1870).[27,28] With the advent of the 'viscose process' (a way of forming fibres) in 1892 by Charles Cross, Edward Bevan and Clayton Beadle, other uses such as rayon textile fibres and cellophane film subsequently appeared.[28]

During this period, the properties of natural rubber (**1**) were being probed and, with the aid of distillation, Charles Williams discovered its monomer unit which he called isoprene (**Figure 4**).[29] Natural rubber has subsequently been the source of much investigation through the years, starting with Thomas Hancock in 1820 who discovered that it becomes more fluid if subjected to high shear forces.[30] In 1839, Charles Goodyear found that heating the rubber with sulphur gave improved elastic properties[31] (coined vulcanisation by Hancock[30]), while his brother, Nelson Goodyear, eventually patented the vulcanisation of natural rubber with large amounts of sulphur in USA (1851) to give a hard rubber also known as vulcanite (it should be noted that a similar patent for vulcanite was awarded to Hancock in the UK in 1843 which led to many disputes with Goodyear).

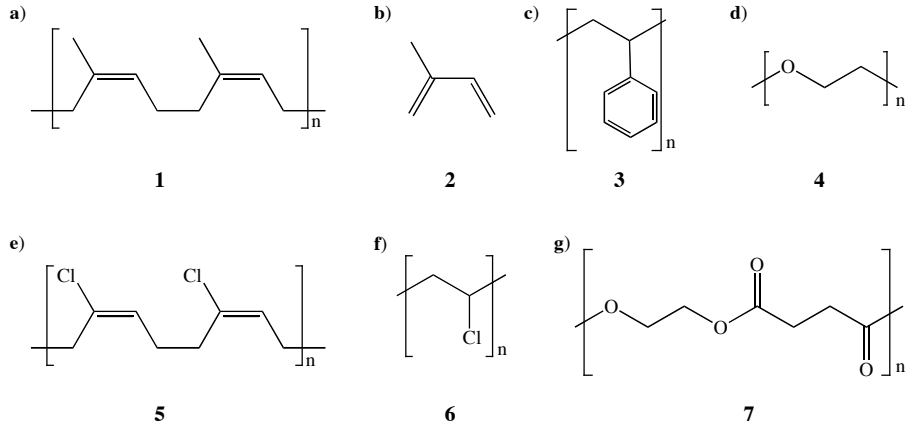

Figure 4. *A selection of molecules discovered from the nineteenth and twentieth centuries. a) Natural rubber, b) isoprene, c) polystyrene, d) poly(ethylene glycol), e) neoprene, f) poly(vinyl chloride) and g) poly(ethylene succinate).*

It was not until the early twentieth century that a synthetic polymer was synthesised; Leo Baekeland reacted phenol with formaldehyde to create Bakelite in 1907.[32] Owing to its nonconductive and heat-resistant properties it was subsequently commercialised in

1909 and later used in a wide range of products. The first polymer to going into mass manufacture was that of *methyl rubber*, developed as a replacement to natural rubber in Germany during World War I using a 2,3-dimethylbutadiene monomer.[33,34]

Even with the commercial success of some polymers, little was still known about their structure, most scientists believed them to be aggregates of small molecules (similar to colloids) held together by an unknown force, a theory that was first suggested by Thomas Graham in 1861 (association theory).[35,36]

In 1922, Hermann Staudinger attributed the properties of polymers to many long chains of atoms linked by covalent bonds (terming the chains *makromoleküles*)[37], an idea that took more than a decade to become widely accepted.[38] Staudinger's discovery had a large impact on polymer science; he commented in 1936 that "it is not improbable that sooner or later a way will be discovered to prepare artificial fibres from synthetic high-molecular products, because the strength and elasticity of natural fibres depend exclusively on their macro-molecular structure – i.e., on their long thread-shaped molecules."[39] He later went on to found the first polymer journal (Die Makromolekulare Chemie, 1940)[40] and receive the Nobel Prize in Chemistry (1953) for his contributions to this field.[40] The theories of Staudinger were used to great effect by Wallace Carothers who, in the 1930s, developed neoprene rubber[41] and polyamide fibres (nylon)[42] among others.[43-48]

The time after World War II saw an explosion in polymerisation techniques and the commercialisation of synthetic polymers such as polystyrene, nylon 6-6 and poly(vinyl chloride) (as a side note, PVC has been discovered on two occasions, first in 1835 by Henri Victor Regnault and then in 1872 by Eugen Baumann).[26] Perhaps the most significant discovery was by Karl Ziegler in Germany, 1955,[49] of new coordination catalysts that allowed the Italian chemist Giulio Natta to develop stereoregular polymers.[50,51] Their work revolutionised the industry as their polymers with controlled stereochemistry were found to possess superior mechanical properties over non-stereoregular polymers. This led to them jointly being awarded the Nobel Prize in Chemistry in 1963 for their development of the Ziegler-Natta catalyst.

Another important name is Paul Flory, whose work with polymers led to him establishing the kinetics of step-growth polymerisation[52] and the Flory-Huggins Solution Theory (a mathematical model of the thermodynamics of polymer solutions).[53,54] He also applied the concept of excluded volume, introduced by Werner Kuhn in 1934, to polymers.[55] Then, in 1974, he was awarded the Nobel Prize in Chemistry "for his fundamental achievements, both theoretical and experimental, in the physical chemistry of macromolecules."

Nowadays, polymers have made their way into most mainstream products, be it as adhesives, lubricants, toys and vehicles. Their properties can be fine-tuned to allow for high strength, degradability, fire-retardancy and, more recently, binding to riboflavin (vitamin B2) to extend the shelf life of bottled beer.[56]

1.2.2 Main Types of Polymers

Though polymers come in a great many compositions, shapes and sizes, the underlying types of structures are not as varied. Most polymers have a polymeric chain, or backbone, to which other groups are attached. *Homochain* polymers contain a backbone made of only one type of atom, usually carbon, whilst *heterochain* polymers are made with a backbone of more than one atom type e.g. a polyether. As has been stated before, a polymer is made up of monomer units, but these can be of different types and arranged in different ways (**Figure 5**).[26,57-59]

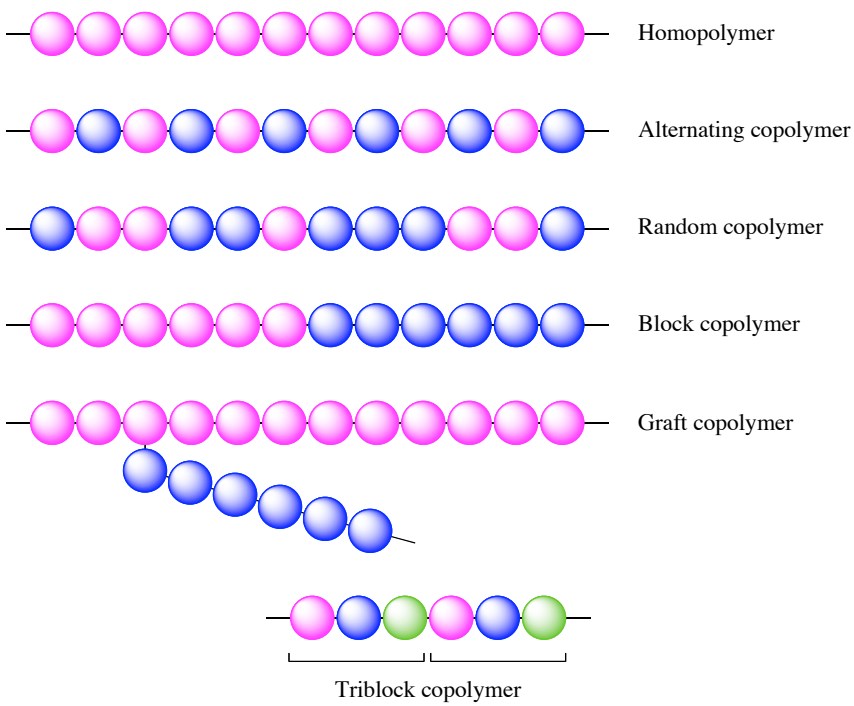

Figure 5. *Representations of a polymer made of its monomer units.*

If a polymer is prepared using only one type of monomer unit it is known as a *homopolymer*, whereas if two or more monomers are involved it is termed a *copolymer*.[58,60] In a copolymer the monomer units can be arranged in a number of different ways depending on the reactivity of the monomers and the polymerisation technique employed. This can result in an *alternating copolymer* (where the type of monomer unit alternates throughout the backbone), a *random copolymer* (usually occurs when monomer units are of similar reactivity), a *block copolymer* (the chain propagates in blocks of the same monomer) or a *graft copolymer* (where one polymer branches off the backbone of another). It is useful to note that the blocks of the block copolymer can be arranged in different ways i.e. when the backbone is made of only a single block of each monomer it is known as a *diblock* polymer, while when a repeat unit of three monomers is used it is termed a *triblock*.

Polymers can also be described through their overall structure, that is to say, whether they are *linear*, *branched* or *network* polymers.[26,58-60] These polymeric structures can be homopolymers or copolymers depending on their monomer.

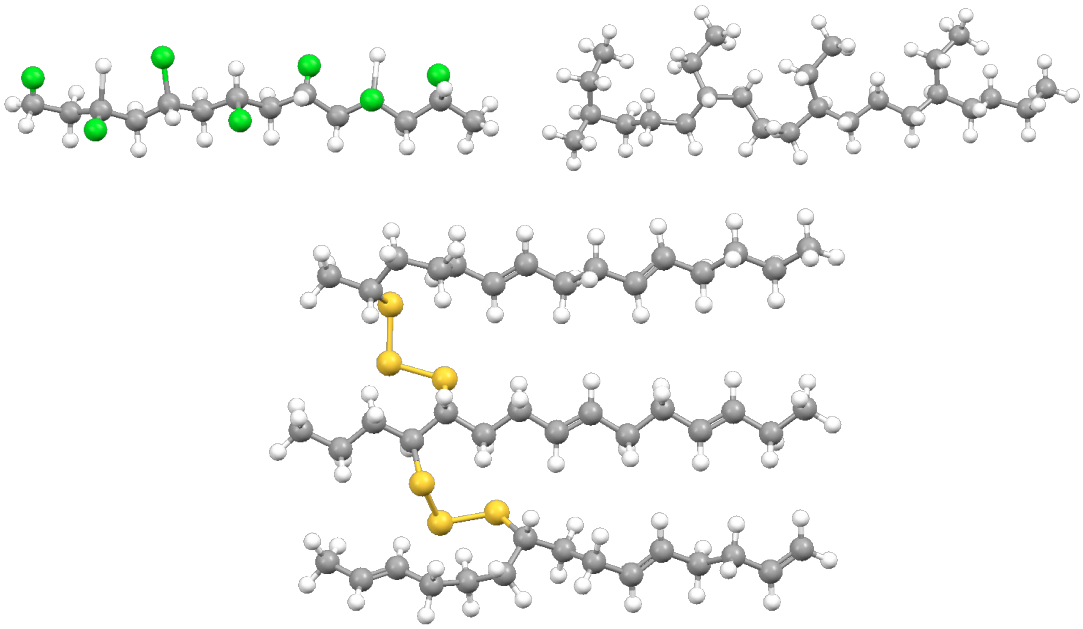

Figure 6. *Structures of polymers, linear (top left), branched (top right) and network (bottom).*

Linear polymers are the simplest of all polymers as they are composed of many chains. Examples include poly(vinyl chloride) (PVC),[61] which is one of the most valued commercial products in the chemical industry and is used in wire insulation and construction, and nylon that is used in ropes, parachutes and vehicle tyres.[61] Branched polymers have the same basic structure as linear polymers, but in this case some of the repeat units contain side chains. This means that, in the polymer, individual chains can find it harder to move past each other, resulting in a more rigid structure. However, these same branches could equally lead to a polymer that has weaker intermolecular forces making for a flexible material, such as low-density polyethylene (LDPE).[57] Network polymers begin life as a linear or branched polymer, but the monomer unit contains a reactive site that can give a covalent bond. The polymer can thus be cross-linked to give covalent bonds between chains. Excessive cross-linking gives rise to very strong network polymers. The synthesis of the different types of polymers stem from only a handful of techniques, some of which are described below.

1.2.3 Synthesis

Polymer synthesis, traditionally, falls into one of two categories, *addition polymerisation* or *condensation polymerisation*.[26,59,60] A polymer is put into one of these classifications based on whether or not all the atoms from the monomer unit are present in the polymer, a concept first proposed by Carothers.[62] A repeating unit in an addition polymer contains all the atoms from its monomer, whilst a condensation polymer contains fewer (as a by-product is released during the polymerisation). Nowadays, however, a polymerisation reaction is classified by its mechanism, namely either *step-growth* (reaction proceeds in a stepwise fashion) or *chain-growth* (reaction of a monomer with a reactive end-group on the growing chain). It should be noted that ring-opening techniques could fall into either of these classifications.

Though the categories of polymerisation were changed in 1994, and others introduced by the International Union of Pure and Applied Chemistry (IUPAC), they all stem from the two classifications above:[63]

- *Polycondensation* – as step-growth polymerisation with concurrent formation of by-products of low molecular weight.
- *Polyaddition* – as step-growth polymerisation without formation of by-products.
- *Condensative chain polymerisation* – as chain-growth polymerisation with the formation of by-products of low molecular weight.
- *Chain polymerisation* – as chain-growth polymerisation without the formation of by-products.

Step-growth Polymerisation

There are two main ways to prepare linear step-growth polymers.[26,57] The first requires a monomer that has two different reactive groups in it whilst the other uses two monomers that are each difunctional.

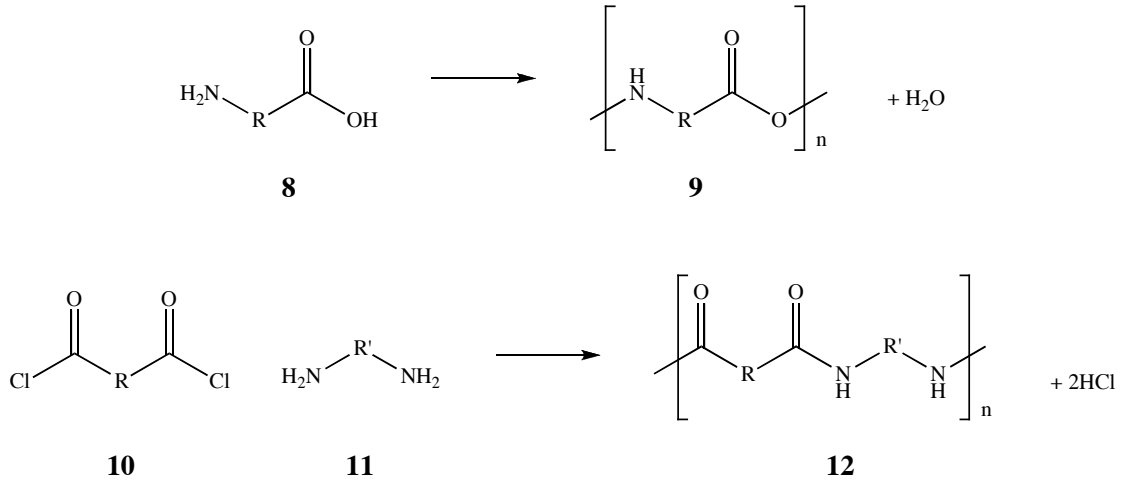

Figure 7*. Examples of monomers used in step-growth polymerisation.*

Most polymerisations by this method are of the condensation type i.e. a small by-product is formed. The rate of reaction proceeds quickly at first, as there are many reactive groups present; this leads to the formation of very small polymer chains (dimers, trimers etc).[57,62] As the monomers are consumed by this process, the rate drops, but since the short chains still have reactive groups they start to create longer chains. This continues until the number of end-groups becomes so low that the rate of polymerisation falls (another rate determining factor is the viscosity of the formed chains). A schematic representation of this process is shown below. Overall, the average molecular weight increases slowly whilst the monomer is rapidly consumed.

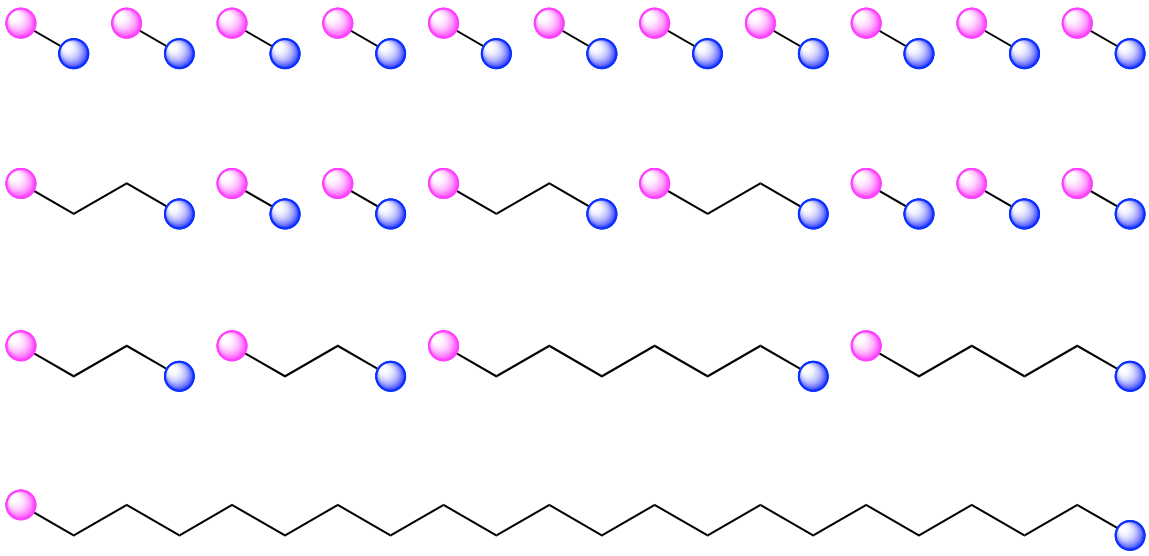

Figure 8. *Schematic of step-growth polymerisation. Top to bottom; increased amount of polymerisation and chain length. Pink and blue spheres represent complimentary reaction groups.*

Perhaps the most well-know polymers prepared by this route are polyamides, first produced in 1935 by Carothers at DuPont.[64] By condensing monomer units of varying lengths that contain both an amine and a carboxylic acid group, a flexible polymer can be made. This type of polymer later became more commonly known as nylon. The length of the monomer chain is indicated by a suffix (**Figure 9**), and can be used to show where a copolymer is used e.g. nylon 6-6, patented by DuPont,[64-66] is made from 1,6-diaminohexane and butane-1,4-dicarboxylic acid (adipic acid).

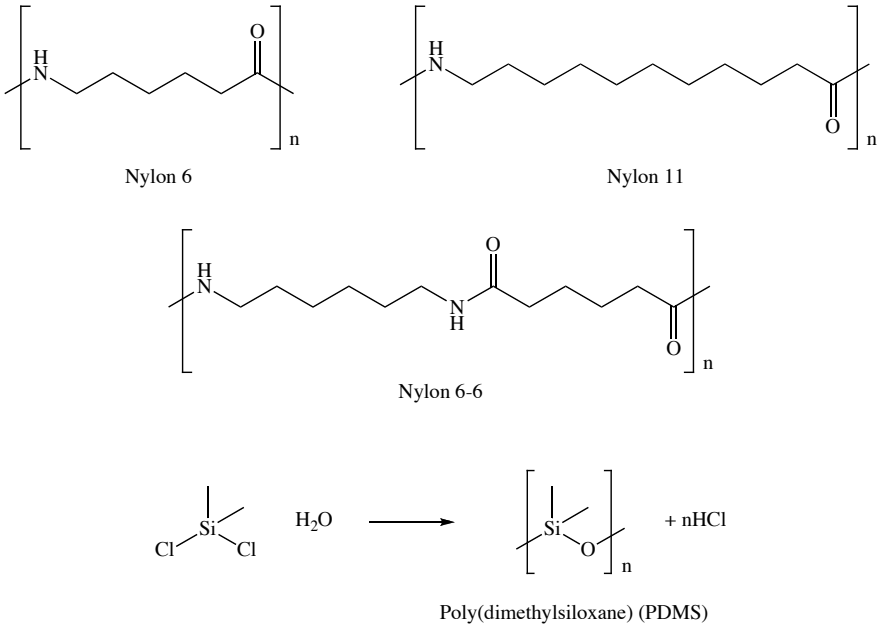

Figure 9. *Examples of step-growth polymers.*

Chain-growth Polymerisation

Polymerisations of this type are generally of the addition type, that is to say, all the atoms of the monomer unit are present in the polymer repeat unit.[58,61,67] This type of polymer growth has three stages, *initiation, propagation* and *termination*. The type of initiation depends on the monomer unit used, for example, a free-radical can be used as the initiator for a monomer that contains a double bond, whilst an anion can be used to open an epoxide group (**Figure 10**).[26,57,68]

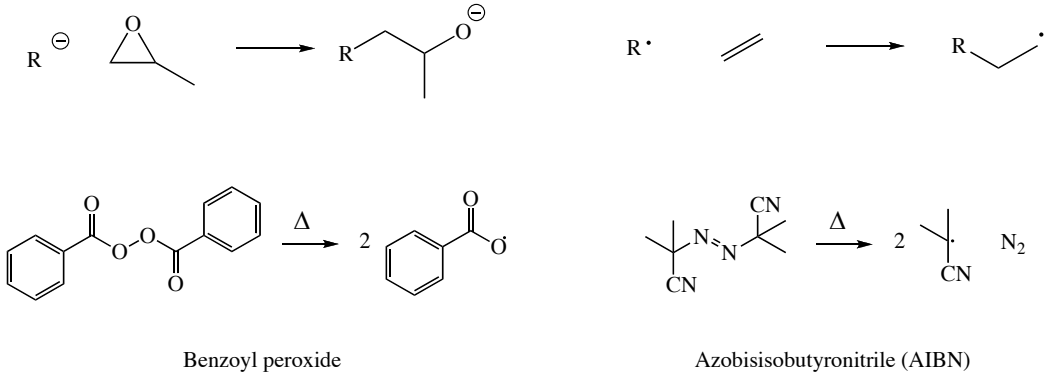

Figure 10. *Examples of initiation (top) and radical initiator (bottom).*[26]

Once a monomer unit is initiated, the free-radical (or anion/cation depending on initiator)[59,67] is located on the terminal group of the chain and is then free to react with another monomer (this is known as chain propagation) which leads to a fast increase in molecular weight. The propagation of the chain will only end when a termination step occurs e.g. by a combination of radicals, or when all the monomer has been consumed.

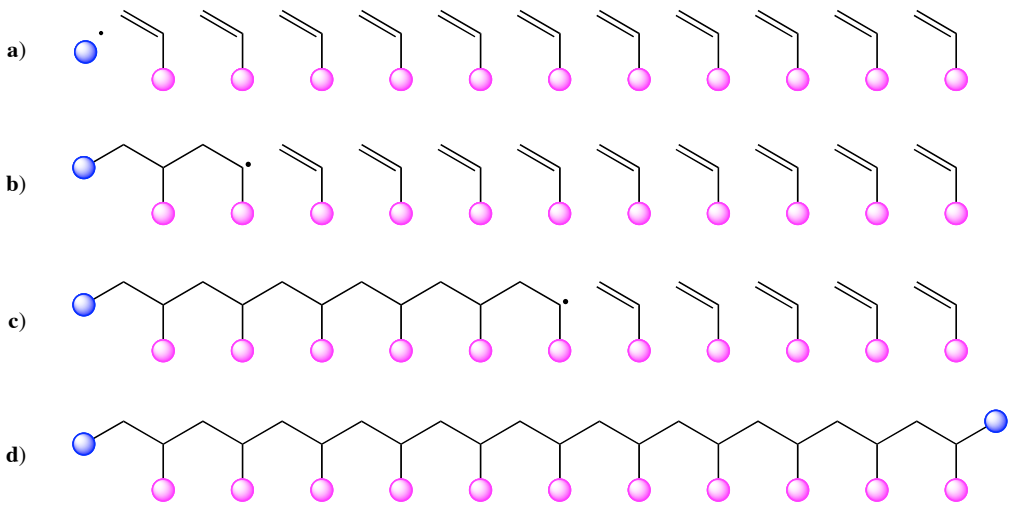

Figure 11. *Schematic representation of radical chain-growth. a) initiation, b) and c) propagation, d) termination. Pink sphere represents a pendant group, blue sphere represents an initiator/terminator radical group (could be another initiated polymer chain).*

Examples of this technique include vinyl polymers, perhaps the most well known of which include poly(vinyl chloride) (PVC), polyethylene (polythene, PE) and polystyrene.[61]

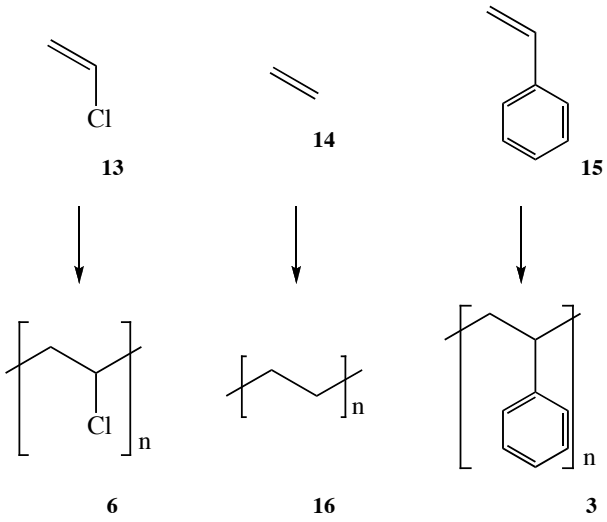

Figure 12. *Structures of PVC, PE and polystyrene respectively.*

Branched and Network Polymers

As the name suggests, branched polymers are polymeric chains that contain branches. These branches can be introduced a number of ways, for example, they can be part of the monomer or can be introduced as part of a graft copolymer. Another way of introducing branches, though not in a controlled way, is by side reactions during the polymerisation. A good example of this is polyethylene. Depending on the technique used for its synthesis, be it by radical, anion addition, cation addition, or ion coordination, a polymer with different amounts of branching (and thus density) can be achieved.[26,59,67]

Network polymers are formed when a polymer chain becomes linked to another through a covalent bond, which can be achieved in one of two ways. The first involves a monomer unit that has more than one functionality such that it can form the polymer chain and still have a reactive group that can form bonds with other chains (i.e. a branched polymer). The second way involves a process known as *cross-linking*.[57,62] The most popular commercial method of cross-linking is that of *vulcanisation*, developed by Charles Goodyear and first patented in 1844.[31] Named after the Greek god of fire, Vulcan, the process involves the heating of rubber in the presence of a curing agent, the most popular being sulphur.

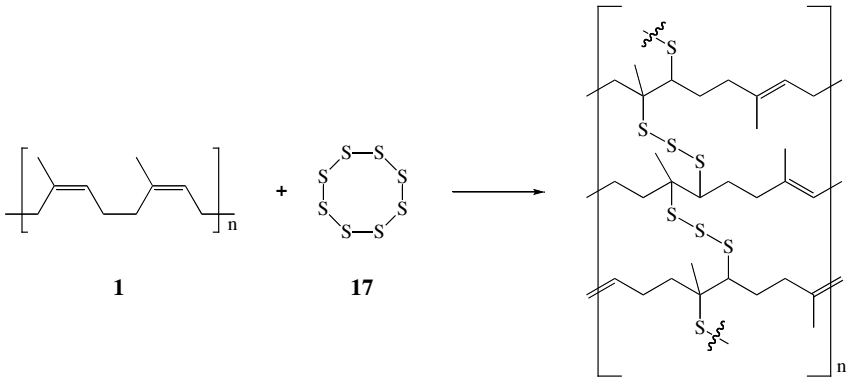

Figure 13. *The vulcanisation process.*

The resulting network polymers become very rigid structures and lose their ability to 'flow', even at high temperature. For this reason they cannot be moulded, making manufacture difficult, and are termed as being *thermoset*. Being so highly cross-linked, thermoset polymers are insoluble, though they may swell as certain solvents can penetrate the structure. Polymers that are not extensively cross-linked are generally soluble and can 'flow' (and be melted); these are said to be *thermoplastic*.[57]

1.2.4 Additional Polymer Types

Despite there being three main types of polymer, namely linear, branched and network, other types exist that have a slightly more unusual structure (**Figure 14**). *Comb polymers* are a type of graft polymer that has a large number of pendent chains.[58,68,69] *Ladder polymers* have a backbone consisting of multiple rings.[70,71] *Polyrotaxanes* are an example of *supramolecular* assemblies, in that molecules are linked through non-covalent means (in this case the polymer backbone is threaded through multiple rings).[72-74] Similarly, *polycatenanes* are synthesised through non-covalent bonding that gives rise to a structure consisting of interlocking rings.[74-76]

Perhaps the most unusual class of polymer is that of the *hyperbranched* polymer, which is an extreme version of branched polymers and has led to the introduction a fourth classification of polymer, that of the *dendritic state*.[57,77] A sub-section of dendritic polymers, known as *dendrimers*, has attracted much attention in recent years.[77-81] They

are ‘grown’ from a central point in a step-wise fashion that allows for controlled growth to a known molecular weight and size. This is unique in the world of polymer science where most polymers are synthesised to a range of lengths and weights.

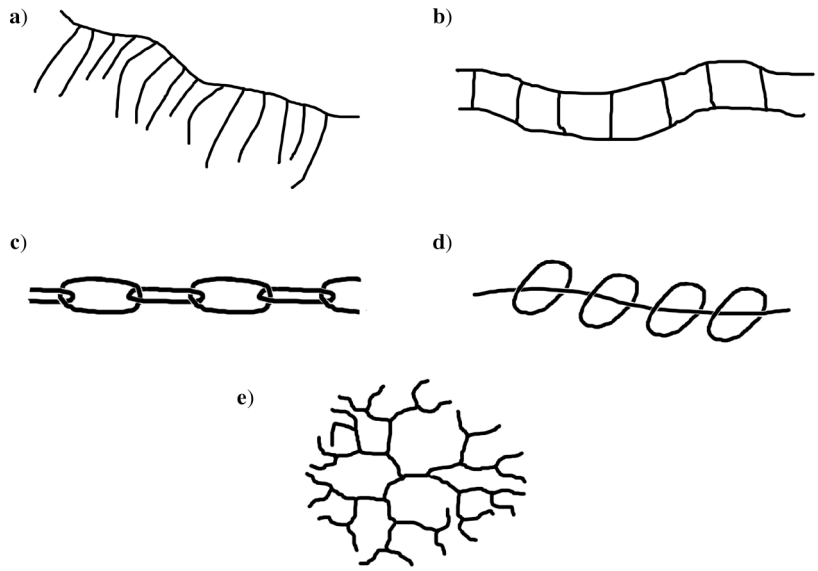

Figure 14. *Representations of a) comb polymer, b) ladder polymer, c) polycatenane, d) polyrotaxane and e) dendrimer.*

1.2.5 A Note on the Properties and Uses of Polymers

The properties of polymers are varied, and depend on a great many things. These include the type of polymer backbone, any branches or cross-links, or whether two or more types of chain are incorporated into the polymer. The variation in length of the chains within the polymeric material (*polydispersity*) also has an effect; polymers that consist of very similar length chains are known as monodisperse. The properties of polymers are too great in number to list here, but a broad selection is shown below, together with more specific examples and their uses (**Table 1**).[58,82,83]

- Good stability to both oxidation and temperature.
- High strength
- Fire retardancy
- Conductance
- Bio-degradability
- Elasticity
- Adhesive

Table 1. *Examples of polymers and their uses.*[57,59]

Polymer type	Uses
Poly(vinyl chloride) (PVC)	Construction, piping, wire insulation
Polystyrene (PS)	Packaging, foam insulation, toys
High-density polyethylene (HDPE)	Bottles, piping, wire insulation
Low-density polyethylene (LDPE)	Toys, coatings, household wares
Epoxy	Protective coatings, adhesives, industrial floorings
Phenol-formaldehyde (PF)	Automobile parts, utensil handles, plywood adhesives
Unsaturated polyester (UP)	Boat hulls, corrosion-resistant ducting, Construction

The addition of *additives* into the polymer can greatly enhance its properties, as well as making them easier to process and can range from small molecules and solvents, to wood-flour (a by-product of saw mills).[57,84-87] The most common type of additive is known as a *plasticizer*,[88,89] and is usually a small molecule that increases polymer flexibility and reduces the overall melting temperature making it easier to mould. These plasticizers can leach out of the polymer, thus reducing its overall effectiveness. In fact, it is this slow release of plasticizer that gives rise to the 'new car smell'. Examples of additives and their function are shown below.

***Table 2**. Polymer additives.*[57]

Type	Function
Plasticizer	Increase flexibility, reduces melt viscosity
Reinforcing fillers	Increase strength properties
Impact modifiers	Increase impact strength
Heat stabilizers	Prevent degradation at high temperatures
Blowing agents	Manufacture stable foams
Cross-linking agents	Cross-link polymer
Lubricants	Prevent sticking to machinery
Antistatic agents	Prevent static charge on surfaces
Antifogging agents	Disperse moisture droplets on films
Flame retardants	Reduce flammability
Biocides	Prevent mildew
Antioxidants	Prevent oxidative degradation
Dyes	Add colour
Odorants	Add fragrance
Deodorants	Prevent development of odour

Polymers as Histone Replacements?

The vast majority of synthetic polymers are linear and have a random molecular weight. Though the length of the chain can be controlled to a certain extent, this still results in a random distribution. In terms of an artificial histone, a polymer could be designed to bind to DNA but this would result in bound polymeric strands, not coils. In order to accurately mimic the properties of a histone, a spherical polymer would be advantageous as this would allow the DNA to coil and condense. For such an application dendrimers are the most suitable option. This type of polymer is synthesised in a step-wise fashion that allows for very good control over the molecular weight and overall size (as described in detail in the following section).

1.3 Dendrimers – The Fourth Polymeric Architecture

1.3.1 Discovery

Though the idea of macromolecules synthesised in a step-wise fashion is relatively new, the first reported synthesis occurring a little over 30 years ago,[90] the concept of three-dimensional branching structures can be traced back to Paul Flory[91,92] and Stockmayer[93] in the mid 1940s. In 1943, Paul Flory introduced the term *network cell*, which he described as "the recurring branch juncture in a network system as well as the extended volume associated with this branch structure".[91] This concept was taken further using statistical modelling to reduce these networks to *branch cells,* and further to graph theory, which mimics the morphological branching of trees.[94-97] These models, together with *cascade theory* mathematics,[98] led to a reasonable understanding of network forming events.[99]

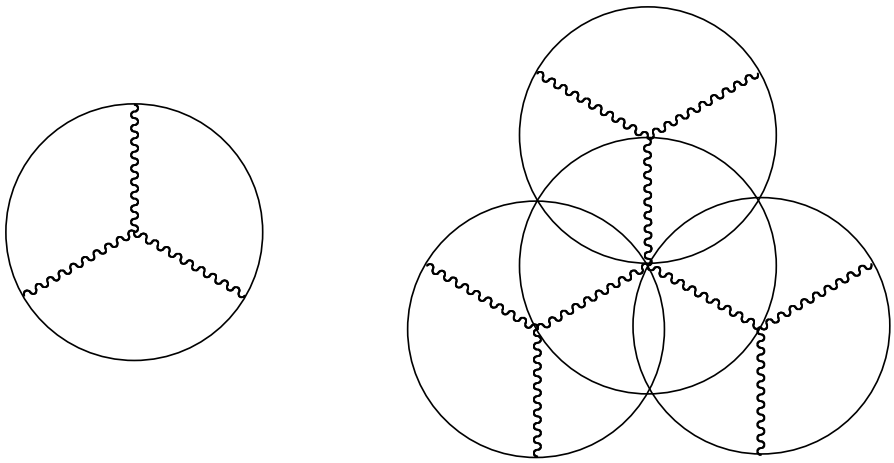

Figure 15. *Two-dimensional projections of a branch cell (left) and a branch cell assembly (right).*[100]

In 1978, Vögtle *et al*.[90] demonstrated the synthesis of two types of molecule, which they describe as *cascade* and *non-skid-chain* structures, both of which were made by the repetitive addition of small molecules. Three years later, Denkewalter *et al*.[101] filed a

patent describing the synthesis of a highly branched macromolecule based around repeating units of L-lysine, which in the following year were shown to be monodisperse.[102]

Around the same time as these discoveries, the Dow Chemical Company was working on their own version of highly branched molecules. In 1979, a group led by Donald Tomalia discovered a methodology whereby acrylate and diamine monomers were sequentially added to a central molecule in what they eventually termed a *divergent synthesis* (**Figure 16**).[77] This research continued until, in 1983, corporate approval was given to publicly present their findings at the Winter Polymer Gorgon Conference (Santa Barbara, CA). Having attended this conference, de Gennes published data predicting the surface congestion properties of these molecules,[103] something that is now referred to as the *de Gennes dense packing* phenomenon. Such was the excitement and controversy over this new type of polymeric architecture that Tomalia was invited to speak at several conferences during 1984-1985, during which time the term *dendrimer* (from the Greek word *dendron*, meaning tree, that can be traced back to A. J. Vogel[104]) was used to describe them.

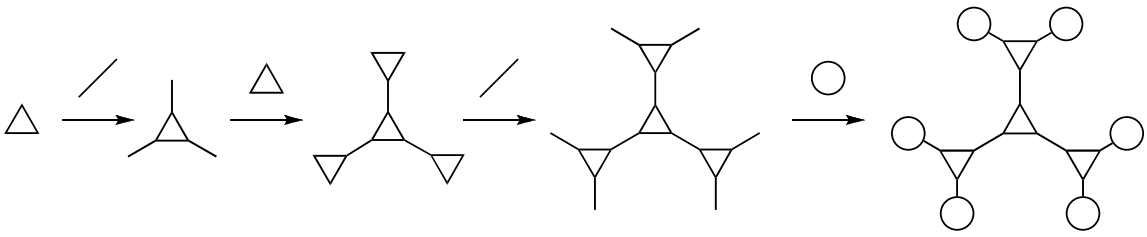

Figure 16. *Schematic representation of the divergent synthesis developed by Tomalia.*

Having filed many patents pertaining to these dendrimers,[105-113] Tomalia *et al*. finally published their findings in 1985, showing a divergent method that produced a series of dendrimers based on methyl acrylate and ethylene diamine.[77] They coined this class of dendrimers poly(amidoamine) (PAMAM) owing to the number of amide bonds and amine surface (later registered to the Dow Company as *Starburst*® dendrimers because of their starburst branching pattern). They ranged in molecular weight from a few hundred to over a million Daltons and were synthesised with high purity, something that Vögtles' cascades failed to achieve as a result of low yields and poor purity.[114] The

paper went on to describe detailed analysis and introduced the idea of *defects* in the dendritic structure. At the same time as this publication, George Newkome *et al.*[115-117] reported their own findings about a series of branched polymers based around a simple mathematical progression (derived from an architectural model of trees, specifically the Leeuwenberg model[118]) to give a cascade structure that could act as a micelle, something they termed *arborols* (from the Latin word *arbor*, meaning tree; this class of polymer later became accepted as a sub-category of dendrimers).

In spite of great interest in this new form of polymeric architecture, many scientific journals remained sceptical, making it hard to publish results. Some reasons cited by critics of the period are shown below:[99]

- Dendrimers are no different from 'microgels' – they are probably highly cross-linked particles akin to latexes.
- Dendrimers are not really discrete chemical structures – they are non-descript materials.
- Back-folding of terminal chain ends into the interior of dendrimers will prohibit any 'guest-host' properties – expectations for unimolecular micelle-like properties are absurd!

The following decade saw an explosion in publications and a general acceptance of dendritic polymers, stemming from several key events in the early 90s. A review by Tomalia *et al.*[100] published in Angew. Chem. in 1990 served to greatly increase awareness by giving an overview to the basic concepts of dendrimers. Another key point was the introduction, in 1989, of a new synthetic route for making dendrimers. Work between Jean Fréchet and Craig Hawker found that instead of growing a dendrimer from the inside out, it was possible to start from the outside and grow inwards towards a core, in a process now widely known as the *convergent synthesis* (***Figure 17***).[119-122] Also of note are the contributions between Tomalia and Nicholas Turro in comparing the photo-physical properties of PAMAM dendrimers to those of micelles and DNA.[123]

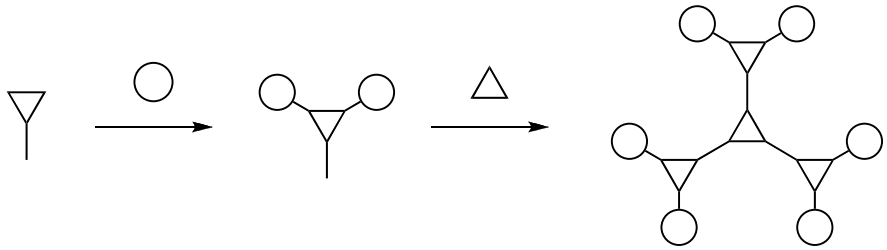

Figure 17*. Schematic representation of the convergent synthesis developed by Fréchet.*

Many groups have since been able to demonstrate the flexibility of the convergent synthesis, though Fréchet and Hawker were definitely the early pioneers; they demonstrated its use to create poly(benzyl ether) dendrimers with more than one type of functionality on the surface.[124,125] They also developed the first double stage convergent synthesis,[126] and produced dendrimers to act as macromonomers along with their subsequent polymerisation,[127,128] and created a range of dendritic architectures.[129] Other work at this time also produced the first solid-phase synthesis of a dendrimer.[130]

In recent years a wide range of dendritic systems have been created, ranging from new components to new architectures. Perhaps the most unusual architectures are those of the *dendrigraft* and *dendronized* polymers. First made in 1991 by Tomalia *et al*.[131] and Gauthier *et al*.,[132] dendrigraft (also known as *arborescent*) polymers are dendrimers where the monomer units are themselves polymer chains, making for flexible polymers with very high molecular weight.[99,133,134] Dendronized polymers are a sub-category of comb-polymers and consist of a linear polymeric backbone from which are attached dendritic arms.[135,136] Also known as 'rod-shaped polymers', their cylindrical structure can be modified for stiffness and surface decoration for uses such as catalytic supports and electricity conducting materials.[137]

1.3.2 Dendrimer Forerunners

The first instance of a dendritic-type step-wise synthesis was reported in 1978 by Vögtle *et al.*[90] They demonstrated how two types of molecule could be made with increasing size from either mono-amines or diaza monocyclic rings in an approach described as 'non-skid-chain like' synthesis.

To create their 'cascade' molecules, mono- or di-amines were reacted with acrylonitrile to form two nitrile groups per amine. These were then reduced to amines using cobalt (II) chloride hexahydrate and sodium borohydride (**Scheme 1**). Further iterations of these steps led to monodisperse materials that possessed increasing cavity size capable of host-guest interactions. This 'growth' type process itself would later become the forerunner to dendrimer synthesis.

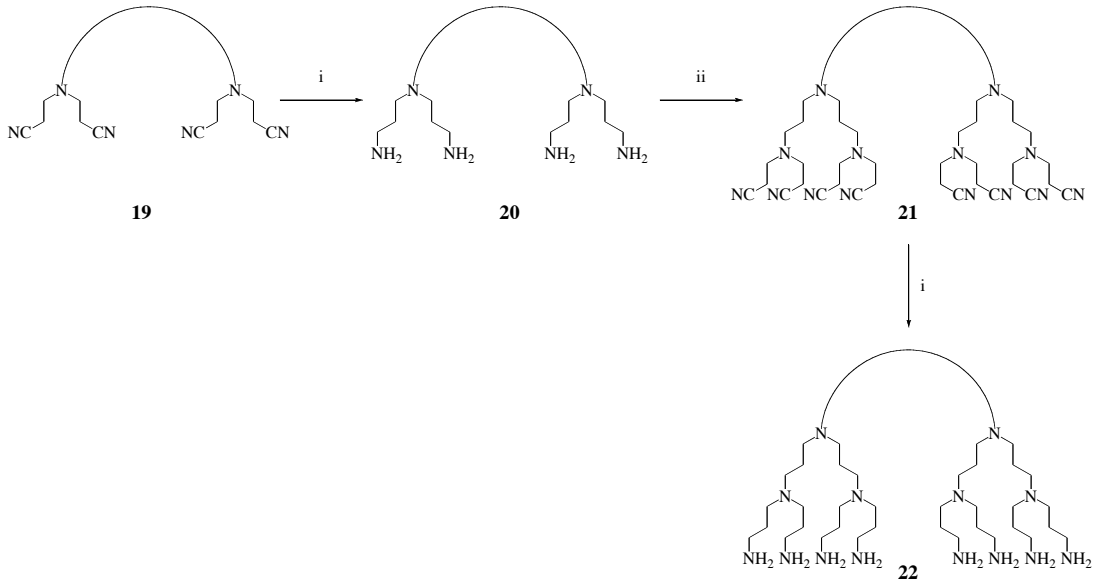

***Scheme 1**. Synthesis of the first 'cascade' molecules. i) $CoCl_2 \bullet 6H_2O$, $NaBH_4$, MeOH, 2 hr; ii) $CH_2=CH\text{-}CN$, AcOH, 24 hr.*

A problem that occurred was that the cobalt (II) used in the reaction formed a complex with the resulting amines, so the cobalt was removed as the amine complex and the product was then extracted into chloroform. This, however, caused difficulties at larger molecule sizes such that these could not be completely purified.[114]

The second molecule type reported by Vögtle *et al.*[90] was a series of cyclic structures grown using the 'non-skid-chain' methodology (**Scheme 2**). This work is similar to that of the cascade molecules in that an amine is reacted with acrylonitrile, followed by a reduction step. The two resulting amines, however, then react with a dicarboxylic acid dichloride at high dilution to form a cyclic system (the amide then being reduced). This process can then be repeated to introduce multiple rings into the system.

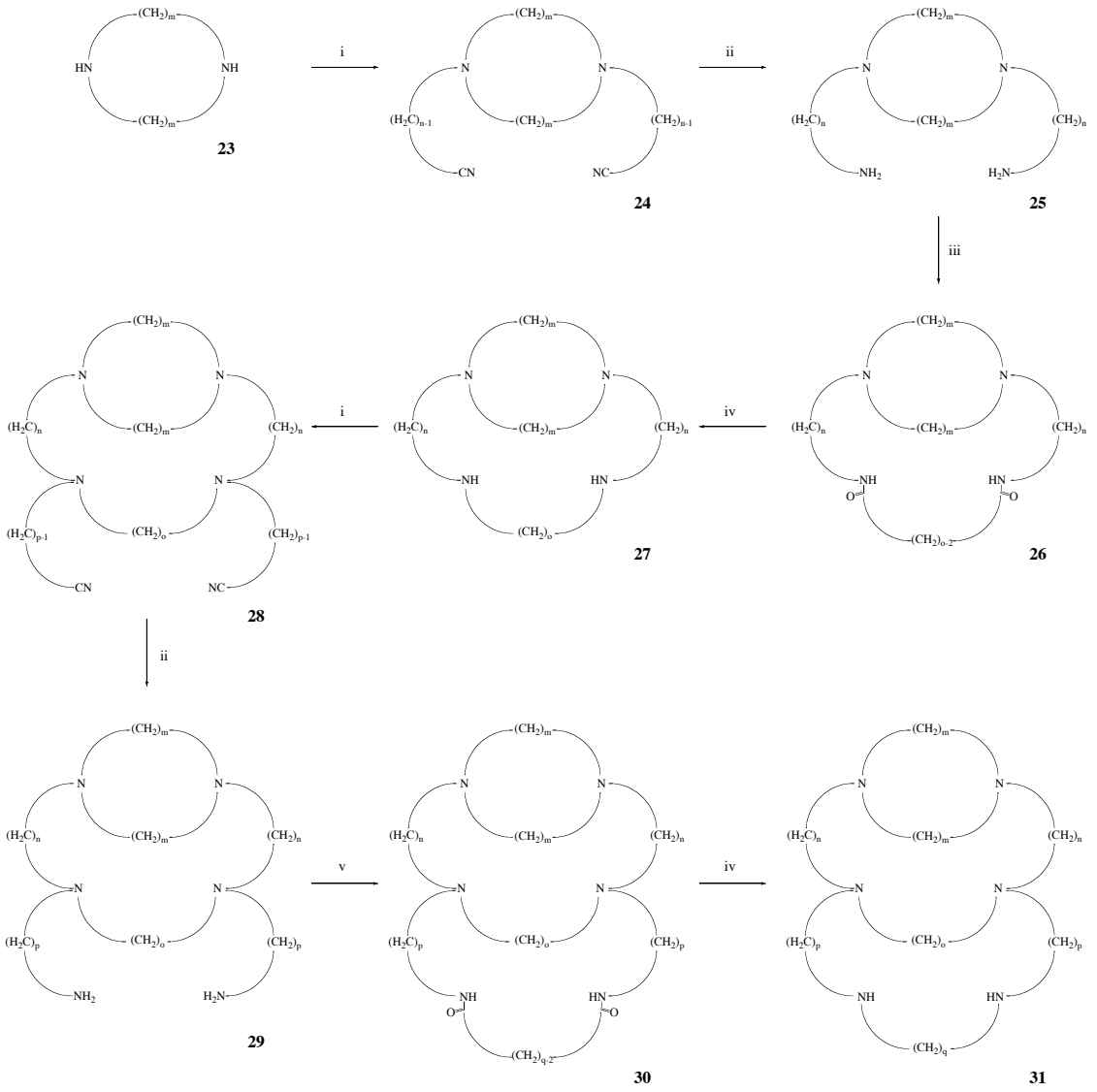

Scheme 2. *'Non-skid-chain' synthesis of polymacrocycles. i) CH_2=CH-CN, AcOH, 24 hr; ii) $CoCl_2$•$6H_2O$, $NaBH_4$, MeOH, 2 hr; iii) $ClC(O)(CH_2)_{O-2}C(O)Cl$, benzene, 7hr; iv) $LiAlH_4$, THF; v) $ClC(O)(CH_2)_{q-2}C(O)Cl$, benzene, 7hr.*

A patent in 1981 by Denkewalter *et al.*[101] demonstrated the synthesis of a macromolecule based on repeating units of lysine using a step-wise growth from a 'source molecule' to give well-defined molecular weight, something akin to Vögtle's cascade and non-skid-chain molecules.

This synthesis (**Scheme 3**) is based around the coupling and deprotection of the amino acid L-lysine, the major repeating steps being the coupling of an activated ester of Boc-protected lysine to the amino groups of a separate lysine group using dicyclohexylcarbodiimide (DCC), and subsequent deprotection using trifluoroacetic acid (TFA).

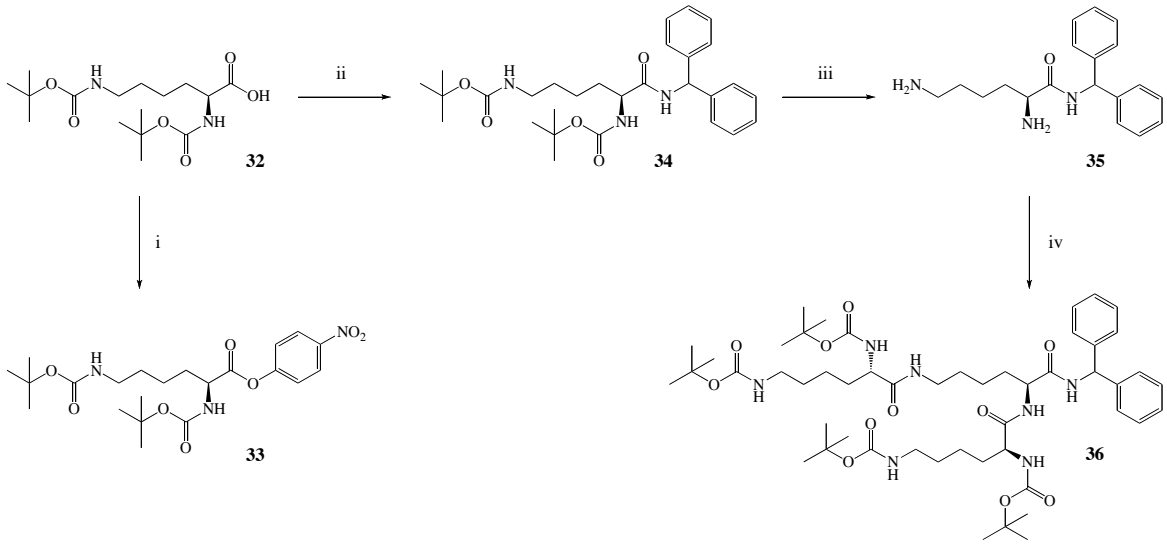

Scheme 3. *Initial stages of Denkewalter's highly branched macromolecules. i) p-Nitrophenol, DCC, DCM; ii) benzhydrylamine, DCC, DCM; iii) TFA, DCM; iv)* ***33****, DCC, TEA, DMF.*

The patent shows that these molecules can be synthesised to a very high molecular weight, having a surface of up to 1024 lysine groups (and an interior of 1023 groups), and suggests that a) further iterations may be possible and b) that other groups could be attached to the surface *via* reactive groups such as anhydrides, acid halides and isocyanates.

The solution properties of this structure were subsequently probed in 1982, revealing the molecules to be both monodisperse and non-draining spheres.[102] It was proposed

that they "may be useful as molecular markers in chromatography and/or spectroscopy of unknown low to moderate molecular weight polymers in certain organic solvents. Their density and non-draining nature minimize size variability with changes in solvent quality".

Though not true 'starburst' type molecules owing to their asymmetric branching, they clearly demonstrate the step-wise approach that helped kick start interest in dendrimer science.

1.3.3 Synthesis

Dendrimers are made *via* a step-wise process that gives rise to a structure that contains three distinct parts, namely the *core*, the *interior* and the *surface*. The dendrimer core is the central point of the structure and acts as a focal point from where the initial branching occurs and can consist of either a small or large molecule (e.g. ammonia[77], calixarnes[138,139] or C_{60}[140]). The choice of core helps determine the properties of the resulting dendrimer, primarily by the number of branching points it provides (the greater this number the faster the density will increase), but also by its shape and properties (i.e. the core could possess the ability to bind metal ions[141]).

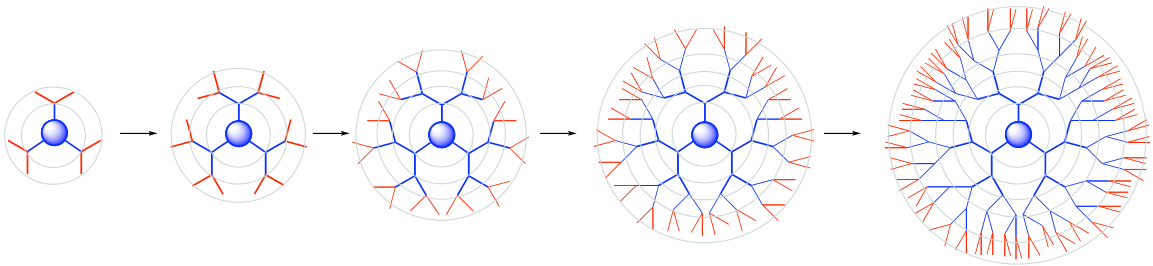

Figure 18. *Schematic representations of dendrimers. Sphere represents the core, blue lines represent the interior, red lines represent the surface.*

The interior consists of a combination of branching points and lengthening groups, which allow the dendrimer to 'grow', each successive inclusion of a branching point being known as a *generation* (which can be denoted as Gn where n is the number of

generations). For a macromolecule to be classed as a dendrimer this branching must be symmetrical. The monomer units used in the interior also help to determine dendrimer properties, helping increase/decrease solubility and viscosity as well as a wide range of other properties. As with other classes of polymers, different types of dendrimers are named based on their monomers; for example, poly(propylene imine) and poly(arylethers).

Perhaps the most important part of a dendrimer is its surface, as this is where its properties can most easily be changed, allowing for wide and varied applications. It has been the surfaces of dendrimers that have captured the imagination of so many scientists and has led to their applications in light harvesting and drug delivery to name but a few (see **Sections 1.3.7 – 1.3.9**).

As previously mentioned, a dendrimer is synthesised in a step-wise fashion, but this can be achieved in one of two ways, namely by the divergent or convergent approach. Unlike any other type of polymer, dendrimers can only be synthesised up to a certain generation as steric hindrance at the surface prevents further growth. This is known as the *starburst limit* and is different for each dendrimer depending on the size of the core, the length of monomer unit and the number of branches in each generation.

Divergent Synthesis

This type of synthesis was developed by Tomalia *et al*.[77] in the early 1980s (though Vögtle used a similar route in 1978[90]), and for over a decade remained the only way to synthesise dendrimers. The term divergent refers to the way that the dendrimer is 'grown' outwards from a central point. Starting from the core, two (or more) steps are required to create a new generation but the type of steps depends on the type of monomer units to be used. Below is shown the synthesis of two common dendrimer types; poly(amidoamine) (PAMAM, developed by Tomalia[77,106]) and poly(propylene imine) (PPI, developed first by Vögtle,[90] then by Meijer[142]).

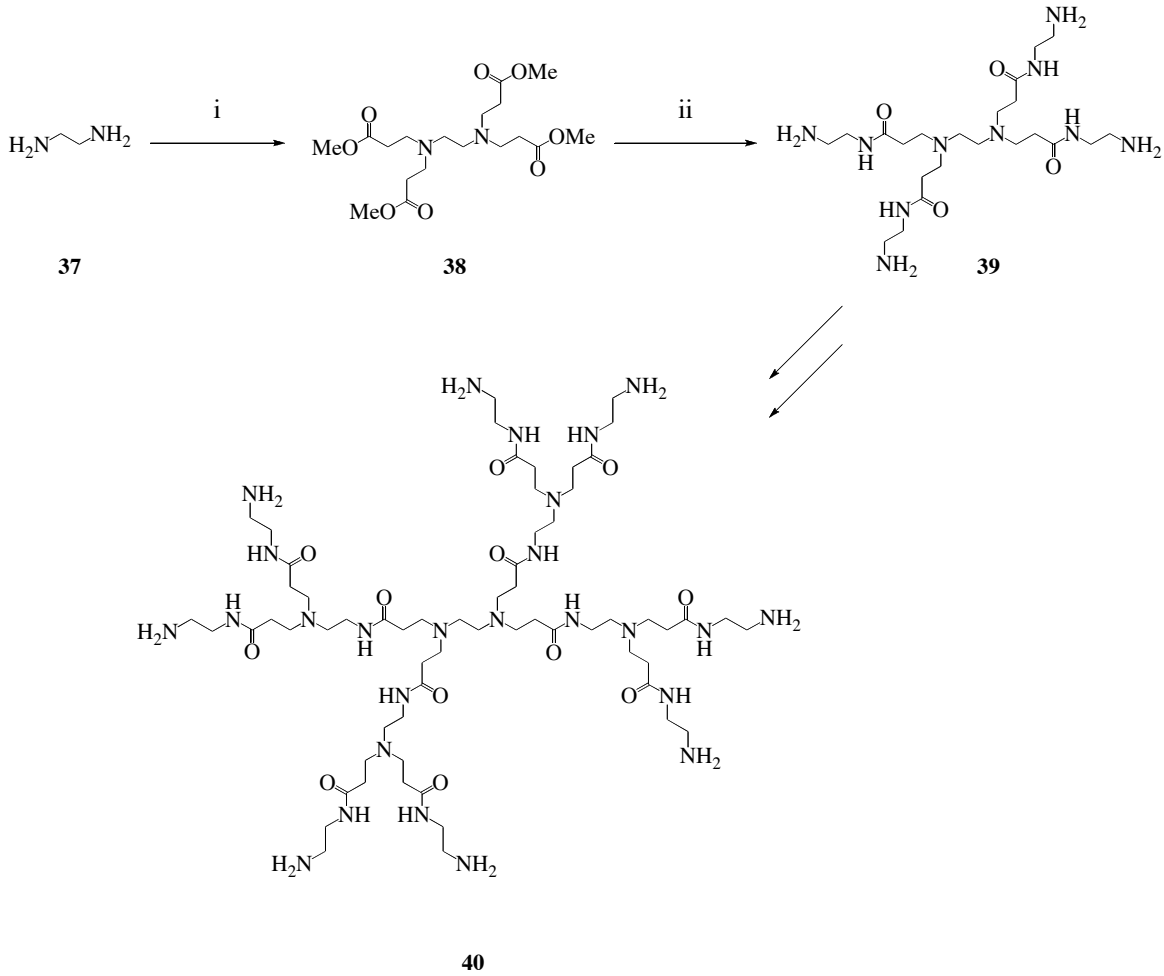

Scheme 4. *Poly(amidoamine) (PAMAM) synthesis. i) Methyl acrylate, MeOH; ii) ethylene diamine, MeOH.*

The first step in PAMAM synthesis involves the addition of a 'lengthening' unit to the core, for which methyl acrylate is used. This is then reacted with an excess of ethylene diamine (to avoid cross linkage of terminal groups) to give a surface that can act as a branching point (i.e. R-NH_2). These two steps, which together make a single generation, are then repeated to give rise to a highly branched structure.

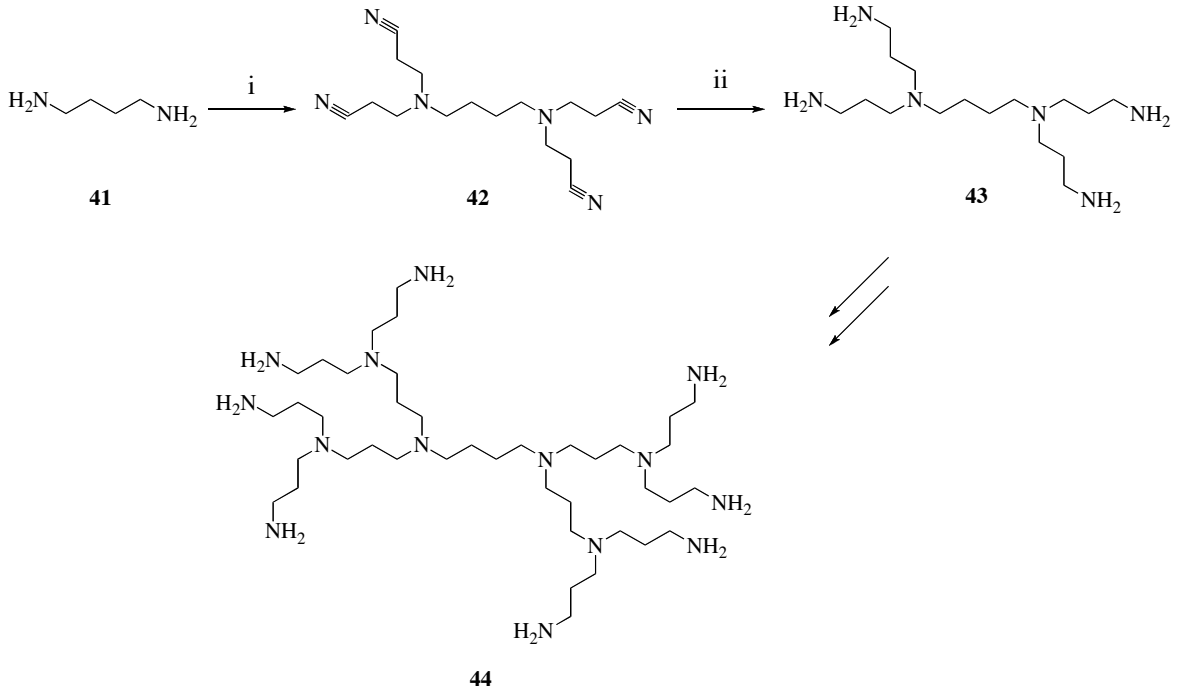

Scheme 5. *Poly(propylene imine) (PPI) synthesis. i) Acrylonitrile, H_2O; ii) H_2, Raney/Cobalt, H_2O.*

Unlike with PAMAM synthesis, PPI dendrimers are made using only one type of monomer unit, namely acrylonitrile (CH_2=CH-CN), which acts as both the lengthening and branching unit. This is achieved by reducing the nitrile group to an amine, which will allow for the double Michael addition of acrylonitrile. So despite only one monomer being used, two reaction steps are required to successfully add a generation.

This synthetic route creates large structures very quickly, which can lead to problems with purification. Similarly, at high generations the number of surface groups is quite high meaning that a large number of monomer equivalents are required to achieve complete surface conversion; not to do so will create defects in the dendritic structure making it unsymmetrical (thus harder to characterise) and lowering the polydispersity (giving a wide range of molecular weights and sizes).[143]

Convergent Synthesis

As previously mentioned, the major drawback of the divergent synthesis is the introduction of defects into the structure that are hard, if not impossible, to remove. In response to this major issue, Fréchet and Hawker[121,122] developed the convergent approach in 1990, which was rapidly taken up by others such as Miller.[144,145] This approach starts at what will be the dendrimer surface and grows inwards creating a wedge shape, or dendron. Several dendrons are then coupled to a core to create the final dendrimer (examples of which are shown below).

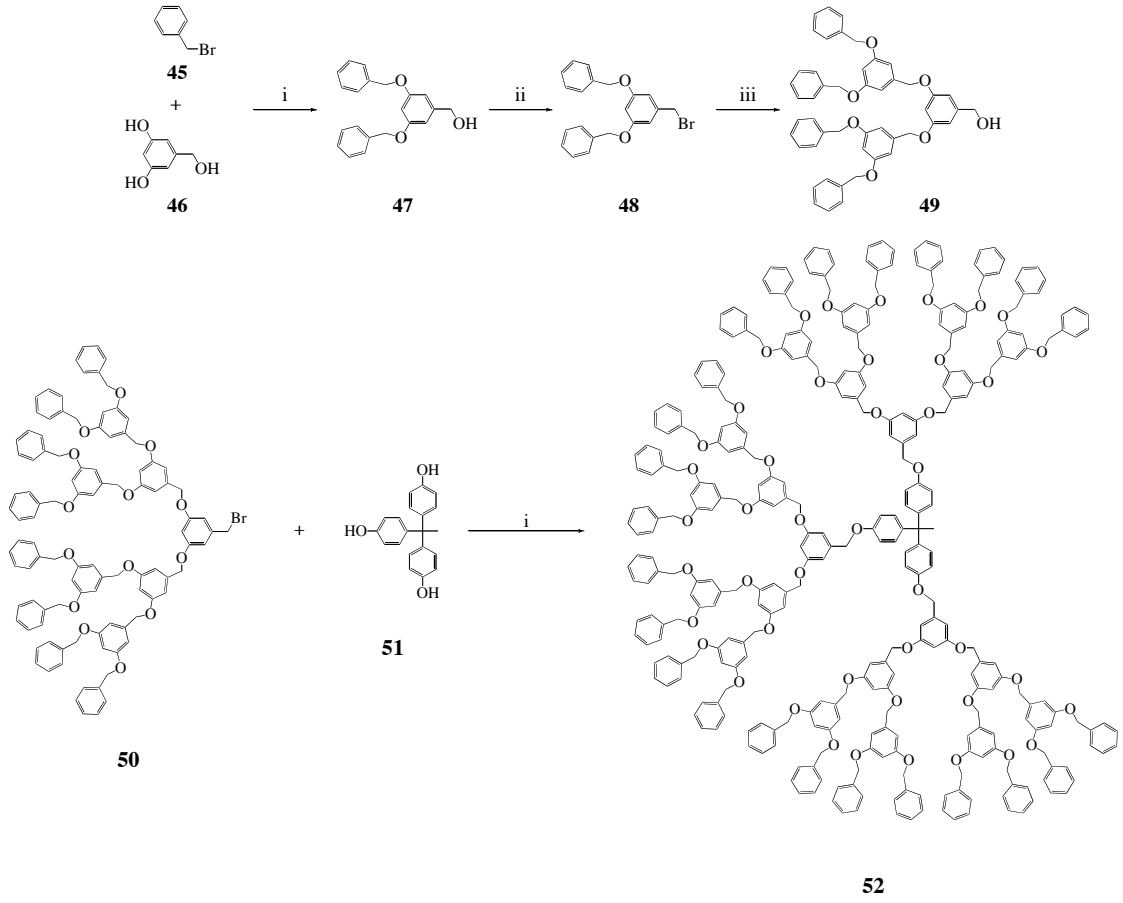

Scheme 6. *Poly(benzyl ethers) developed by Fréchet.[122] i) K_2CO_3, 18-Crown-6, acetone; ii) CBr_4, PPh_3, THF; iii)* ***46****, K_2CO_3, 18-C-6, acetone.*

Similar to the divergent synthesis, the branching motif requires two stages. The first, **47** to **48**, is an activation of the dendron while the second, **48** to **49**, is a coupling of two dendrons to another monomer unit. These steps are then repeated to gain higher generations. Finally, the dendrons are coupled to a central core (**52**).

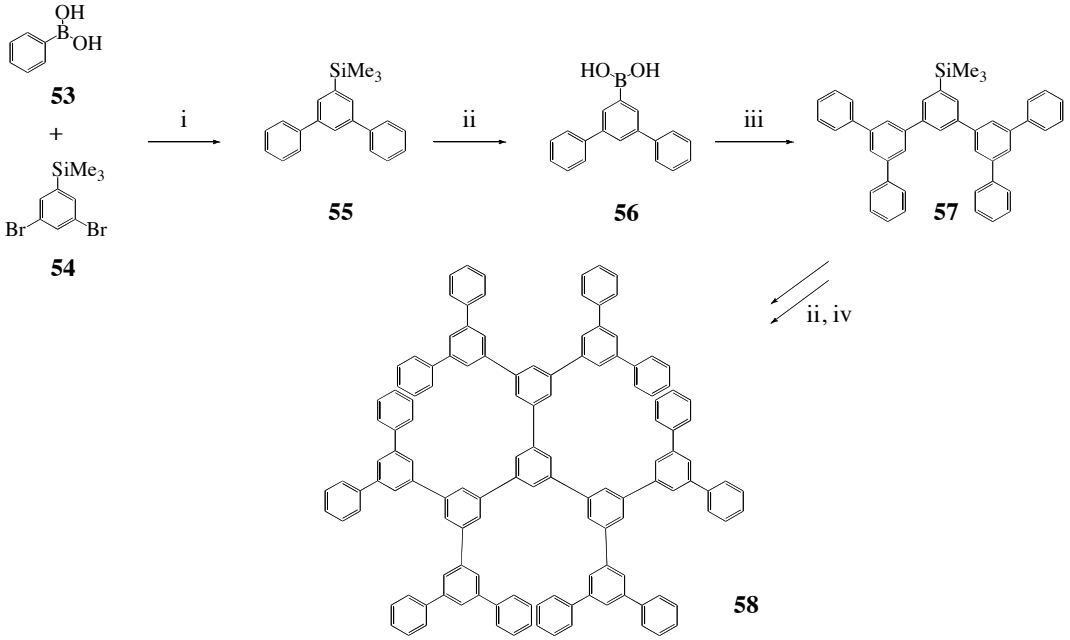

***Scheme** 7. Polybenzene aromatic dendrimers developed by Miller.[145] i) $Pd(PPh_3)_4$, Na_2CO_3, EtOH; ii) a) BBr_3, DCM, b) KOH, H_2O; iii) **54**, $Pd(PPh_3)_4$, Na_2CO_3, DCM/THF; iv) 1,3,5-tribromobenzene, $Pd(PPh_3)_4$, Na_2CO_3, THF.*

The major advantage of the convergent synthesis is that the dendrons are of relatively low molecular weight compared to the final dendrimer, making reactions easier and with fewer defects (which are easier to remove). However, this methodology suffers from low yields as a result of steric problems that occur when the dendrons are coupled to the core.[146]

1.3.4 Examples of Dendrimer Architectures

Branching Monomers

For a dendrimer to 'grow' it requires a multifunctional core as well as monomers that can act as branching points. There are a great many branching architectures used to make dendrimers, some examples of which are shown below (adapted from ref[146]).

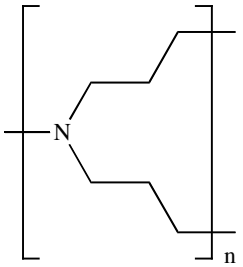 **59**	Poly(propylene imine) (PPI) dendrimers were first synthesised by Vögtle *et al*. in 1978,[90] but their method did not allow for high generations. This methodology was improved upon by Meijer *et al*. in 1993[142] and has since been synthesised to 10th generation. Synthesis is achieved by double Michael-type addition of acrylonitrile to a primary amine, followed by a reduction of the nitrile (**Scheme 5**).
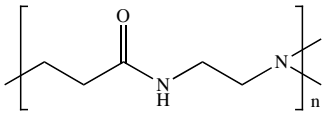 **60**	Developed by Tomalia *et al*. in the early 1980s,[77,105] the poly(amidoamine) (PAMAM) dendrimers were the first to be synthesised and fully characterized. Synthesis is achieved using the divergent approach by double Michael addition of methyl acrylate to a primary amine, followed by reaction of the ester with a diamine (**Scheme 4**). High generation dendrimers (up to 10th) tend to have unavoidable defects.
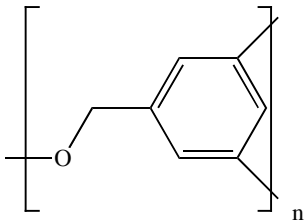 **61**	The poly(benzyl ethers), synthesised by Fréchet and Hawker in 1990,[122] represent the first use of the convergent synthesis. Increased dendrimer generation is achieved by bromination of a benzylic alcohol, followed by reaction of the benzylic bromide with a phenol (**Scheme 6**).

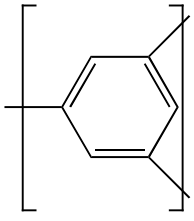 **62**	Created by Miller and Neenan in 1990,[144,145] these were the first all hydrocarbon dendrimers. Synthesis is accomplished by conversion of an aromatic trimethylsilane to an aromatic boronic acid, followed by a Suzuki coupling (**Scheme 7**).
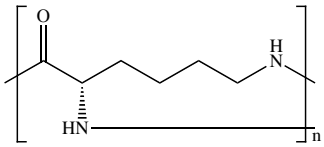 **63**	This poly(L-lysine) macromolecule was patented by Denkewalter *et al*. in 1981.[101] Synthesised by Boc protection/deprotection and peptide coupling using DCC.
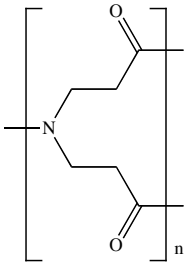 **64**	Created by Fréchet and Uhrich in 1992 using Boc deprotection and DCC couplings.[147]
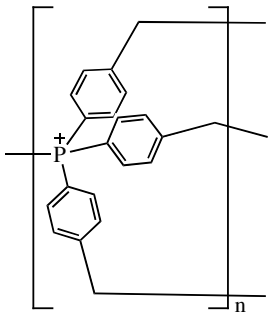 **65**	The 'phosphonium cascade molecules', synthesised in 1991 by Rengan and Engel,[148] are the first example of an ionic dendrimer, and also of one containing phosphorous. Growth is carried out by conversion of a benzyl methyl ether to a benzyl iodide, followed by its displacement by a triarylphosphine.
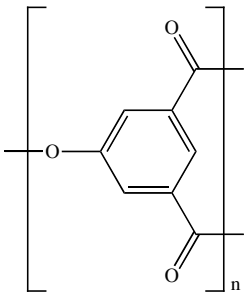 **66**	Synthesised first by Miller *et al*. in 1993[149] in a one-pot synthesis to give an unsymmetrical dendritic structure, then by Feast *et al*. in 1994[150] to give convergent dendrimers. Prepared using acetyl deprotection and aryl acid chloride coupling.

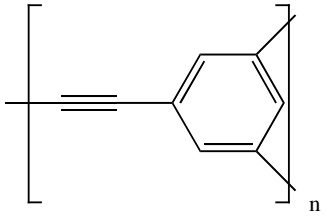 **67**	Created by Moore *et al*. in 1995[151] using a 'double exponential growth' approach. Branching is achieved by palladium-catalysed cross-coupling of a terminal acetylene to an aryl halide. Monomers are prepared by either TMS deprotection of the acetylene, or removal of the focal triazene to give an aryl iodide.
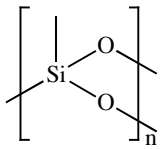 **68**	First prepared by Zhdanov *et al*. in 1990.[152] Synthesised by silylation of sodium bisethoxy methylsiloxide with methyl trichlorosilane, followed by formation of chloro-silyl by cleavage of the ethoxy groups using thionyl chloride.
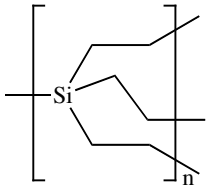 **69**	Prepared by Seyferth *et al*. in 1994.[153] Synthesised by platinum-catalysed addition of trichlorosilane to an alkene, followed by substitution with vinylmagnesium bromide.
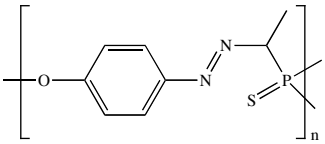 **70**	Created by Majoral *et al*. in 1995.[154] Formation achieved by reaction of a phenoxide with a phosphorous chloride, followed by a condensation between an aldehyde and a primary amine from a hydrazine.
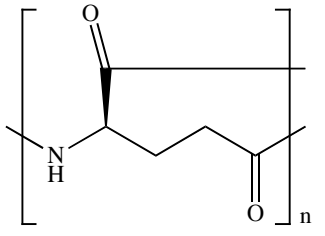 **71**	Based upon repeating units of L-glutamic acid, these dendrimers were created by Mitchell *et al*. in 1994[155] and were the first chiral dendrimers to be fully characterized. Synthesis was performed using Cbz protections and a DCC coupling reagent.
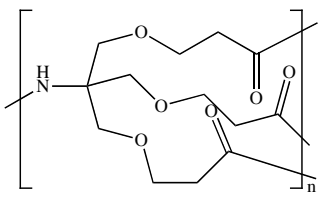 **72**	Developed by Newkome *et al*. in 1985[115,116] using DCC couplings and base-promoted hydrolysis of an ester.

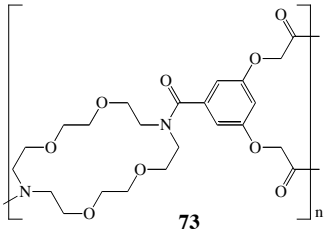 **73**	These so called 'crowned' arborols were synthesised by Shinkai *et al*. in 1992[156] using an amide bond formation (using pivaloyl chloride) followed by ester hydrolysis and Cbz deprotection.
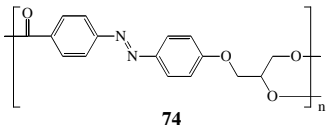 **74**	Synthesised by Shi *et al*. in 2007[157] by formation of an ester bond between two azobenzene molecules, followed deprotection of a carboxylic acid.
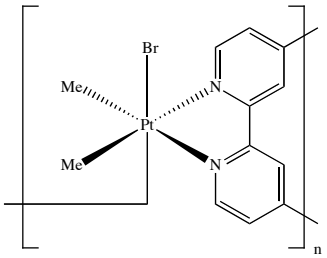 **75**	Created by Achar and Puddephatt in 1995[158] by oxidative addition of a benzylic bromide to a square planar dimethylplatinum species followed by its coordination to a 2,2'-bipryidine.
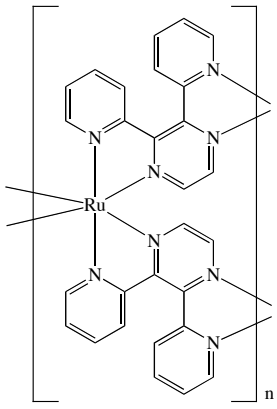 **76**	An interesting architecture developed by Balzani *et al*. in 1995 to study electrochemical and luminescence properties.[159,160] Synthesis is achieved by protection of a pyridine by methylation, displacement of chloride ligands from a metal centre, followed by removal of methyl protection.

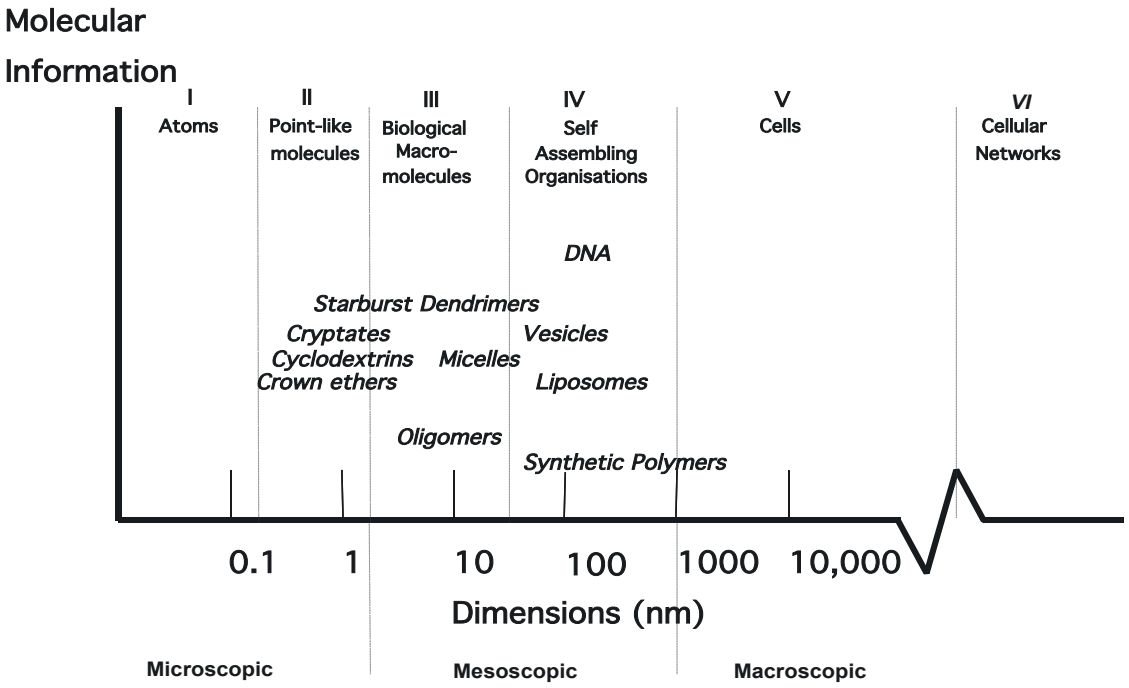

Figure 19. *Relative macromolecular sizes.*

The information in **Figure 19** gives an idea as to the relative size of dendrimers compared to other polymers and biological systems. Similarly, **Table 3** gives an idea as to how a dendrimer's size varies with its generation as well as its branching structure. The first thing to notice is that the more branching sites the core has, the larger the hydrodynamic radius, as demonstrated by the PAMAM examples, one of which has 3 core branches (NH_3) and the other has 4 (EDA). It is also noticeable that the longer the branching repeat unit the larger the radius, for example, a PAMAM branch consists of 7 atoms and has a larger diameter than the corresponding generation of a PPI dendrimer, whose branches only have 4 atoms. It should be noted that some of these radii have been found using different techniques so they cannot be directly compared with each other, though the overall trends can be usefully explored.

Table 3. *Comparison of dendrimer sizes (Å).*

Generation	0	1	2	3	4	5	6	7	8	9	10
PAMAM [a] (NH_3 core) [100,161-163]	10.8	15.8	22.0	31.0	40.0	53.0	67.0	80.0	92.0	105.0	124.0
PAMAM [a] (EDA core)[99,100,161,162]	15	22	29	36	45	57.0	67.0	88.0	97	114.0	130.0
Polylysine [b] [100,101]	–	–	16.0	20.0	25.8	–	39.8	59.2	–	86.8	–
Polyether [a] [100]	–	9.8	18.6	25.0	–	–	–	–	–	–	–
Poly(ethylene imine) (PEI) [a] [100]	7.9	15.1	20	–	–	–	–	–	–	–	–
Poly(propylene imine) (PPI) [c] [99]	4.4	6.9	9.3	11.6	13.9	–	–	–	–	–	–

[a] SEC, [b] Small X-ray scattering, [c] Neutron scattering

Arborols

As already mentioned in **Section 1.3.1**, a series of branched polymers based around the geometric growth of trees was synthesised by Newkome *et al*. in 1985,[115] a structure that they termed arborols (it should be noted that this was at a time before the word dendrimer had been attached to this type of structure). An arborol is, in effect, a one-directional cascade macromolecule, which Newkome synthesised using what is now recognised as the divergent approach (the number of surface groups an arborol possesses is shown as [n]).

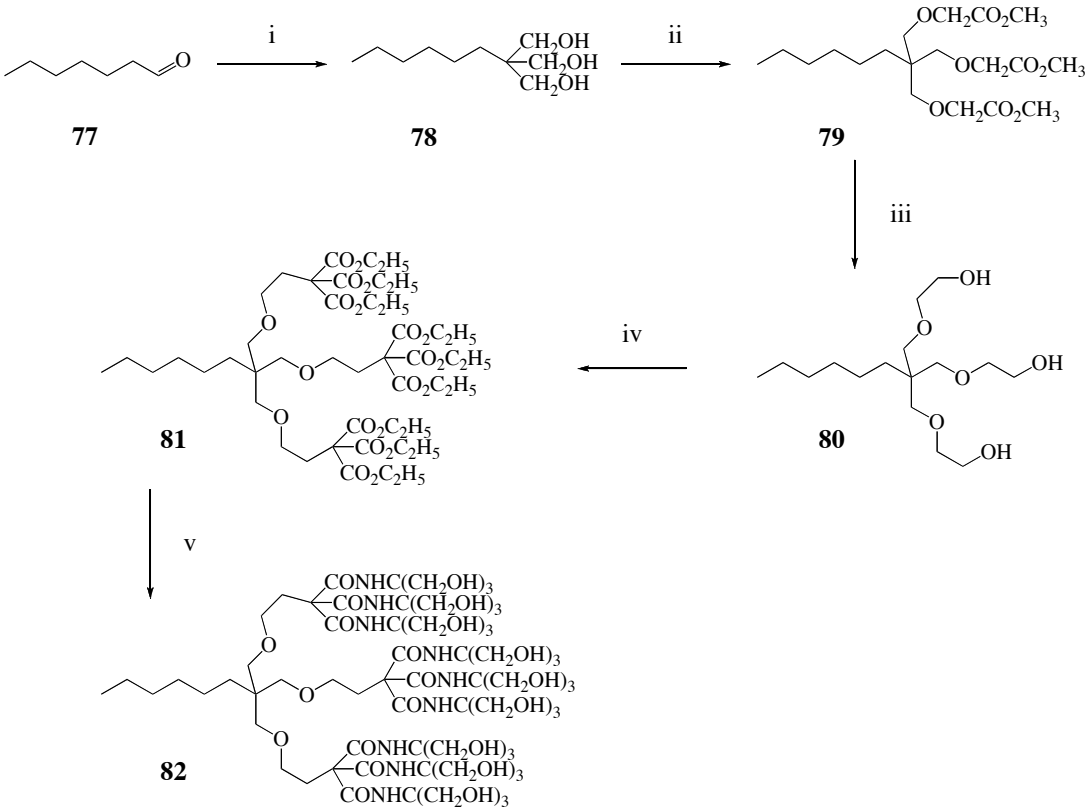

Scheme 8. *Formation of a [27]-Arborol.*[115] *i) EtOH, OH⁻, H_2CO; ii) a. Chloroacetic acid, $^tBuOK/^tBuOH$; b. MeOH; iii) $LiAlH_4$, ether; iv) $NaC(CO_2C_2H_5)_3$, benzene/DMF; v) $H_2NC(CH_2OH)_3$, DMSO, K_2CO_3, 70ºC.*

In the following years, Newkome developed two- and three-directional arborols based on the same branching pattern as shown in **Scheme 8**. The three-directional arborols ([9]^3-Arborol)[116] were synthesised by growing three cascades from a tri-functional benzene core (to give water soluble products that aggregated to form an assembly with a diameter of ca. 200 Å by electron microscopy), whilst the two-directional arborols ([9]-n-[9]-Arborol)[117,164] were grown from varying lengths of dibromoalkanes. Of all the carbon chain lengths used, it was found that only one formed a gel in water, that of [9]-10-[9]-Arborol. This was studied under electron microscopy and was found to consist of rods of uniform diameter, ca. 35 Å. It was proposed that, owing to their 'dumbbell' shape, an interlocking structure occurs whereby one molecule sits on top of another but at a 90º angle as shown in **Figure 20**.

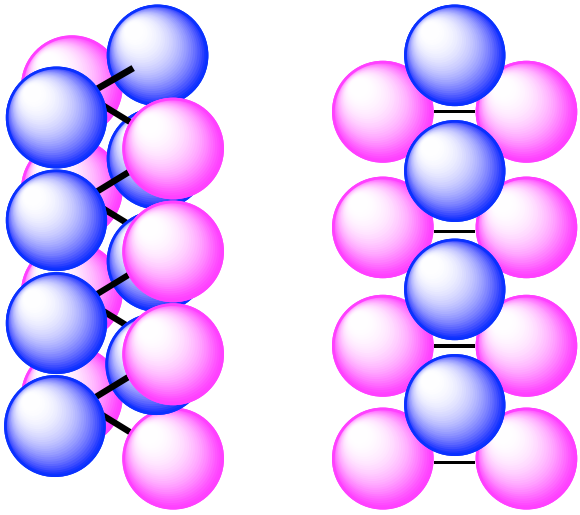

Figure 20. *Proposed aggregation of [9]-10-[9]-Arborol fibres.*[117]

Interesting Architectures

With the number of branching monomers and different types of dendrimer constantly on the increase, a number of interesting architectures have appeared over the years. Majoros, Tomalia and Baker Jr[165] have synthesised a dendrimer that possesses a PPI core up to generation 4, and then continues the branching using PAMAM units. The advantage of this type of synthesis is that it becomes much faster to produce a PAMAM-type surfaced dendrimer at high generation. Similarly, the use of a different

branching monomer can take place in the interior of the dendrimer (similar to a dendrigraft polymer), making for a more dense structure as demonstrated by Majoral *et al*.[166]

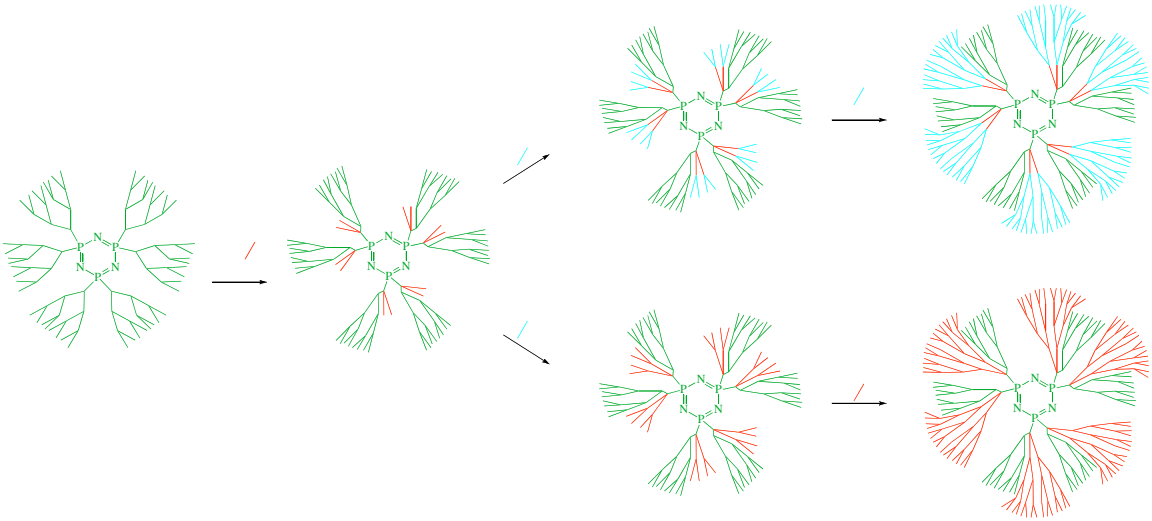

Figure 21. *Stepwise build up of an internal dendrimer.*[166]

Their formation of dendrimers under thermodynamic control has been demonstrated by Stoddart *et al*. using a rotaxane assembly of Fréchet-type benzyl ether dendrons.[167]

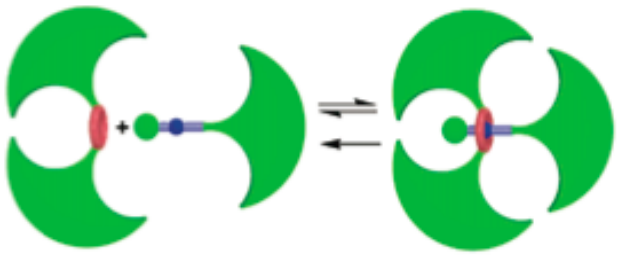

Figure 22. *Rotaxane-type dendrimers developed by Stoddart et al.*[167]

In 1999, Zimmerman *et al*. showed that an alkene surface of a poly(benzyl ether) dendrimer could be cross-linked using a ring-closing metathesis and the core itself could be removed (**Figure 23**)![168] The core consisted of an aromatic ester that could be removed under basic conditions once the surface had been cross-linked.

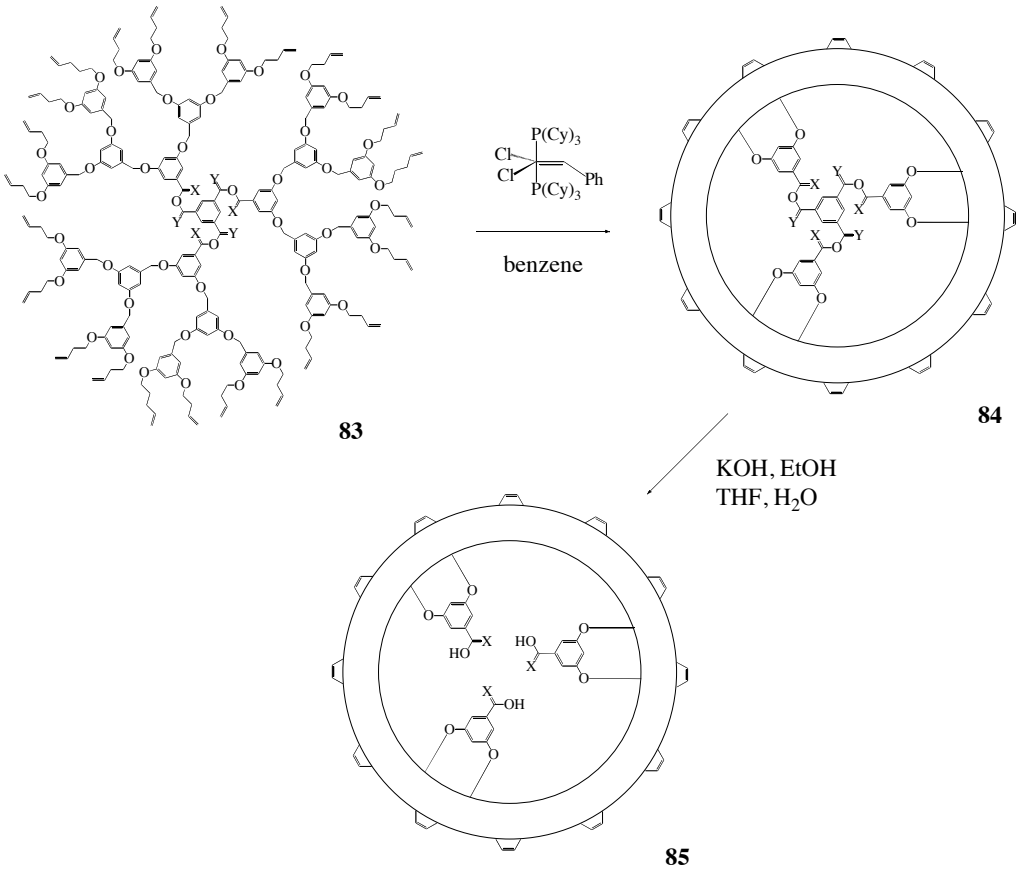

Figure 23. *Synthesis of a 'cored' dendrimer (X = H, H; Y = O or X = O; Y = H, H).*[168]

The Use of 'Click' Chemistry in Dendrimer Synthesis

In recent years a new type of reaction has emerged that has greatly changed small molecule synthesis as well as the surface modification of larger macromolecules. Known as an 'azide-alkyne Huisgen cycloaddition', this reaction uses an azide and an alkyne to form a 1,2,3-triazole using a copper (I) catalyst. This reaction can occur in a wide range of solvents and is generally very high yielding, giving no by-products; it's this effectiveness and simplicity that has led to it being known as a '*Click'* reaction.[169,170]

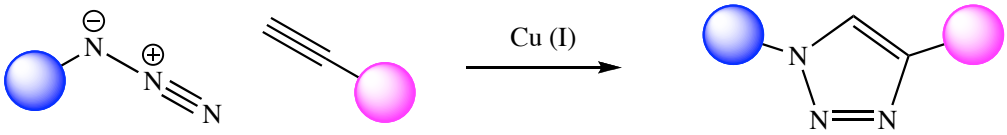

Figure 24. *The 'Click' reaction.*

In 2004, Fréchet and Hawker combined click chemistry with the convergent synthesis to make a series of dendrons containing multiple triazoles.[171] These were then coupled to a series of polyacetylene cores giving dendrimers of sizes up to 4th generation. The following year Hawker synthesised poly(benzyl ether) dendrimers that contained acetylene groups on its outer surface, allowing to various groups to be attached.[172]

Perhaps the most interesting work on dendrimers using a Click chemistry approach has been carried out by Jae Wook Lee *et al*. In 2005 they demonstrated how two dendrons, in this case poly(benzyl ethers), could be joined together[173] and then in 2007 they showed that PAMAM wedges could be joined using a similar strategy.[174] Not only does this mean that dendrimers can be synthesised much faster, it also opens the door to having inequivalent wedges. Lee's work with PAMAM dendrimers showed that a 4th generation wedge could be coupled to a 1st generation wedge, making size-differentiated unsymmetrical dendrimers (**86**). This work was continued to incorporate different types of branching such as half PAMAM half poly(benzyl ether) (**87**)[175,176] and has inspired others to make similarly complex dendrimers.[177]

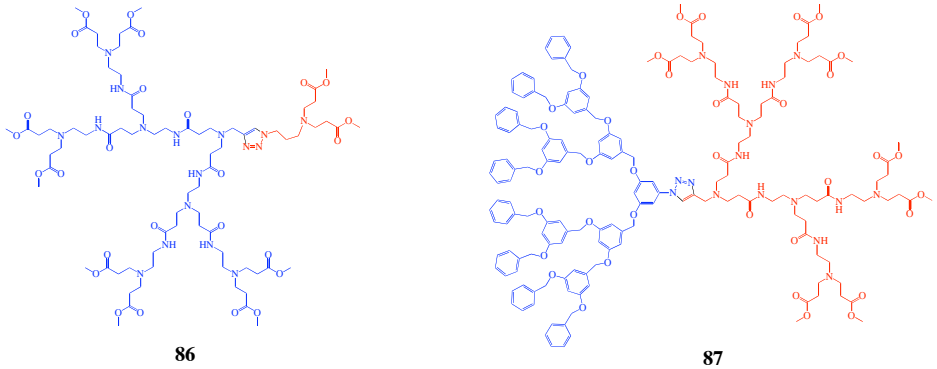

86 **87**

Figure 25. *Diblock codendrimers of PAMAM-PAMAM*[174] *(left) and PAMAM-poly(benzyl ether)*[175,176] *(right) dendrimers.*

1.3.5 Internal Structure of a Dendrimer

Even though dendrimers are synthesised in a step-wise fashion, the arms (dendrons) are polymers and as such can form a wide range of confirmations, making it very hard to determine their relative location experimentally. For this reason, most studies utilize computational simulations, and then compare them to any experimental results available.

When displayed in two-dimensions, a dendrimer appears to be circular with an ever increasing surface density. Computer simulations reveal that they adopt a three-dimensional structure depending on the dendrimer generation. In 1989, Tomalia and Goddard *et al*.[178] modelled the shape of PAMAM dendrimers based on the aspect ratio of the largest to smallest principle moment (I_z/I_x, **Figure 26**). They showed that at low generations (≤4) the shape is that of an ellipsoid, whilst at high generations (≥ 5) they appear as being spherical. This is perhaps to be expected, as the dendrimer surface must reach a point whereby steric hindrance forces the surface to adopt a more three-dimensional (and thus spherical) shape, something that is backed up by molecular dynamics (MD) simulations (**Figure 27**).

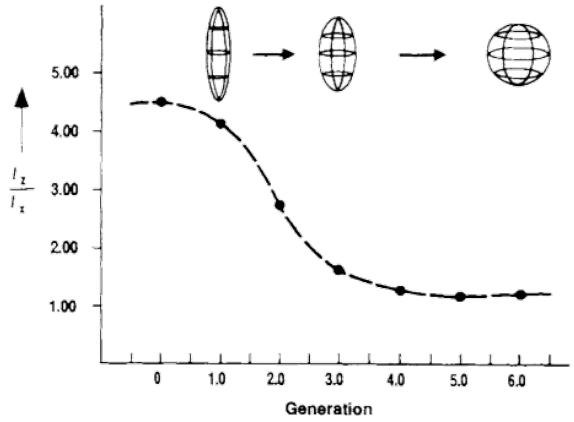

Figure 26. *Comparison of change in PAMAM morphology (aspect ratios, I_z/I_x) as a function of generation.*[178]

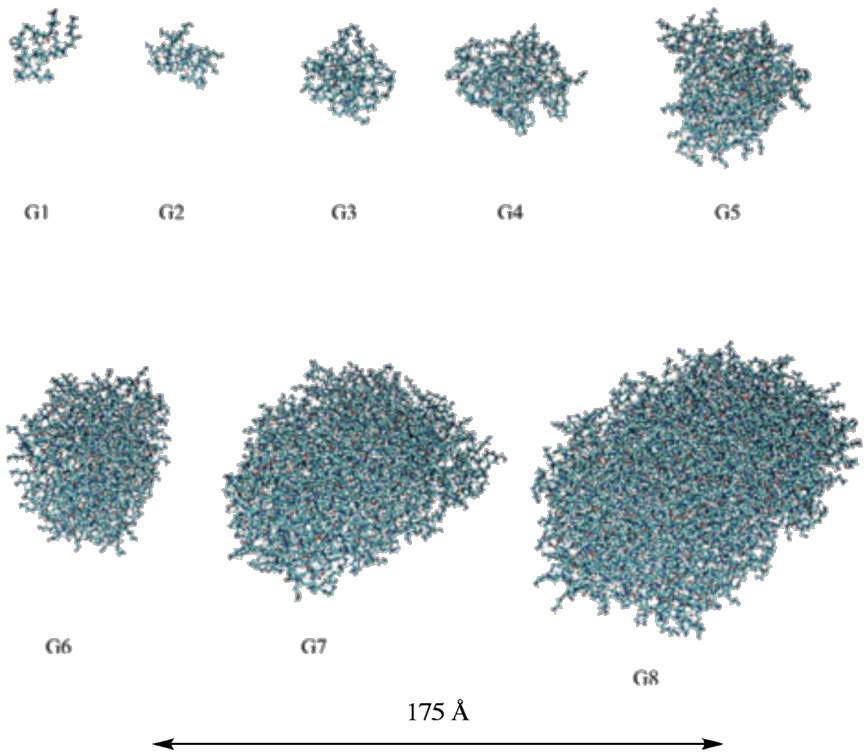

Figure 27*. Snapshots of PAMAM dendrimers, generations 1 to 8, after long MD simulations.*[179] *Blue atoms are nitrogen, red atoms are oxygen and grey atoms are carbon.*

The idea that branched polymers possess internal cavities capable of encapsulation of small molecules was reported in 1982,[180] but it was not until 1989 that experimental investigations were performed to confirm this.[100,178] Measurement of spin-lattice relaxation times (T_1), an NMR technique used to monitor the mobility of nuclei, for a series of half-generation PAMAM dendrimers (ammonia core) when mixed with guest molecules (2,4-dichlorophenoxyacetic acid and acetylsalicylic acid) support the presence of channels and internal cavities predicted by modelling.[178] It should be noted that not all dendrimer architectures possess these cavities; one case being polyethers that have high branching (3 branches per repeat) and short repeat units.[100]

In a joint publication in 1990, Tomalia, Naylor and Goddard described how a quantitative comparison of the internal surface area and solvent-filled volume could be made using the concept of *solvent-accessible surface* (SAS).[100,181] The SAS is determined by 'rolling' a hypothetical sphere of radius *p* around the van de Waals

surface of the molecule, where *p* represents the effective radius of the solvent (e.g. *p* = 1.4 Å for H_2O). This simulation data is then plotted as the square root of the SAS versus *p*, which should result in a linear plot if the molecule is spherical.

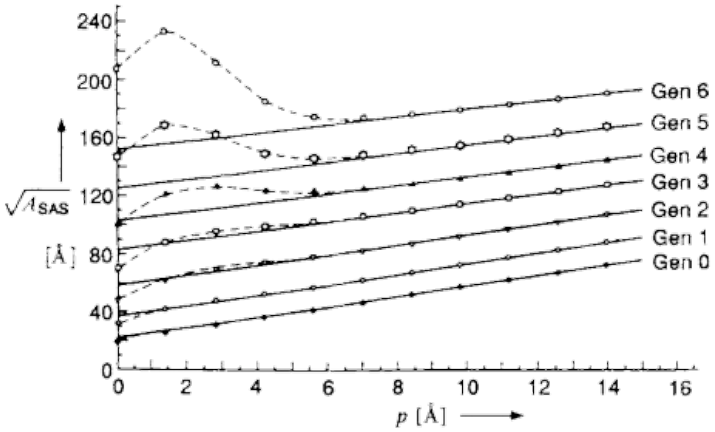

Figure 28. *Variation of the SAS as a function of probe radius for a series of PAMAM dendrimer generations. Solid lines represent linear regression fits (p ≥ 7.0 Å), dashed lines connect the calculated values.*[100]

The results (**Figure 28**) show a linear trend at values of *p* greater than 7 Å, suggesting that the molecules are essentially spherical.[100] Deviations from the linear plot at low probe radius can be explained by the probe 'rolling' into the internal cavities, something that occurs more at higher generation suggesting an increase in internal void space. The fraction of internal over the external surface was calculated at only 1.4% at generation 3. This rises to 29% for generation 4, 69% for generation 5, and 124% for generation 6, suggesting that for the 6th generation PAMAM dendrimer (ammonia core) the internal cavities have a higher surface area than its outer surface! As a point for comparison, polyether dendrimers had fractions of 20% for both 3rd and 4th generations.

A comparison by Tomalia between PAMAM dendrimers and Denkewalter's polylysine cascades demonstrates the importance of branch symmetry for the formation of internal cavities.[182] The Denkewalter cascades possess unsymmetrical branching owing to the L-lysine units that give rise to a dense sphere, something that was not predicted by Maciejewski's calculations[180] when using monomers of the form X-R-Y_2. The hydrodynamic volumes of these cascade were found to have a linear relationship with

their molecular weight suggesting a lack of hollowness, whereas the PAMAMs varied exponentially for both ester and amine surfaces.[102,182]

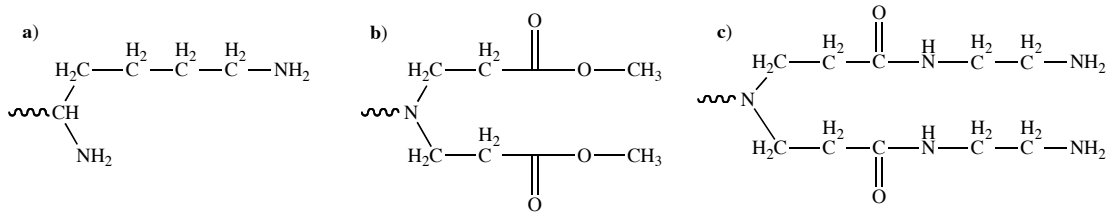

Figure 29. *Dendrimer terminal branches used in Tomalia's calculations; a) lysine, b) PAMAM ester and c) PAMAM amine.*

When looking at calculated densities for these two classes, it was found that that of the cascades should be constant with increasing generation, whereas for the PAMAM series it should decrease up to 5th generation then increase rapidly thereafter.[182] This would suggest the formation of a dense-packed surface, at point where the dendritic arms are unable to extend. Further calculations into the densities revealed that a PAMAM dendrimer with an amine surface induces more internal cavities than for an ester surface, a situation that arises due to the increased steric bulk of the larger amine surface branch. Tomalia also showed that for both classes surface area increased linearly with an increasing number of terminal groups, further suggesting a three-dimensional structure. It therefore follows that since the maximum radial dimensions of the PAMAM are increasing linearly with generation, and the number of surface groups is increasing exponentially, a so called 'starburst limit' should be reached.[182] This is indeed the case for most dendrimers, a limit is reached whereby no further growth can occur owing to surface crowding;[99] for PAMAM dendrimers this limit occurs at generation 10.[99]

The diameters of various dendrimers are shown in **Table 3** and demonstrate how monomer units and the nature of the core molecule affect the size. **Table 4** shows how the calculated hydrodynamic radius for a PAMAM dendrimer with an ammonia core (3 core branches) varies with solvent (published in 1985).[77] It is not surprising to see that dendrimers in methanol and water give very similar radii as they are both very polar solvents that will disrupt any intramolecular H-bonding taking place causing the dendritic structure to swell, but the fact that when HCl is present the radius is lower is

strange. In this case we would expect the radius to be higher than with the other two solvents as the terminal amines would become protonated and seek to move apart, effectively stretching the branches out. Studies carried out since this publication contradict these initial findings, showing that the radius of gyration does indeed increase with lowered pH (**Table 5**).[183]

Table 4. *Calculated hydrodynamic radii for PAMAM dendrimers with an NH_3 core.*[77]

Generation	Solvent	Hydrodynamic radii (Å)
1.0	H_2O	5.7
1.0	HCl	5.1
1.0	MeOH	5.7
1.5	MeOH	6.6
2.0	H_2O	8.6
2.0	MeOH	8.5
2.5	MeOH	9.8
3.0	MeOH	12.2
3.5	MeOH	12.9
4.0	H_2O	16.7
4.0	HCl	14.3
4.0	MeOH	16.6
4.5	MeOH	16.8
5.0	MeOH	24.6

Table 5. *Radius of gyration R_g (Å) for EDA cored PAMAM dendrimers at various solvent conditions.*[183]

					experimental		
					SAXS		SANS
generation	no solvent	high pH	neutral pH	low pH	ref [184]	ref [185]	ref [186]
4	14.50 ± 0.28	16.78 ± 0.15	17.01 ± 0.10	19.01 ± 0.08	17.1	18.60	–
5	18.34 ± 0.37	20.67 ± 0.09	22.19 ± 0.14	24.76 ± 0.14	24.1	23.07	22.1
6	22.40 ± 0.42	26.76 ± 0.11	27.28 ± 0.39	30.89 ± 0.39	26.3	27.50	–

With the knowledge gained of the overall dendritic structure, perhaps the most intriguing structural information lies with the position of the terminal end groups. This is important as dendrimer modifications generally occur at the surface. Back-to-back publications in 1992 by Tomalia[187] and Meltzer[187,188] (and later by others[189-194]) showed how spin-lattice relaxation times could be used to describe a dendrimer's structure. They demonstrated that nuclei (^{1}H and ^{13}C) have a lower mobility at the periphery of the dendrimer when compared with those near the core. They also showed that the terminal groups are not densely packed at the surface (for a 10th generation PAMAM), rather they are folded back into the interior of the molecule. Similar conclusions have also been drawn from neutron scattering experiments.[195,196] This idea of back-folding is supported by computational studies, such as those from Lescanec and Muthukumar,[197] Naylor and Goddard,[100,179,198] and many others.[199-202] These computational studies were best visualized by Goddard *et al*.[179,183] who showed how the terminal group locations varied with pH (**Table 6**). At low pH, when the dendrimer is at its highest radius, the number of terminal groups located on the surface is at its largest, something we would expect as electrostatic interactions push the terminal groups apart. **Figure 30** shows that the terminal nitrogen atoms (magenta spheres) penetrate the interior of the dendrimer, reaching as far as the core.

Table 6. *Number of primary nitrogen atoms located at the surface of the molecules under various solvent conditions.*[179]

Generation	High pH	Neutral pH	Low pH
4	37 (57%)	41 (64%)	45 (70%)
5	48 (37%)	75 (59%)	83 (65%)
6	115 (44%)	152 (59%)	143 (55%)

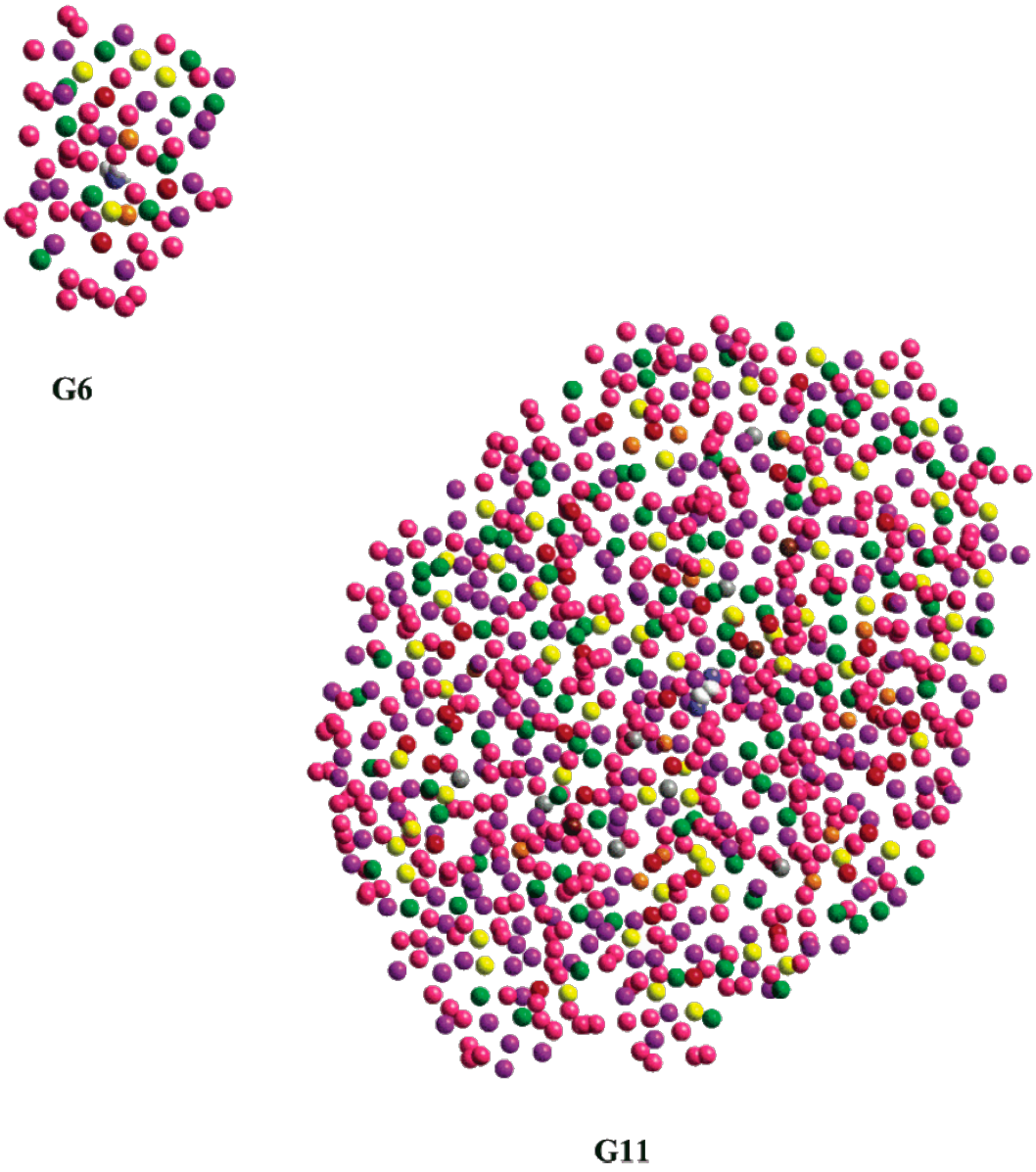

Figure 30. *Instantaneous snapshots showing spatial arrangements of the primary and tertiary nitrogen atoms for 6th and 11th generation PAMAM dendrimers in a slice of thickness 8 Å passing through the centre of mass. White spheres represent the centre of the molecule. For G6, the primary nitrogen atoms are magenta, the tertiary nitrogen atoms of G5 are dark grey, and the tertiary nitrogen atoms of G4 are green. For G11, primary nitrogen atoms are magenta, the tertiary nitrogen atoms of G10 are dark grey, the tertiary nitrogen atoms of G9 are green, the tertiary nitrogen atoms of G8 are yellow, and the tertiary nitrogen atoms of G7 are red.*[179]

1.3.6 Further Subsections of the Dendritic State

With the acceptance of dendritic architectures as one of the main classes of polymer (alongside linear, branched and cross-linked structures) a number of sub-categories have emerged, namely random hyperbranched, dendrigrafts and dendrimers. It is also possible to visualize dendronized polymers (linear polymers with attached dendrons) as being a sub-category of both dendrigraft polymers and dendrimers.

Hyperbranched Polymers

As with most polymers, hyperbranched polymers are made in a one-pot synthesis, i.e. all the reactants are put in together. However, unlike with normal polymers, the monomer units consist of two functionalities and are of the type AB_x, where A will react with B and x is ≥ 2, which means that branching will occur in a statistical fashion. Though Flory first described the concept of this type of polymer in 1952,[92] it wasn't until the late 1980s that interest picked up again, first by Odian and Tomalia,[203] then by Kim and Webster[204,205] (who coined the term hyperbranched polymer).[99]

Examples of this polymer type include the hyperbranched azo polymers of Wang *et al*.[206] and Xie *et al*.,[207] Kim and Websters hyperbranched polyphenylene,[205] Mathias and Carothers' poly(siloxysilanes) (**89**)[208] and Fréchet and Hawker's hyperbranched polyethers.[125,209-211]

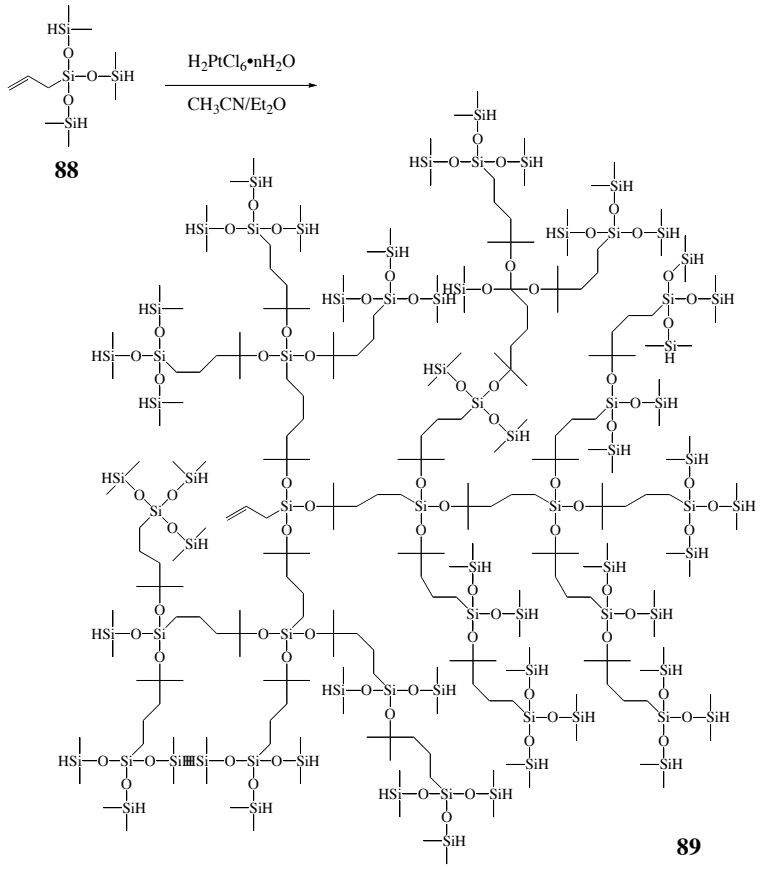

Figure 31. *Hyperbranched poly(siloxysilanes) prepared by Mathias and Carothers.*[208]

Dendrigraft Polymers

Dendrigraft polymers, also known as arborescent polymers, combine features of dendrimers and hyperbranched polymers with linear polymers.[134] Similar to dendrimers, they are grown in a step-wise fashion to give generations, but the monomer unit is of polymeric proportions, meaning that a high molecular weight can be achieved very quickly.[136]

Though the concept of dendrigraft polymers can be traced back to 1991, with the publications of Tomalia[131] and Gauthier,[132] recent reviews by Gauthier (2004[134] and 2007[133]) show just how far this branch of dendritic architectures has come.

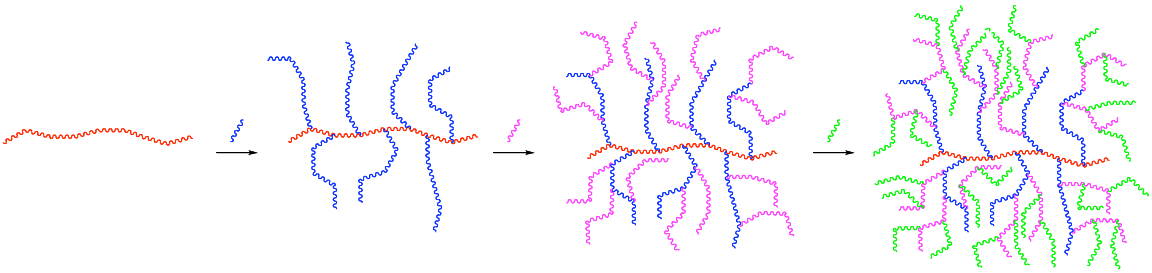

Figure 32. *Schematic representation of the formation of a dendrigraft polymer.*

Dendronized Polymers

Two years after publishing his divergent synthesis of the PAMAM dendrimers in 1985, Tomalia and Kirchhoff filed a patent concerning rod-shaped dendrimers.[212,213] This type of structure consists of a linear backbone with dendritic side chains, making it a sub-class of comb-polymers. Depending on the density and size of the dendrons, the dendronized polymers can be viewed as being rod-like cylinders, which have some interesting properties.[136,137]

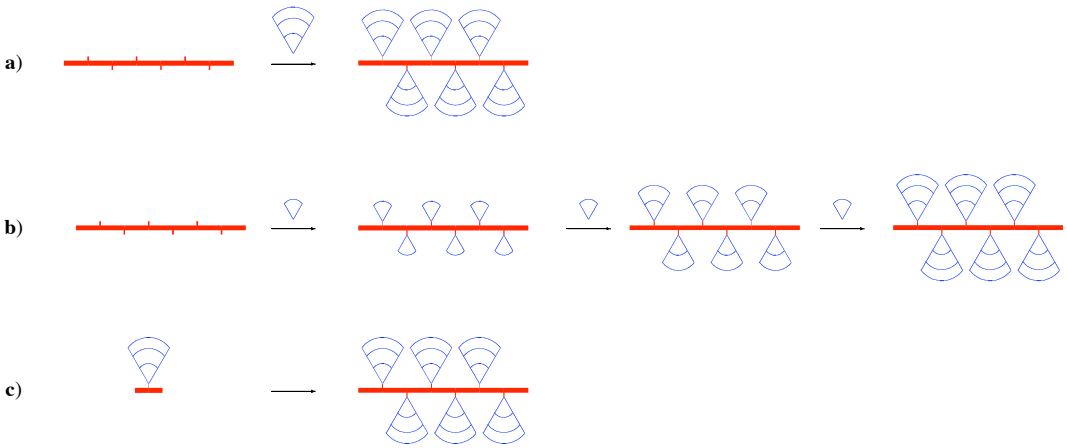

Figure 33. *Synthetic routes to dendronized polymers. a) Graft-to, b) graft-from, c) macromonomer approach.*

The synthesis of this class of structure can be achieved in one of three ways (**Figure 33**). The first two techniques require a functionalised linear polymer onto which dendrons are then coupled using either a divergent (*graft-from*) or convergent (*graft-to*)

synthesis.[214] The graft-on approach allows for limited dendron defects but can suffer from low yields because of steric hindrance, whereas the graft-from approach has a much easier purification (precipitation) and doesn't suffer from steric problems as a result of the small molecules involved.[215] The third synthetic route is known as the *macromonomer* approach, whereby dendrons are synthesised bearing a polymerisable focal point.[136,214] This route has the advantage of giving a polymer that contains a dendron of uniform size on each monomer unit, but suffers steric issues if the dendrons are of too high a generation.[136]

Examples of these structures include Tomalia's poly(ethylene imine) chain with PAMAM dendrons (**90**),[213] Fréchet's polymeric poly(benzyl ethers) using click chemistry (**92**),[80] Cuadrado's polysiloxanes (**91**),[216] Schlüter's polymeric poly(benzyl ethers) using S_N2 substitution[217-219] and Oikawa's polymerisation of dendritic phenylacetylene (**93**)[220] amongst a great many others.

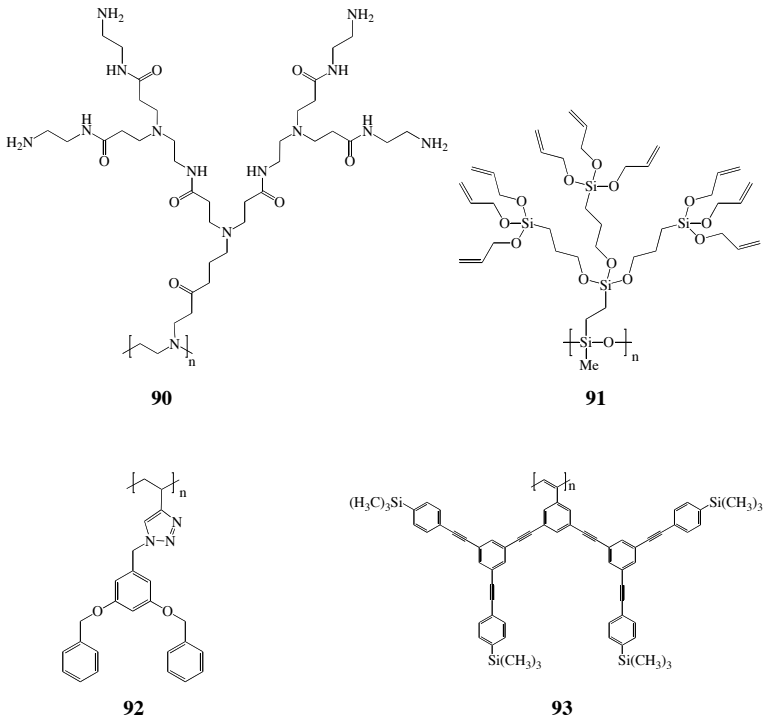

Figure 34. *Dendronized polymers based on (clockwise from top left) PAMAM, siloxane, poly(phenylacetylene) and poly(benzyl ether) dendrons.*[215]

Megamers

Since the mid-1990's, the idea of using a dendrimer as a monomer unit has steadily led to a growing number of publications. [127,128,221-224] These new polymer architectures, known as *megamers*, are formed by the combination of two or more dendrimers, which can be through either *supramacromolecular* or *supermacromolecular* topologies.[99] For example, a PAMAM dendrimer can be made with a carboxylic acid surface so, when this is combined with a PAMAM dendrimer that has an amine surface, a megamer will be formed.

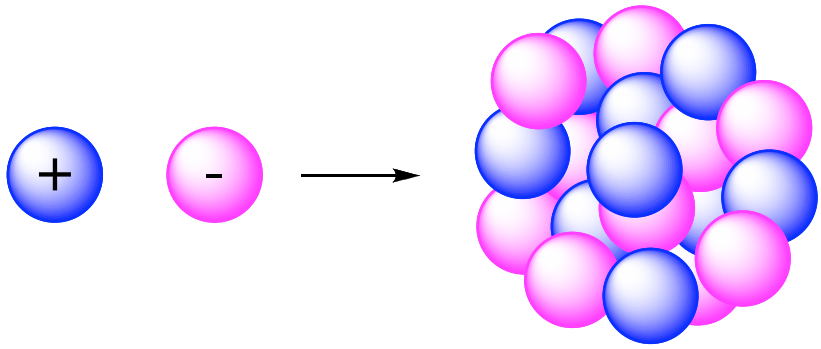

Figure 35. *Schematic representation of the formation of a megamer by electrostatic interactions (balls represent charged dendrimers).*

1.3.7 Surface Modifications

Dendrimers lend themselves to functionalisation very well thanks to their highly branched monodisperse structures that are of the nanometre scale. It is easy to envisage this functionalisation occurring at the dendrimer surface, but it is equally possible, if a little rarer, to do so in the interior. Examples of interior modifications include McGraths chiral branches that contain acetal groups,[225] Fréchets porphyrin cores,[226] and Majorals dendritic growth from inside the dendrimer (**Figure 21**).[166] However, the most common modifications take place at the dendrimer surface where a high number of groups can be reacted. Owing to the equivalent nature of these end groups, only reagents that react selectively and with high reactivity can be used. That said, most

organic reactions can be used, depending on the nature of the surface and the solubility of the dendrimer. Some examples of reactions that have been established for coupling functional groups to polyamino dendrimers are shown in **Figure 36**.

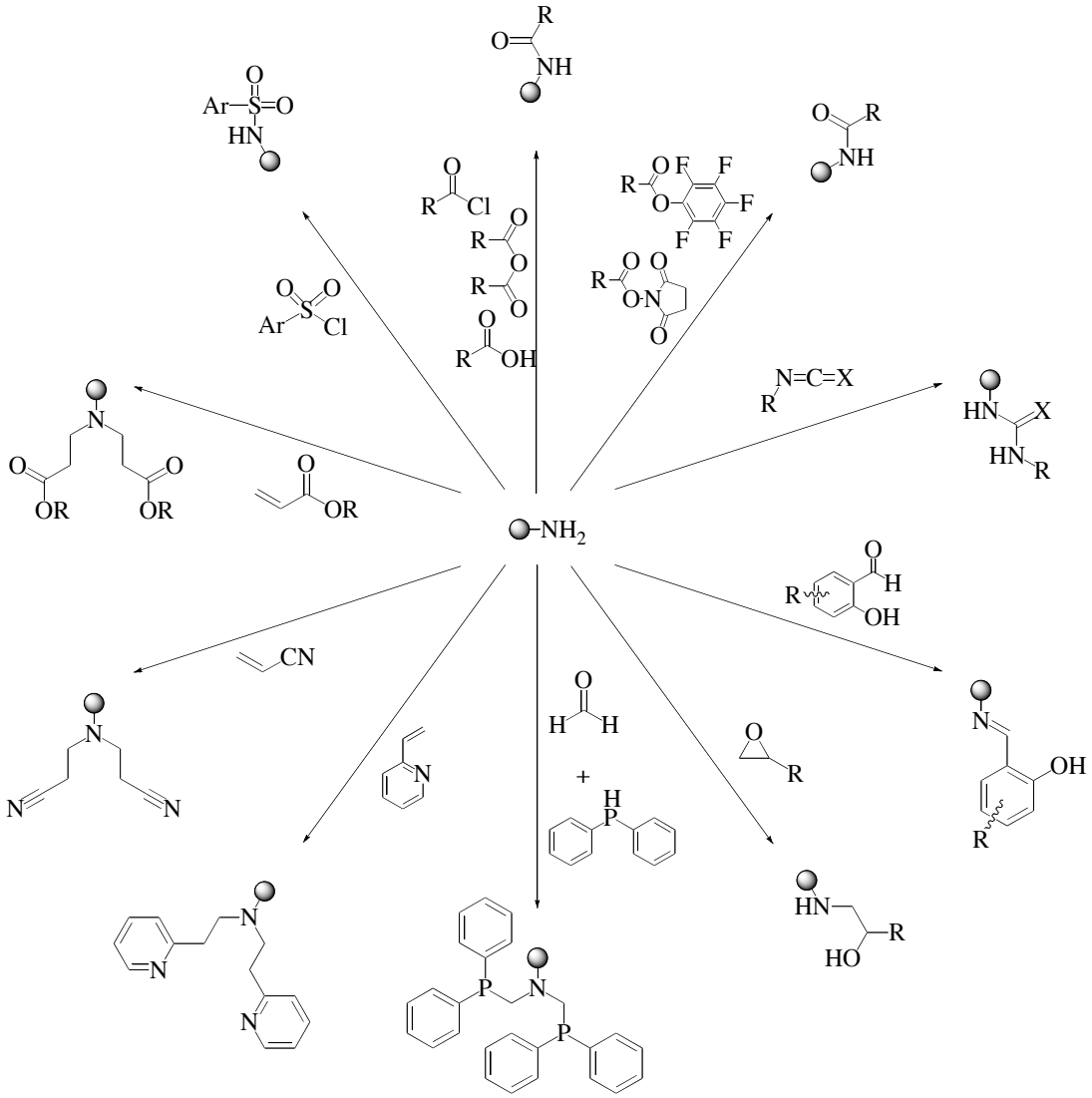

Figure 36. *Reactions coupling functional groups with polyamino dendrimers.*[227]

By using reagents with low boiling points, the dendrimers can be easily purified through distillation, an approach that is used in the synthesis of polyamines and polynitriles.[90,114,142,228] The same strategy has also been used in the functionalisation and construction of polyester[229] and PAMAM dendrimers using acrylic esters.[77,104] Other routes have been established, such as functionalisation with vinyl pyridine to give polypyridines,[230] and the conversion of activated carboxylic acid derivatives, such as carboxylic acid chlorides[231-233] and acid anhydrides,[234] to their respective polyamides.

The use of 'click' chemistry has also been applied to dendrimers in recent years.[80,173,175,177,235] The types of groups that are attached depend entirely on the desired dendrimer properties required; it is for this reason that much work has gone into photoactive and drug-carrying dendrimers (discussed in **Sections 1.3.8** and **1.3.9**).

It is also possible to attach more than one type of group onto the dendrimer's surface; depending on the type of dendrimer used this coverage could be randomly distributed (divergent approach) or densely packed (convergent approach) on the surface. Using the right reagents it is even possible to get the different groups on the same terminal branch (**Figure 37**), which leads to interesting properties such as enzyme mimicry.[227,236,237]

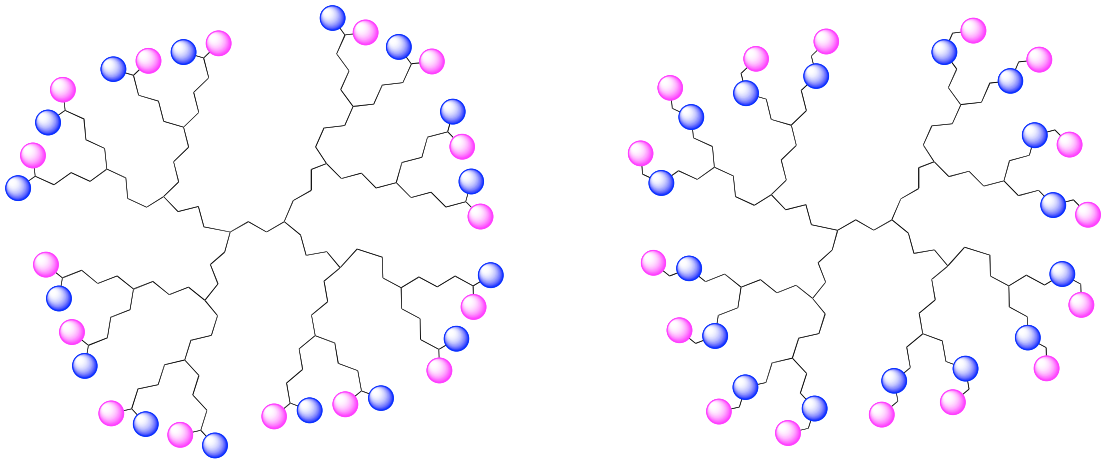

***Figure 37**. Bifunctionalised dendrimers. Coloured spheres represent different attached groups.*

Fréchet *et al*. has demonstrated the linkage of a benzylic ether dendron and a polynitrile dendron to give macromolecules with large dipole moments,[238] whereas the coupling of lipophilic benzyl ether dendrons and hydrophilic carboxylate-functionalised dendrons leads to globular amphiphilic dendrimers (**Figure 38**).[239]

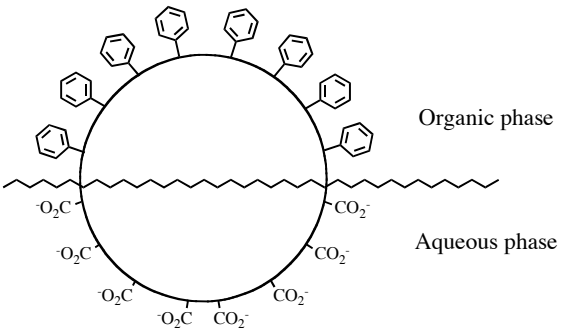

Figure 38. *Globular amphiphilic dendrimers developed by Fréchet et al. Sphere represents a poly(benzyl ether) dendrimer.* [239]

1.3.8 Properties and Uses

Given the wide range of dendritic architectures available and the number of surface modifications possible it is not surprising that a dendrimer's properties can be fine-tuned for a number of uses. This might be to harvest light or to encapsulate small molecules for example. The potential applications of dendrimers are wide and varied. Some of these are described below.

Photoactive Dendrimers

The convergent synthesis of dendrons based on aryl acetylene units was described by Moore *et al*.,[240,241] who found that when a perylene unit is used as the focal point the fluorescence intensity of the emitted light increases with the number of generations of the dendron.[227,242] This process whereby the dendrimer is able to 'collect' light energy is referred to as *light harvesting*. The rate of this energy transfer can be increased by further modification and fine-tuning of the dendron; in this case, additional aryl acetylene units were added into the initial branch (**Figure 39**).[243] This aided the energy gradient from the peripheral groups to the focal point, effectively acting as an energy funnel. There is also interest from many groups, such as Vögtle,[244,245] Aida,[246] and Fréchet,[247] in the fluorescence of metal centres used in the formation of dendrimers, be they bound in a porphyrin core,[138,226,246-248] or as the focal point itself[244,245,249,250] i.e. the dendrons are bound to the metal *via* dative bonds from a bipyridine unit.

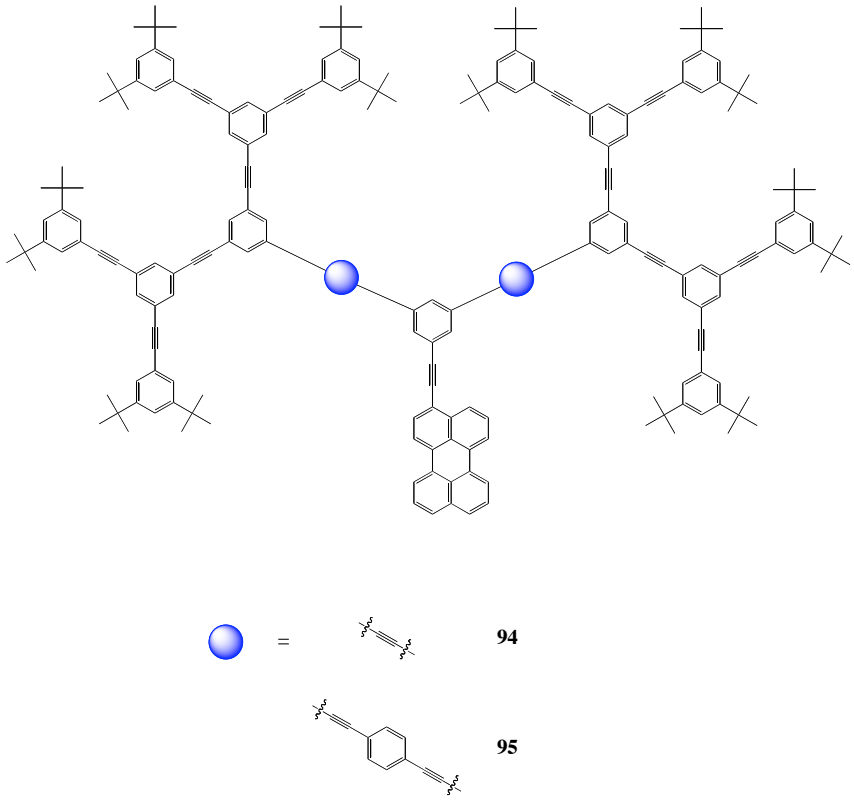

Figure 39. *Fluorescent dendrimers developed by Moore et al.*[242,243]

There is also considerable current interest in the synthesis of photo-responsive dendrimers,[251,252] since the manipulation of dendritic size and shape promises a wide range of potential functions[253] such as drug delivery.[227] One of the most efficient and reversible compounds that give photo-isomerisation is that of azobenzene,[254] and much research has been performed looking into its uses in photo-switchable devices.[255]

These photo-responsive units can be used as the dendrimer core,[251,252] in the branching framework,[254] and on the surface.[256,257] When used within the dendritic structure, the photo-responsive units can give large changes in hydrodynamic volume, though the percentage change varies dramatically with dendrimer type, dendrimer size and its location within the structure[253,255] i.e. by placing the azobenzene unit in the core, a small conformational change will result in a large change in the overall structure.

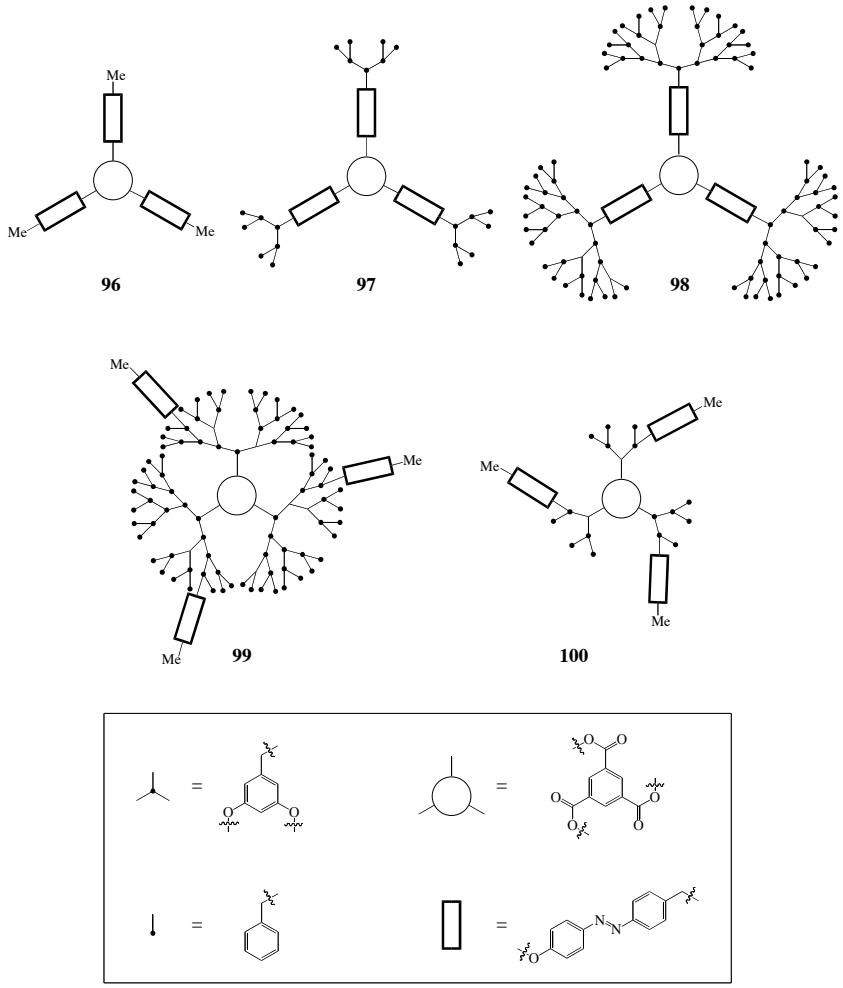

Figure 40. *Photo-responsive dendrimers prepared by McGrath et al.*[258]

McGrath *et al*. have shown that benzyl ether dendrimers can be synthesised containing azobenzene units attached to the core and on the surface, and that they are reversibly photo-responsive (**Figure 40**).[256,258-260] They also show that the change in hydrodynamic volume decreases, upon irradiation with 350 nm light, as dendrimer generation increases. More recent work carried out by Ghosh *et al*. has looked at synthesising PAMAM dendrimers with an azobenzene core and demonstrated photo-switching behaviour up to generation 2.5.[251,261,262]

By attaching fluorescent groups, such as fluorescein and dansyl, onto the surfaces of dendrimers it is possible to use them as sensors for small and large molecules, acids and metal ions,[263-267] as well as allowing dendrimer uptake through membranes to be studied.[268,269]

Guest Encapsulation

As described in **Section 1.3.5**, dendrimers contain internal cavities and voids, the sizes of which depend on the branching architecture. For example, PAMAM dendrimers have larger cavities than PPI dendrimers.[100] Fréchet *et al*.[239] demonstrated that the solubility of small molecules could be aided by the presence of a dendrimer; in this case, a water soluble carboxylate-terminated poly(benzyl ether) dendrimer increased the solubility of 2,3,6,7-tetranitrofluorenone (258 fold), pyrene (120 fold), anthrancene (58 fold) and 1,4-diaminoanthraquinone (56 fold) in water. PAMAM dendrimers have also been shown to act as host molecules. Tomalia *et al*. has demonstrated their encapsulation of charged radicals[270] as well as acetylsalicylic acid and 2,4-dichlorophenoxyacetic acid, the presence of the later being proved using spin-lattice relaxation times.[178]

This ability to 'capture' molecules led Meijer and co-workers to develop a *dendritic box*.[271] The cavities of a 4th generation PPI, whose 64 terminal amines had been protected with Boc-L-phenylalanine groups, were filled with various guests of differing sizes (**Figure 41**) to give dialysis stable complexes.[231,272,273] Upon removal of the terminal Boc groups, the small molecules were found to dissociate from the dendrimer whereas the larger guests remained trapped. When the amino acid groups were removed the remainder of the guests dissociated. This has led to the development of many *slow release* mechanisms for drugs[274,275] and dyes, some based on pH[276] and some using the photo-responsive azobenzene group.[256,277]

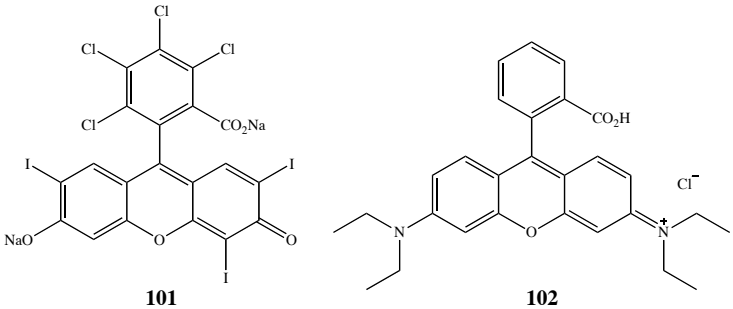

101 **102**

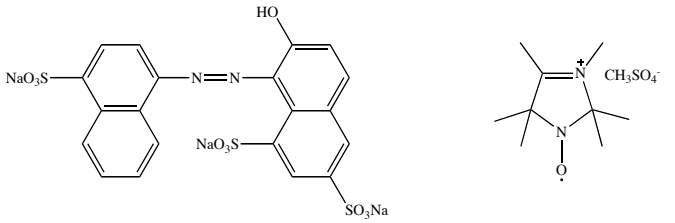

103 **104**

Figure 41. *Guest molecules that have been bound inside Meijers dendritic boxes.*[231,272,273]

Supramolecular Assemblies

The use of non-covalent bonds in dendrimer synthesis has already been touched on with the use of metal centres by Balzani[159,160] and Achar,[158] and with the use of rotaxanes by Stoddart (**Figure 22**).[167] Aside from the encapsulation type interactions described above, supramolecular interactions can lead to the formation of dendrimers, as well as some interesting surfaces.[278]

Reinhoudt *et al*. have demonstrated the formation of dendrimers by applying methods of palladium coordination chemistry and hydrogen bonds.[279,280] Similarly, Zimmerman *et al*. have demonstrated the formation of a hexameric aggregate consisting of six equivalent dendrons with focal hydrogen bonding sites (**Figure 42**).[281-283] Depending on the sterics of the dendron, linear or disk-like structures could be achieved. They also found that by changing the position on the aromatic functional groups, the number of dendrons per aggregate could be reduced to three.[281] Other assemblies based on gallic acid have been prepared[284] and have been shown to form cylindrical or spherical aggregates which can then coordinate with each other to form even larger structures, the

former forming hexagonal columnar phases whilst the latter forms cubic superstructures. Other liquid-crystalline dendrimers have also been observed.[285,286]

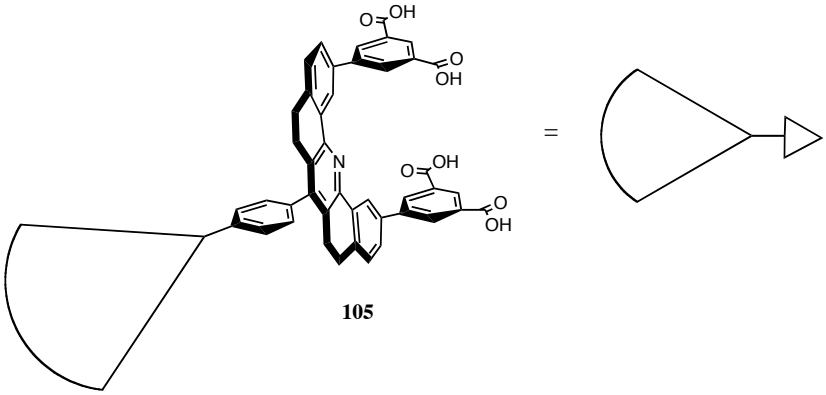

105

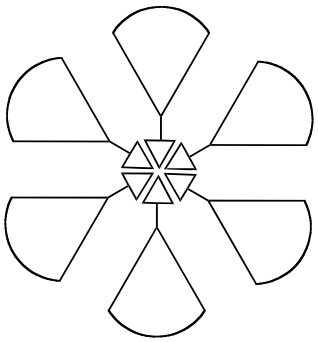

106

Figure 42. *Supramolecular aggregates by Zimmerman et al. The wedge represents a poly(benzyl ether) dendron.*

Other interesting assemblies include Gibson's[72,287] and Smith's pseudorotaxanes,[278,288,289] both of which make use of crown ethers, and Fréchet's 'bow-ties' (**Figure 43**).[290] Similarly, groups can be non-covalently bound to the surface of the dendrimer, such as Kims's cucurbiturils, to give swollen structures.[291,292]

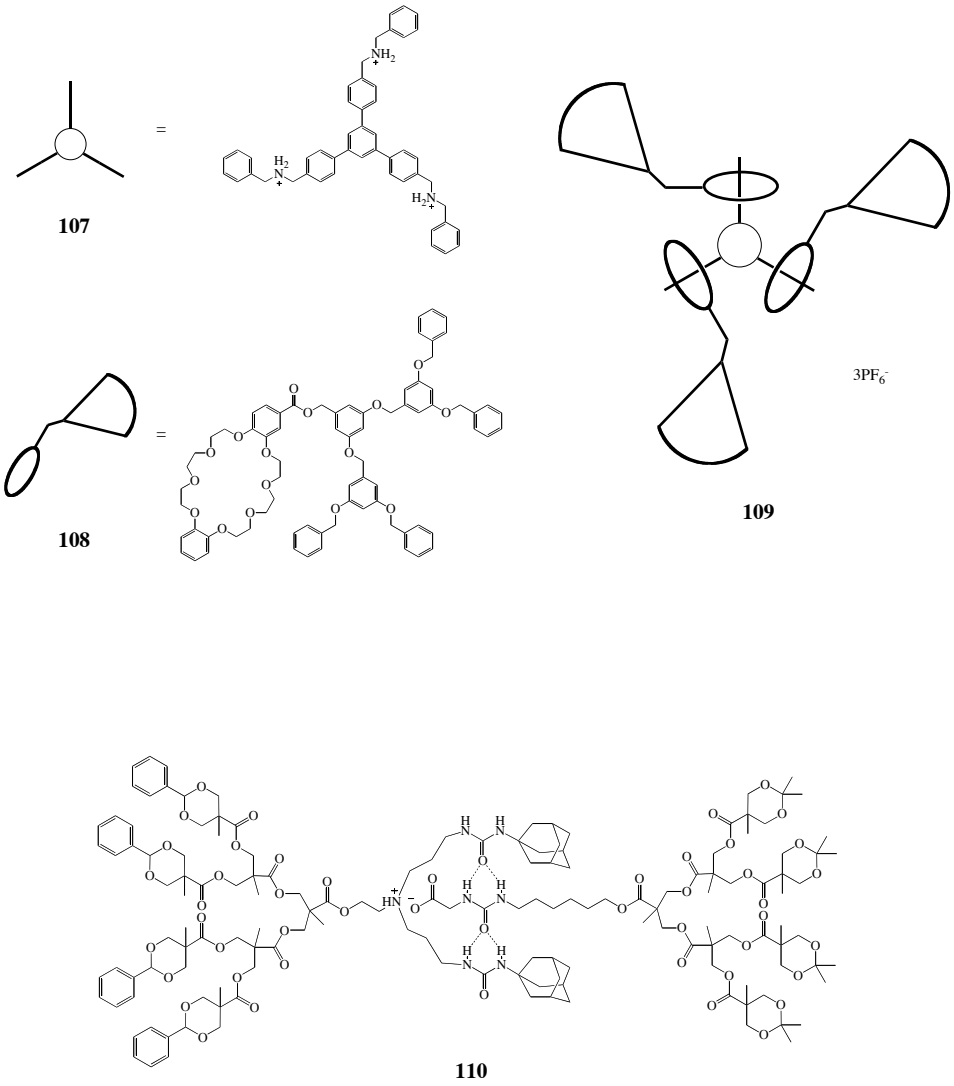

***Figure 43**. Pseudorotaxane by Gibson et al.[72] (top) and 'bow-tie' by Fréchet et al.[290] (bottom).*

Other Uses

Numerous other modifications and architectures are possible. Chirality can be introduced anywhere in the structure to allow for the binding of specific guests, or to give interesting chromatographic properties.[227,293,294] Attachment of chiral units to the surface can also lead to the dendrimer having catalytic effects as well as acting as an enzyme mimics.[146,227,295-297]

Units such as ferrocene can be attached to the surface in order to study electrochemical sensing,[233,298] or drugs can be used, turning the dendrimer into a drug delivery system

(in this case the drug molecule is covalently bound to the surface unlike those of the encapsulated type). [275,299-302] Thermoresponsive gels can also be formed through supramolecular interactions,[303-305] and some examples of photo-responsive gels have been reported such as those from Chen *et al*. shown below.[306]

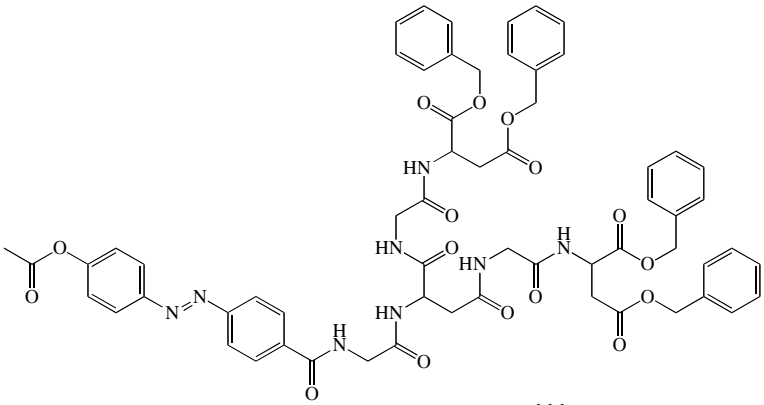

111

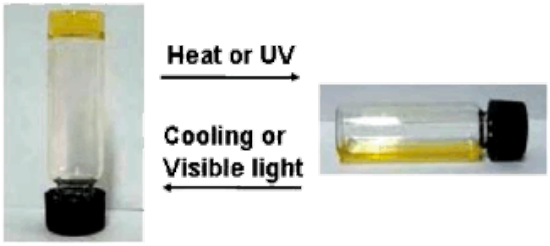

Figure 44. *Structure and behaviour of photo-responsive gel made by Chen and co-workers.*[306]

1.3.9 Dendrimers as Biological Mimics

With the ability to design dendrimers with specific properties, it is not surprising that there is considerable interest in their use in biological systems. PAMAM dendrimers, for example, possess sizes comparable with those of various proteins and bioassemblies, such as those shown in **Figure 45**. With an ammonia core, PAMAM dendrimers of generations 3, 4 and 5 closely resemble the size and shape of insulin (~30 Å), cytochrome C (~40 Å) and haemoglobin (~55 Å) respectively.[13,307] Similarly, larger generations share sizes with histone clusters, explaining why these large dendrimers form such strong complexes with DNA making them ideal 'histone mimics'.[308-310] The biomimetic properties of dendrimers[307,310-312] (thanks to their step-wise synthesis and

branching) have led to them being referred to as 'artificial proteins' and offer a variety of uses, some of which are described below, while others have been commercialised e.g. the use of PAMAM dendrimers as globular protein replacements for immunodiagnostics and for *in vivo* gene expression applications.[313-315]

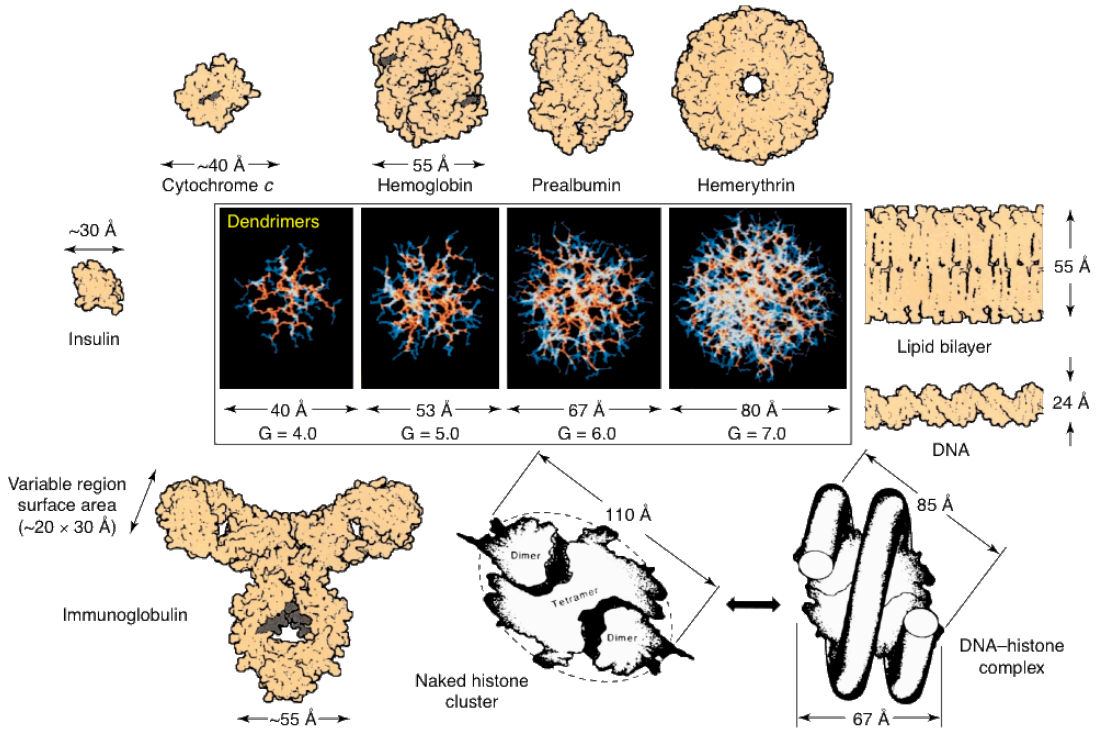

Figure 45. *A dimensionally scaled comparison of a series of PAMAM dendrimers with a variety of proteins.*[13]

Unimolecular Micelles

The idea that dendrimers could act as micelles came in 1985 when Newkome *et al*. published work on arborols.[115] At the same time, Tomalia and co-workers reported that electron microscopy could be used to show the 'hollowness' of PAMAM dendrimers, and also demonstrated how the branching affects the size of the internal cavities.[77,102,182] Further work looking at the hydrodynamic dimensions of PAMAM dendrimers revealed these to be similar to those of traditional micelles (nanometre scale),[182] supporting the idea that dendrimers could act as 'unimolecular micelles' and liposomes.[104,316] Turro *et al.* have demonstrated that the properties of a dendrimer can be tuned to give behaviour

similar to regular or inverse micelles depending on the nature of the interior and surface groups.[123,317,318]

These unimolecular micelles have been shown to be able to encapsulate small molecules (**Section 1.3.8**) using Meijer's dendritic box concept,[271] and work is ongoing with regard to using this encapsulation effect as a drug delivery system.[300,319,320] The binding of multiple metal ions by dendrimers also makes them a viable option in radioimmunotherapy where the radioactive dose applied to a tumour can be increased thanks to the dendrimer's multiple branches.[321]

Enzyme Mimics

Dendrimers have also been shown to mimic the function of enzymes; in this case the enzyme cofactors have been placed at the core of the molecule. This has been demonstrated in a number of cases, such as Diederich and co-workers'[322] mimics for pyruvate decarboxylate, and Breslow and co-workers' use of PAMAM dendrimers with a pyridoxamine core (which gave a 1000-fold rate increase in transamination reactions when compared with pyridoxamine alone).[323] This type of mimic behaviour has also been shown in dendritic peptides where the catalytic properties depend on the sequence of amino acids used.[319,324]

Binding and Transfer of Genetic Material

Arguably the most interesting use of dendrimers is that of the transfer of genetic material into cells, something that PAMAM dendrimers are typically used for as a result of their nonimmunogenic properties.[309] This class of dendrimers has been shown to be able to bind, condense (into structures similar to chromatin), and transport DNA as well as oligonucleotides into a variety of cells, whilst having low cytotoxicity *in vitro*.[247,325-329] Owing to their well-defined size and surface charge density, PAMAM dendrimers (particularly of generations ≥ 7)[308-310] are well suited as artificial histone-mimicking agents. The biophysical characterisation of DNA-dendrimer complexes has been studied by several groups and has been shown to be largely electrostatic, though few studies have looked at DNA condensation at low charge ratios.[330] Smith *et al*. have

demonstrated the release of DNA from a dendrimer using an optical trigger, but this also results in the degradation of the dendron.[331]

The uptake of PAMAM dendrimer-DNA complexes into cells is largely due to *endocytosis*, a process whereby a molecule is engulfed by the cell membrane,[309] and is followed by the release of the genetic material. This technique lends itself to the development of therapeutic proteins in the cells where they are most needed.

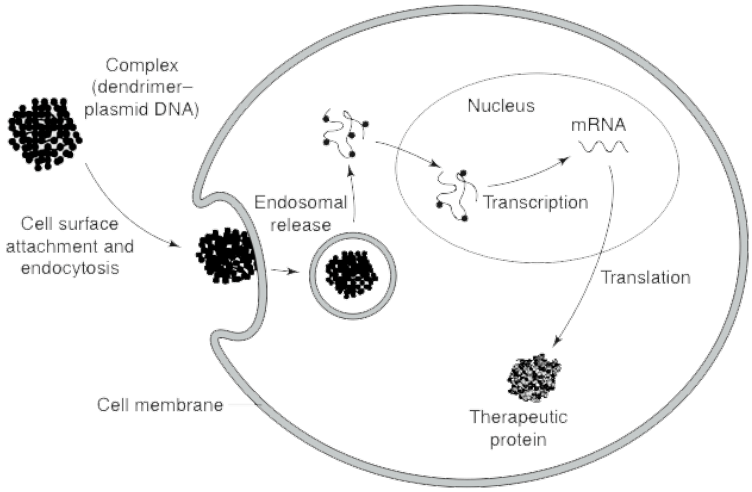

Figure 46. *The mechanism of dendrimer-mediated gene delivery into cells. The complex composed of dendrimer and plasmid DNA attaches electrostatically with the negatively charged phospholipids on the exterior surface of the cell membrane stimulating complex uptake by energy-dependent endocytosis. The DNA (alone or attached to the dendrimer) must escape the endosomal-lysososmal cavity before enzymatic or acidic degradation and translocate to the nucleus where it is transcribed into mRNA (messenger RNA). The mRNA template is transported into the cytosol where it is translated to the therapeutic protein.*[309]

Biological Sensing using Fluorescent Groups

Another biological application for dendrimers is in the field of biosensing.[237,332-336] The surfaces of PAMAM and PPI dendrimers (whose biocompatibility make them ideal) can be tailored to provide a sensing unit that has a high affinity for a particular analyte such as enzymes and proteins, while the rest of the surface is functionalised with fluorescent

units that change their fluorescent properties upon interaction with the biomolecules.[337] A good example of this was demonstrated by Shinkai *et al*. who reported that a water soluble PAMAM dendrimer functionalised with boronic acids and naphthyl units could be used for the sensing of saccharide sugars.[332]

As has been mentioned before, making use of fluorescent properties can give valuable information regarding concentration of dendrimers and bound molecules. This is no less important in biological systems where dendrimers have been shown to quench the fluorescence of tryptophan residues in bovine serum albumin,[338] or to monitor glucose in various biological assays.[339] This fluorescence can even be used to monitor dendrimer uptake into cells,[340] as demonstrated by Baker *et al*. who showed that a 5th generation PAMAM functionalised with 6-carboxytetramethylrhodamine fluorescent units and folic acid targeting units could be used to label human epidermoid carcinoma cell tumours *in vivo*.[269]

1.4 Aims and Objectives

The primary goal of the Neonuclei project[341] is to develop self-assembling particles capable, like the nuclei of living cells, of sustaining gene transcription. Partners involved in the project will aim to start with simple model systems and build up to structures of increasing complexity. This will give an alternative to biotechnological businesses that currently use live cells as protein production units.

Part of this project involves the synthesis of a molecule that can replicate the properties of histones i.e. a molecule that can compact DNA reversibly in response to physical or chemical stimuli. To that end, PAMAM dendrimers were chosen, as there is a wealth of published data that support their biocompatibility, binding and coiling of DNA, but little with respect to the reversibility of this process and behaviour at low charge ratios.

In order to study these DNA-dendrimer interactions, a series of PAMAM dendrimers up to generation 4 will be synthesised, characterised and functionalised to allow for different binding properties. Though higher generations have been reported to be more

effective at binding DNA, their synthesis is lengthy and they are not required in order to demonstrate the types of surface modifications to be carried out. Such surface functionalisations include:

- Using molecules to give different amounts of dendrimer surface charge whilst retaining the same approximate size as the unmodified surface.
- Using photoactive units that allow for cell uptake to be studied and that can be used to reversibly bind DNA.
- The introduction of pH sensitive units.

The behaviour of dendrimers in biological membranes is a relevant topic in medicinal chemistry, particularly when it comes to developing drug delivery systems. In order to gain a greater understanding of how PAMAM dendrimers interact with lipid membranes, initial computational and experimental studies will be performed and the results of these will be compared.

Chapter 2 PAMAM dendrimers

2.1 Nomenclature

The widely accepted naming of PAMAM dendrimers was developed by Tomalia[13,77,100] and incorporates the dendrimer size (or generation), its core type, the number of surface groups and the nature of these surface groups, i.e.

G-[C]-N-F

where G = generation, C = core type, N = number of terminal groups and F = functionality

Each dendrimer generation consists of a branching unit and a lengthening unit; the lengthening unit (methyl acrylate) being termed a half-generation (ester surface), whilst the addition of a branching unit (ethylene diamine, EDA) gives a full-generation (amine surface). So as a dendrimer 'grows', its generation advances in steps of 0.5 (**Figure 47**).

Before Tomalia's naming scheme became commonplace, the numbering of the generations began with the core molecule being termed generation 0. Whilst this worked well with cores that contained amines (and could thus initiate dendritic growth) it became problematic when using larger cores, such as 1,3,5-trihydroxybenzene. This core type would first have to be reacted upon to give amine branching points. Tomalia thus termed generation 0 to be the first instance of an amine surface that has been build out from the core. This means that in the case of 1,3,5-trihydroxybenzene, this molecule is the core, but not generation 0. It is for this reason that some dendrimers are called generation -1.0 and -0.5 (**Figure 47**).

Ethylene diamine core

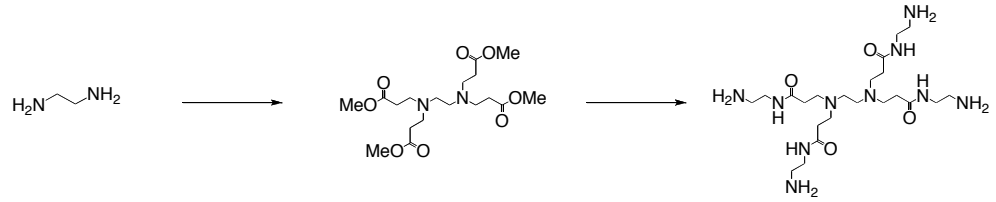

37 **38** **39**

Full generation (-1) Half generation (-0.5) Full generation (0)

Trihydroxybenzene (phloroglucinol) core

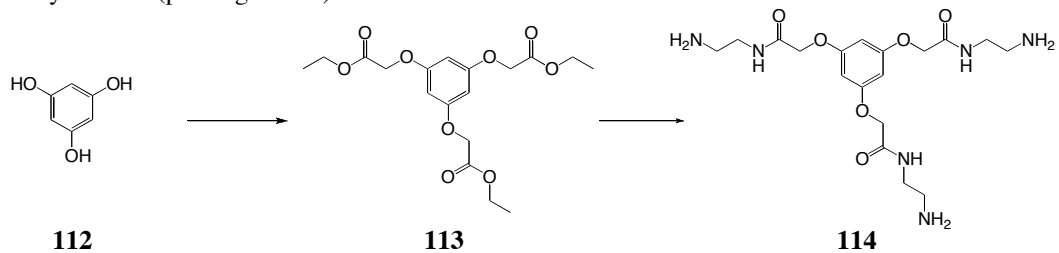

112 **113** **114**

Full generation (-1) Half generation (-0.5) Full generation (0)

Figure 47*. Naming of dendrimer generations.*

The next stage is to determine the number of end-groups, and their functionality. So a 4th generation dendrimer having 64 terminal amine groups based on an EDA core would be written as:

4.0-[EDA]-64-Amine

This approach is very useful when the surface of the dendrimer has been modified, but for simplicity if the surface has not been changed we can use 'G4' to denote a 4th generation dendrimer. If this notation is to be used as a specific example, then the core must also be stated, i.e. for G4 (EDA) we assume the correct number of terminal groups and an amine surface. Similarly, G0.5 (EDA) would denote 8 surface ester groups based on an EDA core.

2.2 Preparation

2.2.1 General Synthesis

A range of PAMAM dendrimers up to generation 4 have been prepared in this study using the methodology described by Tomalia.[77,106,187] Dendrimers with an EDA core were the first to be synthesised owing to their ease of handling, others are described in detail in **Section 2.4**. The synthesis of higher generations served little purpose as some of the surface attachments to be trialled had not been performed before; thus avoiding a lengthy synthesis if the attachments proved to be unsuccessful.

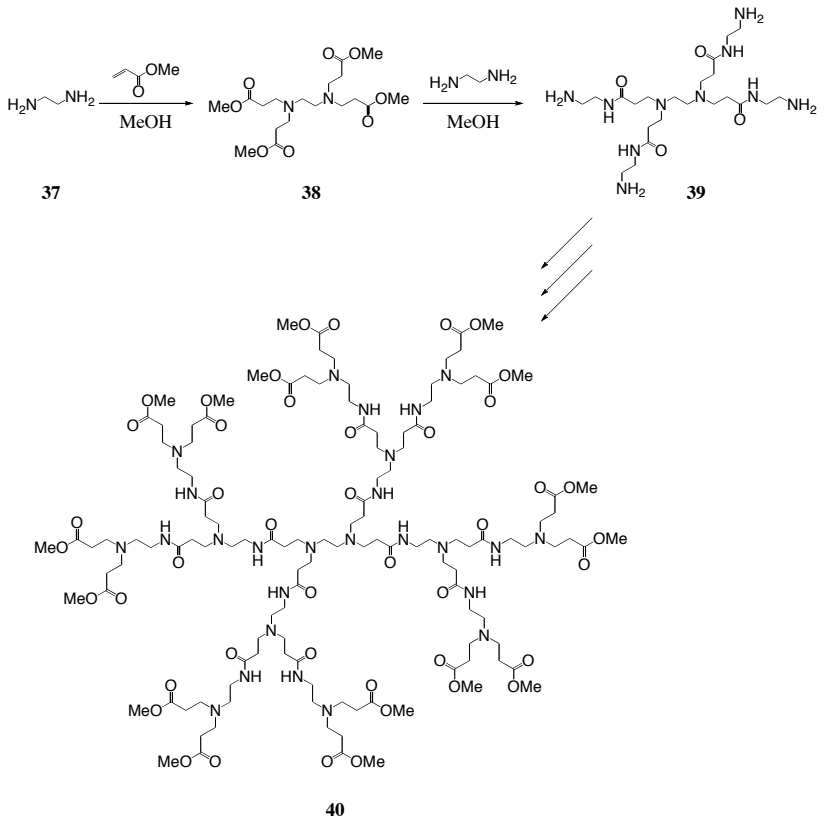

***Figure 48**. PAMAM dendrimer growth of 1.5-[EDA]-16-Ester (**40**).*

The first step in PAMAM dendrimer synthesis involves the creation of the core from an initiator. This involves a Michael addition of an electrophilic reagent (e.g. methyl acrylate) to a multifunctional initiator (e.g. EDA or ammonia) to give G-0.5. An amine

surface (G0) is then achieved by an amidation of the ester with EDA. A further repetition of these two steps will give a G1 dendrimer with an amine surface. This process is repeated to give progressively larger generations with greater numbers of surface groups.

***Table 7**. Number of surface groups associated with different cores.*

	No. of surface groups	
Generation	Core with 3 branching points (NH_3, phloroglucinol)	Core with 4 branching points (EDA)
0	3	4
1	6	8
2	12	16
3	24	32
4	48	64
5	96	128
6	192	256
7	384	512
8	768	1024
9	1536	2048
10	3072	4096

2.2.2 Remarks on PAMAM Synthesis

In preparing half-generation dendrimers a large excess of methyl acrylate is used, about 6 equivalents per amine terminated branch. The reason for this excess is that if any unreacted amines were left, they could react with the ester units on the surface giving rise to branch termination (**Section 2.2.3**). This is not a serious problem during this step of the dendrimer synthesis as the kinetics of the Michael addition is fast enough to prevent amidation occurring.[77]

As described by Tomalia,[77,187] these reactions were typically carried out under an inert atmosphere in dry methanol and allowed to stir for 2 days at room temperature. The

solvent and excess reagent were then removed under reduced pressure to give a yellow oil (it is important not to heat the samples to high temperature (>70ºC) as retro-Michael reactions can occur).[77,342,343] All generations then underwent an azeotropic distillation; the dendrimer is dissolved in methanol to open up the arms and disrupt the H-bonding[179] (see **Section 2.5.3**), and toluene is then added to flush out any impurity.

At low generations (≤ G1.5) these oils are not very viscous and can be purified by column chromatography (5 – 15% methanol in DCM) to give colourless oils. At higher generations (> G1.5) the oils are quite viscous, column chromatography is not possible due to the high molecular weight of the dendrimers (> 3000 g mol^{-1}) and because the high percentage of methanol in the eluent would start to dissolve the silica so little purification is possible (aside from azeotropic distillation).

For the preparation of full-generation dendrimers, the half-generation dendrimer (in dry methanol) and EDA (containing 10% methanol) were first deoxygenated by passing nitrogen through them. Whereas the number of equivalents of reagent used to make the half-generation is constant, the amount of EDA required varied depending on the generation involved; the higher the generation, the more EDA would be needed. This is because of the possibility of a single molecule of EDA reacting across two esters on the surface, either from the same dendrimer causing 2 branches to be terminated, or from two dendrimers causing bridging (see **Figure 50** and **Section 2.2.3**). Tomalia found that 50 equivalents by weight were required to go from G0.5 to G1.0 with a > 95% purity, but this increases to 2870 equivalents for G8.0.[77,187]

Table 8. *Excess EDA used in PAMAM dendrimer synthesis.*[77,187]

Generation	Equiv. of EDA[a]	Generation	Equiv. of EDA[a]
1	50	6	730
2	60	7	1440
3	100	8	2870
4	200	9	5740
5	370		

[a] By weight

Once the two solutions were degassed, the dendrimer solution was transferred dropwise into the EDA solution (over ice) *via* a cannula and the mixture was stirred at a temperature less than 10ºC (this slows the kinetics of the reaction, further inhibiting defect formation). The initial EDA solution was made containing 10% methanol as neat EDA melts at 9ºC. The length of stirring also varies with generation, low generations can be stirred for one week whilst larger generation preparations (≥ G3.0) need to be stirred for 4 weeks.

The reactions were worked up by removing the solvent and reactant under reduced pressure to give crude product as a viscous yellow oil; these oils were found to be more viscous than the half-generation dendrimers used to synthesise them. The excess EDA used was recovered and re-distilled from CaH_2. Since a large number of amines are now present on the surface the dendrimers cannot be purified by column chromatography. Residual EDA was easily detected by NMR and its characteristic odour, but it was found to be troublesome to remove solely under reduced pressure. This is because the EDA becomes trapped within the dendritic structure; the larger the dendrimer the greater the number of carbonyl groups that can form hydrogen bonds to the amine groups of the EDA (**Figure 49**). At low molecular weights, the best way to remove this EDA was found to be by azeotropic distillation.

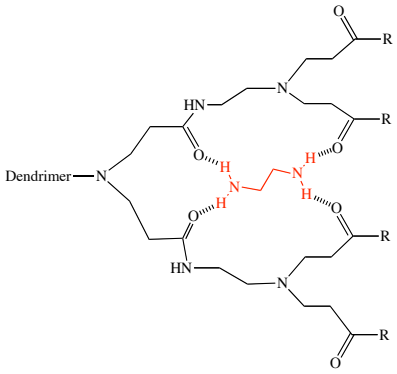

Figure 49. *EDA captured by dendritic branches.*

At high molecular weights (> 4000 $gmol^{-1}$) the dendrimers can be purified by dialysis. Though this technique is typically used to purify peptides, it can be modified to be used with dendrimers. An appropriate piece of cellulose dialysis membrane is first selected

(the membrane is porous and has a molecular weight cut-off below which molecules can freely pass through the membrane) and prepared by stirring in a large volume of 2% sodium bicarbonate and 1 mMol EDTA at 80ºC for 30 min followed by deionised water for 1 hr. The bottom of the tubing is clipped closed and the dendrimer, dissolved in water, added into the tubing. A glass marble is added to the tubing (for weight) and the top clipped closed leaving a small amount of air inside (this allows the tube to remain vertical when put into the bulk). The tubing is then placed in a large volume (5 L) of slowly stirred deionised water where a diffusion gradient will become established. Any impurity, such as EDA, inside the tubing will be forced into the bulk by this gradient assuming that the impurity is of lower molecular weight than the membrane cut-off (the bulk can be replaced after a day to help purify the product by setting up a new gradient). Though deionised water is most commonly used with this technique, organic solvents such as DCM and methanol can be used, but this can lead to pore deformation and product loss. The purified dendrimer solution can then be azeotropically distilled to remove water from the branches, though there may still be some solvent trapped leading to products with artificially inflated yields (over 100%).

2.2.3 Defects

It is very important to ensure that the dendrimer is as pure as possible at all stages of its synthesis as any impurity, be it a branch termination or left over reactant, could be carried through further reactions leading to purification issues. The most common branch termination defects occur when too small an excess of EDA is used (or the reaction proceeds too fast) in reacting a half-generation to make a full-generation dendrimer (**Figure 50**).[77] Termination during the formation of the half-generation is also possible, either by incomplete reaction, or by a retro-Michael addition when the sample is heated to too high a temperature (**Figure 51**).

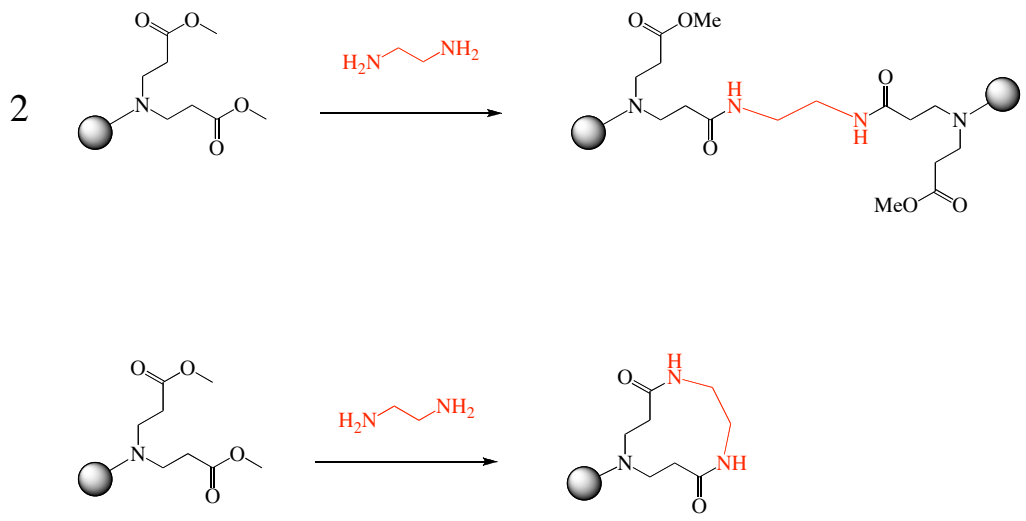

Figure 50. *Possible intermolecular (top) and intramolecular (bottom) defects resulting from an incomplete EDA addition step.*

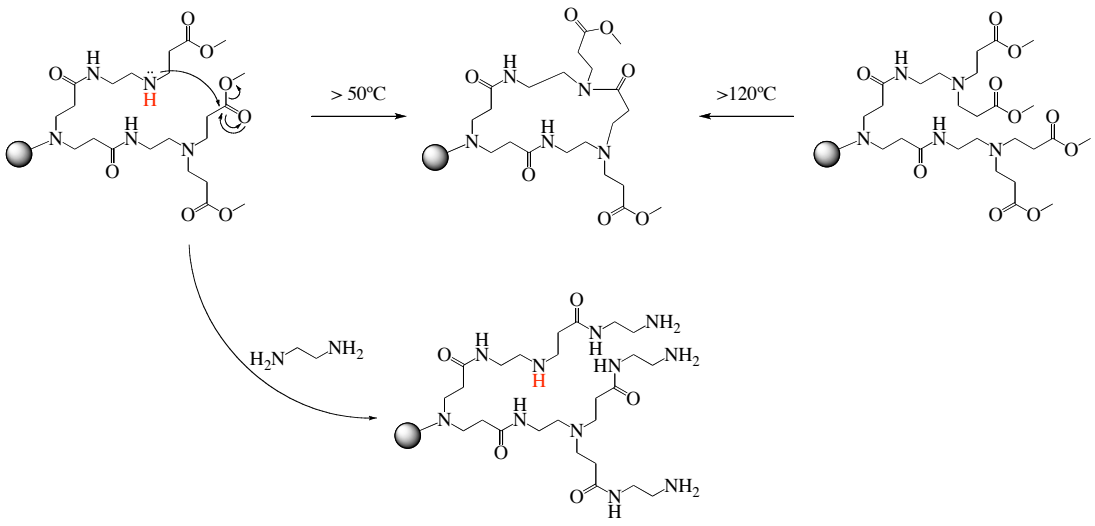

Figure 51. *Possible defects resulting from an incomplete methyl acrylate step.*[77]

If methyl acrylate or EDA is taken through to the next step of the dendrimer synthesis it will react with either EDA or methyl acrylate respectively to make small dendrimers, which if allowed to remain, will themselves form larger dendrimer contaminants that will greatly affect the monodispersity of the product.

Though not a defect in the strictest sense, a problem that can also occur is the precipitation of dendrimer clusters as a gel-type solid from solution. It is suspected that this occurs when the dendrimer concentration is very high; under these conditions the arms of separate dendrimer units can intercalate with each other and form large clusters that become insoluble. It is therefore advantageous to store samples at low concentrations as solutions in methanol (< 60 $mgmL^{-1}$).

2.3 Characterisation

Though this section will focus on PAMAM dendrimers with an EDA core (as this class was used extensively in this report), the characterisation information is applicable to all the dendrimers studied in **Section 2.4**.

2.3.1 ^{1}H and ^{13}C NMR Spectroscopic Studies of Dendrimers

Given the highly symmetrical nature of dendrimers, perhaps the most useful analytical technique is that of nuclear magnetic resonance (NMR). The equivalency of the various proton and carbon environments can lead to well defined spectra, though peak overlap and branch mobility can cause line broadening in ^{1}H NMR. The introduction of defects and surface modifications disrupts the symmetry and thus leads to a more complex spectrum.

At low dendrimer generations (< G1) ^{1}H NMR can give a very accurate idea of sample purity. All the peaks are well defined and can be readily integrated, but at higher generations the peaks begin to overlap and broaden, making analysis hard. Despite this problem, ^{1}H NMR at high generations can be used to determine the degree of surface coverage of any modifications that have been made.

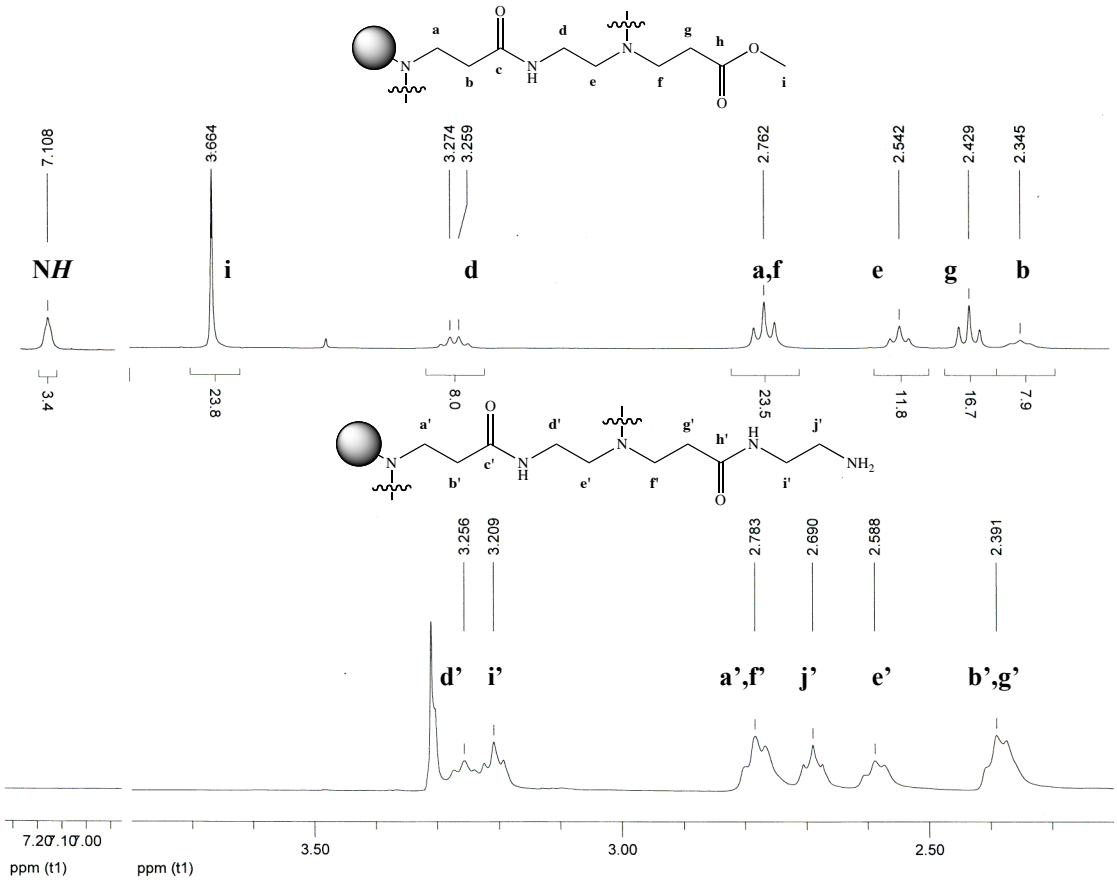

Figure 52. *^1H NMR spectra of 0.5-[EDA]-8-Ester (top, $CDCl_3$) and 2.0-[EDA]-16-Amine (bottom, D_2O).*

By studying the proton spectrum at each stage of dendrimer growth, and with the aid of 2D NMR techniques such as COSY, it is possible to make the assignments shown in **Figure 52**. The half-generation example was run in deuterated chloroform, which helps to prevent H-bonding between branches and thus gives well defined peaks. Peaks at δ 7.11 and 3.66 ppm were assigned as the amide (N*H*) and methyl ester protons (**i**) respectively, the latter giving us useful information about the extent of surface coverage. It can be seen that methanol is still present despite extensive drying which is most likely the result of the solvent becoming trapped within the dendritic structure. As there are no methylene protons that can give rise to the quartet at δ 3.27 ppm, it is most likely to be an overlapping doublet of triplets, implying that this peak arises from the methylene unit next to the amide nitrogen (**d**).

The 4 remaining triplets are from the methylene units (**a**, **b**, **e**, **f**, **g**) of the inner and outer branches. Peaks at δ 2.76 and 2.43 ppm are primarily due to the outer branches (integrals aid this interpretation) and were assigned as methylene units nearest the nitrogen (**f**) and nearest the carbonyl group respectively (**g**). As these peaks should integrate to 16H, an underlying peak of 8H (**a**) can explain the fact that the peak at δ 2.76 ppm integrates to 24H. This is due to the repetitive nature of dendrimer growth, where a methylene unit further inside the structure lies in a similar environment. It is not surprising then to find that the internal methylene units which are next to the carbonyl groups (**b**) appear upfield (δ 2.35 ppm) when compared to similar units in the outer-most shell, the latter being more deshielded by the ester group. The remaining methylene groups located next to the tertiary nitrogen before the point of branching (**e**) appear at δ 2.54 ppm and have a combined integral of 12H.

The observed proton spectrum for a full-generation dendrimer was found to be very similar to that of the half-generation; only the signals arising from methylene units in the outer generation change. There is no longer a peak at δ 2.43 ppm as we have lost the ester functionality. New peaks appearing at δ 3.21 and 2.69 ppm arises from the newly introduced EDA units, and are assigned as being the methylene group nearest the amide (**i'**) and that nearest the amine (**j'**) respectively. At higher generations the number of protons dramatically increases (1248 at 4.0-[EDA]-64-amine) which causes further peak broadening and makes it difficult to obtain accurate integrals.

As with ^{1}H NMR data, ^{13}C NMR spectra rely heavily on the fact that each dendrimer generation, except the outer-most, is identical with respect to its environment. Unlike ^{1}H NMR data, in which the surface change can be hard to observe at high generations, the change from half to full-generation is easily observed at all generations synthesised.

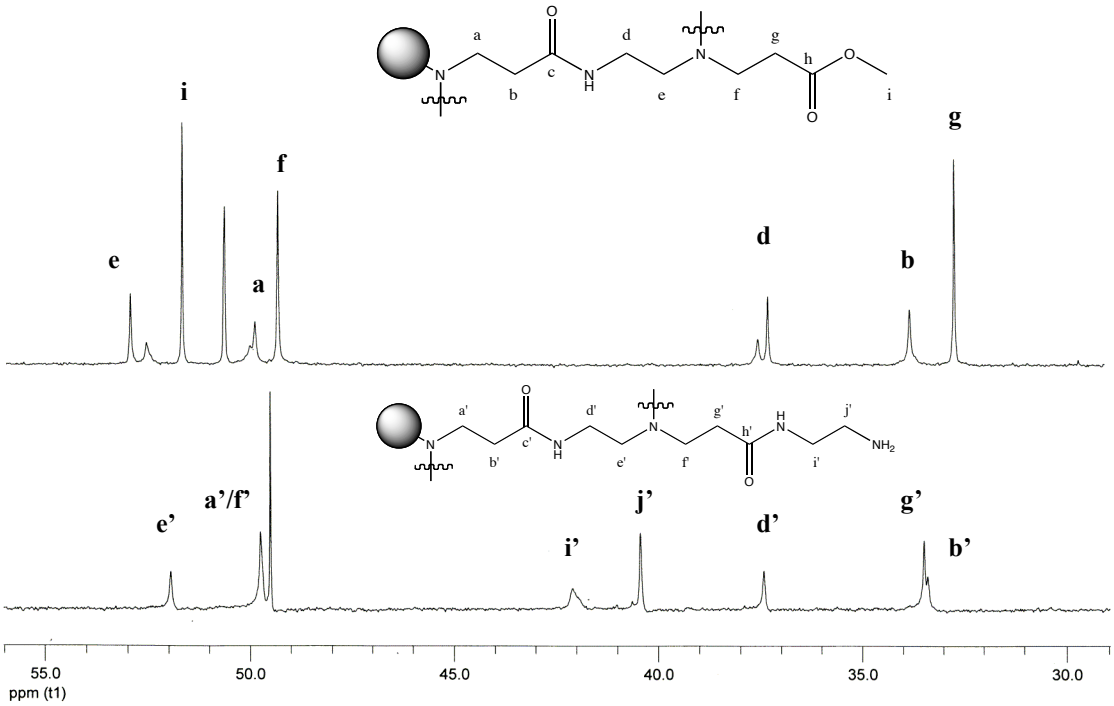

Figure 53. *^{13}C NMR spectra of 3.5-[EDA]-64-Ester (top, $CDCl_3$) and 3.0-[EDA]-32-Amine (bottom, D_2O).*

The assignments of the half and full-generation ^{13}C NMR spectra (**Figure 53**) were arrived at from studying dendrimer growth in combination with 2D NMR techniques such as HMQC and HMBC. It was observed that there are two types of signal in each case, those for the outer most generation and those due to the inner generations.

For half-generation dendrimers, peaks arising from inner generations are typically smaller, slightly broader and located within a few ppm of their larger outer generation counterparts. For example, peak **g** has been assigned as the outermost methylene unit whilst the peak slightly downfield from it, **b**, relates to a similar unit further within the structure. The reason for the slight line broadening is due to small changes in the environment such as H-bonding of nearby functionality, chain motion and branch folding (for more information about the folding of terminal groups, see **Sections 1.3.5** and **2.5**). The two unassigned peaks at δ 52.4 and 37.4 ppm relate to internal EDA units similar in environment to **e** and **d** respectively.

Though it is useful to be able to assign the carbon resonances of the inner generations, it is the peaks relating to the outermost generation, and how they move when going from an ester to an amine surface, that is of primary importance. As can be seen in the case of the half-generation dendrimer, peaks **f**, **g** and **i** relating to the outer methyl ester appeared at δ 49.2, 32.6 and 51.6 ppm respectively. The outermost EDA unit, peaks **d** and **e**, were assigned at δ 37.2 and 52.8 ppm respectively. As expected, it was observed that peaks relating to the methyl acrylate units are approximately twice as large in comparison with those of the EDA.

When replacing the ester functionality with an EDA unit, the signal at δ 51.6 ppm (**i**) disappears whilst two new peaks at δ 42.0 and 40.4 ppm are observed. These two new signals relate to methylene groups of the outer EDA unit **i'** and **j'** respectively. Since the methyl acrylate unit is no longer the terminal unit, peaks **f** and **g** both move downfield to become part of the inner generation signals (**a**/**a'** and **b**/**b'** respectively). This movement also occurs for peaks **d** and **e**. Whilst these two signals do not move far, they completely overlap their inner generation counterparts suggesting that only the outer most generation can be clearly observed. It is not known why **i'** is broader than **j'**, but this may be due to a combination of the adjacent amide bond and branch folding.

When going from an amine to an ester surface, peaks **i'** and **j'** move considerably upfield and downfield respectively to become part of signals **d** and **e**. The appearance of **i** is also noted. By observing these 5 major peaks the sample purity and surface coverage can be easily determined using inverse gated proton-decoupled experiments which allow the ^{13}C NMR spectrum to be integrated.

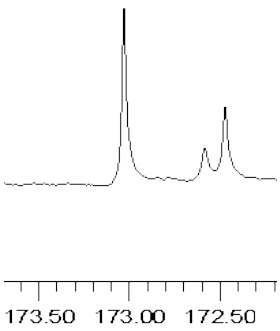

Figure 54. *Carbonyl peaks from ^{13}C NMR spectrum of 3.5-[EDA]-64-Ester ($CDCl_3$).*

Though the carbonyl signals show little movement between half and full-generation dendrimers, it can be seen that the outermost carbonyl peak is located downfield compared to those located for inner generations. This outer carbonyl resonance is often isolated, whereas those for the inner carbonyl groups occur at a similar chemical shift (often overlapping).

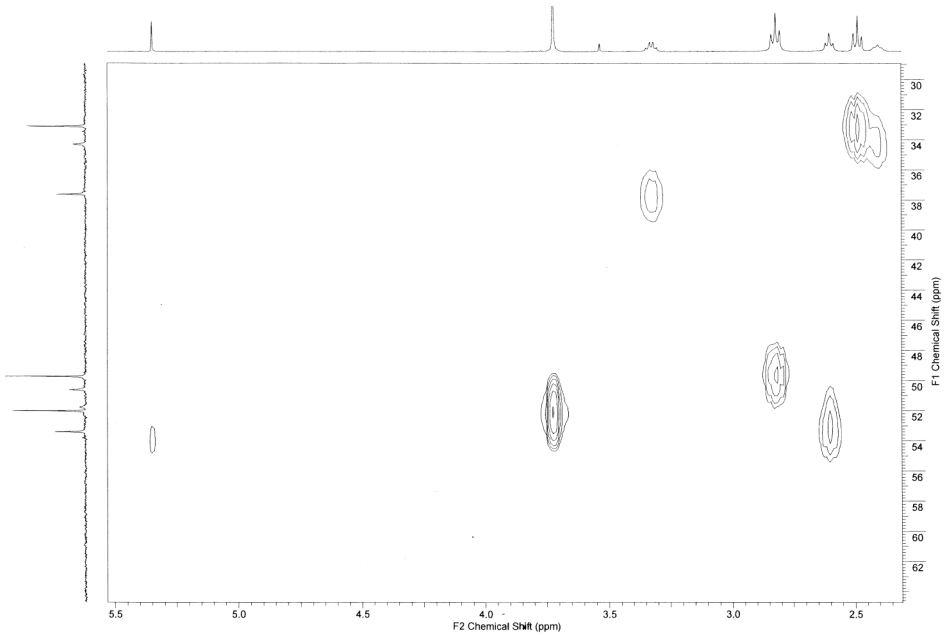

Figure 55. *HMQC coupling spectrum of 0.5-[EDA]-8-Ester ($CDCl_3$).*

The use of 2D NMR techniques can reveal connectivity relationships between nuclei, such as H-H (COSY) and H-C (HMBC, HMQC shown above) correlations. These experiments allow for the final assignments to be confirmed, as well as giving information about the local environment (**Figure 55**).

2.3.2 NMR Complexity

A number of factors can lead to increased spectrum complexity. In general as the dendrimer size increases, the spectral resolution decreases. It is for this reason that samples above G2 are typically run with extended scans (> 4000). The introduction of defects, be they located on an inner or outer generation, and surface modifications,

disrupts the dendrimer symmetry leading to extra peaks and extensive peak broadening in both ^{1}H and ^{13}C NMR spectra. The spectrum shown in **Figure 56** contains a defect that occurred during the preparation of 4.0-[EDA]-64-Amine. Three small peaks at δ 47.8, 45.1 and 36.0 ppm were observed and assigned to the surface capping of two esters with one EDA unit, whilst the peak at δ 39.3 ppm may be due to bridging between two dendrimers. It should be noted that unsymmetrical dendrimers require a great many more scans in order to observe all the environments.

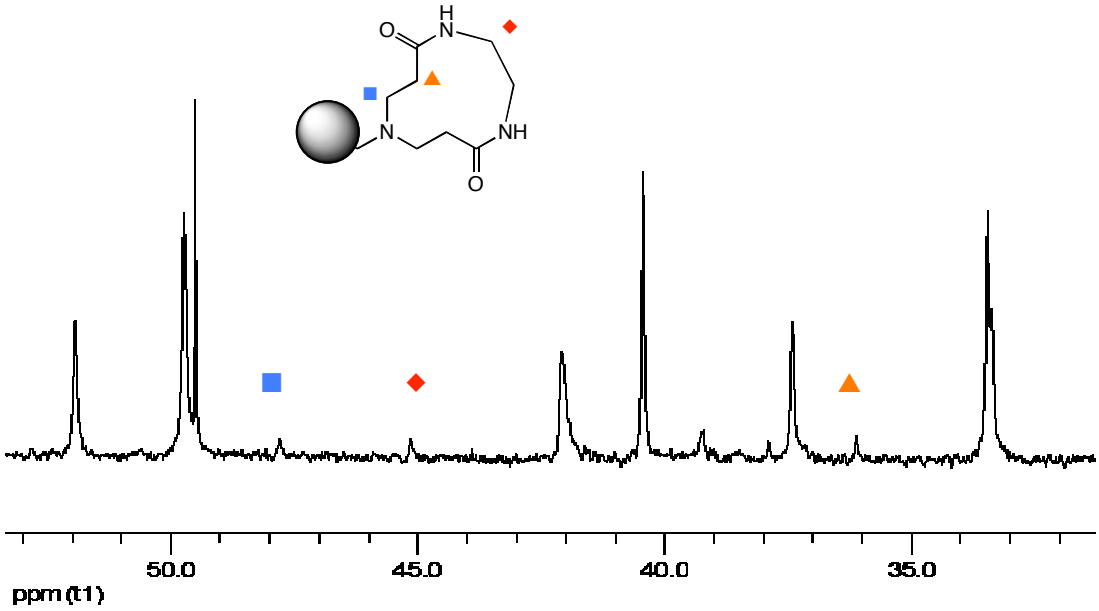

***Figure 56**. ^{13}C NMR spectrum showing a surface capping defect.*

2.3.3 Mass Spectrometry

Mass spectrometry of PAMAM dendrimers has been reported using many techniques such as fast atom bombardment (FAB)[174,175] and matrix-assisted laser desorption/ionisation (MALDI),[344,345] but perhaps the most prevalent technique is that of electrospray ionisation (ESI).[81,309,346-348] This is due to the fact that PAMAMs can be readily protonated (or deprotonated[346]) and thus be analysed by positive electrospray (ES^{+}) because their structures contain a high ratio of nitrogen.

Despite the LRMS ES^+ system used throughout this study only having a measurable range of 120 – 2000 Da so whilst the $[M + H]^+$ peak can be seen for low generation dendrimers (**Figure 57**) it can not be detected for most dendrimer samples, it uses a soft ionisation technique that has the advantage of not fragmenting the structure, allowing for easier identification of defects.

Since there are many nitrogen atoms in the dendritic structure, this ionisation technique can easily lead to multiple protonation of the sample giving rise to many peaks in the spectrum such as $[M + 2H]^{2+}$ and $[M + 2H + Na]^{3+}$. This ability to pick up multiple charges makes analysis of larger dendrimers possible.[348]

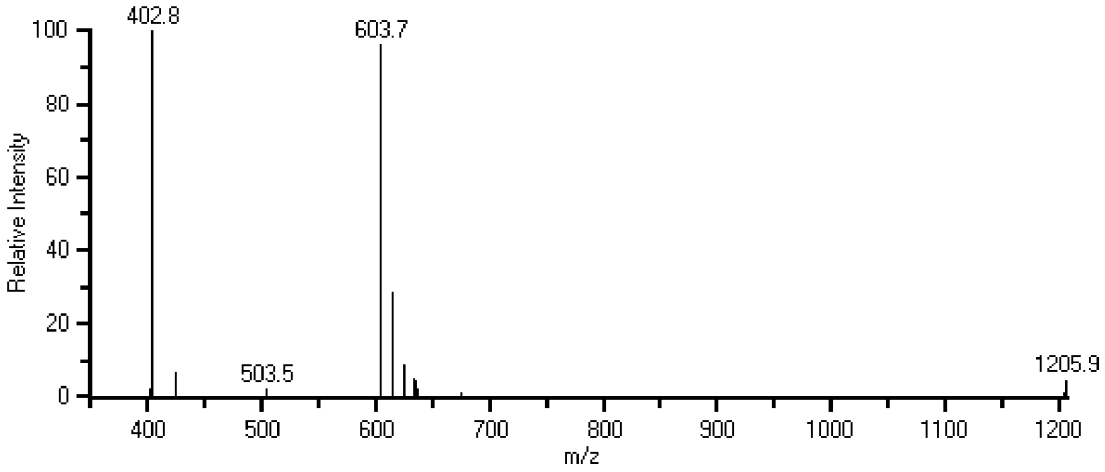

***Figure 57**. A multiply charged MS spectrum of 0.5-[EDA]-8-Ester (MW 1205 Da).*

Dendrimers larger than generation 3 become harder to analyse as they typically have a molecular weight greater than 6500 Da. Even with multiple charging of the sample it is hard to find the relevant peaks amongst the noise, and if defects have been introduced the spectrum becomes very hard to interpret. Of the spectra that could be collected it was found that the ester-surfaced dendrimers were much more ionisable and were thus much easier to analyse. It is believed that some of the dendrimers with amine surfaces had become overly protonated so that no multiple charge pattern could be deduced.

2.4 Specific Dendrimers Prepared in this Study

2.4.1 EDA Cored Material

This series of dendrimers was synthesised up to generation 4.0 following the procedures of Tomalia[77,349] and Amabilino,[350] and is based on an EDA core. These systems have four main branches making them the largest dendrimers synthesised in this study. These dendrimers were primarily synthesised so that their surfaces can be modified with the aim of studying DNA-dendrimer interactions and complex formation. The half-generations, up to G2.5, were used to study spin-lattice relaxation times in the hope of better understanding branch interactions.

The generation -0.5 material (**38**) was prepared by dropwise addition of a solution of EDA in methanol to a stirred solution of methyl acrylate in methanol over 6 hours. This was allowed to stir for 48 hours at room temperature before the solvent was removed and the crude product was then purified by column chromatography to give the product as a colourless oil (72%). A solution of -0.5-[EDA]-4-Ester in methanol was then added *via* a cannula into a cold (< 5ºC) stirred solution of EDA (50 fold excess) in methanol to give 0-[EDA]-4-Amine (**39**). The excess EDA was removed under reduced pressure and set aside to be re-distilled. These steps were repeated to give higher generation dendrimers as described in **Section 2.2**. The ^{1}H NMR spectrum (D_2O) of the G0 dendrimer shows the (equivalent) core methylene groups at δ 2.57 ppm, clearly distinguishable from the other signals. Similarly in the ^{13}C NMR spectrum, the core methylene groups are visible and appear at δ 50.7 ppm. At higher generations these are no longer visible as a result of overlying signals from the other branches.

2.4.2 Phloroglucinol Core

This series of PAMAM dendrimer is based on a phloroglucinol (1,3,5-hydroxybenzene) core and was synthesised up to generation 4.0 following the procedures of Tomalia[77,349] and Amabilino,[350] with the aim of studying their spin-lattice relaxation times and surface modifications. Since this core contains no amines, it first had to be built up to zero generation as shown in **Scheme 9**.

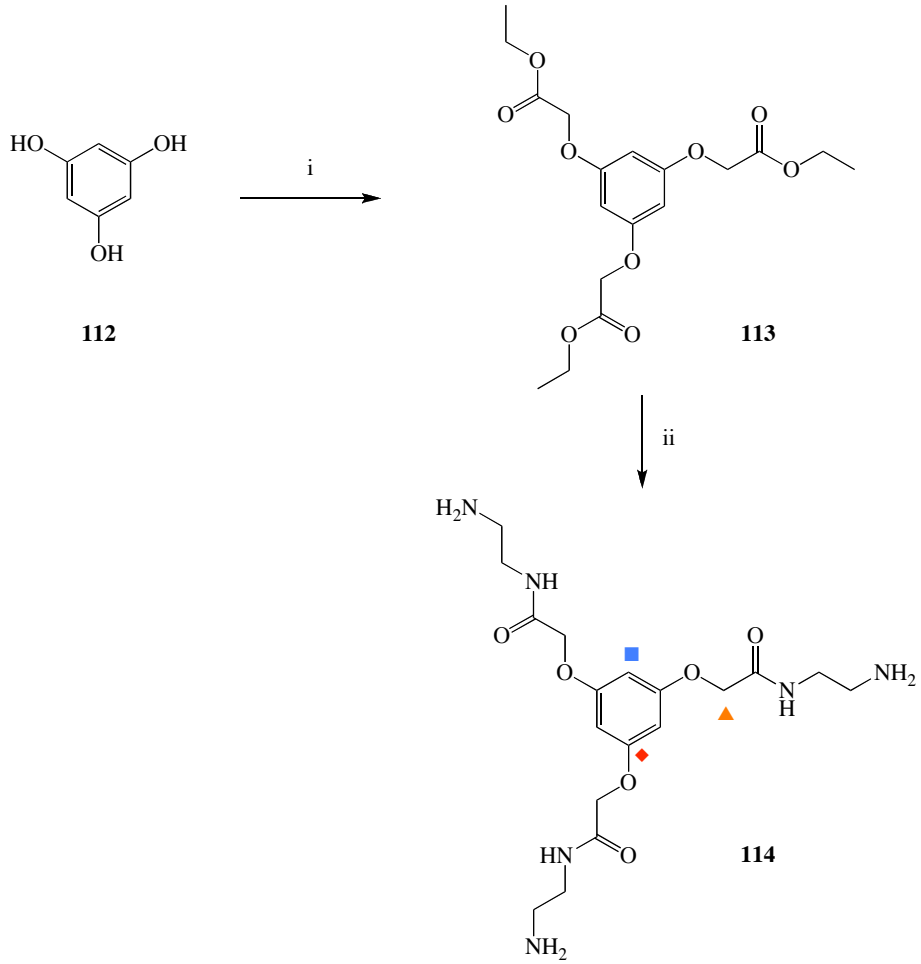

Scheme 9. *i, KF, ethyl bromoacetate, MeCN, reflux; ii, EDA, diethyl ether.*

Phloroglucinol was added to a mixture of potassium fluoride and ethyl bromoacetate in acetonitrile and stirred at reflux for 72 hrs to give the crude product **113** as a white precipitate, which was crystallised as white crystals (31%). Analysis of this ethyl ester, -0.5-[Phloroglucinol]-3-Ester, by NMR, melting point (61 – 62ºC) and elemental

analysis (expected C 56.25%, H 6.29%; found C 56.16%, H 6.32%) showed it to be consistent with published data.[350,351]

The ethyl ester was then added to a large excess of EDA in diethyl ether to give 0-[phloroglucinol]-3-amine **114** as a white solid (65%). Analytical data was found to be consistent with previous work carried out within the Grossel group.[350] By introducing hydrogen donors onto the surface we would expect the number of possible intermolecular H-bonds to increase giving rise to a higher melting point; this is indeed what was observed as this product required over twice the temperature to melt (146 – 148ºC).

Subsequent generations were built up as described in **Section 2.2** to give a series of dendrimers as viscous pale yellow oils. It was found that the full-generation dendrimers in this series gave unrealistic yields, typically over 100%, as well as poor MS data. These observations were expected and are described in more detail in **Sections 2.2.2** and **2.3.2** respectively.

^{1}H and ^{13}C NMR data obtained for this series gave similar spectra when compared to those of the EDA series; the only difference being the appearance of peaks assigned to the aromatic core. In the ^{1}H NMR spectra (D_2O or $CDCl_3$), singlets at δ 6.29 and 4.54 ppm were assigned to the aromatic proton (■) and the methylene unit closest to the ring (▲) respectively. What is perhaps surprising about these two peaks is that, unlike the EDA core, they can be observed even at high generations. The presence of aromatic peaks was also evident in ^{13}C NMR spectra. Signals at δ 159.3, 96.1 and 67.5 ppm were assigned to the quaternary aromatic (◆), tertiary aromatic (■) and the methylene unit closest to the ring (▲) respectively. Unlike in the ^{1}H NMR spectra, these peaks are only observed up to G2.5, which may be a result of the spectra becoming dominated by the exterior carbon resonances.

2.4.3 Ammonia Core

A series of PAMAM dendrimers based on ammonia as the core up to generation 1.5 were synthesised using the standard route described in **Section 2.2** with the aim to study their spin-lattice relaxation times. The core itself was synthesised by passing ammonia gas through deoxygenated methanol and recording the mass increase, before adding methyl acrylate (4 equiv) *via* a cannula. After characterisation of the G-0.5 material, it was reacted with EDA (50 equiv per end group) to give generation 0 material which was then grown further. Similar to the phloroglucinol series, these dendrimers have one fewer initial branch in comparison with the EDA dendrimers and as such possess about ¾ the molecular weight at each generation. The ^{1}H spin-lattice relaxation times are discussed in **Section 2.5** but the generated spectra showed the series to be of high purity.

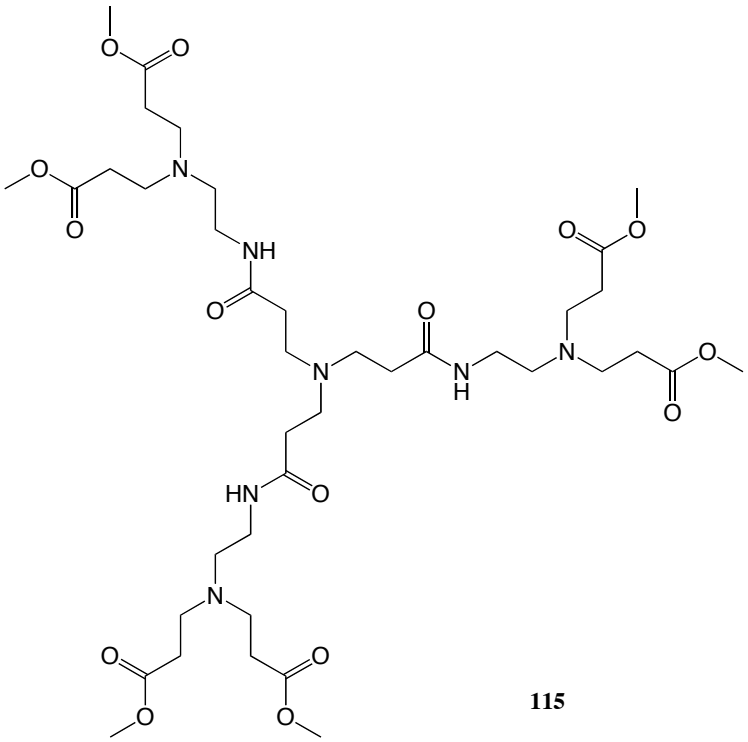

115

Figure 58. *Branching structure of 0.5-[Ammonia]-6-Ester.*

2.4.4 Dendritic Wedges for Coupling to Cores using Convergent Approach

A series of PAMAM wedges (dendrons) were synthesised using the divergent method with the aim of attaching them to a reactive core in a convergent-type reaction. Normal PAMAM dendrimer growth was achieved using ethanolamine as a starting point to give products as colourless oils in high yields. When these dendrons are coupled to a core, any unreacted material needs to be easily removed by dialysis, so the dendrons were only synthesised to G2.5 (MW 1435 Da) as they then have a MW lower than the cut-off for the tubing (MW 3000 Da). It should be noted that the naming of this series takes into account the addition of a core, so the amine of the ethanolamine would be the first amine surface, i.e. generation 0 (**Scheme 10**).

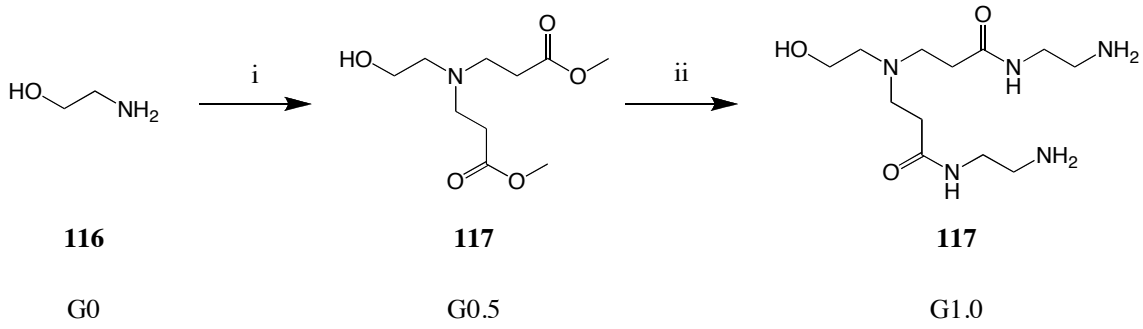

116 **117** **117**

G0 G0.5 G1.0

Scheme 10. *i, Methyl acrylate, methanol; ii, EDA, methanol.*

The reason that ethanolamine was selected as the starting material for these dendrons was because of the lack of reactivity of the alcohol to any of the PAMAM growth reagents. Once the dendrons reached the desired size (a half-generation is required due to the reactivity of an amine surface) the alcohol could be used to couple them to a reactive core (e.g. one which contains an acid chloride). Another possible starting material is mono-protected EDA, the protection being removed before core coupling. This approach however was discarded, as the deprotected amine would be free to react with the ester surfaces of the wedges leading to large polymeric impurities that would not be removed by dialysis.

Analysis of this series by mass spectrometry showed predominantly multiply charged species for all samples except for G2.5 where no spectrum could be obtained. NMR studies revealed normal PAMAM spectra (**Figure 52** and **Figure 53**) with the addition of peaks relating to the alcohol methylene unit; a triplet at δ 3.60 ppm in ^{1}H NMR (D_2O or $CDCl_3$) and a singlet at δ 59.3 ppm in ^{13}C NMR spectra. Since these signals lie outside the normal range for PAMAM branching units, δ 3.25 – 2.30 ppm and δ 53.0 – 32.0 ppm respectively, they can be seen at all generations. This means they could be used to assess the effectiveness of core couplings, as is described in **Chapter 5**.

2.5 Spin-Lattice Relaxation NMR

2.5.1 Background

NMR spectroscopy plays a key role in the determination of PAMAM structure and purity, but it can go further than just giving chemical shift values since it can also give information about the molecular dynamics. By analysing a samples' spin-lattice and spin-spin relaxation times (T_1 and T_2 respectively) it is possible to reveal detail about the intra- and inter-molecular mobility. T_1 data is particularly useful to us as it can show which parts of the a molecule are subject to steric hindrance, the extent to which strong intra-molecular or intra-ionic interactions affect the flexibility of the molecule, and which parts of the molecule are rided and which are flexible.[352] Since T_1 information can be acquired for both ^{1}H and ^{13}C spectra, it can greatly aid peak assignment even when signal crowding leads to peaks overlapping.[188,187,353] Though this report is primarily interested in ^{1}H spin-lattice relaxation times for PAMAM dendrimers, a short review of ^{13}C data has been included. The mechanisms that contribute to spin-lattice relaxation are discussed in **Appendix I**.

There is little published literature looking at ^{1}H spin-lattice relaxation times for dendrimers owing to the fact that the signals start to overlap as the generation increases. Meltzer *et al.* overcame this problem by building a series of PAMAM dendrimers (from an ammonia core) that incorporated a deuterium label at varying locations within the

structure.[188] By studying ^{2}H relaxation times they were able to show a slowing of molecular motion with increased molecular size, as well as the chain motion being most rapid near the terminus and slower in the interior. These results are not altogether surprising as we would expect steric hindrance to increase with higher generations, and a higher degree of movement at the chain ends reflecting less steric crowding when compared with the interior. Similar results were observed by Zhu *et al.* using modified poly(propylene imine) dendrimers.[191]

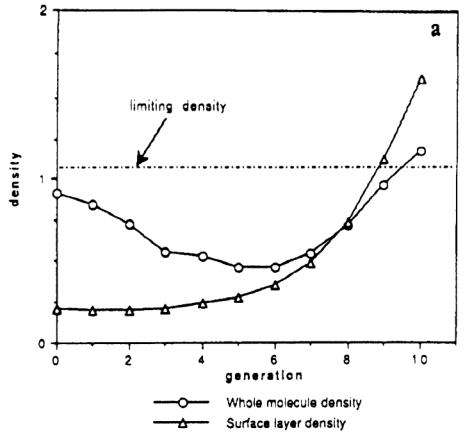

Figure 59. *Calculated molecular and surface densities for PAMAM dendrimers under ideal (defect-free) branching.*[187]

Perhaps the most interesting results come from the analysis of ^{13}C spin-lattice relaxation times, as ^{13}C NMR spectra of PAMAM dendrimers give more structural information than that from ^{1}H NMR. Work by *Meltzer* and *Tomalia et al*. (in a consecutive publication to his ^{2}H NMR study) showed that as the dendrimer size increased (G0 – 10) there was a gradual slowing of molecular motions, suggesting that, as no limiting state is reached, the terminal groups are not densely packed at the surface.[187,188] This led them to study the density of various generations and conclude that their data is consistent with the folding back of terminal groups into the interior of the molecule as suggested by dynamic modelling.[100,197,354] **Figure 59** illustrates calculated density changes during dendrimer growth and shows that the surface would be extraordinarily dense if compared with amorphous nylon (density cf. 1.1 g mL^{-1}).

2.5.2 Methodology

In order to compare how molecular size, branching density and solvent system effect T_1 measurements, three PAMAM dendrimer types were studied (cores of EDA, phloroglucinol and ammonia). Since work by Meltzer and Tomalia *et al.*[188,187,349] gives a comprehensive view of amine-surfaced dendrimers, ^{1}H T_1 data was obtained for half-generations up to G1.5 (G2.5 for EDA core) in two different solvents ($CDCl_3$ and MeOD), the dendrimers first being purified by column chromatography. ^{13}C NMR T_1 data could not be obtained because of the large amount of dendrimer required for these experiments to give accurate results (1 g mL^{-1}) whilst time constraints prevented the synthesis of higher generations.

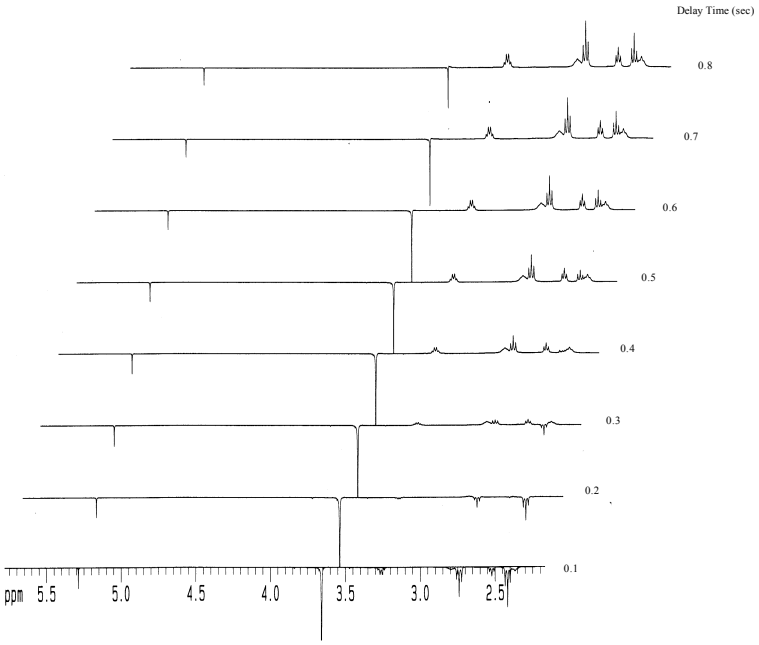

Figure 60. *An inversion-recovery NMR experiment from which the T_1 of 0.5-[Ammonia]-6-Ester was calculated.*

Dissolved oxygen is known to aid some spin-lattice relaxation mechanisms (**Appendix I**). Though this mainly affects small molecules, samples were degassed for 10 minutes with nitrogen prior to their spectra being obtained. An example of the inversion-recovery spectrum from which T_1's are calculated is shown in **Figure 60**.

As stated above, little data is available for direct comparison, indeed it has been shown that T_1 values are sensitive to a number of factors,[189] though overall trends in the data can be compared.

2.5.3 Discussion

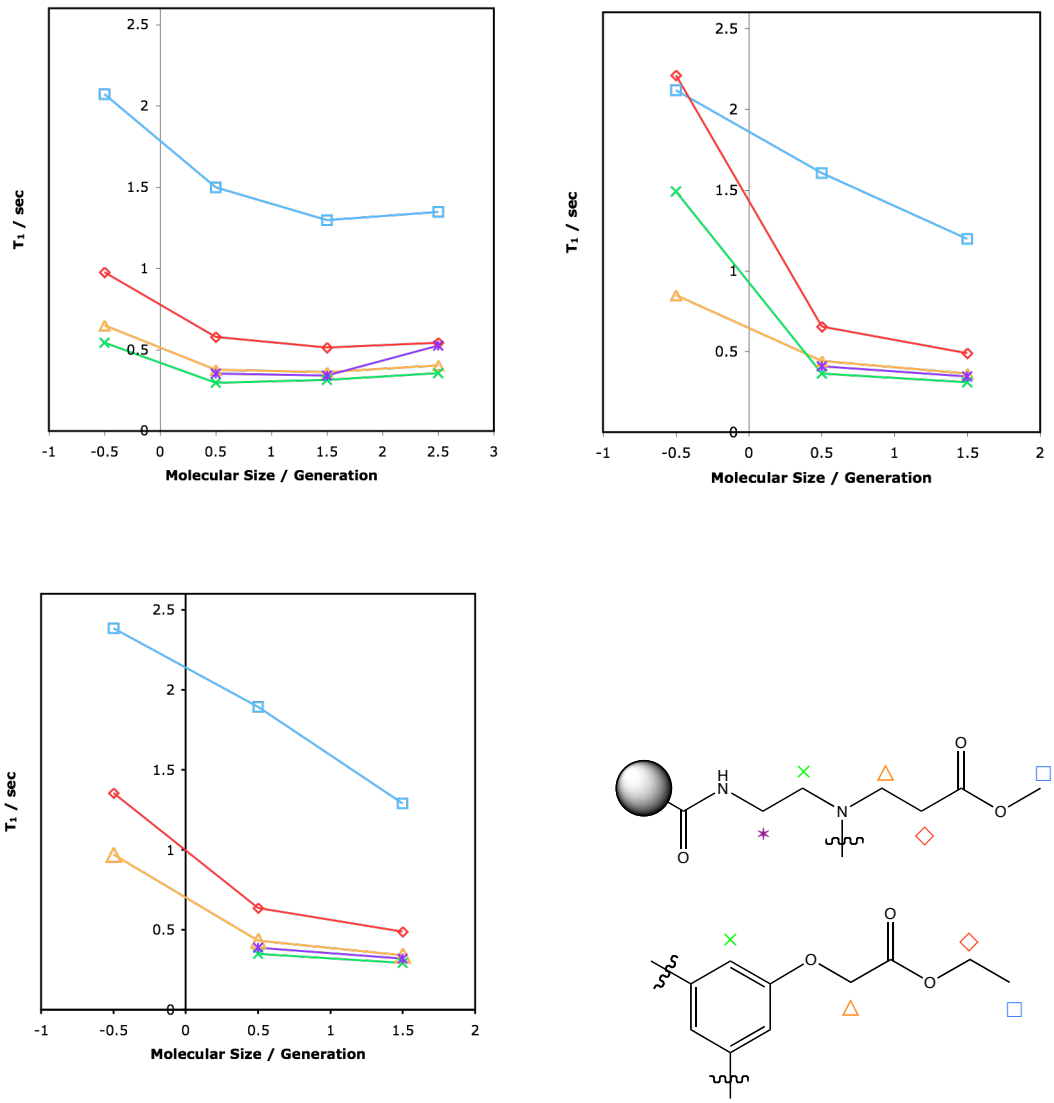

Figure 61. *Dependence of T_1 on molecular size for half-generation dendrimers of different cores (100 MHz, $CDCl_3$, 25°C), EDA (top left), ammonia (top right), and phloroglucinol (bottom left). Structure assignments are shown in the bottom right. Error bars not included owing as no repeat experiments available.*

The first observation that can be made from the T_1 data for ester-terminated dendrimers (**Figure 61**) is that the relaxation is much faster for nuclei closer to the core, which would suggest an increase in steric hindrance at the interior of the dendrimer. The outer methyl units relax much more slowly compared to all the others as we would expect, as they have a greater degree of movement. In agreement with published data,[187,188,191] we observe a downward trend in T_1 values as the size of the dendrimer increases. This too is the result of steric interactions; as the size of the dendrimer increases so the chains become more closely packed and their interactions increase, giving faster relaxation times. It should be noted that, in the case of generation 2.5 (EDA core), the relaxation time for the innermost observable methylene unit increases with respect to the others, possible due to the overlapping of interior signals.

In all cases it can be seen that the interior sites appear to plateau. This we would expect as the environment (particularly at sites × and ✶) changes very little with respect to generation and because of overlapping signals from other internal sites. The terminal methyl groups (□), however, do not show this behaviour at low generation as they encounter much less hindrance on the surface. It was expected that, as with the amine surface, the terminal groups will plateau at a much higher generation.[188] It is interesting to see that in the case of the EDA core this plateau appears to have been reached, though further measurements at higher generation would help to confirm this. It should be noted that G-0.5 (Phloroglucinol) has a different branch structure and as such cannot be used as a comparison in this case.

Next, the branching densities for these dendrimers were studied by comparing T_1 values as a function of the location of each particular atom on the branch. **Figure 62** shows the relaxation times of the three dendrimers as a function of their position from the surface.

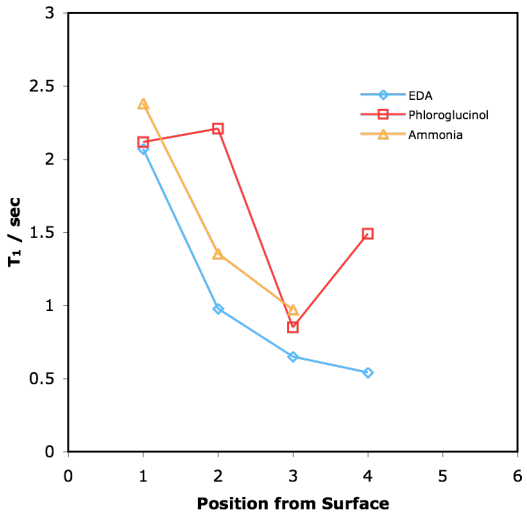

Figure 62. *Dependence of T_1 on location in branch for G-0.5 dendrimers (100 MHz, $CDCl_3$, 25°C). Error bars not included owing as no repeat experiments available.*

At generation -0.5 it can be seen that the sites on the ammonia-cored dendrimer have a slower relaxation time than the corresponding centres of the EDA-cored material. We would expect this as the EDA-cored dendrimer has an extra branch and thus increased steric interactions (and density). It can also be seen that a certain parallelism exists between these two core types, suggesting similar types of interactions between branches. In the case of the phloroglucinol core, these results cannot be directly compared to the others at this generation as it has a different branch structure as well as an ethyl instead of a methyl-terminated surface. Despite this, it is an interesting case in which the internal methylene (*site 2*) has a slower relaxation time than the terminal site. This could be due to a combination of factors; the conformation could be such that the terminal group is folded closer to the core, or, more likely, the methylene unit has a slow relaxation time because of its proximity to the ester group whilst the terminal methyl site can freely move (and rotate). Both these possibilities are supported by the fact that the T_1 value for *site 2* (2.210 s) is very similar to those of the terminal groups in the other two dendrimers (EDA: 2.072 s, ammonia: 2.384 s). Also of note is *site 4* which, as an aromatic proton, has a natural slower relaxation time than the methylene units.[355]

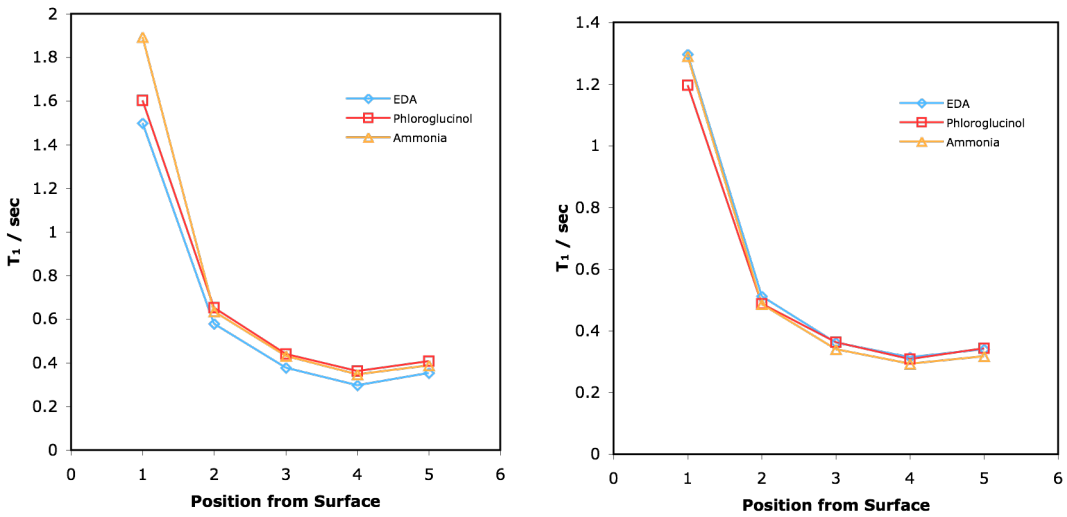

Figure 63. *Dependence of T_1 on location in branch for G0.5 (left) and G1.5 (right) dendrimers (100 MHz, $CDCl_3$, 25°C). Error bars not included owing as no repeat experiments available.*

In contrast to the generation -0.5 data described above, the trends shown for the generations 0.5 and 1.5 materials are completely different. The first thing to note is that all three dendrimers share similar T_1 values at similar sites for their respective generation. In the case of generation 0.5, the EDA cored dendrimer has a slightly lower relaxation time because of its extra branch, though this effect is negligible in the case of generation 1.5. It is suspected that, since we are only looking at the branches and not the cores, this is because the relative environment is the same. There is also a slight upwards inflection in the plots at *site 5*, which suggests a greater freedom of movement towards the interior. To help confirm this, the methylene unit closest to the core of the phloroglucinol dendrimer (δ 4.55 ppm) was studied and found to have a higher relaxation time compared to the outer branches, further suggesting that density is lower at the core (**Table 9**). The terminal sites retain their high relaxation times, which leads to a theory that this is an area of maximum density as commented on by *Meltzer et al.*[187,188]

Table 9. *Spin-lattice relaxation times of sites on phloroglucinol-cored dendrimers (100 MHz, $CDCl_3$, 25ºC).*

Generation	Site 4	Site 5	Methylene unit (δ 4.55 ppm)
-0.5	-	-	0.850
0.5	0.362	0.408	0.457
1.5	0.308	0.344	0.370

It is important to note an observation relating to the terminal methyl groups; as the generation increases, their relaxation times become more similar. This is something we would not expect to see at low generation, as the geometry of the cores should still allow for different branch separations (**Figure 64**). If we look first at the cores that have three branching points (i.e. ammonia and phloroglucinol) we can see that the surface groups of the ammonia-cored dendrimers have a longer relaxation time suggesting more movement at the surface. We can relate this information to the core structures (**Figure 65**), where we can see that the phloroglucinol core restricts the conformation so that at low generations it is mostly planar (or disc-like) whilst the ammonia core has much greater freedom of movement.

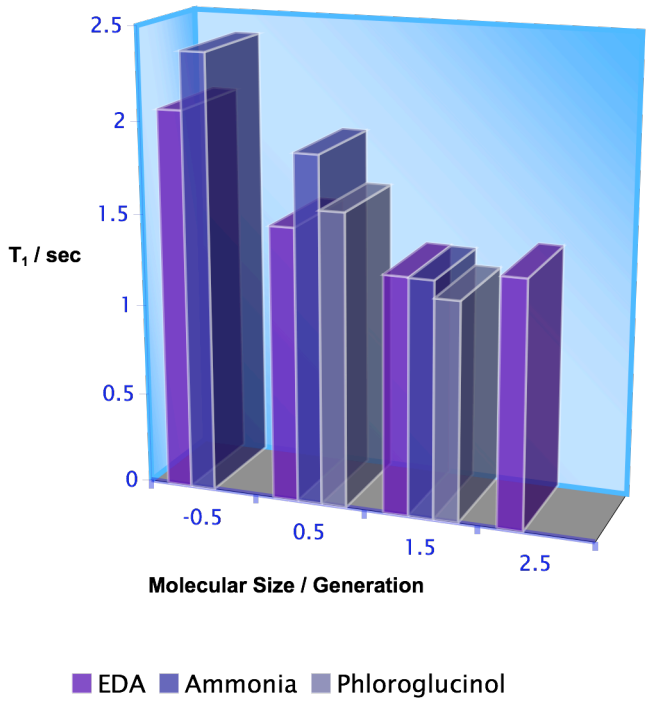

Figure 64. *Spin-lattice relaxation times of methyl ester surfaces (100 MHz, $CDCl_3$, 25°C).*

This core structure information also shows us that the addition of a branch (in the case of EDA) causes increased steric interactions and thus lowers the relaxation times. However, it is the overall trends that are most interesting. It is known that all T_1 values for the respective dendrimers decrease as the generation increases, but what is curious is that by generation 1.5 the terminal groups all have very similar relaxation times. This suggests that the core geometries no longer have any bearing on the overall structure as the branches are now long enough to be able to move to reduce any steric hindrance. The fact that the EDA-cored surface appears to plateau faster than that of the other two is attributed to the increased branching of the core.

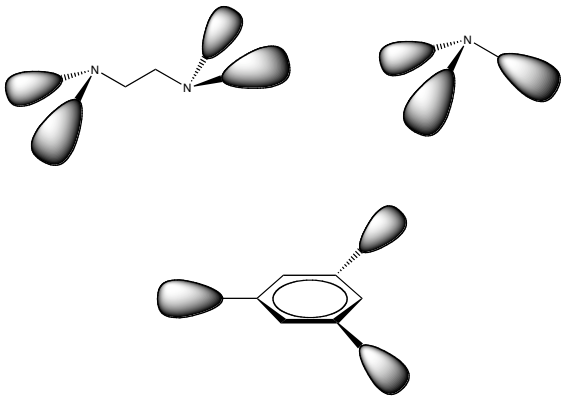

Figure 65. *Core geometries for EDA, ammonia and phloroglucinol dendrimers.*

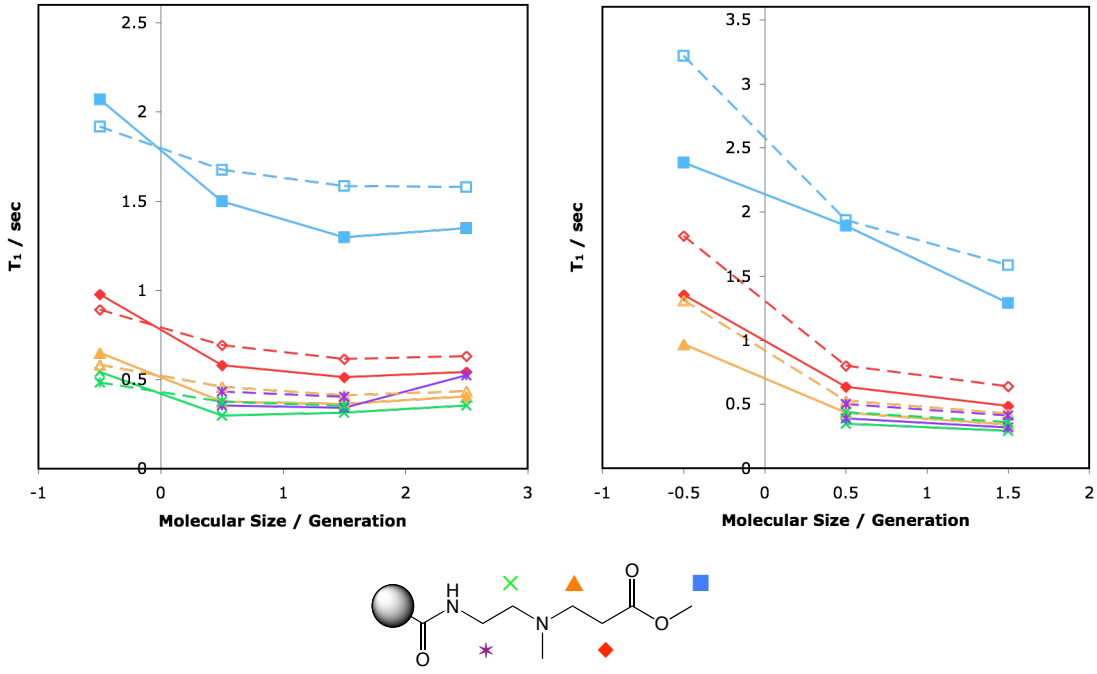

Figure 66. *Comparing T_1 values in different solvents for dendrimers with an EDA core (left) or an ammonia core (right). Solid lines represent $CDCl_3$, dashed MeOD (100 MHz, 25°C). Error bars not included owing as no repeat experiments available.*

A major factor in dendrimer growth and surface modification is that of the solvent system. The two graphs in **Figure 66** show that relaxation time measurements taken in deuterated methanol are generally higher when compared with those measured in deuterated chloroform, suggesting that the dendritic structure swells in methanol, most

likely due to the methanol breaking the internal H-bonds. The only exception to this observation is the generation -0.5 EDA-cored dendrimer, whereas the sample in chloroform gives higher T_1 values than in methanol for all sites.

2.6 Conclusions and Further Work

In order to study DNA-dendrimer interactions, a series of PAMAM dendrimers based around either an EDA or a phloroglucinol core were synthesised up to generation 4. These dendrimers were characterised by NMR and MS techniques, which gave valuable information that could be related to surface modification experiments performed in later chapters.

Spin-lattice relaxation times (T_1) of low generation dendrimers with ester surfaces (up to G1.5: having EDA, phloroglucinol and ammonia cores) were collected and used to probe the dendritic structure, showing that nuclei nearest the branch terminus move fastest. T_1 values for nuclei within the interior of dendrimers having an EDA core were shown to reach a plateaux after generation 1.5, suggesting that the relative environments for the interior sites remains constant at these generations (experiments on larger generations could give more information as to the interior environment near to the core). It was also demonstrated that, for similar generations, cores that contained three branches generally had slower T_1 values than those that had four branches, though these times became more similar with increasing generation. It was observed that the T_1 values for the outer methyl groups became similar across all the cores used, suggesting that even though some cores have different geometries or numbers of branches, a point is reached whereby the environment at the surface becomes very similar. What is surprising about this observation is that it occurs at such a low generation, showing that the core geometry plays a diminishing role as generation increases. This could be further studied by using a range of other cores and larger generations, giving a more comprehensive picture as to the influence of each core.

Chapter 3 Surface Attachments and Biological Studies

The binding of DNA to dendrimers can only be accomplished if the surface of the dendrimer possesses a positive charge, i.e. electrostatic interactions between the positive dendrimer and the negative DNA (backbone) cause them to become attracted to one another. Similarly, if one of these charges were removed (for example, on the dendrimer) they would unbind from each other. This gives rise to the idea that a pH sensitive dendrimer can bind/unbind (compact) DNA; in fact, there is plenty of published data to support this.[161,356-359] However, there is little data relating to the use of modified dendrimers. The surface modification of 4th and 5th generation PAMAM dendrimers, and their interactions with DNA and lipid bilayers, are discussed herein.

3.1 Surface Modifications

3.1.1 Acetylated Surface

The acetylation of a PAMAM dendrimers surface is a technique used to reduce the number of primary amines, and thus reduce the overall charge, that the dendrimer can possess.[199,234,360-362] This is typically achieved using either acetic anhydride (PAMAM)[234,360] or acetyl chloride (PPI)[363] depending on the dendrimer type and relative solvent solubility. Herein we describe the synthesis and characterisation of acetylated (Ac) PAMAM dendrimers using the method described by Baker *et al.*[234] that will then be used in either DNA or lipid bilayer binding experiments.

Acetic anhydride was added to solutions of dendrimer in dry methanol in the presence of triethylamine and the mixture was allowed to stir overnight. The solutions were then dialysed against deionised water and the surface coverages were determined through NMR analysis. Phosphate buffer at pH 8.0 was originally used but was found to promote intermolecular interactions that led to the formation of insolubles.

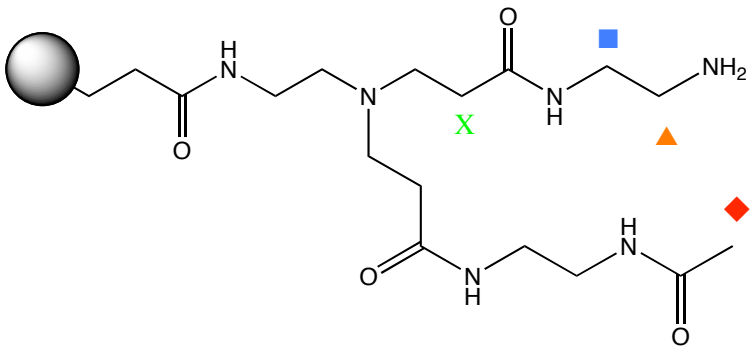

***Figure 67**. Terminal branching structure of a partially acetylated dendrimer.*

***Table 10**. Acetylation experiments involving 1st generation dendrimers and resulting coverages as determined by ^{1}H NMR spectroscopy.*

Compound no.	Dendrimer used	Expected no. Ac groups	Integral of ◆ relative to 24H (X)	Calculated no. Ac groups[a]
119	1-[EDA]-8-Amine	2	8.9	3
120	1-[EDA]-8-Amine	4	14.8	5
121	1-[EDA]-8-Amine	6	19.7	7
122	1-[EDA]-8-Amine	8	26.5	9

[a] Results higher than expected due to trapped solvent.

In order to gain a better understanding of this reaction and the related analysis, 1st generation PAMAM dendrimers (8 amine surface groups) were acetylated to varying degrees (**Table 10**). We would expect to see a new singlet around δ 2.00 ppm in the ^{1}H NMR (D_2O) relating to the acetyl group (◆) that increases in intensity with higher coverages, along with a change in dendritic peak integrals as ▲ (~ δ 2.80 ppm) moves to an environment similar to ■ (~ δ 3.25 ppm). The first thing to note from the ^{1}H NMR of these products is the presence of the resulting acetic acid – triethylamine salt as, although the samples were dried under vacuum prior to analysis, no further purification was possible. The triethylamine triplet and quartet signals appear at δ 1.24 and 3.16 ppm respectively, together with the acetic acid singlet at δ 1.87 ppm. New peaks are observed at δ 3.41, 3.03 and 1.94 ppm, the first two of which were broad and remain unassigned as they had been in work carried out by Baker *et al*.[234] The third peak was a

sharp singlet and corresponds to the acetyl group on the dendrimer surface (◆). If this integral is compared with that of a peak relating to the dendrimer interior at δ 2.40 ppm (X and similar environ) it can be seen that it increases in intensity with higher surface coverage, but is always slightly higher than expected. This is most likely due to solvent being trapped within the dendrimer sample at the time of weighing, causing the relative number of acetic anhydride equivalents used to increase. This is confirmed in the case of **122**, where a higher than possible coverage is seen. It was also observed that as the coverage increases the dendritic signals shift downfield and, in some cases, have their integrals reduced to zero (possibly due to poor relaxation).

Table 11. *Acetylation experiments of 4th and 5th generation dendrimers and resulting coverages as determined by ^{1}H or ^{13}C NMR spectroscopy.*

Compound no.	Dendrimer used	Expected no. Ac groups	Calculated no. Ac groups
123	4-[EDA]-64-Amine [a]	16	– [d]
124	4-[EDA]-64-Amine [a]	32	34
125	4-[EDA]-64-Amine [a]	48	40
126	4-[EDA]-64-Amine [a]	64	46
127	4-[EDA]-64-Amine	16	16
128	4-[EDA]-64-Amine	48	47
129	4-[EDA]-64-Amine	64	54
130	4-[EDA]-64-Amine [b]	48	50
131	5-[EDA]-127-Amine-1-FITC (**132**) [c]	64	67

[a] Dialysis in phosphate buffer. [b] Acetic anhydride-d_6 used. [c] Reaction performed with the aid of a 4th year undergraduate, L. Carrington. [d] Product found to be insoluble

This reaction was repeated using larger dendrimers (namely 4th and 5th generation), the results of which are shown in **Table 11** and **Figure 68**. The first attempt at acetylating 4th generation dendrimers (**123** – **126**) involved dialysis in a phosphate buffer (pH 8.0) and resulted in the formation of precipitates during workup, thus lowering the resulting yields. It was believed that these are the result of the dendrimer arms inter-colating with

each other, which led to reduced solubility and thus lower than expected coverages. In the case of the 25% coverage (**123**), the resulting product could not be dissolved at all. The acetylation of 4th generation dendrimers was repeated without the use of the dialysis in buffer step which gave much better results (**127** – **129**), suggesting that the buffer promotes the formation of the previously observed insolubles. The highest coverage was found not to give total coverage, possibly as a result of some amines remaining in the interior of the dendrimer[179] or because defects on the surface resulted in fewer than expected amine groups being present (^{13}C NMR data can help determine this).

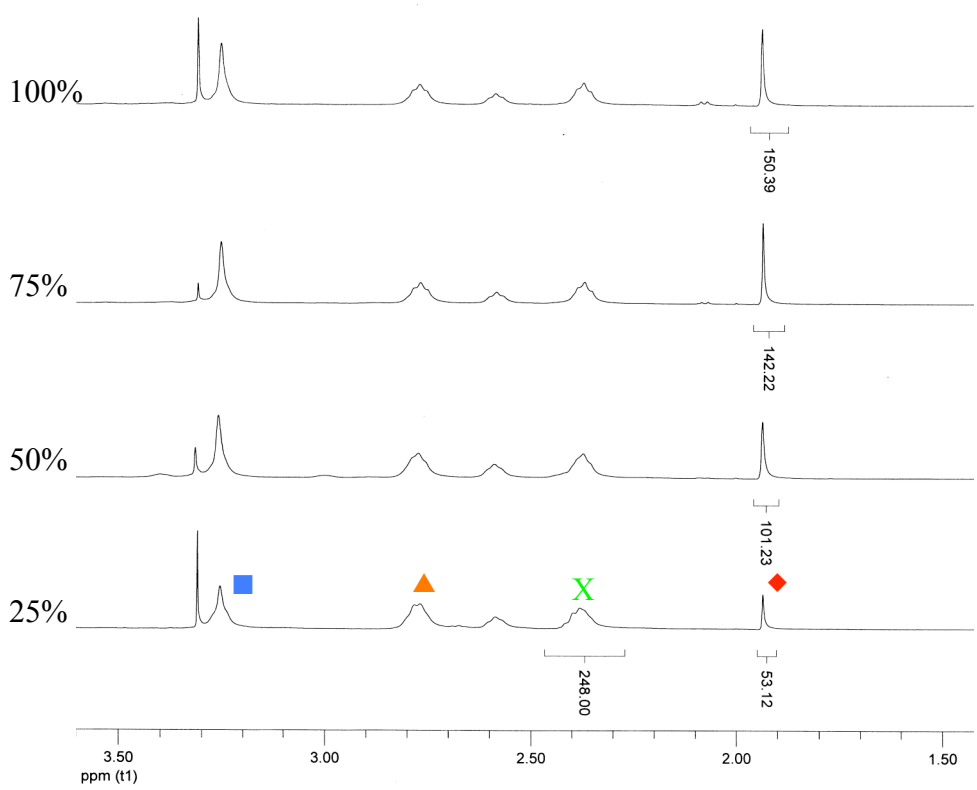

Figure 68. *^{1}H NMR (D_2O) spectra of 4th generation dendrimers with differing acetyl coverages, bottom to top:* ***127, 124, 128, 129***.

The ^{13}C NMR spectra (D_2O) of these acetylation experiments (**127** – **129**) show peaks relating to unreacted amine branches at δ 41.3 (■) and 40.3 ppm (▲), and acetylated branches at δ 39.3 and 39.2 ppm. These are present in the spectrum of the 25% coverage sample but resonances for the unreacted branches are absent in the 75% and 100% material. This would be expected in the case of the 100% coverage (if the reaction had gone to completion), but not for the 75% case. This may suggest that the

dendrimer used contains defects such that the 75% coverage covers all available amine groups. It is unlikely, however, that 25% of the surface is covered with defects, since the 100% coverage gives 54 acetyl groups instead of 64. The loss of the amine branch signals may be explained by the more abundant acetyl branches distorting them, possibly by forcing them to bend into the dendrimer interior or changing the symmetry of the structure.

Using inverse gated decoupled ^{13}C NMR it is possible to estimate the degree of defects present in the acetylated dendrimers as the signals can be integrated. By standardising the dendrimer carbonyl groups (other major peaks were masked by the solvent – methanol-d_4) with an integral of 124, as there should be that number of groups present, it was found that both defect peaks (see **Section 2.2.3**) present at δ 46.6 and 37.0 ppm have integrals of 8; though if integrated relative to other peaks, a lower defect integral is obtained. This suggests that up to 8 surface groups are cross-linked with EDA, which is supported by the observation that higher degree acetylation experiments were not giving complete coverage.

The acetylation was also attempted using deuterated acetic anhydride (**130**) and found to produce a surface coverage of 79% (the target was 75% coverage) as analysed using inverse-gated ^{13}C NMR. A sample of previously modified 5th generation dendrimer (with 1 fluorescein group, **132**) had 50% of its surface acetylated (**131**) so that it could be used in fluorescence studies with lipid bilayers (**Section 3.3**).

3.1.2 PEG Surface

There are many reported examples of the synthesis of PEGylated dendrimers, primarily as a way to reduce cytotoxicity.[364] Generally the PEG chains are attached to the dendrimer *via* an activated ester and their surface coverages are characterised by MS and NMR.[364-368] Whilst this is a very valid route, the use of NMR in this case to determine the coverage is hindered by the broadness and overlapping of all peaks involved. Elemental analysis gives an accurate idea of ratios between nuclei which is very useful for small molecules but less so for a dendrimer, as these typically contain solvent within their interiors. By introducing a non-common nucleus into the PEG

chain it becomes possible to study its ratio with the nitrogen atoms of the dendrimer (assuming that no nitrogen-containing solvent is present). To this end, a route was devised that would allow for the incorporation of a sulphur atom as part of a thiourea linker derived from an isothiocyanate. Aside from the linker group, the type and length of the PEG chain to be attached is also important. In the present study, a monomethyl PEG with an average molecular weight of 550 Da is used as chains of this length have been shown to aid drug encapsulation and delivery.[299,302,369] To use longer chains may result in added surface bulk such that no DNA binding can take place (NOESY experiments have shown there to be no penetration of PEG chains into the central PAMAM domain[370]), whilst shorter chains may not give any increased benefit.

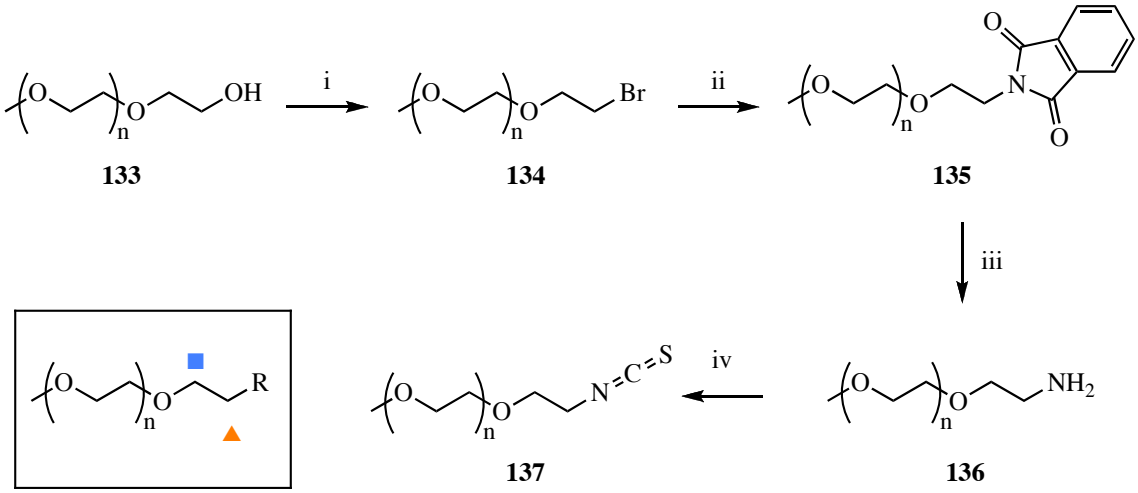

133 **134** **135** **136** **137**

Scheme 11. *Synthesis of α–methyl-ω-isothiocyanatopoly(ethylene glycol). i, PBr_3, DCM 0°C; ii, potassium phthalimide, MeOH, reflux; iii, hydrazine, MeOH, reflux; iv, $CSCl_2$, Na_2CO_3, chloroform, RT. (n = 5 – 16)*

In order to attach PEG chains to the surface of a dendrimer they must first be given the functionality to do so (**Scheme 11**). Half an equivalent of phosphorus tribromide[371] was added to a solution of monomethyl PEG (**133**) in DCM and cooled over ice. After 2 hours, ice was added to quench the reaction and the product was extracted into DCM to give **134** as a colourless oil in an 82% yield. ^{1}H NMR ($CDCl_3$) gave a singlet at δ 3.36 ppm that relates to the methoxy group whilst 2 triplets at δ 3.79 and 3.45 ppm have been assigned as ■ and ▲ respectively. A broad singlet at δ 3.62 ppm arises from the methylene repeat unit. It should be noted that other signals were visible and are assigned as methylene protons nearest the methoxy (CH_3-O-CH_2-) and ■ groups. The

^{13}C NMR spectrum showed 5 major signals, the strongest of which being for the methylene repeat unit at δ 70.5 ppm (**Figure 69**). Peaks at δ 71.9, 71.1 and 59.0 ppm show no change from the starting material and are assigned as (CH_3-O-CH_2-), ■ and the methoxy group respectively. The remaining peak at δ 30.3 ppm is assigned as ▲ and shows a large upfield shift compared to the starting material. Mass spectrometry (MS, ES^+) showed a large distribution of peaks with spacings of 44 Da (m/z 559.3 Da relates to n = 9 at 100%) confirming that the PEG product had been formed. FTIR also confirms the formation of **134**, showing the loss of the O-H stretch from the starting material whilst gaining a C-Br stretch at 653 cm^{-1}.

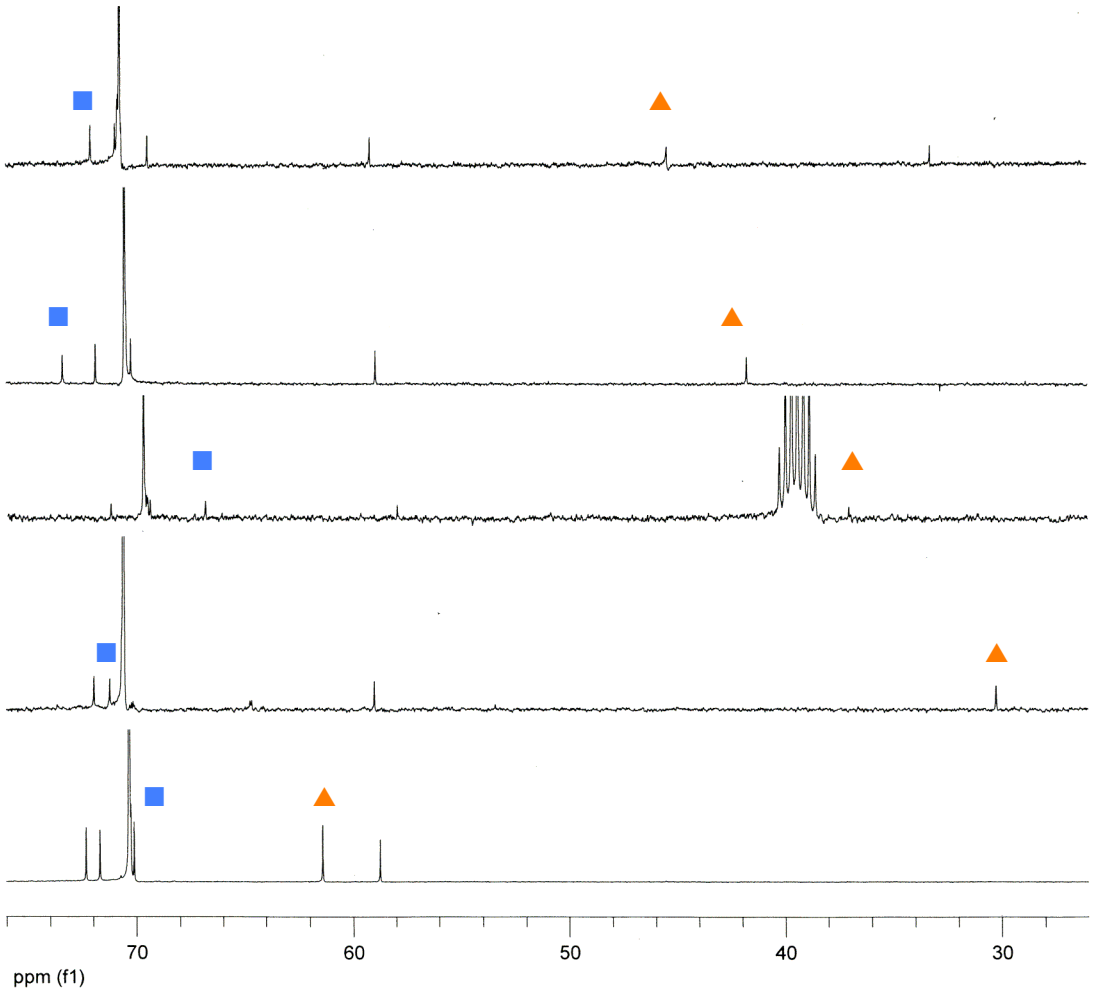

Figure 69. *^{13}C NMR spectra of PEG products **134** ($CDCl_3$), **135** (DMSO-d_6), **136** ($CDCl_3$) and **137** ($CDCl_3$), together with starting material **133** ($CDCl_3$).*

Potassium phthalimide was added to a solution of **134** in dry methanol and allowed to reflux in the first step of the Gabriel Synthesis.[372,373] After 22 hours, the methanol was removed and the product was isolated by partioning between ethyl acetate and water to give **135** as a white oily solid in a 20% yield. The reason for this low yield is suspected to be due to product being lost through repeated washings with other solvent systems (in order to find a system that worked). ^{1}H NMR studies (DMSO-d_6) revealed new peaks in the aromatic region relating to the phthalimide group. The triplet relating to ■ moved upfield to δ 3.62 ppm whilst the triplet of ▲ moved downfield to δ 3.75 ppm. ^{13}C NMR data confirmed the presence of the phthalimide group (aromatic region not shown in **Figure 69**) and showed a downfield shift of ▲ to δ 37.3 ppm. MS (ES^+) again showed a distribution, the most abundant being at m/z 679 Da (n = 9). FTIR indicated the formation of **135** by peaks at 3059 cm^{-1} ([Ar] C-H stretch) and 1709 cm^{-1} (C=O stretch).

The second stage of the Gabriel Synthesis was accomplished by the addition of hydrazine[372,373] to the phthalimide derivative (**135**) in methanol which, after 72 hours at reflux, resulted in a lime green solution. The crude material was dissolved in basic water (pH 11, NaOH) and the product extracted into DCM to give the amine **136** as a colourless oil in a 44% yield. ^{1}H NMR ($CDCl_3$) showed that ■ and ▲ had moved upfield to δ 3.49 and 2.85 ppm respectively; this is a large shift in the case of ▲ a result of the deshielding effect of the amine. There were no longer any signals in the aromatic region, these having been replaced with a broad singlet at δ 1.50 ppm relating to the amine. The signal assigned to ▲ moved to δ 41.8 ppm in the ^{13}C NMR spectrum. MS and FTIR confirmed the product as **136**.

A solution of amine **136** in chloroform was added very slowly to a stirred solution of thiophosgene and sodium carbonate in chloroform.[373] After stirring at room temperature for 72 hours the remaining solids were removed by centrifugation to give isothiocyanate **137** as a yellow oil in a 76 % yield. Analysis of this product by ^{1}H NMR ($CDCl_3$) revealed that the majority of the peaks were overlaid with the methylene repeat unit at δ 3.67 ppm. ^{13}C NMR data failed to show evidence of the isothiocyanate group, though a downfield shift of ▲ was observed (δ 45.2 ppm). MS confirmed the presence of **137**, whilst FTIR showed a characteristic N=C=S stretch at 2116 cm^{-1}.

With the successful preparation of isothiocyanate **137**, the PEG chains were then attached to the amine surface of various dendrimers. A solution of isothiocyanate **137** in 1,4-dioxane was added dropwise to a stirred solution of dendrimer in water in the presence of triethylamine. The resulting crude material was then purified by dialysis in water, giving final product as a viscous orange oil. As expected, the resulting PEGylated dendrimers were found to be soluble in DCM owing to the solubilising effect of the PEG chains. NMR spectroscopy was not used to analyse these dendrimer samples because of the large number of nuclei present; elemental analysis was used instead. By looking at the ratio between the nitrogen (predominantly from the dendrimer) and sulphur atoms (from the PEG units) we can get an accurate idea of the degree of surface coverage (carbon and hydrogen nuclei are not used as these will be affected by the inevitably trapped solvent). For the PEGylated dendrimers prepared, fairly accurate coverages were obtained (**Table 12**). These were then used to study dendrimer-DNA (**Section 3.2**) and dendrimer-lipid interactions (**Section 3.3**).

***Table 12**. PEGylated dendrimers synthesised and resulting coverages as determined by elemental analysis.*

Compound no.	Dendrimer used	Expected no. PEG groups	Calculated no. PEG groups
138	4-[EDA]-64-Amine	16	23
139	4-[EDA]-64-Amine	16	18
140	5-[EDA]-128-Amine	32	26
141	5-[EDA]-128-Amine	32	25
142	5-[EDA]-127-Amine-1-FITC (**132**) [a]	64	57

[a] Reaction performed with the aid of a 4th year undergraduate student, L. Carrington.

3.1.3 Fluorescent Surface

The incorporation of fluorescent groups onto/into a dendritic structure has been the source of much investigation in the literature (**Section 1.3.8**). The principle use is to make dendrimers visible by fluorescence microscopy during DNA binding studies. Indeed, the attachment of groups such as dansyl chloride (**142**) and fluorescein isothiocyanate (**143**) is easily accomplished (**Figure 70**).

Reported literature has shown that the surface of a PAMAM dendrimer can be wholly dansylated by using an excess of dansyl chloride in basic aqueous conditions (Schotten-Baumann procedure) to give high fluorescence.[267] This method was modified to give a low surface coverage (4 groups) of a 4th generation dendrimer that would still allow the remaining free amines to bind to DNA.

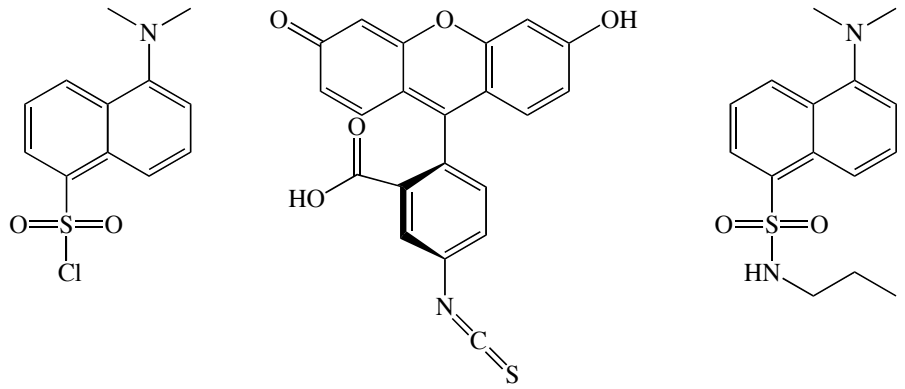

142 **143** **144**

Figure 70. *Structures of dansyl chloride (**142**), fluorescein isothiocyanate isomer I (FITC) (**143**) and 5-(dimethylamino)-N-propylnaphthalene-1-sulphonamide (**144**).*

Analysis of this product by ^{1}H NMR studies ($CDCl_3$) revealed the presence of aromatic signals suggesting that the attachment was successful. Integral data suggests the presence of 7 dansyl groups, but since only 4 equivalents were used this is unlikely (such a large discrepancy is likely to be the result of integrating over such a large area, δ 7.80 – 6.30 ppm). However, it is possible that a slightly higher than expected coverage is possible as solvent may still have been present during the weighing of the dendrimer, effectively decreasing the amount of dendrimer and thus increasing the effective

number of dansyl equivalents used (the same problem was observed for the acetylation of 1st generation dendrimers). UV/Vis experiments were performed (**Figure 71**), but in order to get an accurate picture of the absorbances involved a small dansyl derivative (**144**) was also synthesised.[374]

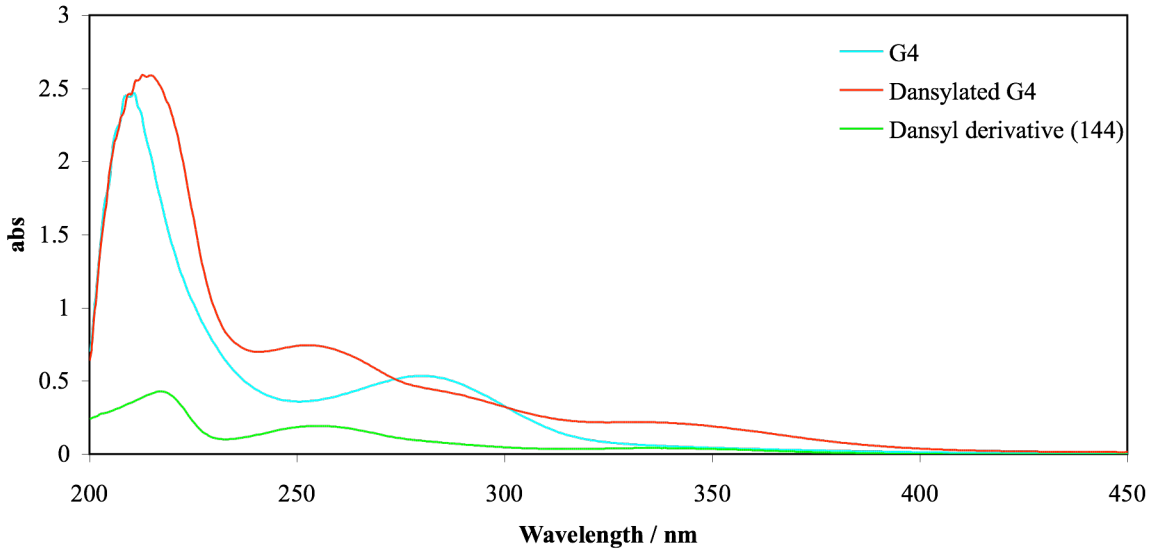

***Figure 71**. UV/Vis spectrum showing 4th generation dendrimer (9.95 x 10^{-6} M, λ_{max} 280 nm, ε 67,500), dansyl modified G4 dendrimer (9.58 x 10^{-6} M, λ_{max} 217 nm, ε 262,500) and small dansyl molecule **144** (9.33 x 10^{-6} M, λ_{max} 217 nm, ε 45,500).*

Figure 71 shows that the modified dendrimer sample has dansyl groups on its surface, as demonstrated by the addition of a strong absorbance at 255 nm not present in the spectrum of the unmodified PAMAM dendrimer. That this absorbance is attributed to the dansyl group is demonstrated by molecule **144**. Other absorbances of note are the dendrimers' absorbance at 280 nm (carbonyl n-π*) and the dansyl absorbances at 217 (naphthalene unit), 255 and 330 nm, further confirming the presence of dansyl groups on the modified dendrimer.[263,374] By normalizing concentrations and absorbances it was possible to calculate the number of dansyl groups present on the dendrimer using the relative extinction coefficients; surface coverage was estimated at 6 groups, showing that the UV/Vis data compares well to that determined by NMR.

It was found that visualising dansylated dendrimers, when bound to DNA, proved difficult so it was decided that use of a fluorescein group would be explored instead. This group should be easier to locate within the cell nucleus as the microscopy visualisation technique used can be more readily calibrated to its transmission frequencies. To that end, fluorescein isothiocyanate (**143**) was added to a series of 4th and 5th generation dendrimers in DMSO. These were then dialysed against water, and their composition analysed using elemental analysis to give an estimate of the level of surface coverage (shown below).

Table 13. *FITC dendrimers synthesised and resulting coverages as determined by elemental analysis.*

Compound no.	Dendrimer used	Expected no. FITC groups	Calculated no. PEG groups
145	4-[EDA]-64-Amine	2	1
146	4-[EDA]-46-Amine-18-PEG (**139**)	2	2
147	5-[EDA]-128-Amine	2	23 [b]
132	5-[EDA]-128-Amine [a]	2	1
148	5-[EDA]-103-Amine-25-PEG (**141**)	1	3

[a] Reaction performed with the aid of a 4th year undergraduate student, L. Carrington.
[b] Sample contaminated with DMSO.

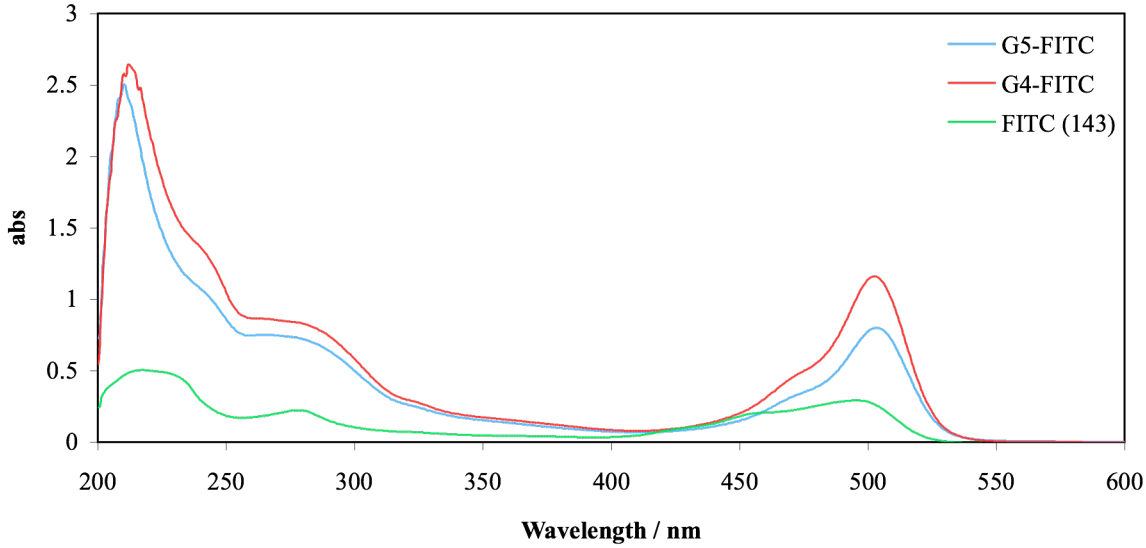

Figure 72. *UV/Vis spectrum showing FITC modified 5th generation dendrimer **147** (9.12 x 10^{-6} M, λ_{max} 503 nm, ε 89,100), FITC modified 4th generation dendrimer **145** (9.67 x 10^{-6} M, λ_{max} 503 nm, ε 122,100) and FITC **143** (9.49 x 10^{-6} M, λ_{max} 495 nm, ε 25,600).*

The UV/Vis spectra of **145** and **147** are shown in **Figure 72** and compared with that of FITC (**143**). It can be seen that the main absorbance of the fluorescein group appears at ~ 500 nm[375,376] and thus this has been successfully attached to the dendrimers. These FITC-modified dendrimers were then used in DNA and lipid binding studies (**Sections 3.2** and **3.3**).

3.2 Dendrimer–DNA Interactions

The DNA condensation induced by a selection of PAMAM dendrimers synthesised in previous sections was studied in collaboration with PhD student Kristina Fant (Chalmers University, SE)[330,377] and her results are included in this report to give better idea for their applications (results reproduced with permission). Interactions between DNA and dendrimers were investigated at various charge ratios (commonly defined as the concentration of positive amines on the dendrimers over the concentration of the negative phosphates on the DNA) to aid in the understanding of complex formation.

3.2.1 Comparing DNA Binding of Unmodified and PEGylated Dendrimers.

By varying the charge ratio between unmodified 5th generation dendrimers and DNA it is possible to use linear dichroism (LD) and ethidium bromide titrations to gain an idea of the structure of the resulting complexes.

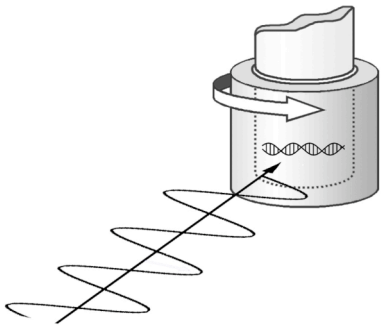

Figure 73. *Representation of a flow Linear Dichroism setup.*

Linear dichroism uses polarized light to give detailed information about the orientation of a given sample. In this work, the sample was orientated by introducing a shear flow gradient, i.e. the sample was placed in a narrow gap between two quartz cylinders; the inner cylinder then being rotated to align long molecules in the sample (**Figure 73**). In our case, the samples consist of complexes formed between the dendrimers and DNA, the results of which are shown in **Figure 74**.

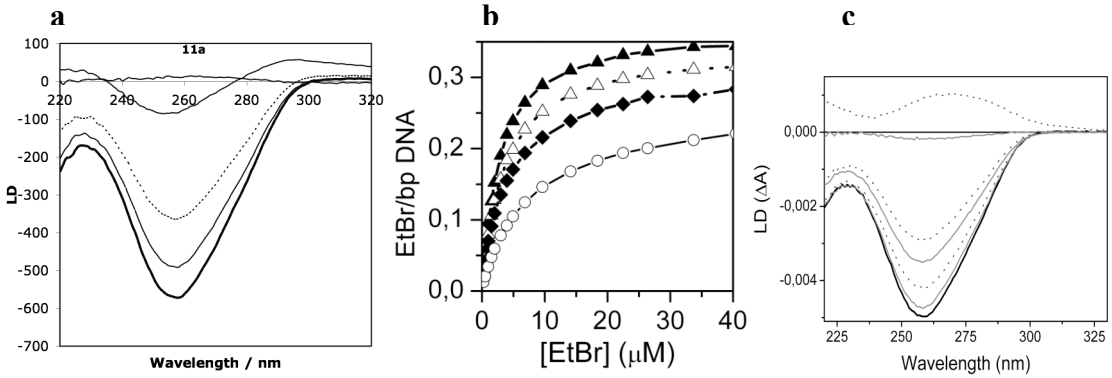

***Figure 74**. Characteristics of dendrimer-DNA complexes as a function of charge ratio (r). a) DNA compaction using unmodified G5 dendrimers shown by flow LD of the DNA absorption band. b) Ethidium cation binding isotherms of unmodified G5 dendrimer complexes as determined by emission measurements. c) DNA compaction comparing unmodified G4 and PEGylated-G4 (25%, **139**) dendrimers shown by LD of the DNA absorption band. Data for 'a' and 'b' corresponds to uncondensed DNA (— or ▲); r = 0.2 (---); r = 0.5 (···· or △); r = 1 (-·- or ◆); r = 1.5 (—); and r = 2 (○). Data for 'c', solid lines represent PEGylated G4, dashed lines represent unmodified G4, at charge ratios r = 0.25, 0.5 and 1.*

It was found that, as expected, the alignment of the DNA disappears as the amount of dendrimer is increased, and when the DNA is sufficiently condensed the LD signal vanishes (**Figure 74a**). This shows that the DNA is becoming condensed to such a point that there is no/very little free DNA present in the sample. **Figure 74b** shows results of an ethidium bromide titration which sought to discover the number of remaining binding sites present on the DNA (its fluorescence increases considerably once it intercalates with DNA[378]). This was modelled by estimating ethidium bromide binding constants as well as determining the remaining fraction of available binding sites using the 'nearest neighbour model'.[379] The data (**Table 14**) shows that a large amount of binding sites remain available on the condensed DNA, which together with the LD measurements, suggests the condensed complexes have a relatively loose structure with a high degree of flexibility.

Table 14. *Apparent binding constants (K) and remaining binding sites after DNA condensation for ethidium bromide bound to unmodified 5th generation dendrimer/DNA complexes.*

Ratio	K (x 10^6 M^{-1})	% Remaining binding sites [a]
Uncondensed DNA	0.33	100
r = 0.5	0.17	97
r = 1	0.13	91
r = 2	0.05	82

[a] Binding site size was estimated to 2.5 base pairs and assumed not to change upon dendrimer binding to DNA.

When the behaviour of unmodified 4th generation dendrimers is compared with that for PEGylated derivatives (25% surface coverage, **139**) it can be seen that, from preliminary results, the PEGylated samples do not condense DNA to the same extent, thus giving 'looser' structures in which the DNA is better orientated (**Figure 74c**). It should be noted that these comparisons were made at the same *charge* ratio, not molar ratio. This means that the observed difference in binding cannot be attributed to the fact that the PEGylated dendrimer possess fewer positive charges. Ethidium bromide binding titrations were carried out with DNA complexes (unmodified 5th generation and 25% PEGylated 5th generation dendrimers) formed under one of two sets of conditions: in water or in cell growth medium (Ham's F12).[380] The binding isotherms (**Figure 75**) indicate that complexes formed in water are much more dense when compared with those in growth medium, as shown by the higher amount of intercalation of the latter. They also show that, regardless of conditions, unmodified dendrimer samples give a higher density complex with DNA. This interpretation of the binding results is supported by dynamic light scattering experiments (DLS), which shows that complexes formed in the growth medium are much larger than those formed in water (**Figure 75**). The size of the complexes was also studied as a function of time; complexes formed in water were found to be stable over a 2 hour period and remained at a size beneficial to endocytosis[381] (G5 ~ 80 nm, G5-PEG ~ 110 nm), whilst those formed in growth medium continued to grow into large aggregates.

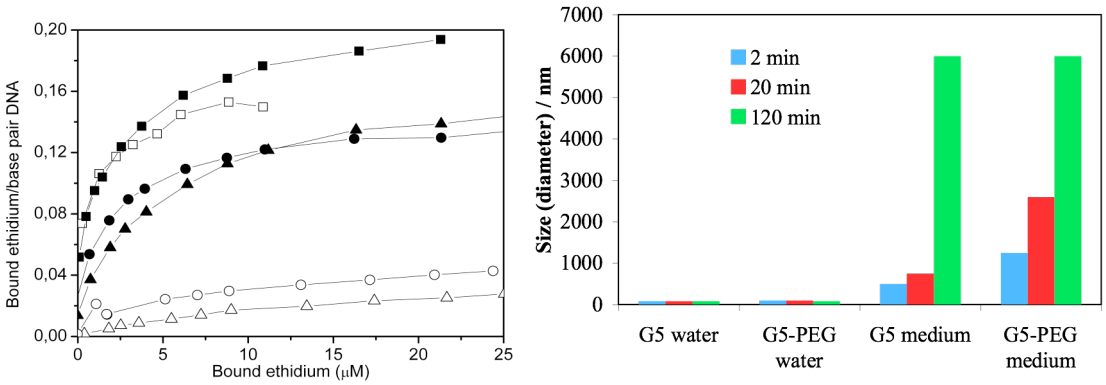

Figure 75. *Effect of buffer conditions on morphology of unmodified and PEGylated dendrimer (**140**)-DNA complexes as shown by ethidium cation binding isotherms (left) and dynamic light scattering (right). Binding isotherms for G5 (△ and ▲) and PEG-G5 (○ and ●) complexes as well as uncondensed DNA (□ and ■), formed in water (open symbols) or cell growth medium (filled symbols).*

3.2.2 Uptake in Mammalian Cells

Confocal images were taken using fluorescence microscopy showing the uptake of fluorescein labelled 4th and 5th generation dendrimers (**145** and **147** respectively) in live CHO-K1 cells. These reveal that the fluorescent dendrimers (green) locate themselves within the cells. It was observed that some of the fluorescent clusters are bigger and brighter than others, suggesting that they have interacted with DNA and become compacted. Similar observations were noted in the literature using HeLa cells.[382]

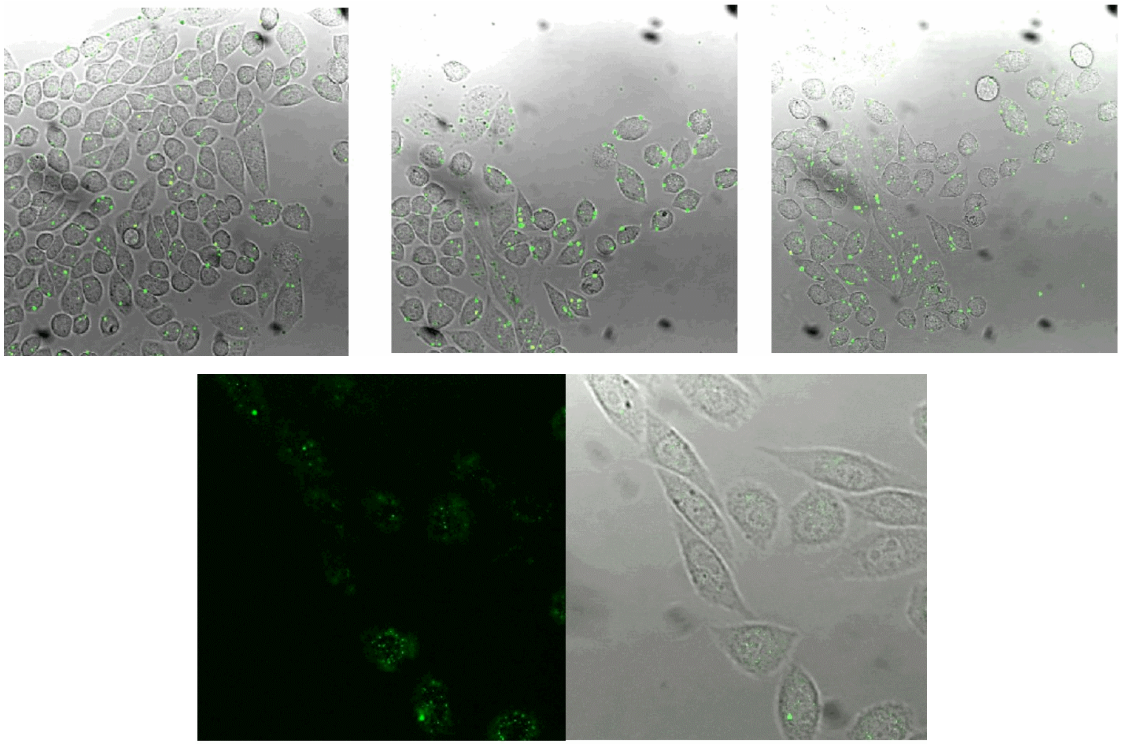

Figure 76. *Confocal images of the uptake of FITC-labelled G4 (**145**, top) and G5 (**147**, bottom) PAMAM dendrimers in CHO-K1 cells. All images were acquired after 1 hr incubation at 37ºC.*

3.2.3 Cytotoxicity of Modified Dendrimers

Preliminary results for *in vitro* cytotoxicity in cultured mammalian cells of various modified dendrimers and their corresponding DNA complexes are shown in **Figure 77**. 4th Generation dendrimers with PEG or acetyl surfaces appear to significantly lower the toxicity compared to the control, whilst others raised toxicity.[326,327,364] The results for the complexes differ somewhat compared to the unbound dendrimers, which is not surprising considering they have very different properties regarding size, morphology and surface charge.

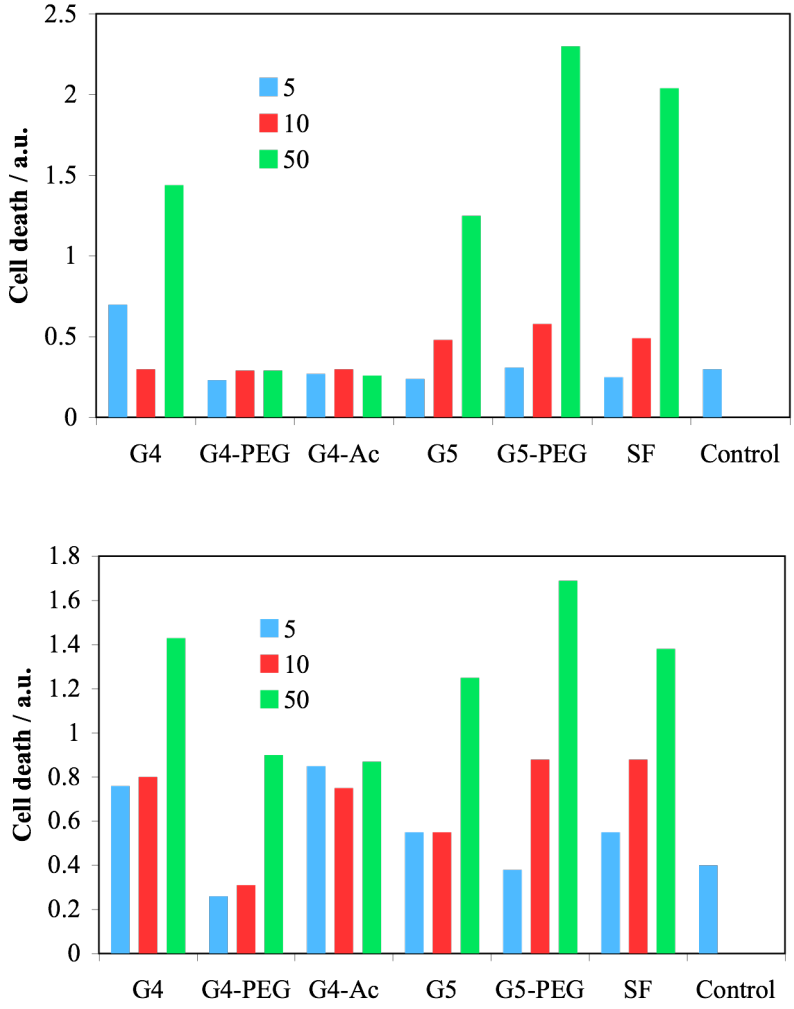

Figure 77. *Cytotoxicity of functionalised dendrimers in CHO-K1 cells following 48 hrs incubation of dendrimers alone (top) or dendrimer/DNA complexes (bottom). The amount of dendrimer corresponds to charge ratios 5, 10 and 50 when incubated with 1 μg DNA. The amount of dead cells was determined through measuring leakage of cytoplasmic lactate dehydrogenase, an early indicator of cell death. Data has been averaged over 3 experiments.*

3.3 Dendrimer–Lipid Bilayer Interactions Studied using Fluorescence Microscopy

Fluorescence microscopy of phospholipids is a convenient tool for the study of model biological membranes. Lipid systems can adopt a variety of liquid-crystalline phase structures by varying the water content and/or temperature (shown in **Figure 78**), the formation of which is driven by the hydrophobic effect.[383] Lyotropic (can form a liquid crystalline phase) lipids provide an accessible medium in which to monitor the absorbance and uptake of fluorescently labelled dendrimers. The lamellar liquid crystal phase is comprised of amphiphilic lipids arranged in bilayer sheers separated by layers of water. This phase is useful for the study of dendrimer-lipid bilayer interactions as each bilayer is a prototype of the arrangement of lipids in cell membranes. The interaction of dendrimers with an inverse hexagonal phase can also be studied. In this phase the amphiphile molecules are aggregated into cylindrical structures giving long-range orientational order. Using fluorescence microscopy, it is possible to visually observe the distribution and association of fluorescein-tagged dendrimers with such lipid liquid crystals. This study was carried out in collaboration with Prof. G. Attard (Southampton), Dr M. Dymond (Southampton) and a 4th year undergraduate project student, L. Carrington.

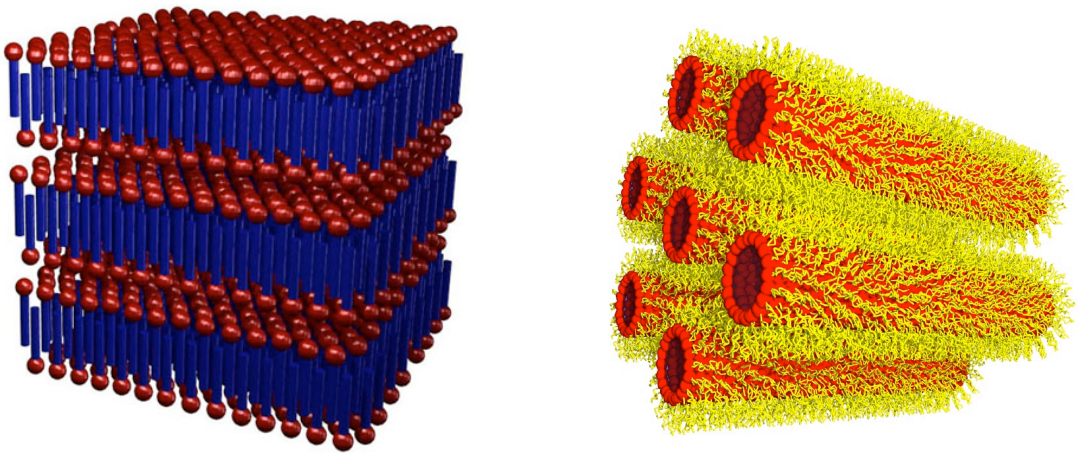

***Figure 78**. Schematic representations of a lamellar (left) and inverse hexagonal (right) phase of liquid crystal lipid bilayers.*

3.3.1 Fluorescence Studies - Results

5th Generation PAMAM dendrimers containing the fluorescent group fluorescein isothiocyanate (FITC) (**132**) were synthesised and modified to possess either a 50% acetyl (**131**) or 50% PEG (**142**) surface as described in previous sections, the FITC tag allowing the dendrimer uptake to be monitored by fluorescence microscopy. These dendrimer samples, either in neutral or acidic conditions (**Table 15**), were then added to different lipid phases (**Table 16**). The dendrimer solution was kept as concentrated as possible in order to give a greater chance of an interaction being visualised. For each lipid sample (the anionic mixture of 1,2-dioleoylphosphaditylcholine (DOPC) and oleic acid gave the best results), it was found that water and acidified water had minimal effect on the lipid and thus ensured that results seen could be attributed to the dendrimer-lipid interaction.

Table 15. *5th Generation PAMAM dendrimers used to study interactions with lipid bilayers.*

Dendrimer sample	Surface [a]			Concentration	Overall charge
	Amine	PEG	Acetyl		
A	127	–	–	0.135 mM	Neutral
B	66	57	–	0.185 mM	Neutral
C	63	–	60	0.130 mM	Neutral
D	127	–	–	0.0675 mM	Cationic [b]
E	66	57	–	0.0925 mM	Cationic [b]
F	63	–	60	0.0650 mM	Cationic [b]

[a] Dendrimer has a single FITC group. [b] Made cationic by the addition of 0.5 M HCl.

***Table 16**. Liquid crystal lipid composition and phase.*

Liquid crystal	DOPC (%)	Oleic acid (%)	Water or saline	Phase
A'	60	40	Water	Inverse hexagonal
B'	60	40	Saline	Inverse hexagonal
C'	80	20	Water	Lamellar

The images from the fluorescent microscopy studies are shown in **Table 17** and **Table 18**. Where possible, a 'before and after' image was taken for comparison. The pale grey areas represent the fluorescent dendrimer solution; dark grey areas are the lipid samples. Whilst in most samples, the lipid edge remained fluorescent once it had been in contact with the dendrimer solution, this was not counted as an interaction, it is merely a reflection from the dendrimer solution left on the glass slide. Interactions were perceived as absorption of fluorescent material into the inner parts of the lipid sample or as evidence of a liquid crystal phase change.

Table 17*. Fluorescence microscopy images of neutral dendrimers with liquid crystal lipid samples.*

Lipid Phase	Sample **A**	Sample **B**	Sample **C**
A'	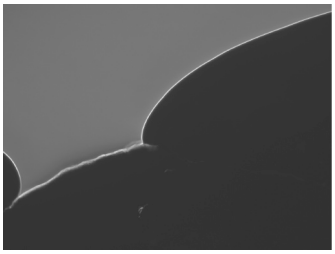		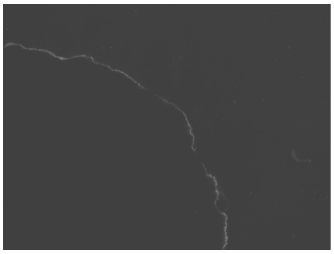
B'	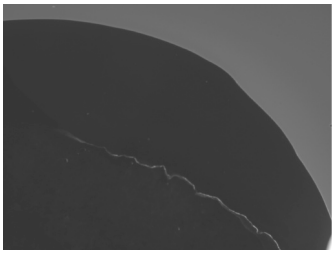	 ↓ 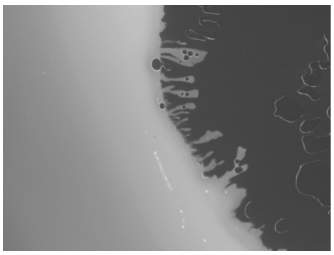	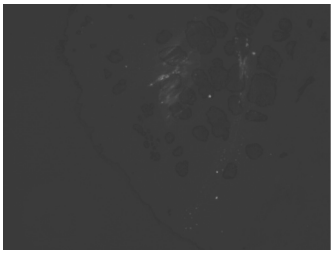 ↓ 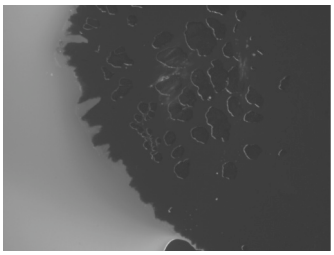
C'	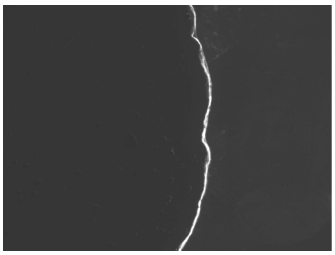	 ↓ 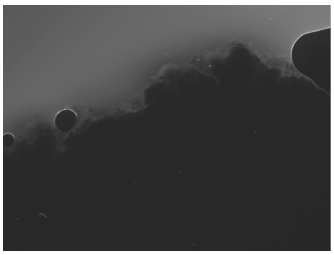	 ↓ 

Table 18. *Fluorescence microscopy images of cationic dendrimers with liquid crystal lipid samples.*

Lipid Phase	Sample **D**	Sample **E**	Sample **F**
A'	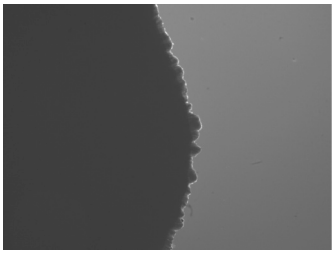	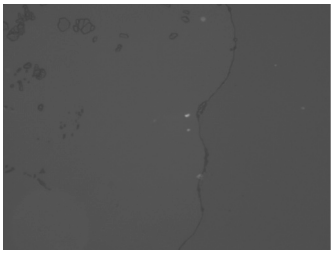 ↓ 	
B'	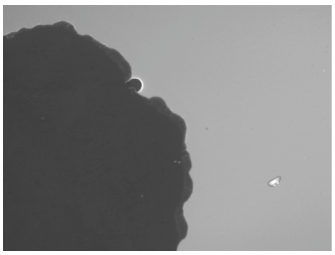		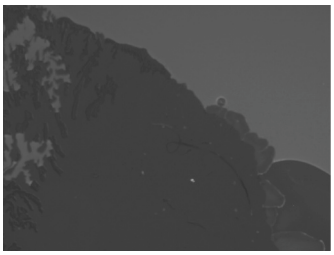
C'	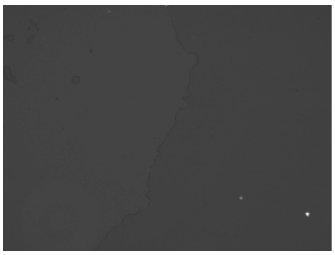 ↓ 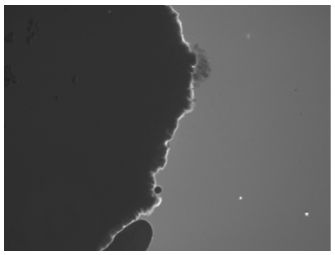	 ↓ 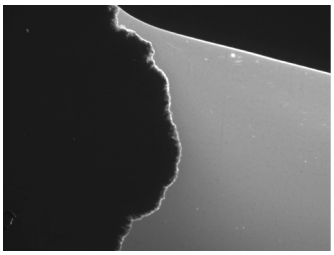	 ↓ 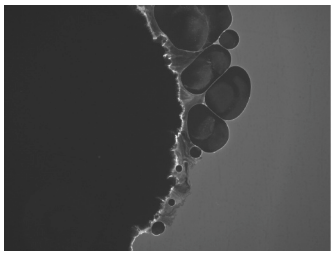

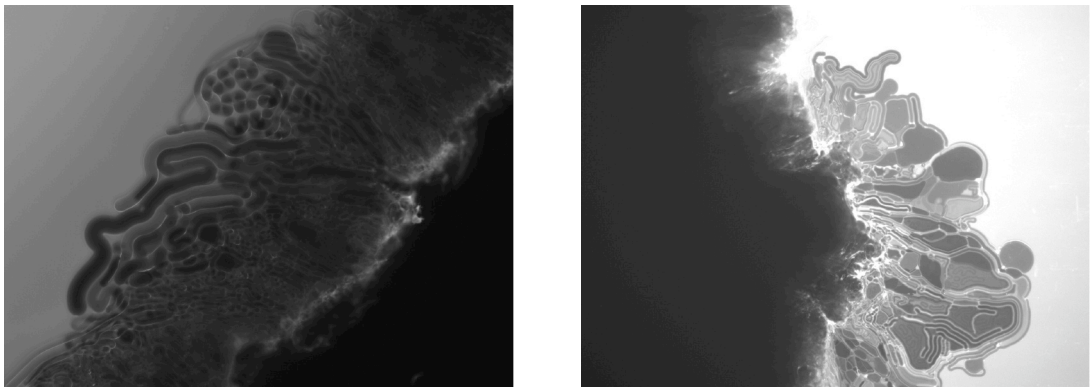

Figure 79. *Myelin sheaths found in the lamellar phase when using acetylated dendrimers.*

3.3.2 Fluorescence Studies – Effect of Dendrimer Surface Functionality

From the images shown in **Table 17** and **Table 18** it can be seen that the type of surface functionalisation has a significant effect on the dendrimer-lipid interaction. It was first noticed that unmodified dendrimer samples showed little to no interaction with any of the liquid crystalline lipids used, which is not wholly unexpected as previous studies have shown that the size of the dendrimer plays a vital role in this type of interaction.[384] It is not then unsurprising to see that PEGylated samples show the most interactions as their molecular weight is over double that of the unmodified dendrimer (the size of these dendrimers is unknown and merits further investigation). The most profound effect was observed with an inverse hexagonal phase (**EA'**); the PEGylated dendrimer solution was quickly taken up by the liquid crystal phase and absorbed through to its centre.

Acetylation of the dendrimer surface has been reported to decrease the hydrodynamic radius[234] so we would expect to see no interactions as observed with the unmodified samples. Interactions were not seen between acetylated dendrimers and the inverse hexagonal phase for neutral or cationic samples, but the same could not be said for the lamellar phase. In the lamellar phase (**CC'**, **FC'**), though no dendrimer absorption was observed, phase expansion and the formation of myelin sheaths suggests an interaction (**Figure 79**). This can be partly attributed to the effect of water on the lipid phase, as

water content is essential to the type of liquid crystal phase formed. However, it can be inferred that some of this effect is due to the interaction with the dendrimer solution as when none is present the myelin sheath formation is slow. This data compares favourably to that published by Orr and coworkers[268,384] who showed that whilst larger PAMAM dendrimers (7^{th} generation) caused hole formation in lipid bilayers, smaller dendrimers (3^{rd} generation) did not. Similarly they demonstrated that the acetylation of 5^{th} generation dendrimers reduced its hole-forming ability.

3.3.3 Fluorescence Studies – Effect of Dendrimer Surface Charge

There is no significant evidence to suggest that protonating the unmodified dendrimer samples has any effect on their interactions with the lipid bilayers. It was believed that the largest interaction would be observed between a cationic amine surface (**D**) and the lipid (made anionic by DOPC/oleic acid) as this dendrimer possesses the highest charge density, but as with the neutral dendrimer, no absorption was seen. This finding (i.e. no difference in behaviour between charged and uncharged amine surface) could be because the neutral dendrimers are becoming protonated when in contact with the lipid (by oleic acid) and thus there would be little difference in the surface charge between the assigned as 'neutral' and 'cationic' dendrimers. Futhermore, irregular effects such as the absorption of dendrimers in some areas of the lipid sample, but not everywhere, could reflect uneven mixing of the DOPC and oleic acid.

The cationic PEGylated dendrimer was seen to permeate strongly into the inverse hexagonal phase hydrated with water but not into the phase hydrated with saline. It is thought that this results from some screening of the electrostatic components of the lipid molecules, thus not giving as strong an interaction. Whilst not as highly charged as the amine-surfaced dendrimer (**D**), the PEGylated (**E**) and acetylated (**F**) dendrimers (with only half the sites available for protonation) show the biggest evidence of disruption of the lipid. This suggests that the interaction between dendrimers and lipids may be more influenced by the dendrimer surface functionality than overall surface charge. This could provide significant insights into the biological applications of dendrimers owing to their cytotoxicity when they are polycationic.[385]

3.3.4 Fluorescence Studies – Effect of Liquid Crystal Phase

The absorption of modified dendrimers was primarily observed in the inverse hexagonal phase, whilst lipid edge disruption and expansion was seen in the lamellar phase. The use of saline instead of water as the hydrating agent appeared to aid absorption in the case of neutral dendrimer samples, but was found to prevent the absorption of cationic samples. This indicates that the mechanism by which the dendrimer is absorbed into the lipid varies depending on its phase. Further studies would help clarify the mode of these interactions, as well as confirm the permeation of the dendrimers through the lipid bilayers.

3.4 Dendrimer–Lipid Bilayer Interactions Studied using Molecular Dynamic Modelling

Dendrimers have been shown to be efficient at improving drug absorbance into cells but the mechanism by which this occurs is difficult to study experimentally.[386] Molecular dynamics (MD) is a type of molecular modelling that enables the user to calculate the time-dependent behaviour of a given system, making it a very useful tool for the study of biological systems. Previously published computational studies have shown that PAMAM dendrimers interact with lipid bilayers and can, at high generation, cause pore formation.[387-392] However, there are few studies that directly compare simulation data with experimental results. It is used herein to study the interaction between dendrimers of varying surface charge and either neutral or anionic lipid bilayers in the hope that their ability to pass through the layers (and hence be absorbed into the lipid) can be determined. This work was performed by a 4th year undergraduate project student, L. Carrington in collaboration with Dr S. Khalid (Southampton).

3.4.1 Molecular Dynamic Studies – Simulations

The modelling of a solvated dendrimer-lipid bilayer system is difficult to simulate using atomistic MD simulations because of the number of interactions that need to be

calculated, so coarse-grained (CG) simulations were used. This technique reduces the resolution of the system, smoothing out fine detail, as well as reducing the number of interactions and thus allowing longer time-scale dynamics to be studied. This approach is favoured by Lee *et al.*,[389] who has shown that dendrimers are more efficient at increasing membrane permeability than linear polymers, as they can span both lipid leaflets to maximize the number of favourable electrostatic interactions.[387]

Six CG molecular dynamics simulations (using the GROMACS simulation package[393]) were run using different dendrimer-lipid systems as shown in **Table 19**. Two lipid bilayer systems were simulated to investigate the effect of overall charge of the bilayer on dendrimer permeation; a neutrally-charged membrane containing 1-palmitoyl-2-oleoylphosphaditylcholine (POPC - zwitterionic), and an overall anionically-charged membrane containing a 1:1 mix of 1-palmitoyl-2-oleoylphosphaditylethanolamine (POPE) and 1-palmitoyl-2-oleoylphosphaditylglycerol (POPG). 3rd Generation PAMAM dendrimers have been modelled as an extended form by Lee *et al.*[389] and functionalised by representing the terminal groups as either cationic, anionic or polar. By visual inspection, the average simulated G3 dendrimer size agrees with the experimental diameter of ~35 Å. It should be noted that four dendrimers were used in each simulation, which was run with a time step of 40 fs for an overall duration of 100 ns. Specific simulation details can be found in **Appendix II**.

Table 19. *List of CG simulations run (simulation time: 100 ns).*

Simulation	Lipid bilayer charge	No. cationic dendrimers	No. anionic dendrimers	No. polar dendrimers
A	Neutral [a]	4	0	0
B	Neutral [a]	2	2	0
C	Neutral [a]	0	0	4
D	Anionic [b]	4	0	0
E	Anionic [b]	2	2	0
F	Anionic [b]	0	0	4

[a] Composed of POPC. [b] Composed of POPE/POPG.

3.4.2 Molecular Dynamic Studies – Effect of Dendrimer Surface Functionality

Interactions were observed in all the simulations modelled, primarily involving the lipid head-group. In simulations using cationic dendrimers, the dendrimer was observed to open its spherical structure and flatten along the lipid leaflet (**Figure 80**). This is a result of electrostatic interactions being the main influence, the cationic terminal groups of the dendrimer being drawn to the anionic component of the POPC head-group (negative phosphate group). When the results of simulation **A** are compared with those of **D** it is possible to see the strength of this interaction. When an anionic lipid was used, the dendrimers became associated with it in about 8 ns (**Figure 81**), far faster than with a neutral lipid (80 ns). Although this is a strong interaction, no lipid penetration was observed.

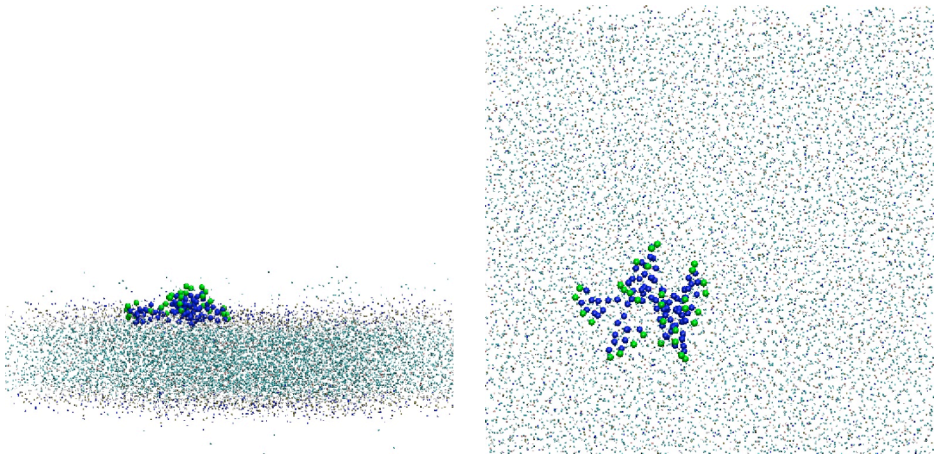

Figure 80. *Interaction between cationic 3rd generation dendrimers and neutral lipid (simulation **A**) after 80 ns. CG dendrimer is represented by blue beads, green beads being the cationic terminal groups.*

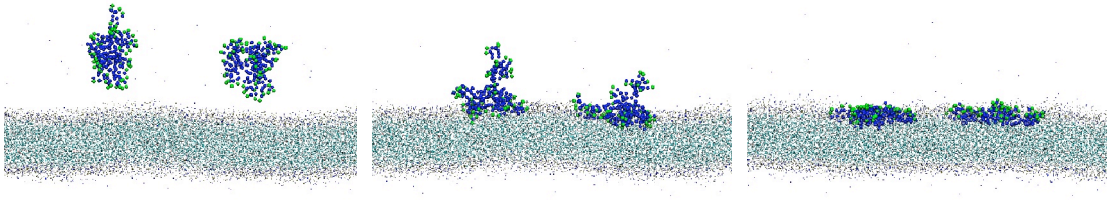

Figure 81. *Interaction between cationic 3rd generation dendrimers and anionic lipid (simulation **D**) after 0.16 ns (left), 1 ns (middle) and 8 ns (right). CG dendrimer is represented by blue beads, green beads being the cationic terminal groups.*

When a mixture of dendrimers with opposite charges was used (simulations **B** and **E**), they were found to agglomerate. Initially, two oppositely charged dendrimers come together, then two of these newly-formed neutral complexes associate (**Figure 82**). This dendritic cluster then interacts with the lipid as described above to be dispersed on the lipid leaflet. Though the size of this cluster is significantly larger than a single dendrimer, it was not seen to insert or pass through the bilayer; a longer time-scale may facilitate this, but this observation may be due to the charges being internalised or to the low dendrimer concentration used.[389,390]

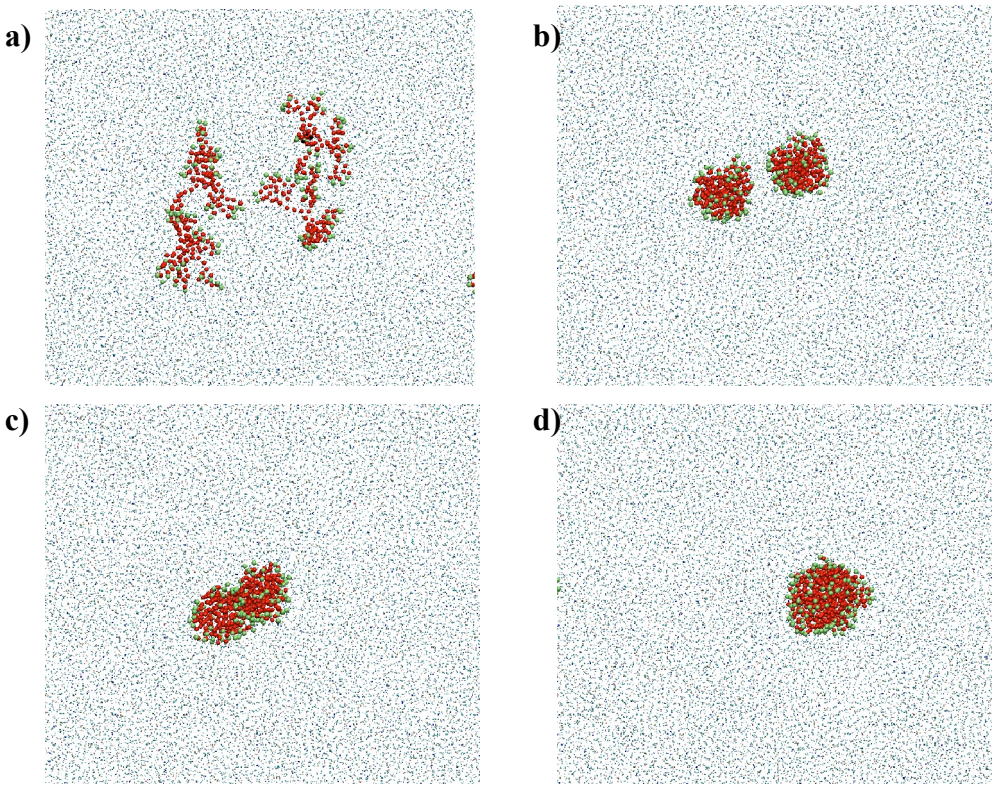

Figure 82. *Interaction between cationic and anionic 3rd generation dendrimers and neutral lipid (simulation **B**) after (a) 0.4 ns, (b) 6.8 ns, (c) 15 ns and (d) 40 ns. CG dendrimer is represented by red beads, green beads being the charged terminal groups.*

Polar-terminated dendrimers were also observed to interact with both lipid systems (simulations **C** and **F**); however, they do so in a different way from the other simulations. Instead of the dendrimer terminal groups interacting primarily with the charged lipid head-groups, they orientate themselves away from the lipid surface allowing the dendrimer interior to interact as seen in **Figure 83**.

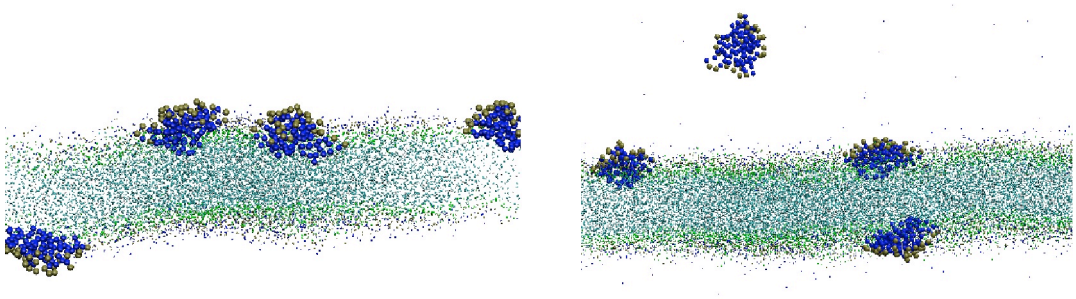

Figure 83. *Interaction between polar 3rd generation dendrimers and neutral (left) or anionic (right) lipid (simulations **C** and **F** respectively) after 100 ns. CG dendrimer is represented by blue beads, gold beads being the polar terminal groups.*

Though no pore formation was observed, in contrast with other studies using larger dendrimers,[388-390] it is clear that the dendrimers modelled interact with the lipid bilayers. This interaction was observed as an opening of the dendrimer structure followed by their flattening on the lipid leaflet. Pore formation is seen in the work of Lee *et al*.[389] using 7th generation dendrimers, where they are large enough to span across the two lipid leaflets in an effort to maximise charge balance. This infers that the 3rd generation dendrimers used in our simulations are not large enough to cross the lipid, thus the most favourable interactions are found by their flattening on the surface.

No significant difference was seen between neutral and anionic lipids, except that cationic dendrimers associate much faster with the latter. It was also observed that in this case (simulation **D**) these electrostatic interactions are too strong to overcome the hydrophobic effect of permeating through the hydrophobic interior of the layer (insertion into the bilayer would increase the number of interactions of polar-nonpolar interactions, which would increase the energy of the system).

3.4.3 Molecular Dynamic Studies – Contacts

Using the results of the MD simulations it is possible to quantitatively compare them in terms of the number of contact points formed between the dendrimer and lipid bilayer. In the neutral lipid bilayer system (**Figure 84**), it is evident that the cationic dendrimers form the highest number of contacts with the lipid, and in the shortest time. This shows that the electrostatic force between the cationic dendrimer and anionic phosphate component of the lipid head-group is significantly stronger than the van der Waals forces and hydrogen bonds formed by the polar dendrimer. The mixture of cationic and anionic dendrimers form the least number of contacts as a large proportion of the dendrimer terminal groups become internalised into the resulting dendrimer cluster, and are thus unable to interact with the lipid bilayer.

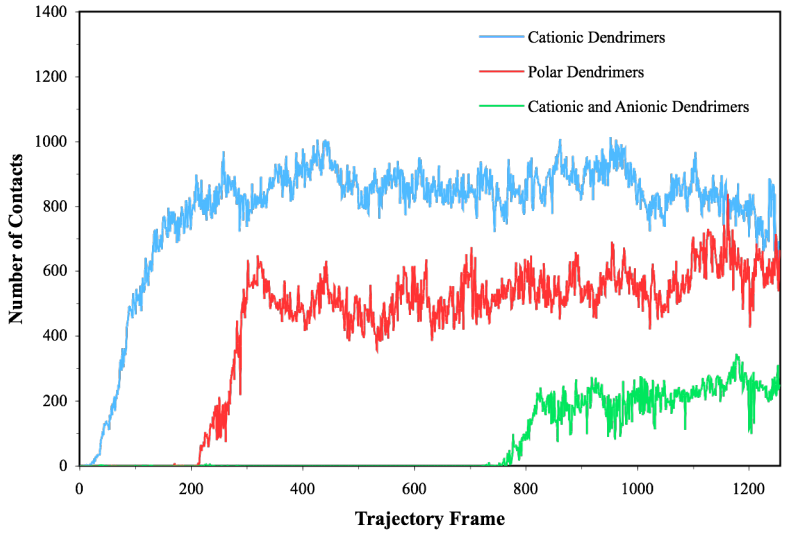

Figure 84. *Number of contacts between dendrimer terminal groups and the neutral lipid bilayer.*

When using an anionic lipid (**Figure 85**), the cationic dendrimers form considerably more contacts (greater than 600) in a much shorter time compared with the neutral lipid. This is not entirely unexpected as the number of electrostatic interactions have been increased. The polar dendrimers form a similar number of interactions when compared with the neutral lipid as their interaction is not driven by electrostatics; though it should be noted that these contacts take longer to form when using an anionic lipid. Perhaps

the most significant change is that of the cationic and anionic dendrimer mixture. Though many of the terminal groups are internalised (giving the same number of total contacts), the presence of the charged lipid makes the contacts form much faster.

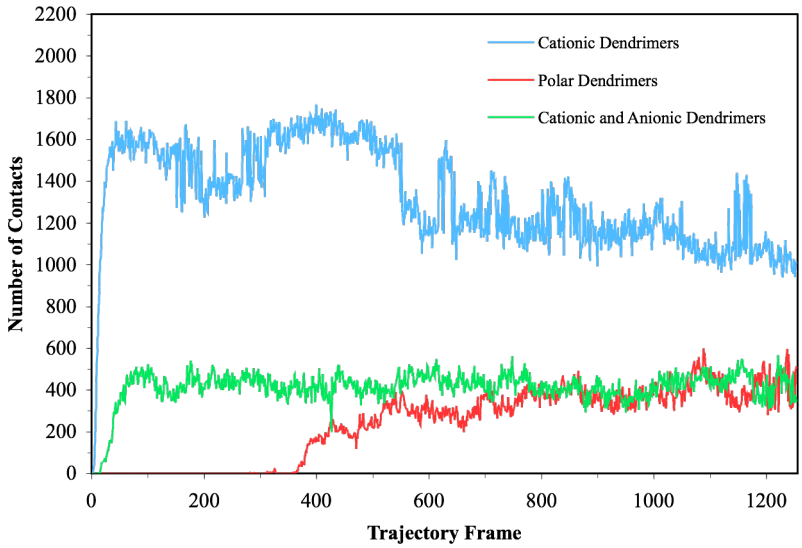

Figure 85. *Number of contacts between dendrimer terminal groups and the anionic lipid bilayer.*

3.4.4 Molecular Dynamic Studies – Radial Distribution Function

A radial distribution function (RDF) gives the relative probability of finding a particle within a certain distance of another.[394] In this study, the RDF has been calculated for the dendrimer terminal groups (cationic or polar) with-respect-to the lipid. For the neutral lipid system (POPC), radial distribution functions were calculated against the negative phosphate (PO4) and the positive choline (NC3) components of the head-group. For the anionic lipid, radial distribution functions were calculated against the neutral lipid component (POPE) and the anionic lipid component (POPG).

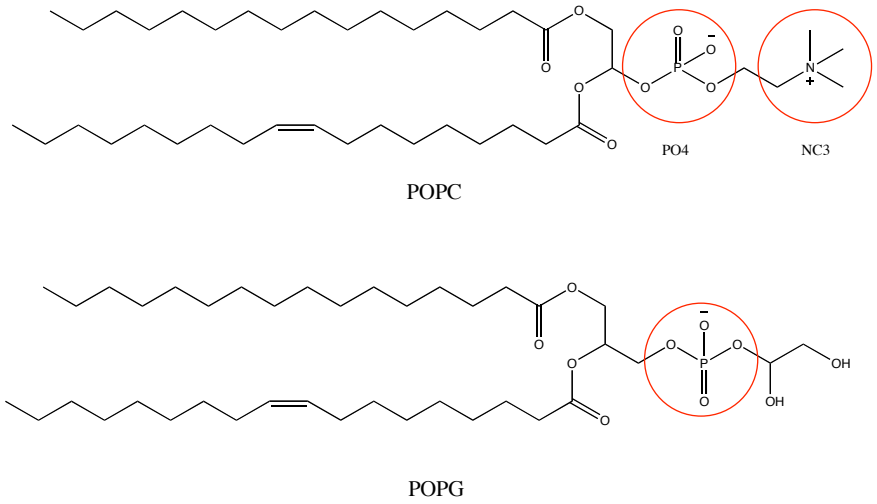

Figure 86. *Structure and assignments of POPC and POPG lipids.*

As we would expect when using positively charged dendrimers, the highest radial distribution functions were observed with the anionic components of the lipids (**Figure 87**). For the neutral lipid, the largest RDF for the charged dendrimer is seen at a distance of 0.5 nm for both components, the negative component having a RDF of ~ 4 whilst the positive component has an RDF of ~ 3. The same relationships were observed for the anionic lipid, the anionic component (POPE) giving a higher RDF (~ 6) compared to that of the neutral component (POPG, ~ 1). It is not surprising that the highest RDF using a cationic dendrimer is seen when interacting with the anionic lipid; electrostatics plays a large role here. Since electrostatic interactions are largely responsible for the high RDF values, it is perhaps surprising that the value for the positive component of POPC is so high. However, this can be explained by the fact that both components of the POPC head-group are close to each other, thus an increase in the RDF for the anionic component will affect that for the positive component. The large difference between components for the anionic lipid is the result of it being composed of two lipids, the neutral one having little interaction with the cationic dendrimer.

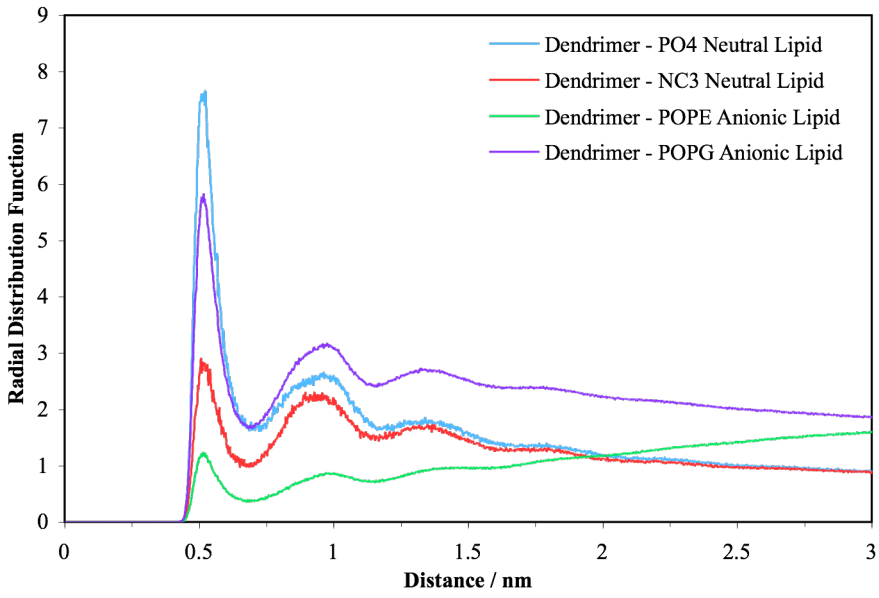

***Figure 87**. Radial distribution function for cationic dendrimer terminal groups with respect to the negative phosphate (PO_4) and positive choline (NC_3) components of the neutral lipid bilayer, and with-respect-to the neutral POPE and negative POPG components of the anionic lipid bilayer.*

For polar-terminated dendrimers, the RDF peaks occur at similar distance to those for the cationic dendrimers (**Figure 88**). It can be seen that the size of the peaks relating to the phosphate/choline bilayer are similar, as too are those of the POPE/POPG lipid bilayer. This shows that, in the case of polar dendrimers, electrostatic interactions with the lipid are not present, and helps explain why their association rate with the bilayers is slower when compared to that for the cationic dendrimers.

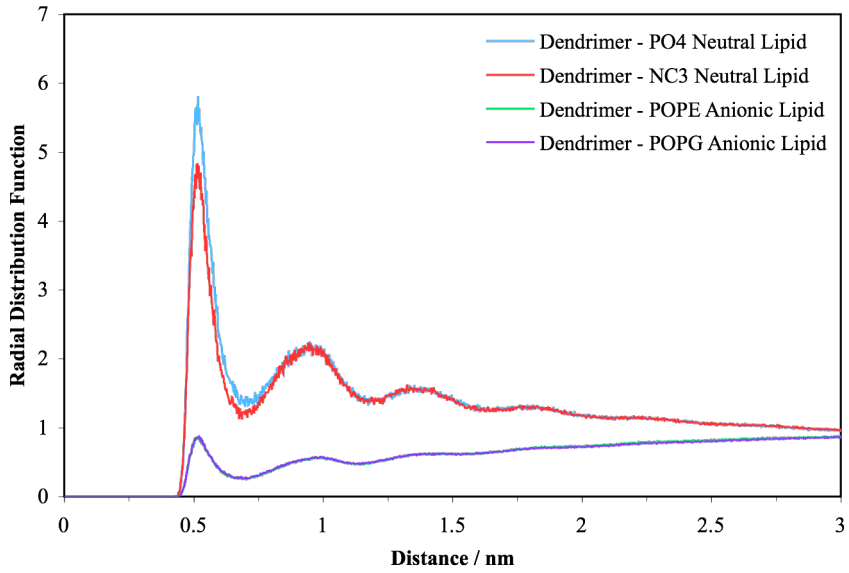

Figure 88. *Radial distribution function for polar dendrimer terminal groups with respect to the negative phosphate (PO_4) and positive choline (NC_3) components of the neutral lipid bilayer, and with-respect-to the neutral POPE and negative POPG components of the anionic lipid bilayer.*

3.5 Conclusions and Further Work

PAMAM dendrimers of 4th and 5th generation were successfully modified with acetyl, PEG and fluorescent groups with various degrees of surface coverage. Acetyl groups were attached to the amine surface of the dendrimers by the addition of a quantitative amount of acetic anhydride to give well-defined coverages that were determined by ^{1}H NMR spectroscopy. A PEG chain was synthesised bearing a terminal isothiocyanate group using the Gabriel Synthesis to convert a terminal alcohol into an amine (*via* the corresponding bromide). The amine was then treated with thiophosgene, and the resulting isothiocyanate used to attach the PEG chain to the dendrimer amine surface. The extent of surface coverage was determined using elemental analysis, by comparing the ratio between nitrogen and sulphur atoms. Fluorescent groups, namely dansyl and fluorescein, were attached directly to the dendrimer amine surfaces at low degrees of coverage so that the dendrimers could be visualized using microscopy techniques.

These dendrimer samples were used by Kristina Fant (Chalmers University, SE) to investigate their complexation and condensation with DNA samples. It was found that, at similar dendrimer to DNA charge ratios, unmodified dendrimers formed more condensed complexes than PEGylated dendrimers. The uptake of fluorescently labelled dendrimers into CHO-K1 cells was demonstrated, and preliminary results pertaining to the cytotoxicity of modified dendrimers where obtained which showed that PEG and acetyl-G4 dendrimers have significantly reduced toxicity compared with unmodified dendrimer samples.

Modified 5th generation dendrimers (namely fluorescein labelled dendrimers with a 50% acetyl, 50% PEG or unmodified surface) were used to study interactions with 3 different lipid bilayer systems (made from DPOC and oleic acid). Protonated and unprotonated dendrimer samples were found to show very few interactions with the lipids in the inverse hexagonal phase, though PEGylated samples were seen to permeate into the lipid interior. This is most likely because of the increase in size of the dendrimer arising from the addition of PEG chains to it. When a lipid in the lamella phase was used, acetylated samples demonstrated a disruption of the lipid surface, as shown by the formation of myelin sheaths at a faster rate than with no dendrimer present. The lack of effect of protonating the dendrimer samples seems to suggest that the lipid itself is protonating them (from the oleic acid), implying that the differences in interaction between dendrimers purely the result of the surface modifications.

A series of coarse-grained molecular dynamic simulations were run to study the interaction of a range of 4th generation dendrimers (cationic, cationic and anionic, and polar surfaces) with either a neutral or anionic lipid bilayers. It was found that all the simulations showed an interaction of the dendrimer with the lipid, principally by electrostatic interactions and thus was viewed as an opening of the dendritic structure and a flattening on the lipid surface. For cationic dendrimers this interaction was strongest (and fastest, 8 ns) when the anionic lipid was used, and, it showed many more contacts compared with those seen for a neutral lipid. When a mixture of cationic and anionic dendrimers were used it was shown that the dendrimers are attracted to each other to form a large dendritic cluster which then flattens on the lipid leaflet. It does this relatively weakly with few contacts, suggesting that the majority of the charges have been internalised. Polar dendrimers also show flattening on the lipid leaflet, but

they do so using the interior of the dendrimer; the polar terminal groups point away from the lipid. Radial distribution functions showed that the cationic dendrimers are (unsurprisingly) most strongly attracted to the anionic components of the lipids, the closest interaction occurring at 0.5 nm from the lipid surface, whilst the use of a neutral lipid demonstrated that polar dendrimers are not attracted by electrostatic interactions. It should be noted that no lipid permeation was observed, possibly because of the size of the dendrimer; rather the dendrimer maximizes its number of interactions with the lipid by spreading out along its surface. Further work should be carried out with these modified dendrimers to help determine at what generation pore formation starts to occur, possibly by increasing the dendrimer concentration and simulation time.

Since the simulations have shown that the dendrimers interact with the lipids, the experimental interactions should be re-visited. It was noted that the edges of the lipids remain fluorescent, but this was believed to be due to reflections of the dendrimer by the glass slides. Further experiments should look to reduce this reflection to help determine if a true interaction is occurring in these cases, as well as providing more quantitative data.

Chapter 4 Histidine surface

The binding between DNA and dendrimers *via* a pH-controlled process has been much studied,[161,330,337,356-359,395-397] so too has the protonation/deprotonation of histidine.[398-405] However, little work has been done to combine these two components,[406] in fact there is no reported evidence linking histidine and PAMAM dendrimers. Work carried out by Kristina Fant (Chalmers University, Gothenburg, Sweden) in conjunction with this project showed that polyhistidines have favourable binding to DNA, so it was decided to incorporate histidine into a PAMAM dendrimer to give a pH reversible binding system. To that end, a number of routes for attaching L-histidine (**149**) onto the surface of a dendrimer were explored. Since the primary amine and the imidazole amine of the histidine are required for binding to the DNA strands, protected histidine (Boc, Cbz or Fmoc) must be used to avoid polymer formation when coupling to the dendrimer amine surface.

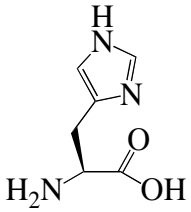

149

Figure 89. Structure of L-histidine (**149**).

4.1 Histidine Dendrimers via Peptide Couplings

Before the protected histidine was coupled to the dendrimers, small scale trial reactions were carried out using Boc-protected EDA (**150**), as this was considered to be a fair approximation to a dendrimer arm, in order to ascertain the most effective reaction conditions.

4.1.1 Small Scale Peptide Couplings

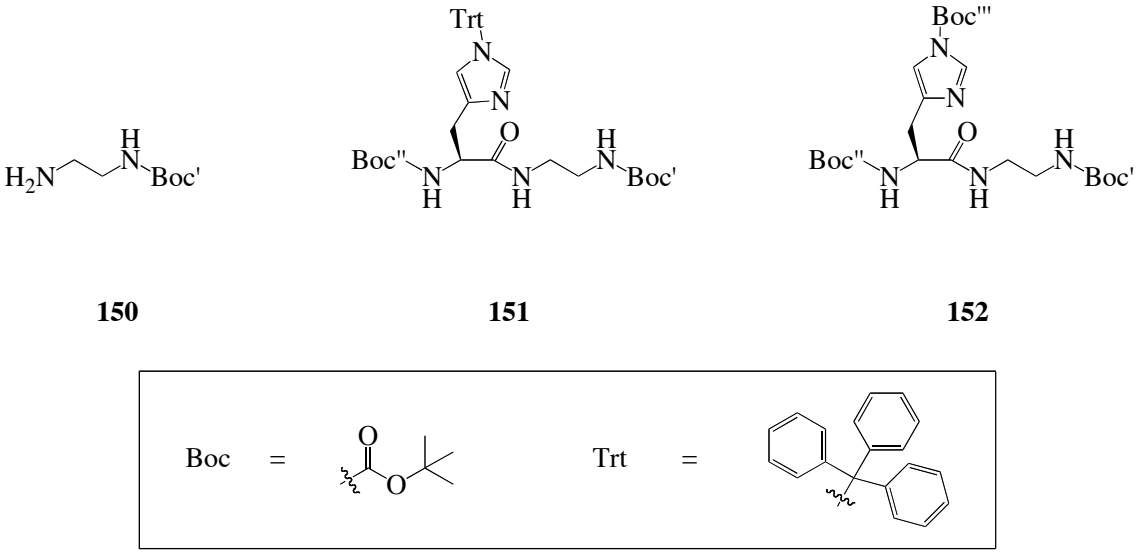

150 **151** **152**

Figure 90. *Structures of synthesised molecules used for simple peptide couplings; Boc-EDA (**150**), Boc-His(Trt)-EDA-Boc (**151**) and Boc-His(Boc)-EDA-Boc (**152**).*

Mono-protected EDA **150** was synthesised by addition of di-*tert*-butyl dicarbonate to an excess of EDA in DCM. This allowed for the formation of the desired product, plus the limited formation of the *bis*-protected form, and was isolated as a colourless oil (79%). The presence of the single Boc group was confirmed by MS (ES^+; m/z 160.2) and NMR spectroscopy ($CDCl_3$, δ ^1H, 1.43 ppm; ^{13}C, 28.4 ppm). **150** was then coupled to either Boc-His(Trt)-OH or Boc-His(Boc)-OH using different solvents (DCM or DMF) and coupling agents (HBTU or EDC) in the presence of DIPEA and HOBt to form **151** and **152** respectively.

The peptide couplings were carried out by first synthesising the activated histidine ester using HOBt at 0ºC. This was followed by the addition of the amine whereupon the reaction was allowed to warm to room temperature. After being allowed to stir (45 min at 0ºC, then 18 hrs at RT), any unreacted material and reaction by-products were removed by repeated acidic and basic washes. The resulting crude material was then further purified by column chromatography (typically 5% methanol in DCM; **151** R_f: 0.33, **152** R_f: 0.28) to give a white solid or foam.

The ^{1}H NMR spectrum ($CDCl_3$) of **151** is seen to possess two Boc groups, one at δ 1.43 ppm (Boc') that relates to the addition of **150**, the other at δ 1.35 ppm from the protected histidine (Boc''). There is downfield shift for the methylene units of the EDA to δ 3.38 and 3.22 ppm. Interestingly, the integrals of these two peaks (relative intensities of 1H and 3H respectively) suggest that the unit closest to the histidine is near enough to the chiral centre to have inequivalent protons. Singlets in the aromatic region at δ 7.39 and 6.66 ppm relate to the imidazole protons, whilst higher multiplicity signals at δ 7.32 and 7.10 ppm show the trityl (Trt) group. The C*H* and diastereotopic CH_2 group of the histidine can be seen at δ 4.30 (as a broad quartet), 3.07 (as a double doublet) and 2.91 ppm (as a double doublet) respectively, whilst the amide singlets can be seen at δ 6.89, 6.13, and 5.58 ppm. While ^{13}C NMR and 2D NMR (COSY and HMQC) spectra confirm these assignments, it should be noted that the methyl substituents of both Boc groups appear at the same chemical shift (^{13}C δ 28.4 ppm). Elemental analysis and HRMS both support the formation of **151**, which has a melting point of 72 – 74ºC.

The ^{1}H NMR spectrum ($CDCl_3$) of **152** is a very similar to that of **151**. The imidazole Boc group appears at δ 1.60 ppm, while the two remaining Boc groups both now appear together at δ 1.44 ppm. This suggests that the different imidazole protecting groups, even though they are not in close proximity, have an intramolecular effect on the remaining histidine Boc' group. The replacement of the Trt with a Boc group also causes a downfield shift of the imidazole protons to δ 8.02 and 7.18 ppm. In the ^{13}C NMR ($CDCl_3$) spectrum, the new Boc group appears upfield compared with the others at δ 27.9 ppm, while the imidazole carbons remain largely unchanged (though there is a small upfield shift of the Boc-N-*C*H-C-CH_2- compared to **151**). Once again, elemental analysis and HRMS indicate the formation of **152**, the melting point of which is lower than **151** at 60 – 62ºC.

***Table 20**. Percentage yields of coupling reactions.*

	Boc-His(Trt)-EDA-Boc (**151**)			Boc-His(Boc)-EDA-Boc (**152**)	
	HBTU	EDC		HBTU	EDC
DCM	69[a]	76		48[a]	75
DMF	84[a]	42		61	52

[a] These reactions contained a small amount of impurity (1,1,3,3-tetramethylurea) that was hard to remove by column chromatography, thus slightly artificially inflating their yields.

For the formation of **151**, the best combination of coupling agent and solvent was found to be EDC in DCM, giving a yield of 76%. The use of HBTU as a coupling agent was found, in this case, to give a by-product that had a very similar R_f to the desired product and which proved hard to remove, artificially increasing the yield. Similar results were obtained for **152**; overall, EDC in DCM gave the highest yields but those using HBTU gave a greater consistency. Unless the dendrimer has been PEG modified, and thus soluble in DCM, it is most likely that the solvent of choice will be DMF, so for that reason HBTU will be the reagent of choice for the couplings because of its higher yields in this solvent.

4.1.2 Couplings using Boc Protected Histidine

As a point of interest, Boc-His(Boc)-OH was coupled to the surface of a 4th generation PAMAM dendrimer with the aim to achieve total surface coverage (**153**). The reaction was performed in DCM/DMF, as it was believed that although the dendrimer was insoluble in DCM the product would be soluble, using HBTU as the coupling agent. When the dendrimer was added to the amino acid/coupling agent mixture the solution changed to dark orange and then to brown. After 18 hrs a brown precipitate had formed. Since it was known that all the starting materials and expected coupling by-products are soluble in the solvent system used, it was reasonable to assume that the formation of a solid was due to the formation of the desired product **153**. Upon closer inspection, the precipitate was found to be an insoluble highly viscous oil (suggesting a dendritic structure) and this was collected by centrifugation (no acid/base washes were performed owing to the likely formation of an emulsion). Normally the product would

be subject to dialysis. However, this material was found to be insoluble in conventional solvents, and only partially soluble in DMSO and so dialysis was not attempted due to safety concerns. The decanted supernatant liquid was reduced to give a brown oil that NMR revealed to contain no dendrimer peaks, but did show the presence of the coupling by-product (1,1,3,3-tetramethylurea).

The poor solubility of the product meant that its surface coverage could not be determined. Attempts were made to remove the Boc protection using TFA, but once again this resulted in the formation of an insoluble product. Published data indicates that the removal of Boc groups from a dendrimer surface is possible,[382,407] but the high density of histidine might be hindering this deprotection. In order to increase the solubility of these dendrimers, lower coverage reactions were investigated.

The initial trial reactions (using DMF as the solvent) were found to have an undissolved component (dendrimer), so a small amount of water was added to aid solubility. Using the same reagents as described above, the expected coverage would have been 10% and 25%, but by ^{1}H NMR studies they were found to be 7.1%, (**154**) and 14.5% (**155**) respectively (it should be noted that where coverage is low, the product dendrimer is soluble in methanol). It was originally surmised that the low coverage was due to the addition of water, which would interfere with the coupling intermediate regenerating the starting material. To test this hypothesis the reaction was tried again using DMSO, but this resulted in only a 16.4% coverage (**156**; 25% expected). These results suggest that the solvent has only a minor effect, the major concern is therefore likely to be the bulk of the intermediate group being added to the surface. Despite these problems, it can be confirmed that protected histidine has been successfully coupled to the dendrimer surface.

TFA was again employed to remove the Boc protecting groups of the histidine, starting at a low concentration (5%) in methanol to avoid any damage to the PAMAM structure (*via* an acid-catalyzed retro-Michael addition). Once the dendrimer had been added, the solution was stirred for 60 minutes before being quenched with $NaHCO_3$ and dialysed against deionised water. This however failed to remove the protecting groups (as monitored by ^{1}H NMR data), so higher concentrations of TFA were used (up to 50%; larger ratios could degrade the dendrimer) together with longer reaction times but this

again showed no signs of deprotection. This may be due to the terminal histidine units folding into the interior of the dendritic structure, a phenomenon often observed with dendrimers, thus helping protect it from the TFA.

4.1.3 Couplings using Fmoc or Cbz Protected Histidine

Since the removal of Boc protecting groups has proved difficult, it was decided to try other forms of protection. Upon trying to attach Fmoc-His-OH (**157**) to a 1st generation dendrimer it was found that the Fmoc group was removed by the surface amines, so Fmoc protection was not used in conjuncture with full generation dendrimers.

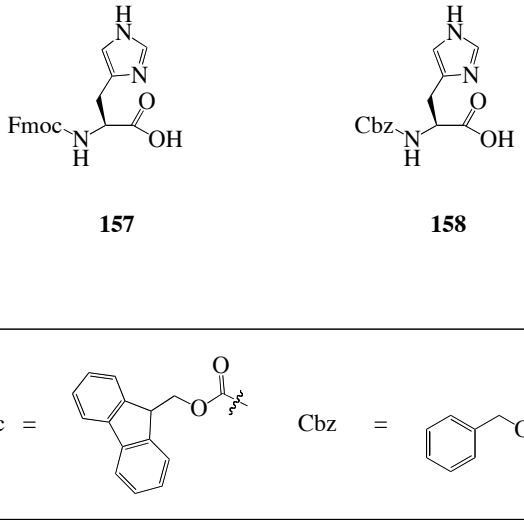

***Figure 91**. Structure of Fmoc-His-OH (**157**) and Cbz-His-OH (**158**).*

It was decided that, since the removal of Boc protecting groups had proved difficult to achieve and Fmoc groups were removed by the dendrimer itself, carboxybenzyl (Cbz) protection should be used as an alternative. Its removal is achieved by catalytic hydrogenation, which was not expected to cause any damage to the dendrimer. Cbz-His-OH was coupled to the surface of a 4th generation PAMAM dendrimer (8 groups) using HBTU/HOBt in DMF/water (25:3 mL). The resulting solution was dialysed in deionised water for 2 days followed by deionised water/methanol (1:1) for 3 days (**159**). Comparison between integrals of ^{1}H NMR (MeOD) spectrum at δ 2.37 ppm (internal dendrimer signal) and the aromatic region δ 8.12 – 7.24 ppm (Cbz and imidazole

groups) suggested 7 Cbz-His groups to be present. ^{13}C NMR data also showed the presence of aromatic signals relating to the Cbz-His group.

The deprotection of **159** was performed in ethanol/methanol (3:1) in the presence of palladium on carbon catalyst under a hydrogen atmosphere. After stirring overnight the catalyst was removed by filtration and the dendrimer was dialysed in methanol. This gave a pale green product (**160**) suggesting that some of the catalyst was trapped in the interior of the dendrimer[293] so it was re-filtered and dialysed to give the final product as a viscous pale yellow oil, the ^{1}H NMR (D_2O) spectrum of which showed the presence of multiple aromatic signals suggesting that the protecting group had not been removed. Analysis of the integrals, however, showed that fewer Cbz groups were present. The ratio of the aromatic signal to internal dendrimer arm for Cbz-His-PAMAM was 5.00 to 24.06H, whereas for the attempted deprotection the ratio was 3.65 to 24.06H. For complete removal of the protecting group we would expect an integral ratio of 0.71 to 24.06H, so the reaction was repeated under the same conditions but with no further effect.

As previously mentioned, the major concerns with putting any group onto a dendrimer surface are reactivity and bulk of the linker groups. If we assume the amine groups of the dendrimer are all located at the surface (unlikely), then it is the steric bulk of the group to be attached which is the major issue, thus leading to lower surface coverage. However, it is more likely (as suggested by computational studies),[179,190,202] that the terminal amines lie within the structure (i.e. not at the surface) in which case a bulky linker group would be hard pressed to penetrate the dendrimer and react. The use of peptide coupling agents, though shown to successfully couple histidine to the dendrimer surface, react slowly and give a low surface coverage. Furthermore, because of the nature of these couplings, protected histidine must be used. To overcome these problems two further synthetic routes were considered, one using an isothiocyanate linker as it is a small and reactive group, the other utilizing ‘Click’ chemistry that exploits the triazole ring formation from an alkyne and an azide.

4.2 Histidine Surface via *an Isothiocyanate linker*

The use of isothiocyanate linker units has already been discussed in **Section 3.1.2** and has been shown to give well-controlled coverage (i.e. when 25% PEG-NCS coverage was aimed for, ~ 25% coverage was achieved). Thus, a protected histidine was modified in such a way as to allow for the formation of a primary amine that could then be turned into an isothiocyanate group as shown below (initial trials into this route were carried out with the aid of a 4th year undergraduate project student, S. Moore).

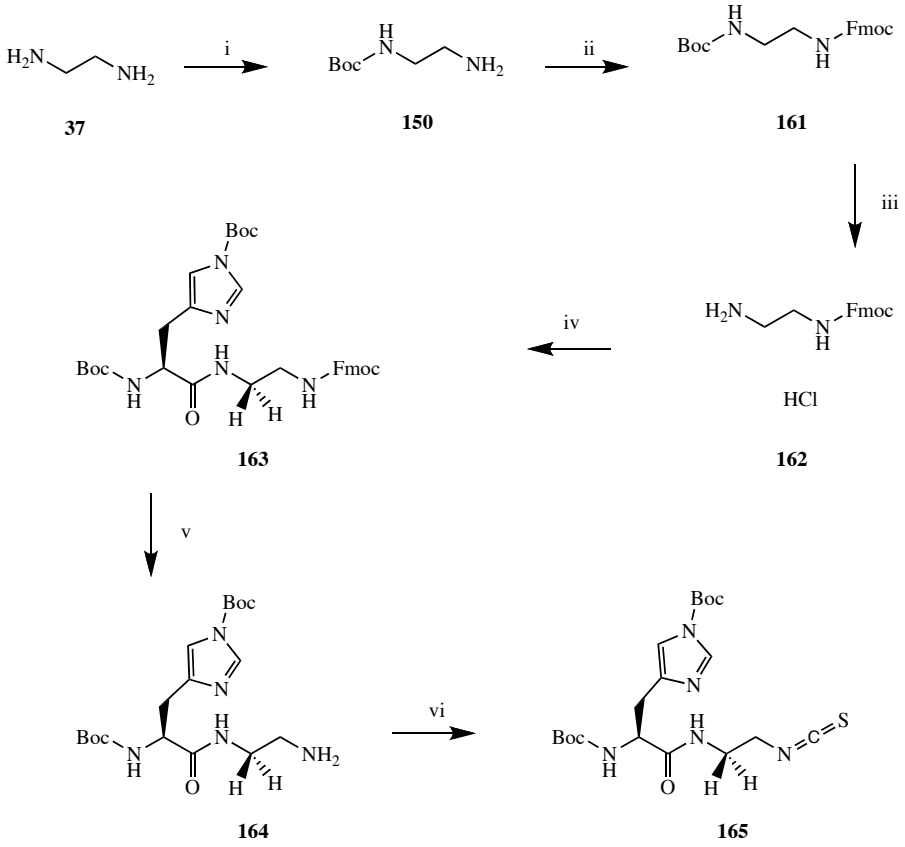

Scheme 12. *i, Boc_2O, DCM; ii, Fmoc-OSu, NaOH, H_2O/MeCN; iii, Conc. HCl, MeOH; iv, Boc-His(Boc)-OH•DCHA, HBTU, HOBt, DIPEA, DCM; v, Piperidine, DMF; vi, $CSCl_2$, Na_2CO_3, $CHCl_3$.*

It was decided that a unit containing an Fmoc-protected amine should be coupled to the Boc-protected histidine as this will provide the extra amine group required to make the isothiocyanate derivative **(Scheme 12**). To that end, the synthesis of **161** was first

attempted by the addition of Fmoc-OSu to stirred EDA but it was found that the amines of the EDA deprotected any of the formed product so a literature route was used.[408] Fmoc-OSu in acetonitrile was added to previously prepared **150** under basic conditions, which caused **161** to precipitate as a white powder in a 71% yield. MS and NMR spectra were consistent with the introduction of the Fmoc group (peaks being observed in the aromatic region for both ^{1}H and ^{13}C NMR spectra) though the melting point (135 – 137ºC) was lower than previously reported (155 – 156ºC).[408] The literature procedure removed the Boc group using a saturated solution of HCl in diethyl ether (prepared by dropping conc. H_2SO_4 onto NaCl and bubbling the resulting gas through diethyl ether) but this was found to be ineffective. Instead, **161** was added to a 50% solution of conc. HCl in methanol and allowed to reflux.[409] Upon cooling, product **162** precipitated and was crystallised from hot methanol and diethyl ether to give the HCl salt as white needles (93%). Since the salt is formed, the primary amine cannot cause the deprotection of the Fmoc group. MS and NMR spectra (no Boc group seen) was again consistent with published data,[408] though no literature melting point (123 – 125ºC) could be found for comparison.

162 was then coupled with Boc-protected histidine using HBTU/HOBt to give **163**, after purification, as a white solid (89%). When EDC/HOBt was used for this coupling only a 9% yield was achieved. Both ^{1}H and ^{13}C NMR (DMSO-d_6) show a shift for the methylene unit adjacent to the amine of **161** (from δ 2.84 to 3.30 ppm and δ 38.5 to 40.3 ppm respectively) suggesting coupling had occurred (interestingly these protons are equivalent unlike in the case of **151** and **152** where they are diastereotopic); 2D NMR (HMQC), MS and elemental analysis confirmed this. The melting point of **163** was found to be 99 – 100ºC which is higher than those for the previous histidine couplings made (**151** and **152**).

Fmoc deprotection is well documented in the literature[408,410,411] and proceeds *via* the deprotonation at the tertiary CH position (usually by piperidine) to give a resonance-stabilized anionic intermediate. This then forms dibenzofulvene and an amine whilst releasing CO_2. It should be noted that the dibenzofulvene reacts further with the piperidine at the double bond to regenerate the tertiary CH. The deprotection of **163** was carried out at room temperature using a 20% solution of piperidine in DMF. The reaction was followed by thin layer chromatography (TLC; 5% methanol in DCM) and

showed that the reaction had gone to completion overnight. Two spots were observed, R_f: 0.96 and R_f: 0.00, the dibenzofulvene-piperidine by-product and product/residual piperidine respectively. No solvent system could be found that would allow for the recovery of the product and separation by crystallization proved unsuccessful. Mass spectrometry (ES^+) was performed on the aqueous phase from the work-up and was found to contain dibenzofulvene-piperidine (m/z 264.3). The deprotection was also carried out using piperazine in an effort to reduce any side reactions taking place (as described by Wade *et al.*[412]), but once again whilst the deprotection by-product was observed, **164** was not.

As a result, a new route to the amine (**Scheme 13**) was explored using the Gabriel Synthesis.[372] Protected histidine was coupled to 3-chloropropylamine to give **167** as a white foam (84%). Compared with other histidine derivatives made, the melting point was relatively low (43 – 45ºC) suggesting that those with extra Boc (**152**, 60 – 62ºC) or Fmoc (**163**, 99 – 100ºC) groups have increased intermolecular interactions in the solid state. NMR ($CDCl_3$) and HRMS spectra confirmed that formation of this product, a chlorine isotope pattern being observed in the latter case.

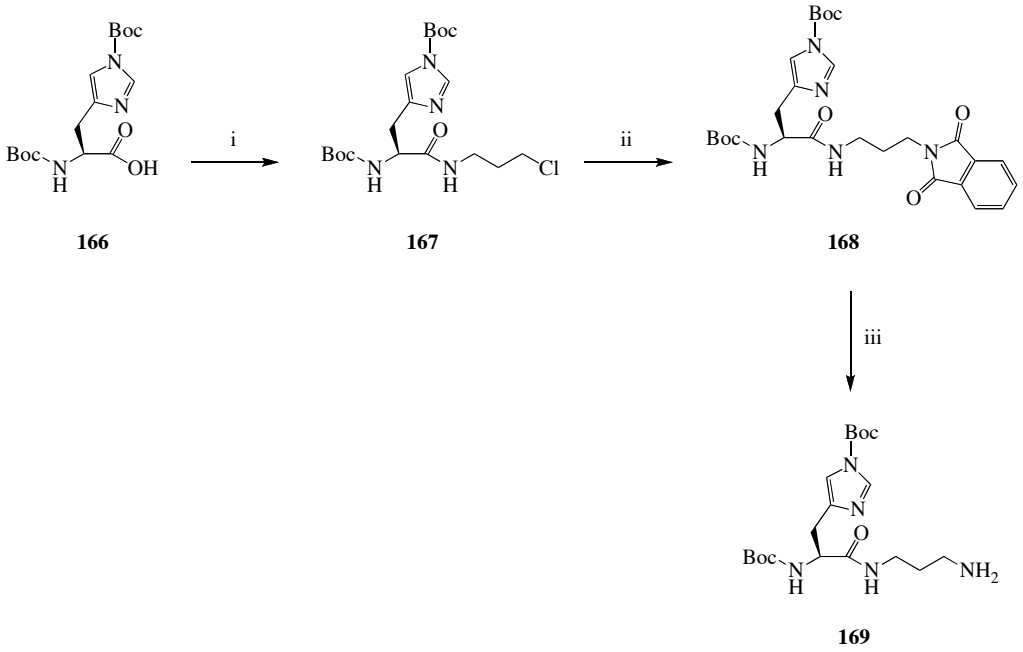

166 **167** **168**

169

Scheme 13. *i, 3-Chloropropylamine•HCl, HBTU, HOBt, DIPEA, DCM; ii, Potassium phthalimide, MeOH, reflux; iii, Hydrazine, MeOH.*

The second step involves the addition of potassium phthalimide to **167** in methanol (at reflux), which will displace the chloride to give **168** and KCl. An aqueous workup was used to remove the salts and the organics were purified by column chromatography. The major product was identified as Boc-His-propylchloride (i.e. starting material minus a Boc group). The ^{1}H NMR spectrum (MeOD) displayed only one Boc group signal at δ 1.35 ppm as well as no new peaks in the aromatic region relating to the phthalimide group (the Boc group that was lost was that attached to the imidazole ring). MS (ES^{+}) data showed a peak at m/z 331.2 (100%) that was assigned as [Boc-His-propylchloride + H]$^{+}$ (showing a chlorine isotope pattern), further confirming that the desired product had not been formed. It seems evident that the conditions used here promote the loss of the imidazole Boc group so the reaction was repeated using less harsh conditions i.e. without reflux. This, however, resulted in the same deprotected material being formed, further suggesting that the imidazole Boc group is not stable in the presence of potassium phthalimide under even mild conditions. Given this information, work on this route was halted, as even using a better leaving group (such as bromide or in the presence of an iodide catalyst) would fail to give **168** in adequate yield.

It should be noted that there are other options that could be explored, for instance the primary amide could be formed and then reduced, but the reduction may effect other functional groups within the structure.[413] It may also be possible to form the isocyanate from the acid via a Curtius Rearrangement, though this may prove to be too reactive for the dendrimer solvent medium.[414-416]

4.3 Histidine Surface via *Click Chemistry*

The routes discussed above have been shown to have some major drawbacks, namely poor attachment to a dendrimer surface and deprotection problems. Whilst using an isothiocyanate linker alleviates one of these issues, the protection on the histidine still needs to be removed which has been shown to be hard to do. A solution to both these problems can be found by using an azide-alkyne Huisgen cycloaddition, also know as a 'Click' reaction.[169,170] By partially attaching a small alkyne-containing group to the

surface of a dendrimer, and modifying a histidine unit to contain an azide group, we can link them together to form a 1,2,3-triazole using a copper (I) catalyst. This avoids the use of any bulky coupling agents as the alkyne-containing group can be attached using an isothiocyanate group (that will also introduce a sulphur atom for elemental analysis) whilst the 'click' step requires little surface space. The modified histidine unit also gives an advantage over previous routes as it can be deprotected *before* it is put onto the dendrimer surface.

4.3.1 Alkyne Surfaced Dendrimer

As with all surface modifications, the best ways to characterise these materials is by $^{1}H/^{13}C$ NMR spectroscopy and elemental analysis. To that end, the alkyne-containing unit was designed in such a way as to be attached to the dendrimer using an isothiocyanate linker and also to contain an easily recognizable group by NMR, the synthesis of which is shown below.

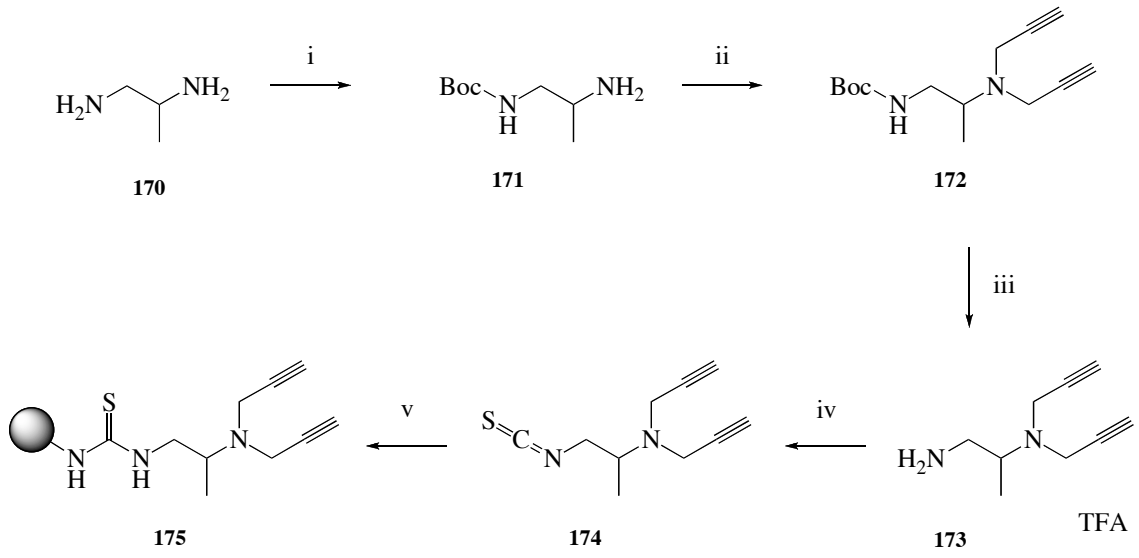

Scheme 14. *i, Boc_2O, DCM; ii, Propargyl chloride, NaI, K_2CO_3, acetone; iii, TFA, DCM; iv, $CSCl_2$, $NaHCO_3$, DCM, 0ºC; v, PEG-G4 (EDA), TFA, DCM.*

We decided to base this unit around 1,2-diaminopropane as it is a similar size to EDA and has a methyl group that lies outside the dendritic region in both ^{1}H and ^{13}C NMR. Since there are two amines present, a large excess of the diamine was used in the Boc protection step together with a large amount of solvent to afford a high dilution. The first attempts gave a high yield (>90%) but low purity, approximately 3 molecules of **171** for every regio-isomer *tert*-butyl 1-aminopropan-2-ylcarbamate. With a higher dilution a lower yield (44%) but higher purity (7:1) was achieved. Given the cheapness of the starting materials involved, this lower yielding but more selective reaction was deemed more suitable. Analysis by ^{1}H and ^{13}C NMR spectroscopy ($CDCl_3$) confirmed that the methyl group lies outside the normal dendritic range, this group appearing at δ 1.05 (doublet) and 21.5 ppm respectively. **171** was then added to a solution of dry acetone containing 2.2 equivalents of propargyl chloride in the presence of sodium iodide and potassium carbonate to give *tert*-butyl-2(N,N-di(prop-2-ynyl))aminopropylcarbamate (**172**). Purification by column chromatography gave the product as a colourless oil in reasonable yield (30%) and also showed that a small quantity of the mono-substituted product was formed. This purification step also removed any of the isomer formed during the previous reaction. ^{1}H NMR data ($CDCl_3$) showed a downfield shift for the chiral C*H* proton from δ 3.11 to 3.22 ppm as well as the introduction of new signals at δ 3.43 (singlet) and 2.22 ppm (triplet) relating to the propargyl units.

The Boc deprotection was first carried out using refluxing conc. HCl in methanol. This was found to remove some of the alkyne groups and give poor NMR resolution so TFA in DCM at RT was then used which gave a quantitative yield of **173**. Mass spectrometry (ES^{+}) revealed two signals (m/z 134.1 (100%) and 151.1) suggesting that one of the alkyne units had fallen off, but integrals in the ^{1}H NMR spectrum (MeOD) showed that pure product had been formed, so this observation is most probably because of the electrospray ionization.

The formation of 1-isothiocyanato-2-(N,N-di(prop-2-ynyl))aminopropane (**174**) was formed by addition of **173** to a stirred solution of thiophosgene in DCM in the presence of sodium bicarbonate. When a slow addition rate was used it was found that two units of **173** became joined by a thio-urea so the reaction was repeated with an even slower

addition rate to yield the desired product as a pale brown oil (96%). ^{1}H NMR data ($CDCl_3$) indicated the presence of the isothiocyanate through a downfield shift of the adjacent methylene unit while ^{13}C NMR data showed a downfield shift from δ 21.7 to 48.6 ppm for the same group. FTIR spectra revealed the presence of alkyne stretches (3292 cm^{-1}) and isothiocyanate stretches (2100 cm^{-1}) whilst MS showed the presence of both the product and the methanol derivative (sample run in methanol).

The attachment of **174** to an unmodified 4th generation dendrimer (in H_2O/dioxane) resulted in a yellow oil that, upon drying, became insoluble in all common laboratory solvents. To aid the solubility of this product, the reaction was repeated using a dendrimer that had been modified with PEG groups (this was achieved *via* a method described in **Section 3.1.2** and was found to possess 18 PEG groups by elemental analysis; **139**). The presence of the PEG groups allowed the reaction to be performed in DCM, thus avoiding any water related by-products. **175** was purified by dialysis in DCM/methanol and found to be readily re-solublised after drying. Elemental analysis showed 28 sulphur atoms to be present; since 18 are known to come from the PEG chains 10 must be due to the alkyne units, thus we have 20 alkynes on the surface of the dendrimer. The presence of the alkyne groups was confirmed by NMR spectroscopy, principally from signals at δ 3.51 (CH≡C-C*H*$_2$-) and 1.38 ppm (-CH$_2$-CH(C*H*$_3$)-N-) in the proton spectrum and δ 71.8 (CH≡*C*-CH$_2$-), 68.1 (*C*H≡C-CH$_2$-) and 13.9 ppm (-CH$_2$-CH(*C*H$_3$)-N-) in the carbon spectrum, though not by FTIR as the spectrum was dominated by the dendrimer stretches.

4.3.2 Azide Modified Histidine

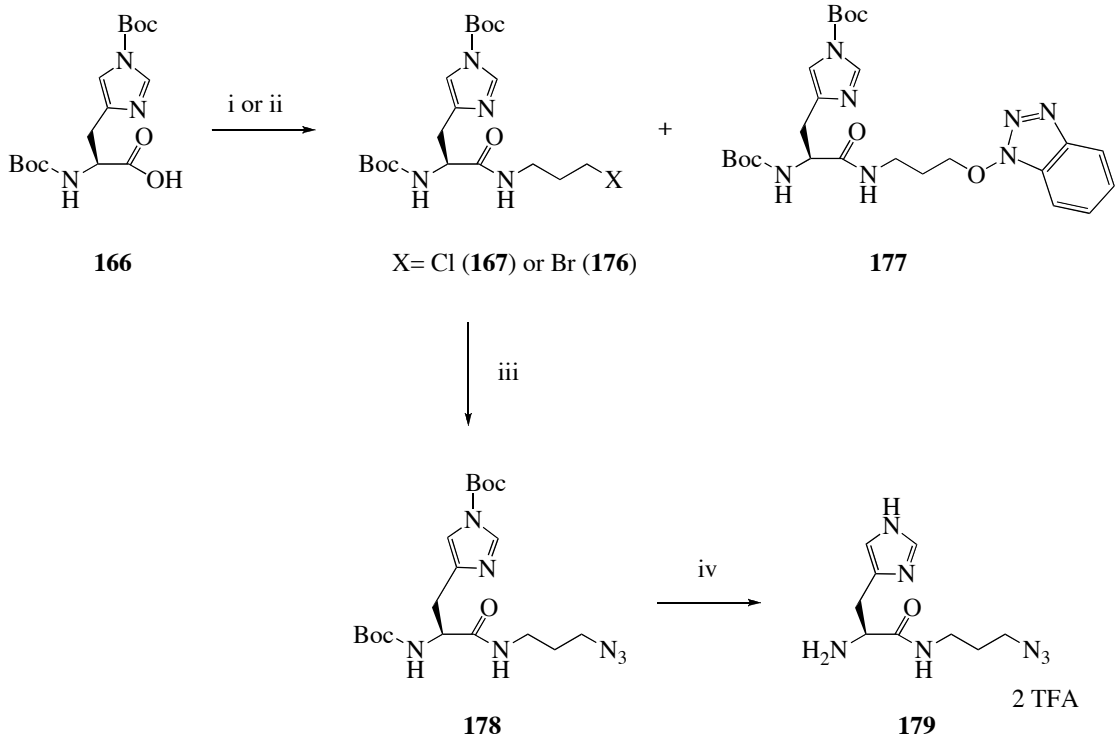

Scheme 15. *i, 3-Chloropropylamine•HCl, HBTU, HOBt, DIPEA, DCM; ii, 3-Bromopropylamine•HBr, HBTU, DIPEA, DCM; iii, NaN_3, DMF, 60ºC; iv, TFA, DCM.*

The synthesis of the azide component of the 'Click' reaction is shown in **Scheme 15**. The Boc-protected derivative of histidine was used in these reactions as this can be easily removed prior to the 'Click' reaction; Trt protection was thought to be too easily removed by repeated acidic workups. **167** was synthesised using standard peptide coupling reagents (as described in **Section 4.2.1**) as a white foam (81%). No azide could be formed from this product, the chlorine being a poor leaving group and no reaction was observed even in the presence of sodium iodide. To check that the Boc groups could be removed, **167** was added to TFA in DCM and gave the desired product **180** (NMR showed no Boc present) in a 98% yield as a white solid (mp: 38 – 40ºC).

To aid the formation of the azide, 3-bromopropylamine was coupled to the protected histidine as the bromine is a much better leaving group. Despite the formation of the desired product **176**, it also resulted in the formation of the by-product **177**. This is due

to HOBt being formed from the HBTU as it reacts (**Figure 92**), which can then displace the bromine. It is for this reason that no extra HOBt was added to make the activated ester intermediate. These products were then separated by column chromatography to give white foams (**176**: 43%, **177**: 12%), the desired product being confirmed by HRMS and NMR data (mp: 40 – 42ºC, similar to that of **167**). This reaction was repeated using EDCI as the coupling agent as this would eliminate the formation of **177**, but it was found to give a reduced yield of the desired product.

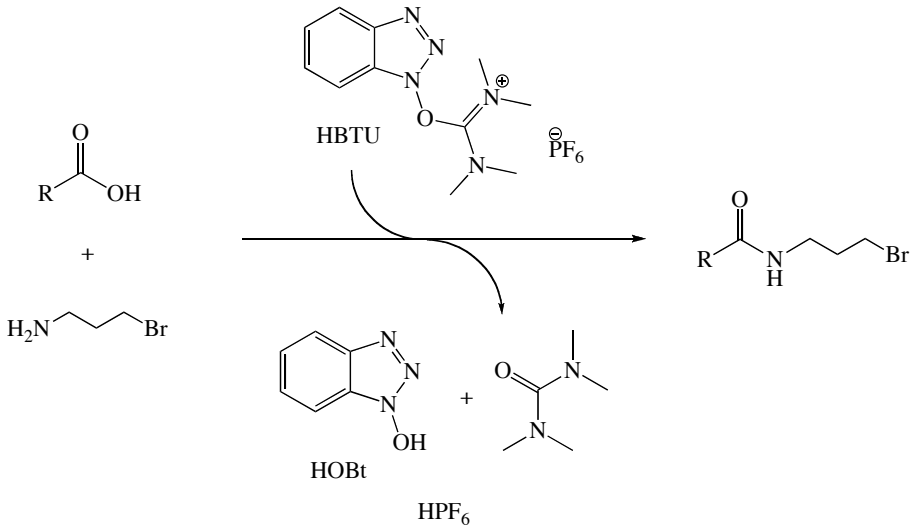

***Figure 92**. HOBt formation during a peptide coupling reaction using HBTU.*

Sodium azide was then added to a solution of **176** in dry DMF and the mixture was allowed to stir at 60ºC.[417] After purification, the product was found to be a colourless glass (32%), NMR and HRMS data confirming formation of the product. The NMR ($CDCl_3$) spectrum of **178** shows a change in the shift values of the aliphatic chain, namely the two methylene units closest to the azide; they move upfield in the proton spectrum (compared to **176**) from δ 3.33 and 1.97 ppm to δ 3.22 and 1.73 ppm respectively, whilst in the carbon spectrum the adjacent methylene carbon moves downfield from δ 30.5 to 32.3 ppm whereas the other moves upfield from δ 32.1 to 28.6 ppm. The final step was the Boc deprotection using TFA, which resulted in formation of the white TFA salt **179** (85%). Though ^{13}C NMR spectra (DMSO-d_6) did not show the presence of TFA, yield calculations suggest that two TFA molecules are present in the salt (which we would expect since two Boc groups are being removed). The ^{1}H

NMR spectrum and MS (ES^+; m/z 250.2) showed that the desired product had been formed, the former indicating that no Boc groups were present.

4.3.3 Click Reaction

Following literature proceedure,[80,174,176] the alkyne surfaced dendrimer **175** and azide modified histidine **179** were placed in THF/water in the presence of sodium ascorbate and copper sulphate. The sodium ascorbate reduces the copper from Cu (II) to Cu (I) which then initiates the 'click' formation of the triazole as shown in **Figure 93** (it should be noted that only the isomer with the least steric hindrance is shown).

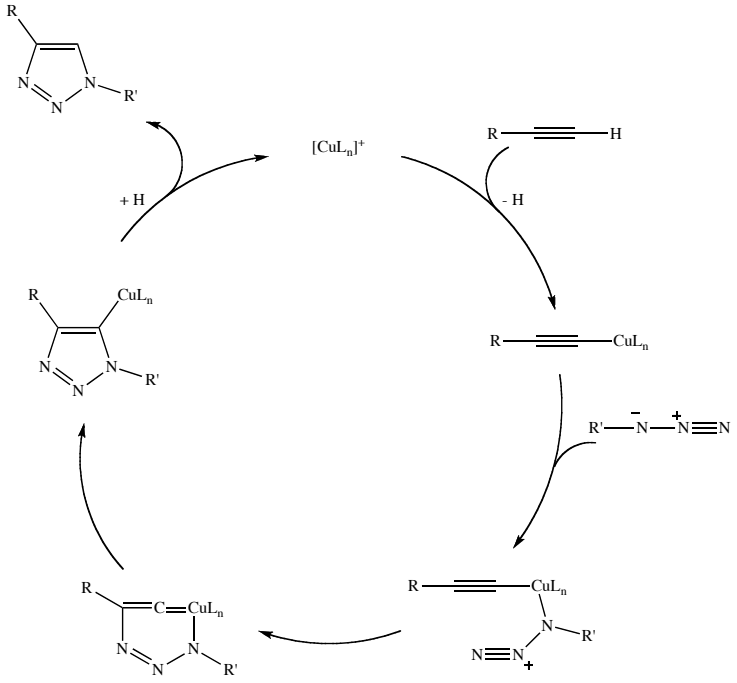

***Figure 93**. Formation of a 1,2,3-triazole during a 'click' reaction.*

If the desired product (**181**) had formed we would expect to see aromatic peaks in the ^{1}H NMR relating to the imidazole from the histidine and the triazole, together with a downfield shift of the methylene units adjacent to the triazole. None of these were observed (**Figure 94**). Instead, it can be seen that the peak relating to the methylene adjacent to the alkyne remains unmoved (MeOD, δ 3.55 ppm), suggesting that some, if not all the alkynes failed to react. It is hard to say whether any reaction took place as it

is impossible to get accurate integral data because of the broad dendrimer and PEG peaks that overlap most methylene signals, though the scarcity of signals in the aromatic region would seem to confirm that no reaction had occurred. In the ^{13}C NMR spectrum (MeOD) once again no aromatic signals were observed, though new peaks appeared at δ 51.2, 40.1 and 34.6 ppm. The peak at δ 51.2 ppm could be due to a methylene unit located next to the triazole though other peaks suggest the alkyne is still present. It remains unclear as to what the other two peaks are, but they could be due to the histidine unit.

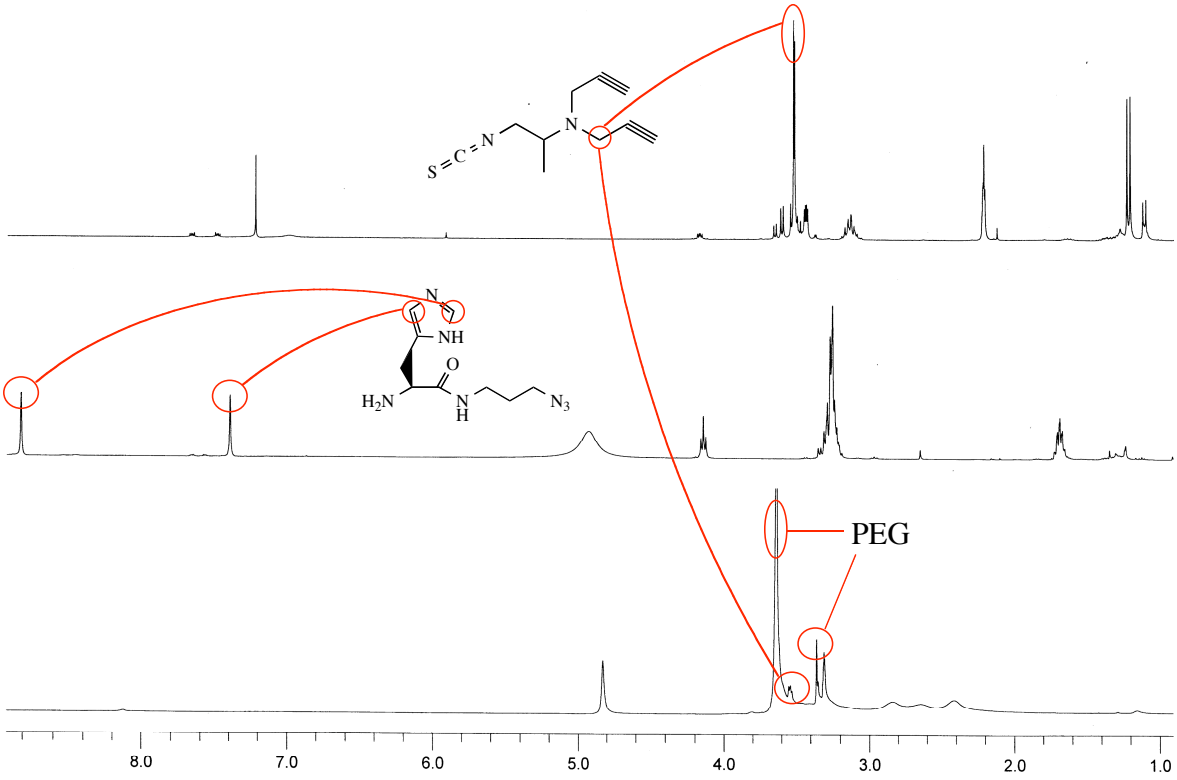

Figure 94. *^{1}H NMR spectra of **174** (top, $CDCl_3$), **179** (middle, DMSO-d_6) and product after Click reaction **181** (bottom, MeOD) all run at 400 MHz.*

If a 'Click' reaction had indeed taken place we would be introducing more nitrogen onto the molecule that should lead to an increase in the N:S ratio observable by elemental analysis. However, this was not seen; analysis showed that when 28 sulphur atoms were present (known from previous experiments), the amount of nitrogen remained the same as the starting material further suggesting that no reaction had occurred.

It has become clear that the key to these reactions lies with the solubilising effect of the PEG chains. Without them the alkyne modified dendrimer becomes insoluble, whilst their presence can provide enough steric hindrance to prevent the reaction occurring.[299] Further work in this area should look at limiting the number of solubilising groups whilst increasing the number of alkynes present. This should lead to increased reactivity as well as better NMR resolution making the reactions easier to follow.

4.4 Conclusions and Further Work

We aimed to attach histidine onto the surface of a PAMAM dendrimer in such a way as to allow for binding to DNA i.e. leaving the primary and imidazole amines free of protecting groups. To that end, trial couplings were made between Boc-His(Trt)-OH or Boc-His(Boc)OH and the small molecule Boc-EDA (to simulate a dendrimer arm) utilizing different reagents and solvents. It was found that HBTU/HOBt in DMF was the system of choice giving consistent yields in a solvent that gave high solubility to PAMAM dendrimers, though EDC in DCM gave higher yields in both cases.

Boc-His(Boc)-OH and Cbz-His-OH were successfully attached to the amine surface of 4th generation dendrimers using the conditions stated previously. In the case of the Boc protected species, high surface coverage resulted in an insoluble product, whilst using less histidine gave higher solubility but lower than expected coverage (approx. 65% of expected value). This was at first attributed to the use of a small amount of water in the reaction, but when it was repeated in DMSO a similar observation was made. It is believed that the bulky nature of the amino acid intermediate is to blame. Furthermore, the terminal amine groups may lie within the interior of the dendrimer. It should be noted however, that when Cbz-His-OH was used an accurate coupling of 8 groups was made, suggesting that it this low coverage was affected by the imidazole protecting group. Couplings made using Fmoc as the protecting group were found to fail as a result of the amines of the dendrimer itself removing the Fmoc group before the histidine could attach. A greater number of couplings would help increase our understanding of how the bulky intermediate affects different surface coverage's as well as showing the highest coverage (whilst retaining solubility) possible.

Reaction of Boc-protected histidine dendrimers with TFA resulted in little deprotection; Cbz was found to be more reliably removed by hydrogenation using a palladium on carbon catalyst.

The synthesis of a histidine unit that could be attached *via* an isothiocyanate linker was attempted using two routes. The first involved the coupling of protected histidine to Fmoc-EDA; the Fmoc group could then be removed to give a primary amine that could be converted into the isothiocyanate. It was found that the removal of the Fmoc group left a product that was hard to isolate, so a second route was tried. This involved using the Gabriel Synthesis to convert a chloride into an amine *via* a phthalimide intermediate. However, the synthesis of this intermediate resulted in the removal of the imidazole protecting group, so work on this route was halted. Further work to explore the introduction of a sulphur atom into the attachment of histidine onto a dendrimer is required, possibly utilizing different protection strategies and linker groups.

The use of a 'Click' reaction between an alkyne and azide was explored. A small alkyne containing molecule was synthesised that contained both an easily recognizable group by NMR and a sulphur atom that would allow for surface coverage calculations *via* elemental analysis. It was found that a dendrimer modified with PEG chains was required as without them, the product was very difficult to solubilise. Boc-His(Boc)-OH was modified to contain an azide group before being deprotected. These two components were then reacted under 'Click' conditions using a Cu (I) catalyst but it was found from NMR spectra and elemental analysis that none of the desired product had formed. This is most likely because of the bulk of the aforementioned PEG chains. By reducing the number and length of the PEG chains on the dendrimer it might be possible to limit their interactions during the 'Click' process whilst retaining this solubilising effect.

Chapter 5 Incorporating Azobenzene into a PAMAM Architecture

Dendrimers containing the photo-responsive group azobenzene have been studied for a wide range of applications, though most work has looked at using these units either as the core or on the surface (**Section 1.3.8**). By building a dendrimer around an azobenzene core, a change in hydrodynamic radius can be observed, though this typically requires stiff extension arms in each shell.[253,258,260] PAMAM dendrimers with an azobenzene core were studied by Ghosh *et al*. and were found to give limited hydrodynamic changes after generation 2.5.[251,261]

It was decided at the onset of this project that a photo-responsive dendrimer would possess advantageous properties for DNA binding, principally the potential ability to compact/decompact the DNA as a response to illumination at a suitable wavelength. Work with photo-responsive groups within this thesis has concentrated on introducing azobenzene units into/onto a PAMAM dendrimer as there has been little reported concerning their inclusion in the interior of the dendritic structure. Different methods of azobenzene synthesis have been investigated here with the aim of incorporating these units into the arms a dendritic structure.

5.1 Azobenzene as the Core

Published literature has shown that azobenzene can be attached to the surface of polyamine dendrimers[257] as well as used as a core,[251] but little data was found about using it as part of the branching structure of PAMAM derivatives. In order to synthesise an azobenzene unit that can do such a task, it must possess a free amine group at one end, as well as a means of attachment to the developing dendrimer at the other.

Work by Ghosh *et al.* was repeated to help give a greater understanding of azobenzene synthesis using aromatic compounds that possess no electron donating groups (which are commonly used in azobenzene synthesis).[261] To that end, a dicarboxylic acid derivative of azobenzene was synthesised from *p*-nitrobenzoic acid in one of two ways (**Scheme 16**).

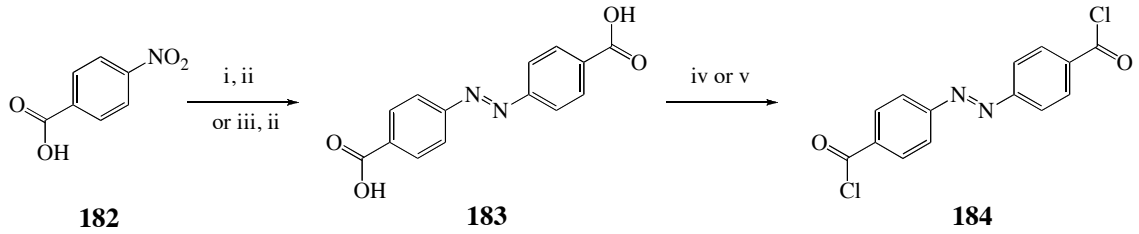

***Scheme 16**. Formation of azobenzene-4,4'-dicarboxylic acid. i, Glucose, NaOH, H_2O, 50ºC; ii, acetic acid; iii, Zn powder, MeOH/H_2O, reflux; iv, PCl_5, 1,2-dichloroethane; v, $SOCl_2$, DCM, cat. DMF.*

In the first instance, glucose in water at 50ºC is added, *via* cannula, to a solution of *p*-nitrobenzoic acid (**182**) and sodium hydroxide in water (also at 50ºC), resulting in an orange precipitate.[418,419] Upon acidification with glacial acetic acid, the solid turned pink and, when dried in an oven, gave product **183** as a brown insoluble solid (60%). Though this procedure was repeated multiple times, no analytical data concerning the product could be acquired because of its insolubility. The second route involved refluxing the starting material with zinc powder followed by an acidic workup, which when dried gave the product (**183**) as a pink solid in a 69% yield.[420,421] Unlike in the previous route, it was found that this product was sparingly soluble in DMSO. ^{1}H NMR (DMSO-d_6) data showed a broad singlet (δ 12.27 ppm) and two doublets (δ 6.73 and 7.74 ppm) relating to the desired product, but also that some starting material remained. In view of its poor solubility no further purification was attempted. These reactions share a common mechanism, namely the reductive coupling of two nitro groups to an azo linkage (it is important to note that the presence of a large excess of the reducing agent will further reduce the azo unit to a hydrazine group).

The di-acid (**183**) was then converted to the di-acid chloride (**184**) using either phosphorus pentachloride (27%)[418] or thionyl chloride (70%). Both gave the product as red crystals which showed a change in the aromatic signals in both ^{1}H and ^{13}C NMR spectra ($CDCl_3$; δ 7.93 and 8.18 ppm, and δ 123.5 and 132.5 ppm respectively), though further analysis by ^{13}C NMR revealed the presence of trace impurities in the higher yielding reaction. These compounds were then introduced to previously prepared dendritic wedges (dendrons), 1.5-[PAMAM dendron]-4-Ester, in dry DCM to see if dendrimers with an azobenzene core could be made (**Scheme 17**). It was found that the major product from this reaction was not 1.5-[Azobenzene]-8-Ester **186**, but a mono-substituted version. It was found that one end of the azobenzene core would react readily with the dendritic wedge, whilst the other was found to react with methanol that had become trapped in the dendritic structure during its' synthesis (**187**). To check this hypothesis a different core was used, that of terephthaloyl chloride, but similar results were obtained.

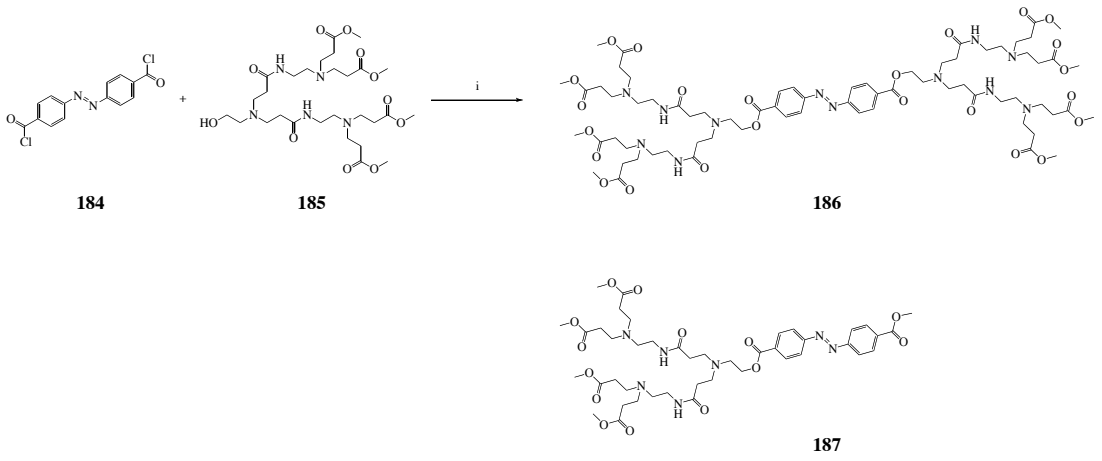

Scheme 17*. Formation of 1.5-[Azobenzene]-8-Ester. i, Triethylamine, DCM.*

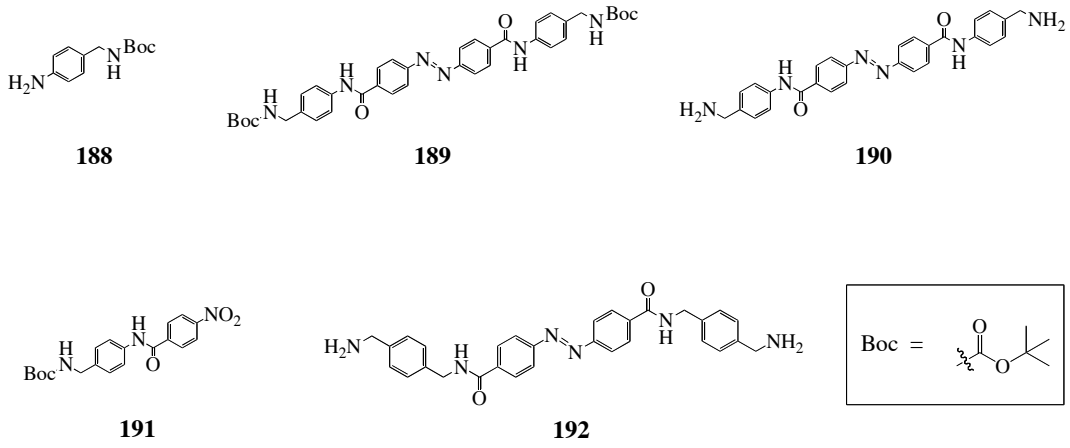

***Figure 95**. Molecules formed to study rigid core.*

A further approach for introducing azobenzene as a dendrimer core is to extend it using rigid groups (to allow for greater hydrodynamic volume change) and grow the dendrimer using the divergent method. To that end, di-acid chloride **184** was added to previously prepared ^{t}butyl-4-aminobenzylcarbamate (**188**, 93%) to give an extended core with protected amines at either end (**189**) in high yield (95%). The product had to be precipitated from DMSO and gave a melting point greater than 300ºC. The complex NMR spectrum suggested that the orange solid was pure (NMR assignments aided by comparison with previously prepared **191**, 48%). Attempts at deprotecting **189** with TFA led to the formation of **188** and **190**, suggesting that the amide bonds in this molecule are not stable to such an acidic environment. The assignments of these products were deduced primarily from ^{1}H NMR, which, though giving a very weak signal as a result of being sparingly soluble in DMSO, showed too few Boc groups for the number of aromatic protons present. The synthesis of **192** was attempted from **184**, *p*-xylylene diamine and triethylamine so as to avoid the deprotection step, but the resulting orange solid proved to be insoluble in all common laboratory solvents.

5.2 Azobenzene at the Interior

Having learnt that methanol may always be present during reactions with dendrons, and that synthesising a more rigid core leads to solubility problems, it was decided that a better approach would be to attach the azobenzene unit to the surface of the dendrimer

in such a way as to allow for continued growth. Initially, two routes were investigated; the first was to use an isothiocyanate linker (**Scheme 18**), the second involved the use of either an acid chloride or *via* peptide coupling with a carboxylic acid (**Scheme 19**).

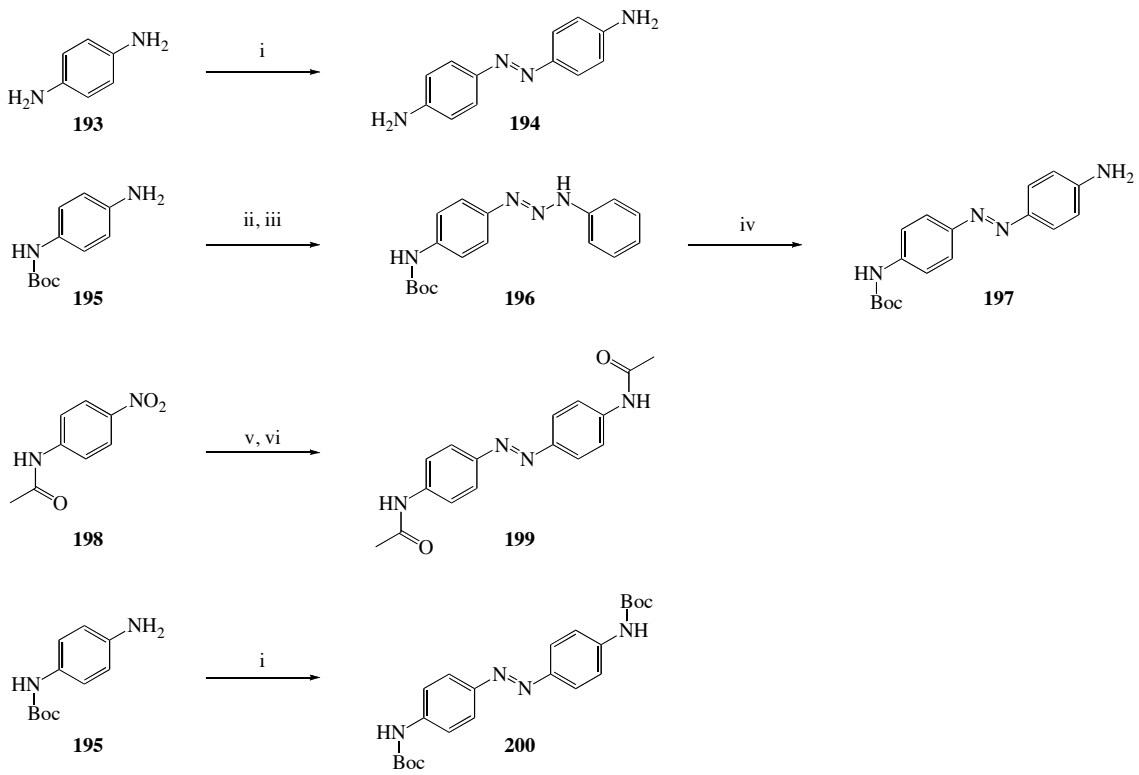

***Scheme 18**. Formation of azo dyes. i, MnO_2, $CHCl_3$, reflux; ii, conc. HCl, $NaNO_2$, H_2O, <5°C; iii, aniline, RT; iv, sodium acetate, NaOH; v, Zn powder, MeOH/H_2O, reflux; vi, H^+ work up.*

The use of isothiocyanate as a linker unit has been discussed before (**Section 3.1.2**), but it should be mentioned again that its main advantage is to introduce a sulphur atom that can be used to determine the level of surface coverage (using elemental analysis). In order for this azobenzene unit to be of use, it requires two amine groups (one at either end): one for conversion into the isothiocyanate and the other to act as the dendrimer surface.

The formation of 4,4'-diaminoazobenzene (**194**) proceeded from *p*-phenylenediamine and manganese (IV) oxide in negligible yield (3%), which is low compared to the literature reports (30%).[422,423] This reaction is believed to proceed *via* radical formation

on the nitrogen (**Figure 96**) generated by the MnO_2, so that two molecules can dimerise to form a hydrazine. The MnO_2 then oxidizes this to the azo group. The low yield is believed to be a result of the formation of a diradical that can isomerise to a quinone diamine; this can then hydrolyze to give the corresponding quinone which can itself be readily polymerised.[423]

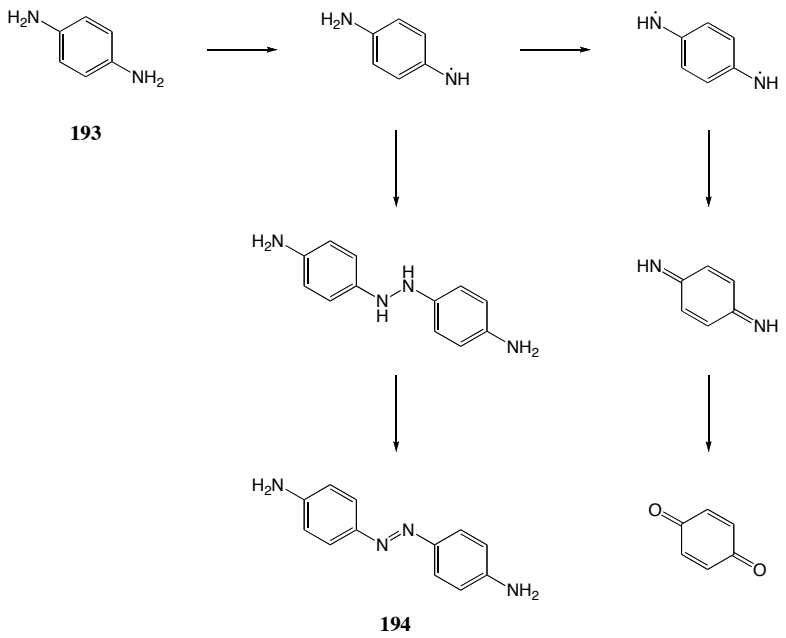

***Figure 96**. Formation of azobenzene **194** and associated side products in the presence of manganese (IV) oxide.*

Preparation of a protected version of **194** was also explored *via* a triazene intermediate,[424,425] though this gave none of the desired product. Protected aromatic amines were then used, one of which possessed a nitro group and the other an amine. The nitro-aromatic (**198**) was reduced to azo-compound **199** using zinc powder (as described in **Section 5.1**) to give none of the desired product, whilst the amine-aromatic **195** underwent an oxidation using manganese oxide. All these azobenzene products were achieved in very poor yield (or none of the desired product was isolated), low enough that there would not be enough material to attach to the dendrimer, so the idea of an isothiocyanate linker was temporarily put aside.

The second of the preliminary routes looked at using a carboxylic acid group for the attachment to the dendrimer surface. Since an amine group on the azobenzene unit would interfere with this coupling, be it *via* acid chloride or using peptide coupling agents, this would first need to be protected with either a Boc or an Fmoc groups (**Scheme 19**). Compounds **188** and **202** were synthesised from 4-aminobenzylamine by reacting with either di(^{t}butyl)dicarbonate (Boc_2O) to give **188** a white solid (93%),[426] or N-(9*H*-fluorenylmethoxycarbonyloxy)succinimide (Fmoc-OSu)[427] to give cream crystals of **202** (35-80%) respectively.

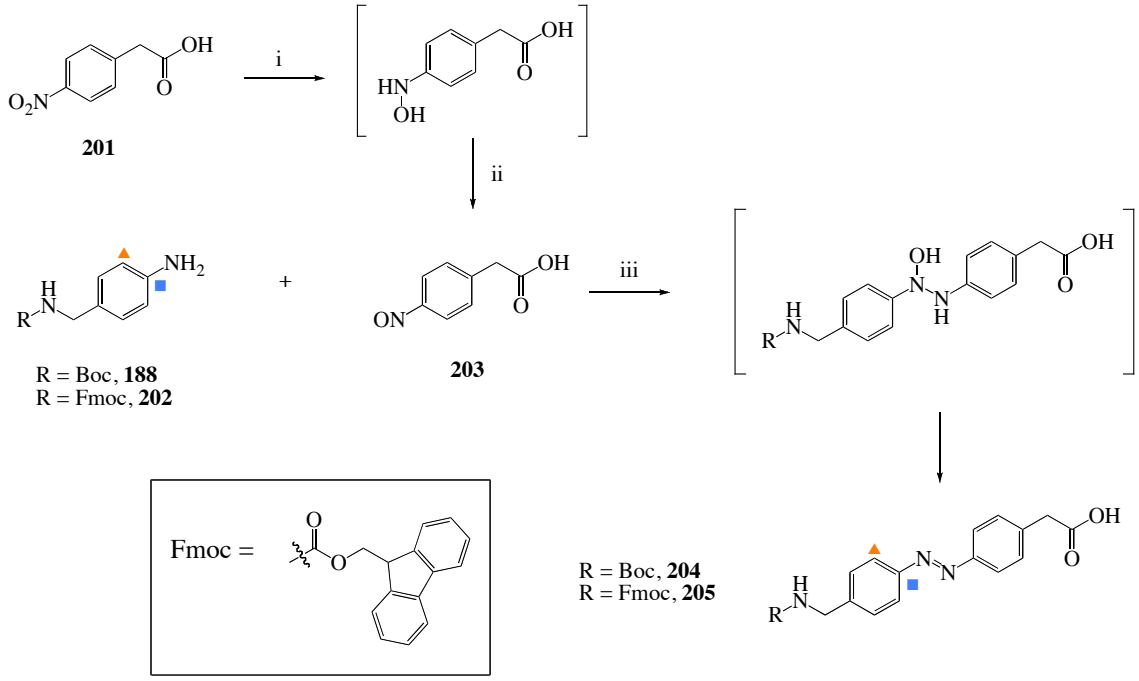

Scheme 19. *Formation of protected amino-acid type azobenzenes. i, Zn powder, NH_4Cl, 2-methoxy ethanol; ii, $FeCl_3$, $EtOH/H_2O$, 0ºC; iii, acetic acid.*

4-Nitrosophenylacetic acid (**203**) was prepared by first reducing 4-nitrobenzoic acid to the corresponding hydroxylamine intermediate using zinc powder as the reducing agent in the presence of ammonium chloride. This was then oxidized *in situ* to the nitroso analogue using iron (III) chloride. The product was extracted into diethyl ether, reduced and dried, to give **203** as a green oil in good yield (51%).[426-428] Nitroso compounds are reputed to be unstable and to readily decompose (even at low temperatures), so the product was used immediately in the next step without further characterisation.

The 4-nitrosophenylacetic acid **203** was added to **188** (or **202**) in acetic acid and the mixture was allowed to stir for 24 hours. The Boc-protected product (**204**) was crystallised from DCM as an orange solid (8%). When compared to the starting material, ^{13}C NMR data (DMSO-d_6) for the product showed a shift in the quaternary carbon attached to the amine (■), as well as that for the adjacent carbon in the ring (▲), from δ 145.7 to 150.6 ppm and δ 115.1 to 122.4 ppm respectively. Further analysis of **204** by NMR spectroscopy, HRMS and elemental analysis shows good purity and a strong correlation with published data, though the melting point was found to be lower than expected, 189 – 190ºC (lit[426] mp: 196 – 198ºC). **205** was purified by column chromatography to give product as an orange solid in a 9% yield (mp: 174 – 176ºC). Analysis, again by NMR, HRMS and elemental analysis, showed a good level of purity and the data compared well with that for **204**, though no published data could be found for direct comparison. From IR data both of these products were found to show that the amine stretch (~3400 cm^{-1}) had been replaced with an azo stretch (~1600 cm^{-1}).

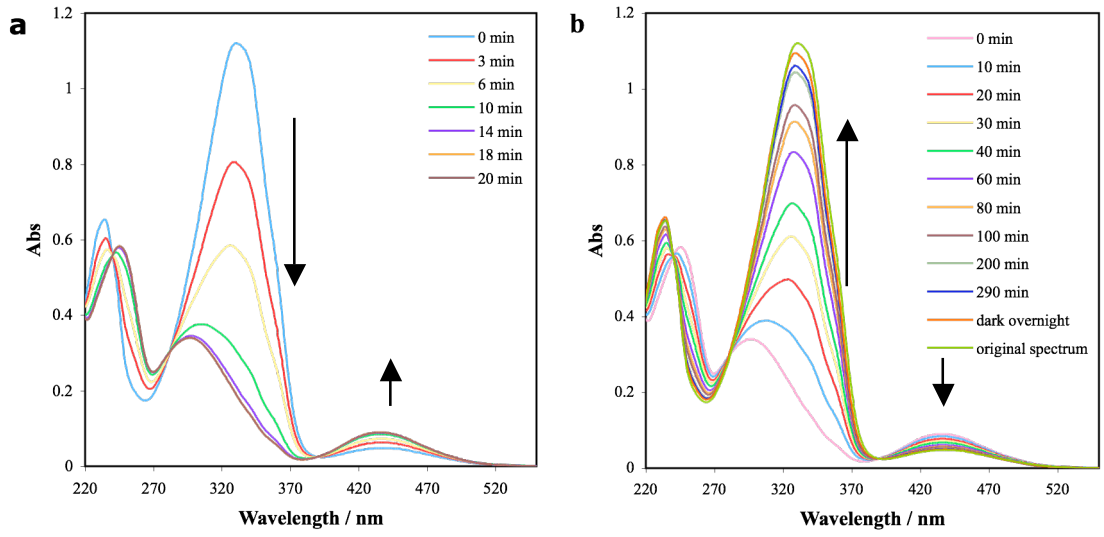

***Figure 97**. UV/Vis absorption spectra of azobenzene **204** (a) switching from trans- to cis-isomer via illumination at 365 nm, and (b) switching from cis- to trans-isomer via illumination in daylight. Measurements taken at 4.77 x 10^{-5} M in methanol.*

In order to show reversible photo-isomerisation of the azo group, compounds **204** and **205** were used in a series of UV/Vis experiments, the results for **204** are shown in **Figure 97**. Methanol solutions of the protected azobenzene molecules were first kept in the dark for 1 week, then irradiated with UV light at a wavelength of 365 nm for up to 20 minutes to isomerise them from the *E* to the *Z* configuration. This was primarily observed as a decrease in absorbance of the respective π-π* bands of the N=N unit (330 nm).[253,418,429,430] It was also seen that the absorbance at 440 nm (n-π*) increased whilst that of 235 nm (σ-σ*) decreased.[428] Furthermore, isosbestic points were observed at 245 and 285 nm in both cases. It was noticed that after 6 minutes of illumination the absorbance peak at 235 nm had equilibrated and there then followed the appearance of a peak at 250 nm which seemed to slightly increase in absorbance with further illumination. Quite why this should occur is unclear as no literature precedence could be found for it relating to this class of molecules.

Published literature has shown that in order to isomerise these molecules from *Z* to *E*, they need to be either placed in the dark for long periods of time (thermal relaxation) or by irradiation at the wavelength of the n-π* transition (approximately 440 nm).[253,418,429,430] Work published by Freitag et al.[431] also showed that daylight could be used to facilitate the *Z* to *E* change. With this in mind, samples of **204** and **205** were exposed to daylight, whilst a duplicate of each was placed in the dark. It was found that the samples that were placed in the dark showed negligible change in their absorbance spectra after 8 hours (though each gave complete conversion after 1 week), so it was decided to discontinue this experiment as this thermal back-isomerisation would be too slow for practical isomerisation (in the Neonuclei project). Samples placed in daylight were found to equilibrate in less than 5 hrs to about 95% conversion, though it was only when they were placed in the dark overnight that complete conversion occurred. This result can be explained by the fact that white light was used for this isomerisation, so that while the sample is being exposed to 365 nm there is also present 440 nm radiation, which is promoting formation of the *E* isomer. This would explain why using daylight gives faster transitions but does not lead to complete isomerisation i.e. while the thermal process is slow, it does give high degrees of *E*-isomer formation.

The samples exposed to daylight showed an increase in absorbance at 330 nm as well as a decrease at 440 nm, and were equilibrated after 290 minutes. It was observed that the equilibrium absorbance value at 330 nm did not reach that of the original *E*-isomer sample, though it did return to its original absorbance intensity after 1 week in the dark.

It was proposed that these carboxylic acids could be attached to the dendrimer amine surface *via* formation of the respective acid chloride (using thionyl chloride), but it was found that when the acid chloride samples were coupled to a G0 (EDA) dendrimer they gave either the methyl ester azo product (as observed with the azobenzene core) or an orange oil that gave an inconclusive NMR spectrum.

Since none of the routes tried up to this point gave high enough yields of suitable material (or satisfactory results) it was decided that the formation of the azobenzene moiety should be developed in such a way as to allow for various different linking strategies. With this in mind, protected aminoazobenzenes were synthesised containing a hydroxyl group (**Figure 98**). This could then be further reacted with an 'extender' unit that would allow for attachment to the dendrimer and for continued dendritic growth.

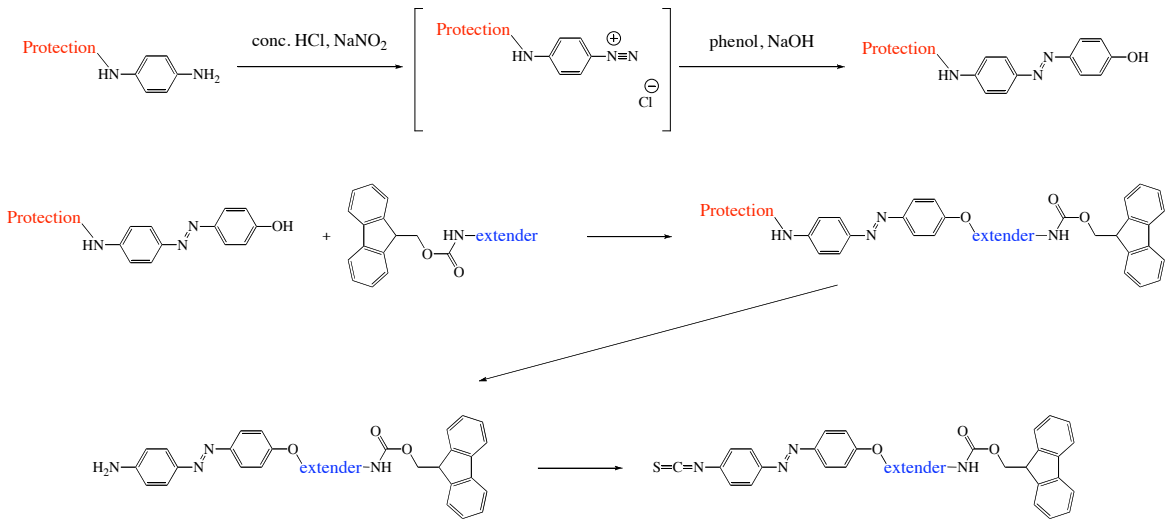

***Figure 98**. Azobenzene formation and proposed isothiocyanate attachment.*

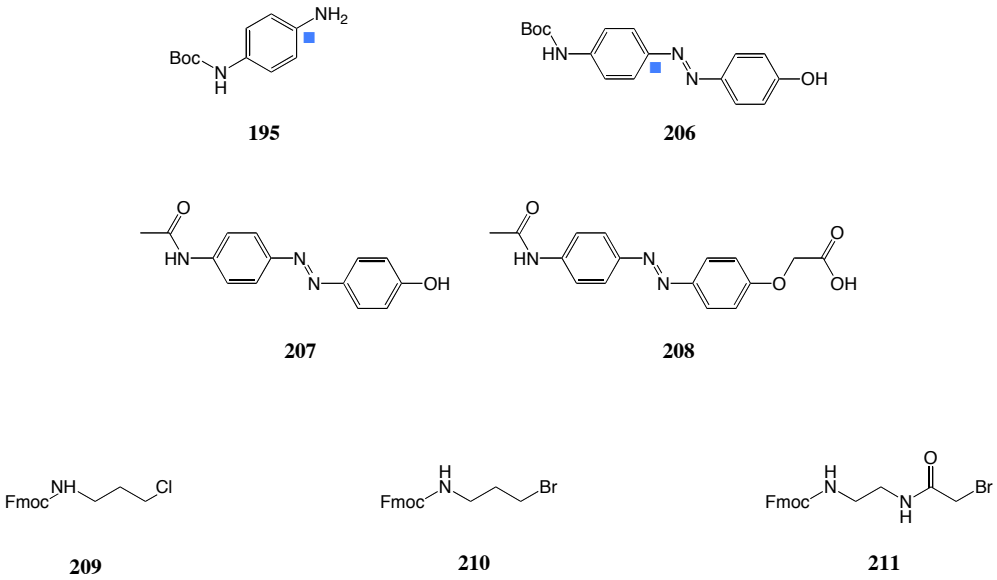

***Figure 99**. Azobenzene molecules and extender units synthesised.*

p-Phenylenediamine was mono-Boc protected in good yield (**195**, 81% mp: 104 – 105ºC) and was then used for the preparation of 4-((4-((ᵗbutylcarbonyl)-amino)phenyl)diazenyl)phenol (**206**). **195** was added to cold (<5ºC) conc. HCl in water and sodium nitrite was then added to form the diazonium chloride salt as a pale yellow solution. To this mixture was then added a solution of phenol in sodium hydroxide and an orange precipitate immediately formed. This was purified by column chromatography to separate the *ortho*- and *para*- isomers, and this gave the desired product as a light orange solid in a high yield (93%, mp: 197 – 198ºC). ^{13}C NMR (MeOD) analysis showed a change in the chemical shift for the quaternary carbon attached to the amine (■) from δ 142.4 to 149.4 ppm, whilst ^{1}H NMR showed a downfield shift of ~1 ppm for both aromatic proton signals of **195** upon azobenzene formation. HRMS and elemental analysis gave very strong correlation with theoretical values, and FTIR data indicated the presence of a N=N stretch at 1590 cm^{-1}. Similarly, 4-((4-acetamidophenyl)diazenyl)phenol (**207**, mp: 192 – 194ºC) was formed with equally high purity but lower yield (25%), and once again the sample showed good comparisons with literature data.[432]

In order that these molecules might be used for the isothiocyanate attachment approach, an extender unit would be required that possessed the ability to allow for continued dendritic growth. The protecting group on the aromatic amine could then be removed and the isothiocyanate be formed. In order to stop any intra-molecular reactions occurring between the linker and the extender group, any other amines should be Fmoc protected (as this group is stable under acidic conditions). Though work carried out looking at histidine attachment had shown that the amines on the dendrimer surface can remove the Fmoc protecting group (see **Section 4.1.3**), it was believed that the amines would react much faster with the isothiocyanate.

Molecule **209** was synthesised by the Fmoc protection of 3-chloropropylamine in good yield (84%, mp: 106 – 107ºC) and was characterised using NMR, HRMS and elemental analysis. This was then added to a solution of dry acetone containing **207**, sodium iodide and potassium carbonate. When no desired product was found *via* S_N2 displacement, it was proposed that this was due to the iodo- intermediate not being formed so molecule **210** was synthesised (68%, mp: 86 – 88ºC) and used, but to no further success. Stronger bases were then used to aid deprotonation; sodium hydride gave no visible difference, but caesium carbonate gave a solution colour change from yellow to red indicating a change in the electron density of the aromatic system. Despite this, no product was formed when **210** and sodium iodide was added. To check that the deprotonation had taken place, the reaction was repeated using a more activated bromo- species, ethyl bromoacetate. Whilst the desired ester was not isolated, the corresponding carboxylic acid (**208**, mp: 229 – 233ºC) was obtained in 31% yield. Since this reaction (partially) worked, **211** was prepared from (9*H*-fluoren-9-yl)methyl-2-aminoethylcarbamate hydrochloride (**162**) and bromo acetylbromide (55%) but once again none of the desired product was obtained when this was reacted with **207** under similar conditions to those described above. It should be noted that where no product could be isolated from these reactions, starting materials were recovered.

5.3 Azobenzene Attachment to PAMAM Dendrimer

As a result of the isolation of **208** it was realised that this could be converted into its acid chloride and thus linked to the dendrimer surface (though the protecting group of the aromatic amine would need to be changed so that it could be removed in the presence of the dendrimer, i.e. Boc, acetyl or Fmoc would not be suitable as these require either strong acid conditions that could cause retro-Michael addition reactions, or basic conditions since the amine surface can cause Fmoc deprotection). Cbz protection was therefore chosen as this group can be removed under relatively mild conditions. The synthetic route is outlined in **Scheme 20**.

Benzyl 4-aminobenzylcarbamate (**213**) was synthesised from benzyl chloroformate and an excess of 4-aminobenzylamine (48%), the excess reagent being required to help prevent the addition of the protecting group at both amines. This was then converted into an azobenzene *via* the diazonium chloride salt intermediate to give **214** as a deep-red solid (40%, mp: 131 – 132ºC), the product being characterised fully by NMR, HRMS and elemental analysis. To synthesise **215**, the phenol group of azobenzene **214** was deprotonated using potassium carbonate, and then allowed to react at reflux with ethyl bromoacetate in the presence of sodium iodide. This gave the ethyl ester product as an orange solid in a 52% yield (mp: 114 – 116ºC). This latter was then hydrolysed to the corresponding acid **216**, using sodium hydroxide. **216** was found to be only sparingly soluble in organic solvents, so no purification other than an extraction was attempted, though the final product was obtained in a very high yield (>99%) as a yellow solid (mp: 202 – 203ºC). FTIR data for **214** showed the presence of the alcohol (3423 cm^{-1}) and an N=N bond (1595 cm^{-1}), the former disappearing upon formation of **215** (an extra C=O stretch was observed at 1770 cm^{-1}). The C=O stretch was replaced with a stretch at 1706 cm^{-1} suggesting complete conversion of the ester to the acid **216**.

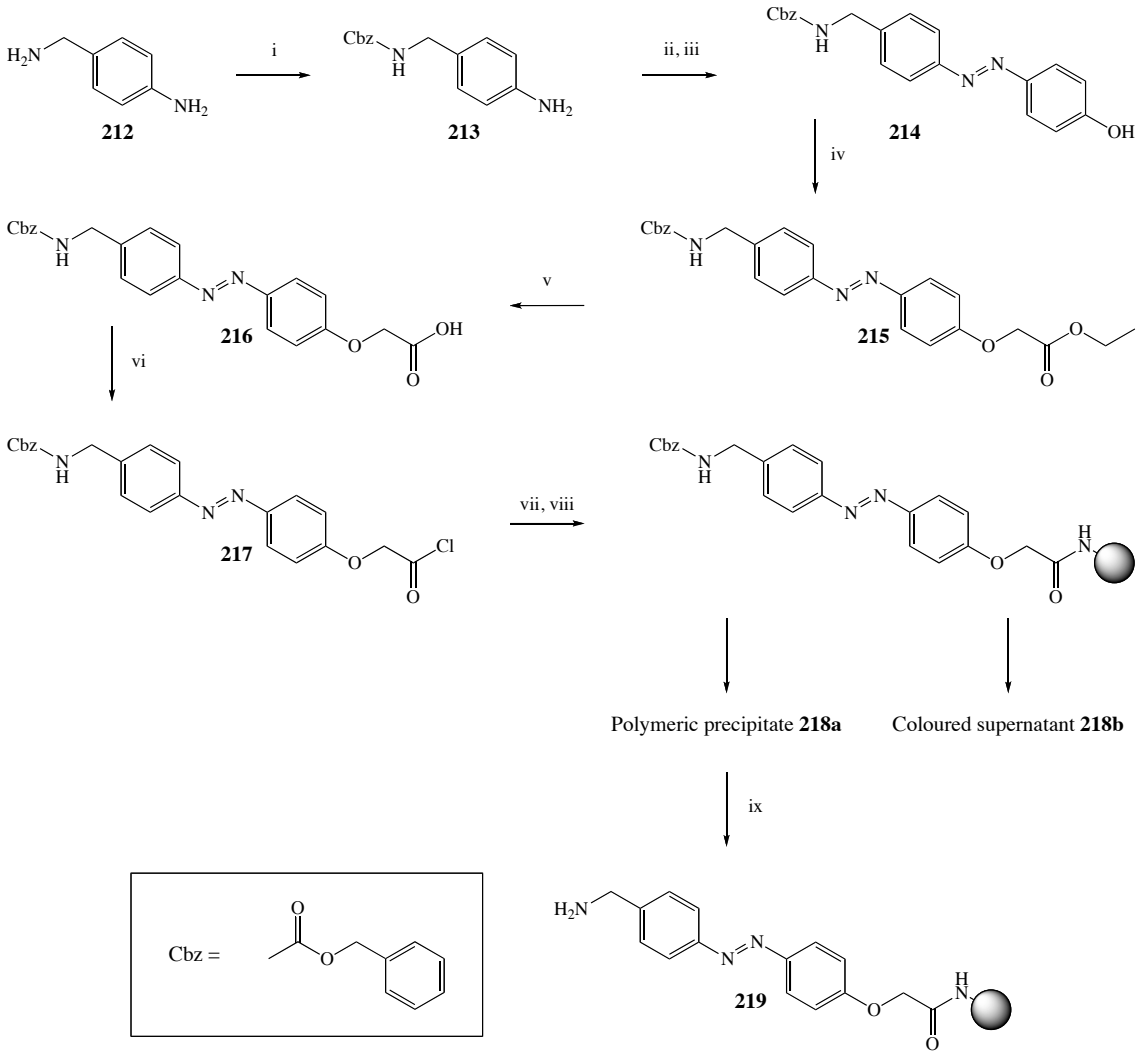

Scheme 20. *i, Benzyl chloroformate, NEt_3, DCM, 0ºC; ii, conc. HCl, H_2O, $NaNO_2$, <5ºC; iii, phenol, NaOH, RT; iv, ethyl bromoacetate, K_2CO_3, NaI, acetone, reflux; v, NaOH, EtOH/H_2O, then H_3O^+; vi, $SOCl_2$, reflux; vii, G4 PAMAM dendrimer, NEt_3, DMSO; viii, acetic anhydride, DMSO; ix, Pd/C, H_2, EtOH.*

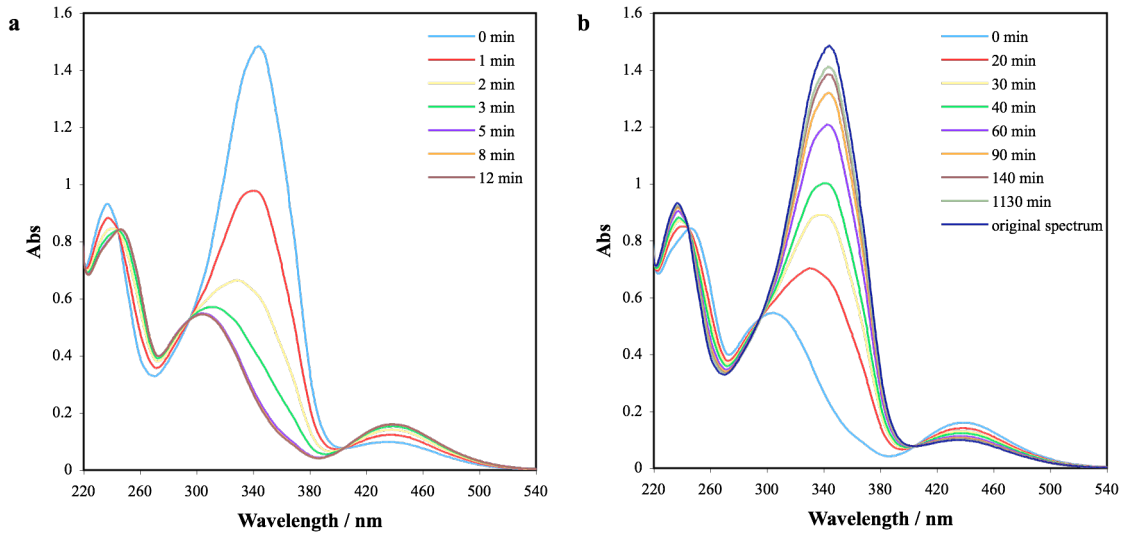

***Figure 100**. UV/Vis absorption spectra of azobenzene **215** (λ_{max} = 344 nm, ε = 45725 $cm^{-1}mol^{-1}dm^3$; λ = 280 nm, ε = 8681 $cm^{-1}mol^{-1}dm^3$). (a) Trans- to cis-isomer switching via illumination at 365 nm. (b) Cis- to trans-isomer switching via illumination in daylight. Measurements taken at 7.40 x 10^{-5} M in methanol.*

The UV/Vis spectra for for azobenzene **215** (**Figure 100**) are almost identical to that seen for **204**, though the λ_{max} was found to be a little higher (344 nm) in the former case. When isomerising from *E* to *Z* by illumination at 365 nm, this peak decreased in intensity whilst the peak at 440 nm increased, showing classic azobenzene photo-isomerisation behaviour.[157,260,431] However, equilibration to the *Z* isomer took 12 minutes, i.e. 5 minutes less than for **204**, possibly because of the electron donating effect of the ester group. In transforming from the *Z* to the *E* isomer the sample was illuminated by daylight and this process was found to take 2 hours to equilibrate, as shown by an increase in absorbance at 344 nm and a decrease in that at 440 nm. Once again, as for **204**, it was observed that the absorbance failed to reach the level of the sample pre-exposed to 365 nm light under these conditions.

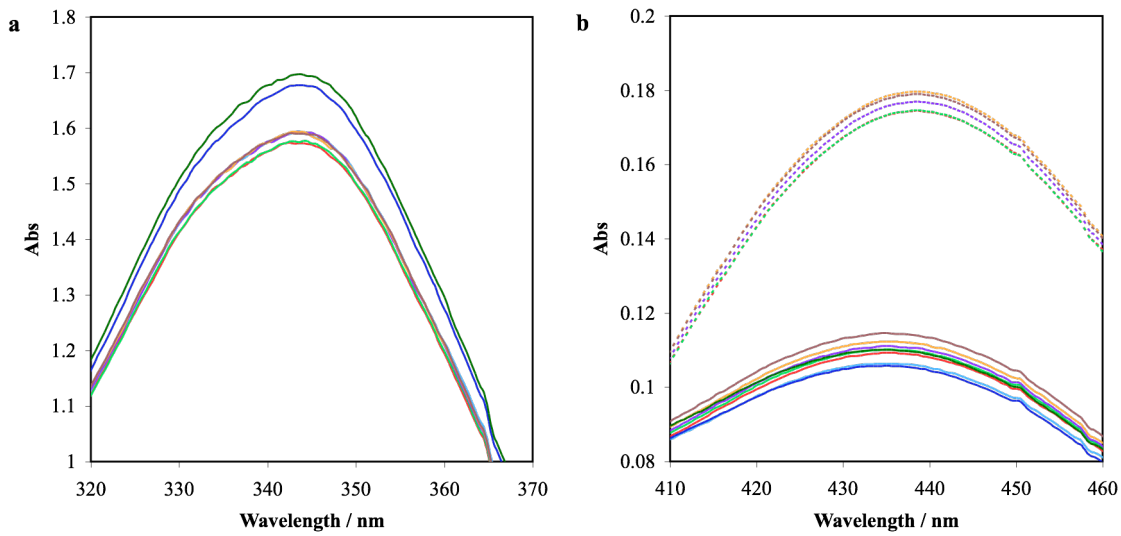

Figure 101. *UV/Vis absorption spectra of azobenzene **215** to show the reliability of repeated switching from (a) Z to E-isomer and (b) E to Z-isomer. Dashed lines; sample after illumination at 365 nm, straight lines; sample after illumination in daylight. Light blue; initial trans reading, red; 1st cycle, green; 2nd cycle, blue; 3rd cycle, orange; 4th cycle, brown; 5th cycle, dark blue; kept in dark for 16 hrs after 2nd cycle, dark green; kept in dark for 16 hrs after 5th cycle.*

In order to explore the reversibility of this photo-isomerisation, a sample of **215** was repeatedly exposed to 365 nm and daylight conditions. Prior to these experiments the sample was exposed to daylight for 8 hours. It was then illuminated at 365 nm for 20 minutes followed by daylight for 2 hours, a UV/Vis spectrum being obtained after each illumination. The data (**Figure 101**) shows that after 5 such cycles no sample degradation was detectable. All illuminations at 365 nm and in daylight resulted in a reproducible change. It is interesting to note that, after the 2nd and 5th cycle, the samples were left in the dark overnight (to promote the slower thermal *Z* to *E* isomerisation) which, for both samples resulted in an identical absorbance value which was larger than that recorder at the start of the experiment. After 1 cycle, this returned to the absorbance values of the other cycles. This suggests that use of daylight, which by its very nature consists of all wavelengths, can only promote formation of the *trans* isomer up to a certain limit. However, the thermal isomerisation (dark) to the *trans* isomer, though far slower and less useful, once again results in complete conversion.

The acid chloride **217** was prepared by refluxing the carboxylic acid **216** in neat thionyl chloride for 18 hours. After drying under high vacuum the product **217** was obtained as a dark red solid and used immediately without further purification. Thirteen equivalents of **217** in DMSO were then added dropwise to a solution of 4.0-[EDA]-64-Amine in DMSO, in the presence of triethylamine. This resulted in a solution colour change from dark red to orange. After the addition of approximately half of the acid chloride solution, a precipitate started to form which coalesced into a polymer-like ball. The supernatant was removed (**218b**) and the solid (**218a**) was added to excess acetic anhydride in DMSO in an attempt to dissolve it. After stirring for 64 hours, some dissolution was observed, but the bulk of the solid remained. 2M HCl was then added and the mixture was stirred for 4 days, resulting in complete dissolution of the solid. The solution was then dialysed against 1M HCl and deionised water. To make sure that all of the surface amines had reacted, ethyl isothiocyanate was added and the sample was re-dialysed against deionised water.

The previously decanted solution (**218b**) also had excess acetic anhydride added to it as it was thought that any product which formed would not be able to be resolubilised. To make sure all the surface amines had been reacted, ethyl isothiocyanate was once again added. It should be noted that during all of the above dialysis steps, the bulk had a slight yellow colour to it suggesting that not all of the azobenzene moiety had reacted with the dendrimer; it is believed that it instead reacted with methanol that was present in the interior of the dendrimer.

Analysis of the ^{1}H NMR spectrum (D_2O) for **218a** (**Figure 102**) revealed none of the observable aromatic signals that would be expected from the addition of the azobenzene group to the dendrimer. However, it was calculated that 19 acetyl (δ 2.00 ppm) and 11 ethyl urea (methyl group δ 1.31 ppm) groups were present on the surface, which left 34 sites unaccounted for.

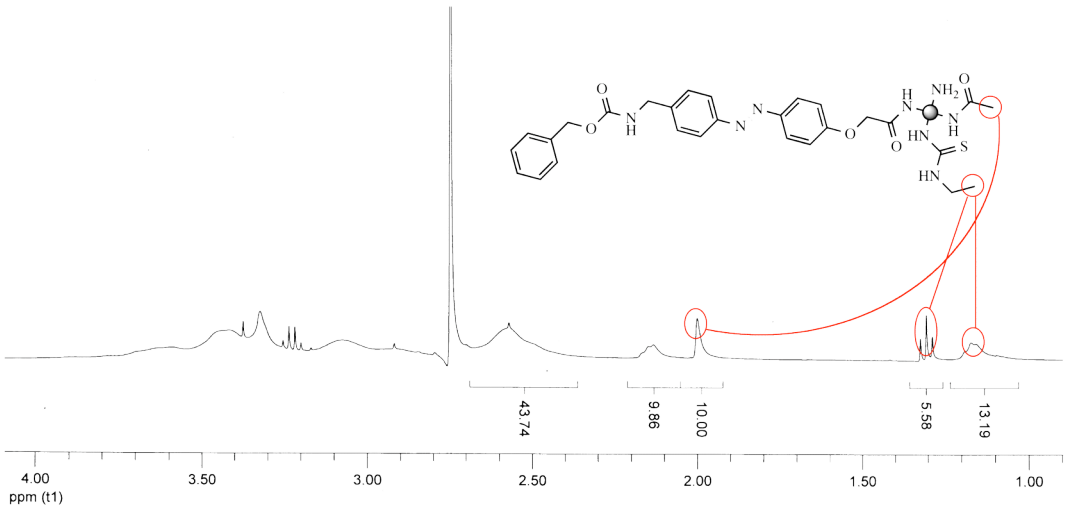

Figure 102. *^{1}H NMR spectrum of **218a** (D_2O; trace DMSO).*

Since the dendrimer is in no way symmetrical anymore, it is possible that the most upfield peak at δ 1.17 ppm (broad) could be arising from either an acetyl or ethyl urea group in a different environment. By integrating the area under this peak we can conclude that it is either the result of 24 acetyl groups, or 24 ethyl urea groups, which would make a total of either 43 acetyl and 11 urea units, or 19 acetyl and 35 urea units respectively. To confirm which one of these two cases has occurred, the sample was analysed by elemental analysis, which revealed that 36 sulphur atoms were present. This then supports the idea that the unsymmetrical nature of the modified dendrimer allows for multiple peaks in the NMR relating to different environments of the same group (i.e. 2 environments for the methyl component of the ethyl urea group), one giving a well defined triplet whilst the other is broad.

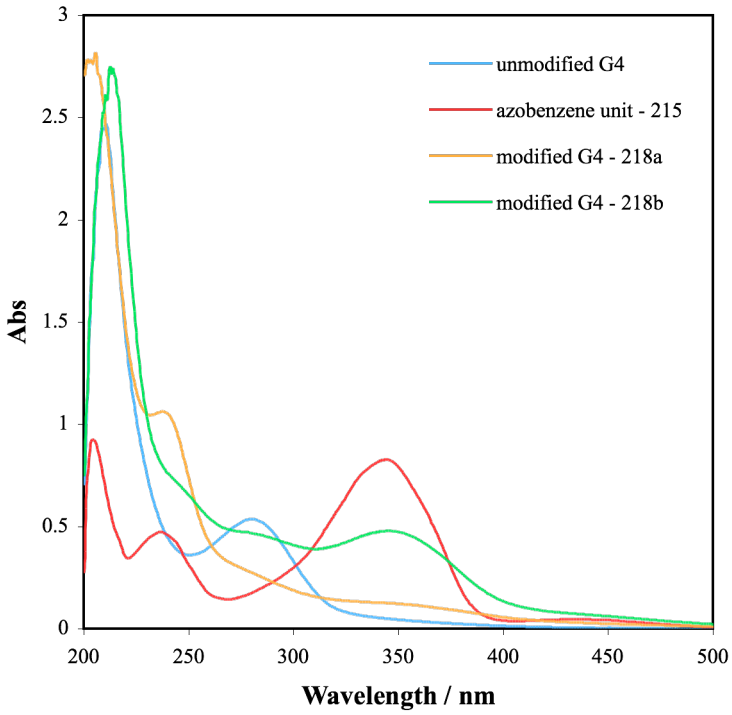

Figure 103. *UV/Vis absorption spectra of Cbz-azobenzene modified G4 dendrimers (**218a** and **218b**), unmodified G4 dendrimer and azobenzene unit **215**. Measurements taken at (—) 9.95 x 10^{-6} M, λ_{max} = 280 nm, ε = 67500 $cm^{-1}mol^{-1}dm^3$; (—) 7.40 x 10^{-5} M, λ_{max} = 344 nm, ε = 45725 $cm^{-1}mol^{-1}dm^3$: λ = 280 nm, ε = 8681 $cm^{-1}mol^{-1}dm^3$; (—) approx 1.21 x 10^{-5} M; (—) unknown concentration.*

In order to see if the remaining sites were covered by azobenzene groups (though it was suspected that only a few were, in view of the lack of signals in the ^{1}H NMR spectrum), UV/Vis experiments were carried out (**Figure 103**). Though photo-isomerisation of this 'azobenzene-dendrimer' was not observed, its spectrum showed a difference when compared with that for the unmodified G4 dendrimer. The absorption peak relating to the dendrimer at 280 nm was not well defined in the case of **218a** because of its low concentration, though weak peaks relating to the azobenzene units at 350 and 240 nm were observed. This lack of surface coverage is confusing, particularly as all the sites should be covered with either the azobenzene, the acetyl groups or the ethyl urea units.

By comparison, NMR data (**Figure 104**) obtained for the sample resulting from the initial solution (**218b**) showed that a higher level of the azobenzene moiety was present, as well as a greater number of acetyl groups (34) but fewer ethyl urea units (13).

Signals in the aromatic region of the ^{1}H NMR suggested the presence of approximately 3 azobenzene groups, and this can be confirmed from the relative extinction coefficients obtained through UV/Visible experiments.

The calculations shown below (assuming that the extinction coefficient is the same for the azobenzene unit once it is attached to the dendrimer) first determine the concentration of the azobenzene unit on the surface of dendrimer **218b** by comparing its absorbance at 344 nm with the extinction coefficient found for **215** at the same wavelength. With this concentration known, we can find its contribution to the absorbance at 280 nm (λ_{max} for G4) and thus calculate the contribution (and concentration of) the G4 dendrimer. By comparing the relative concentrations of the azobenzene on the surface and that of the dendrimer we find that there are approximately 2 azobenzene groups present, a result that relates well to the value obtained from the ^{1}H NMR data (3 groups).

At 344 nm, $\varepsilon_{\mathbf{215}} = 45725\ cm^{-1}mol^{-1}dm^3$, $A_{\mathbf{218b}} = 0.4785$

$$\therefore C_{azo} = \frac{A_{218b}}{\varepsilon_{215}} = 1.047\,x10^{-5}\,mol\,dm^{-3} \qquad \textbf{Equation 1}$$

At 280 nm, $\varepsilon_{\mathbf{215}} = 8681\ cm^{-1}mol^{-1}dm^3$

$$\therefore A_{azo} = \varepsilon_{215}\,x\,C_{azo} = 0.0908 \qquad \textbf{Equation 2}$$

At 280 nm, $A_{\mathbf{218b}}$ = 0.4781, A_{Den} = $A_{\mathbf{218b}}$ – A_{azo} = 0.3876. ε_{G4} = 67500 $cm^{-1}mol^{-1}dm^3$

$$\therefore C_{Den} = \frac{A_{Den}}{\varepsilon_{G4}} = 5.743 x 10^{-6} mol\, dm^{-3} \qquad \textbf{Equation 3}$$

$$C_{Den} : C_{azo} \; at \; 280\, nm$$

$$1{:}1.822 \approx 1{:}2$$

where *azo*, *Den* and *G4* are data relating to the azobenzene component of **218b**, the dendrimer component of **218b**, and 4th generation unmodified PAMAM dendrimer respectively. Subscript numbers correspond to structures.

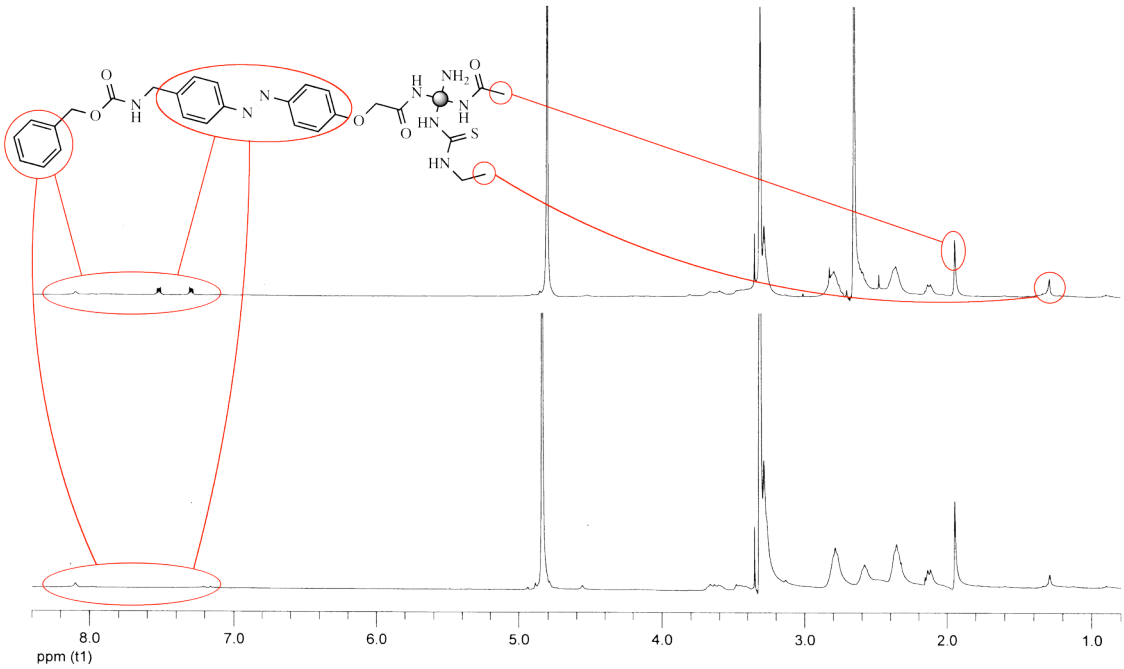

Figure 104. *^{1}H NMR spectra of **218b** (top, MeOD; trace MeOH and DMSO) and resulting deprotection **219** (bottom, MeOD; trace MeOH).*

The total number of surface groups for **218a** and **218b**, including known azobenzene groups, is 54 (19 acetyl, 35 ethyl urea) and 49 (34 acetyl, 13 ethyl urea, 2 azobenzene) respectively out of a possible 64. The fact that complete coverage was not achieved was to be expected in view of the potential folding of dendrimer arms making reaction with them difficult. What is interesting is that **218b** has a higher azobenzene coverage compared with that for **218a**, but a lower total coverage. This may be because the azobenzene groups require more physical space thus preventing further reaction on nearby amines. The fact that **218b** has a higher azobenzene coverage is interesting in itself as we would expect that during the reaction, as the coverage increases on the dendrimer surface, the latter precipitates; but the opposite effect was observed. The precipitate that formed **218a** might be explained by the azobenzene molecules H-bonding to the exterior and interior of the dendrimer causing a decrease in solubility, though further experiments would need to be carried out to confirm this.

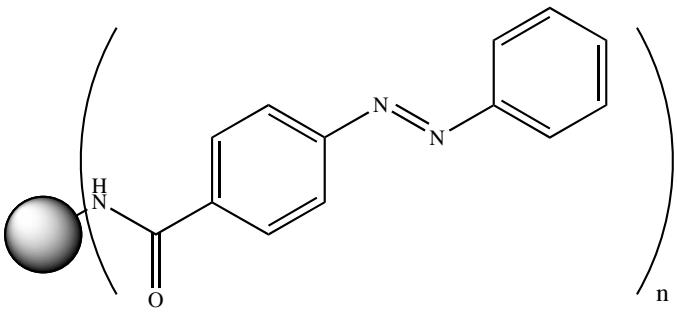

220

Figure 105. *Azobenzene coverage of 4-[EDA]-64-Amine (**220**).*

The UV/Vis data for **218b** (**Figure 103**) can be compared with that for a G4 dendrimer that has a partial surface of azobenzene (**220**). Though a coverage of 32 groups was attempted, only 10 azobenzene groups were attached to the amine surface (as determined by ^{1}H NMR experiments), the remaining unreacted azobenzene reactants forming methyl esters that were removed through dialysis. Dendrimer **218b** was found to have a switching time of 8 minutes for *E* to *Z*-isomer and 210 minutes from *Z* to *E*-isomer, whereas **220** (**Figure 106**) had a longer *Z*-isomer formation time (14 minutes) but a similar *E*-isomer formation time (195 minutes). These values seem to be typical of the azobenzene units studied (and with published literature[157,433]) suggesting that, at

low levels of surface coverage, the dendrimer has little impact upon the photo-isomerisation. It could be said that the faster isomerisation time for *Z*-isomer formation is the result of lower surface coverage of **220b**, though this is not observed for formation of the *E*-isomer because of the longer equilibration times. The difference in line-shape of the UV/Vis spectrum of **220** compared to **218b** can be attributed to the fact that **218b** contains other groups appended to the azobenzene unit, though this line-shape has been observed in other dendrimer types.[260,434]

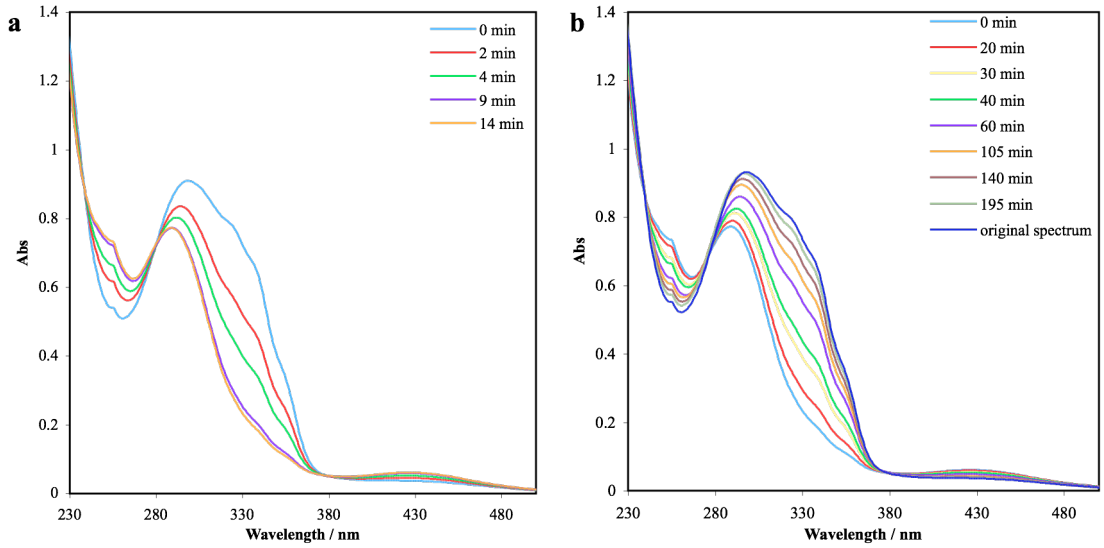

Figure 106. *UV/Vis absorption spectra of **220**. (a) Trans- to cis-isomer switching via illumination at 365 nm. (b) Cis- to trans-isomer switching via illumination in daylight. Measurements taken at 9.47 x 10^{-6} M in methanol.*

For the final preparative step from **Scheme 20**, Cbz-azobenzene-G4 (**218b**) was deprotected using a palladium on carbon catalyst under a hydrogen atmosphere. The ^{1}H NMR spectrum (MeOD) of the product (**219**) showed fewer (and less intense) peaks from δ 7.00 to 8.00 ppm suggesting that, despite the poor resolution, the deprotection had worked to a certain extent (**Figure 104**). Further work would be required in order to increase the surface coverage of the dendrimers, partly for improved NMR resolution, and in addition to allow for a greater chance of continued growth.

5.4 Conclusions and Further Work

The work carried out in this chapter was aimed at incorporating the photo-responsive group azobenzene into a dendritic structure. In the first instance, a dicarboxylic acid derivative of azobenzene was synthesised and coupled to samples of dendritic wedges (dendrons) in an attempt to create a dendrimer with a photo-responsive core (convergent method). From this study it was found that, whilst one dendritic wedge would react with the core, methanol contained within the dendrons also reacted, leading to incomplete dendrimer formation. To alleviate this problem, longer cores containing aromatic groups were synthesised (to increase any change in hydrodynamic radius) with the aim of continuing dendrimer growth using the divergent method. Though the synthesis of this core proved problematic as a result of poor solubility, it confirmed our suspicions that introducing the azobenzene unit onto the dendrimer surface would be more achievable and could give a greater level of control of DNA binding. To that end, two types of azobenzene moiety were synthesised; the first aimed at using the isothiocyanate attachment approach that ultimately proved unfruitful because of low yields, whilst the other more successful approach involved an attachment *via* the corresponding carboxylic acid. An aromatic amine and nitroso group underwent a condensation reaction to give a protected amino-acid type azobenzene unit, the photo-isomerisation of which was observed using UV/Visible spectroscopy. This was further reacted to give the acid chloride and was then coupled onto the surface of a G0 PAMAM dendrimer, but this once again gave a product contaminated with methyl esters.

A series of azobenzene units were synthesised that contained a protected amino group as well as a phenolic moiety. The hydroxy group was reacted with 'extender' units with the aim of allowing for dendrimer attachment *via* an isothiocyanate but it was discovered that an acid chloride linkage could also be made. A Cbz-protected azobenzene moiety was synthesised and fully characterised, and was then reacted to give the corresponding acid chloride. This was then successfully attached to the surface of a G4 PAMAM dendrimer. This azo-dendrimer was fully characterised through NMR, elemental analysis and UV/Vis experiments, and its behaviour was then compared with that of the native azobenzene molecule and of a separately prepared

dendrimer that contained an azobenzene group on its surface. NMR data showed that the Cbz protection was successfully removed though further work is required to fully characterise the resulting dendrimer. More experiments are required to ascertain the highest surface coverages possible, which may perhaps require a change in the attachment route in order to make use of 'Click' chemistry. It should then be possible to further react the new azo-amine surface with a view to continuing dendrimer growth.

Chapter 6 Conclusions

Two series of PAMAM dendrimers based around either an EDA or phloroglucinol core have been synthesised up to the 4th generation and characterised by NMR and MS techniques. Spin-lattice relaxation time NMR experiments were used to investigate the branch mobility of dendrimers (≤ generation 1.5) with varying sized cores, revealing that nuclei nearest the branch terminus are the most mobile. It was shown that cores containing three branches generally had greater mobility than those that had four branches, though it was observed that the behaviour of the outer methyl groups became similar across all the cores used as the generation increased suggesting that, whilst the cores have different geometries and numbers of branches, a point is reached whereby the environment at the surface becomes very similar.

Dendrimers based on an EDA core have had their surfaces modified with acetyl, PEG and fluorescent groups with various degrees of surface coverage. They were then used to study DNA complexation and compaction. It was observed that whilst PEGylated dendrimers have a higher surface area, unmodified dendrimer samples condensed DNA to a higher degree as a result of higher surface charge density. These modified dendrimers were also used to study interactions with lipid bilayers, showing that when charged, they can pass through the bilayer.

Coarse-grained molecular dynamic simulations have been run to study the interaction of a range of charged 4th generation dendrimers with either a neutral or anionic lipid bilayers. No lipid penetration was observed, all the dendrimers flattening on the lipid surface *via* electrostatic interactions.

Various routes to attaching L-histidine to the surface of a dendrimer were attempted, the most successful involving the use of 'Click' chemistry. A small alkyne-containing unit was synthesised and attached to a dendrimer surface (containing 18 PEG groups) using an isothiocyanate group, whilst a histidine unit was modified to contain an azide group. These two components were brought together in the presence of a copper (I) catalyst but were found not to react, possibly as a result of the bulky PEG groups.

The incorporation of azobenzene units into a dendritic structure was attempted in order to introduce a photo-responsive component for DNA binding. Several attempts were made to include an azobenzene group at the core of a dendrimer, but yielded no desired material either because of side-reactions or through solubility issues. Work to attach azobenzene units onto the surface of the dendrimer have resulted in the formation of a Cbz-protected moiety that was successfully coupled to a PAMAM dendrimer and ultimately deprotected, and has been shown to possess photo-responsive properties by UV/Visible spectroscopy.

Chapter 7 Experimental

Procedures and Equipment Summery

Commercially available compounds were purchased from either Sigma Aldrich or Fisher and were used as supplied without further purification. Dry solvents were prepared by distilling them over a drying agent; DCM, EDA and toluene were dried over calcium hydride, methanol was dried over calcium sulphate. Acetone and DMF were dried by passing them through a silica plug.

^{1}H and ^{13}C NMR spectra were collected using either a Bruker AV300 or Bruker DPX400 spectrometer as solutions in a deuterated solvent. ^{1}H NMR experiments were reported at 300 MHz or 400 MHz respectively whilst ^{13}C NMR experiments were reported at 75 MHz or 100 MHz respectively. ^{13}C NMR spectra were collected fully ^{1}H decoupled. The Bruker DPX400 spectrometer was used to collect ^{1}H spin-lattice relaxation NMR spectra and inverse-gated decoupled ^{13}C NMR data. Chemical shift data are given in ppm with multiplicities abbreviated as follows; s (singlet), d (doublet), t (triplet), q (quartet), qu (quintet) br (broad) and m (multiplet). Coupling constants (J) are quoted in Hz. T_1 values are recorded in seconds. Analysis was carried out using either ACD Labs or Mestrec software.

Electrospray mass spectra were obtained using a Micromass Platform II single quadrapole mass spectrometer. High resolution spectra were obtained using a Bruker Apex III FT-ICR mass spectrometer fitted with an Apollo electrospray ionisation source.

IR Spectra were obtained using a Thermo Nicolet 380 FT-IR spectrometer with a SmartOrbit Golden Gate Attenuated Total Reflection (ATR) attachement.

Melting points were measured using a Gallenkamp melting point apparatus and are uncorrected.

Elemental analysis was performed by Medac Ltd. Results are accurate to ± 0.30%.

UV/Vis spectra were recorded from 1000 to 200 nm using Shimadzu UV-1601 UV/Vis spectrometer. Data collection was managed using the UVPC Personal Spectroscopy Software v3.5.

General Procedure for the Synthesis of PAMAM Dendrimers

All PAMAM dendrimer preparations were based on the work of Tomalia *et al*. and found to give material consistent with published data.[77,251,349] Only dendrimers directly referred to in this thesis are given numbers.

Half generation dendrimer synthesis

Methyl acrylate (2.8 mol equiv per dendrimer end group) was added dropwise to a stirred solution of whole generation dendrimer in methanol (20 mL). The reaction vessel was covered with foil and allowed to stir for approximately 6 days at room temperature, before being concentrated *in vacuo*. For generations up to 1.5, the crude product was purified by column chromatography to give a viscous yellow oil. All generations underwent an azeotropic distillation as follows: toluene (120 mL) was added to the product dissolved in methanol (10 mL). The solvents were then removed *in vacuo*. This was repeated a further two times. The product was then dissolved in methanol (10 mL), which was then removed *in vacuo* to give product.

Whole generation dendrimer synthesis

A 10% solution of half generation dendrimer in methanol and a solution of distilled EDA were deoxygenated by bubbling nitrogen through it for 30 minutes. The EDA was cooled over ice and the dendrimer solution was added slowly *via* canula before being allowed to stir at 5ºC. The solvent and excess EDA were then removed *in vacuo*. An azeotropic distillation (as above) was then performed. The product was then dissolved in methanol (10 mL), which was then removed under reduced pressure to give a pale

yellow oil. Dendrimers of 3rd generation or greater were dialysed in deionised water for 5 days (changing water after 2 days), followed by a repetition of the azeotropic distillation to give product as a viscous oil.

-0.5-[EDA]-4-Ester (38)

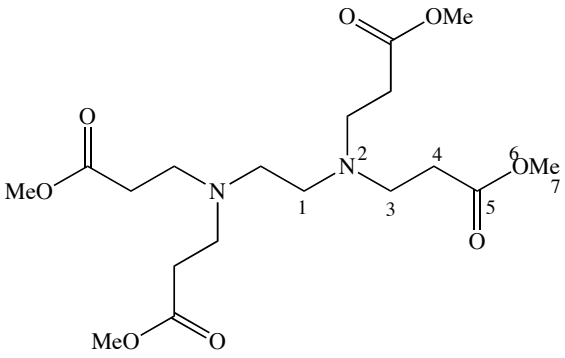

$C_{18}H_{32}N_2O_8$

RMM = 404.47

Methyl acrylate (16 mL; 177.5 mmol)

EDA (2.5 mL; 33.3 mmol)

Duration of stirring: 48 hrs at room temperature

Purification: Azeotropic distillation

Product: Colourless oil (9.64 g; 72%)

MS/ES^+ (m/z): 405.3 (60% $[M + H]^+$).

^1H NMR: (300 MHz, $CDCl_3$) 3.50 (12H, s, **H-7**), 2.60 (8H, t, J = 7.1, **H-3**), 2.33 (4H, s, **H-1**), 2.27 (8H, t, J = 7.0, **H-4**).

^{13}C NMR: (75 MHz, $CDCl_3$) 172.4 (**C-5**), 51.9 (**C-1**), 51.0 (**C-7**), 49.4 (**C-3**), 32.3 (**C-4**).

^1H T_1 NMR: (MeOD) 3.50 (1.918), 2.60 (0.584), 2.33 (0.484), 2.27 (0.891).

^1H T_1 NMR: ($CDCl_3$) 3.50 (2.072), 2.60 (0.651), 2.33 (0.543), 2.27 (0.977).

0-[EDA]-4-Amine (39)

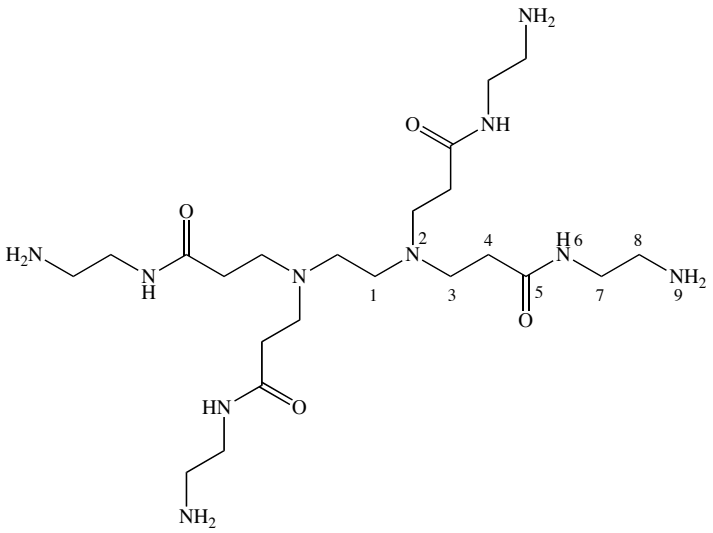

$C_{22}H_{48}N_{10}O_4$

RMM = 516.69

-0.5[EDA]-4-Ester (1.00 g; 2.47 mmol)

EDA (50-fold by weight, 56 mL; 830.7 mmol)

Duration of stirring: 4 days at 5ºC

Purification: Azeotropic distillation

Product: Orange oil (1.60 g; 125%, product contaminated with solvent)

^{1}H NMR: (400 MHz, D_2O) 3.31 (MeOH), 3.21 (7H, t, J = 6.1, **H-7**), 2.77 (7H, t, J = 7.0, **H-3**), 2.69 (8H, t, J = 6, **H-8**), 2.57 (4H, s, **H-1**), 2.40 (8H, t, J = 6.9, **H-4**).

^{13}C-NMR: (100 MHz, D_2O) 174.6 (**C-5**), 50.7 (**C-1**), 49.8 (**C-3**), 49.5 (MeOH), 42.2 (**C-7**), 40.4 (**C-8**), 33.4 (**C-4**).

^{1}H T_1 NMR: (MeOD) 3.21 (0.801), 2.77 (0.309), 2.69 (0.901), 2.57 (0.262), 2.40 (0.393).

^{1}H T_1 NMR: (D_2O) 3.21 (0.937), 2.77 (0.291), 2.69 (1.059), 2.57 (0.256), 2.40 (0.390).

0.5-[EDA]-8-Ester

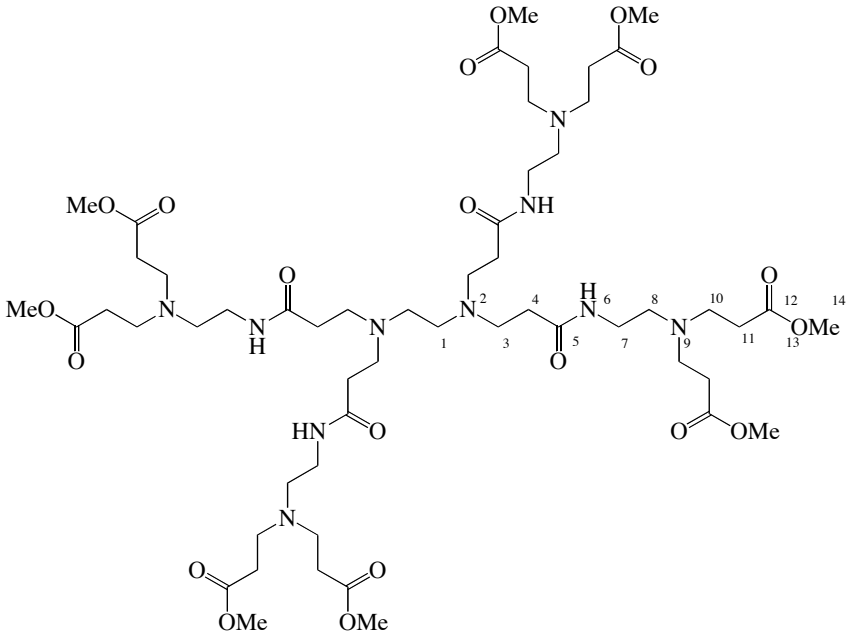

$C_{54}H_{96}N_{10}O_{20}$

RMM = 1205.40

0-[EDA]-4-Amine (3.83 g; 7.42 mmol)

Methyl acrylate (7.5 mL; 83.1 mmol)

Duration of stirring: 7 days at room temperature

Purification: Column chromatography (R_f: 0.33, 12% MeOH in DCM, silica 60)

Product: Viscous yellow oil (4.264 g; 48%)

MS/ES$^+$ (m/z): 402.8 (100% $[M + 3H]^{3+}$), 603.7 (95% $[M + 2H]^{2+}$), 614.7 (30% $[M + H + Na]^{2+}$), 625.7 (10% $[M + 2Na]^{2+}$).

^{1}H NMR (400 MHz, $CDCl_3$): 7.11 (3H, s (br), H-6), 3.66 (24H, s, **H-14**), 3.48 (MeOH), 3.26 (4H, q, J = 5.9, **H-7**), 2.76 (24H, t, J = 6.8, **H-3/10**), 2.54 (12H, t, J = 6.1, **H-1/8**), 2.43 (17H, t, J = 6.7, **H-11**), 2.36 (8H, t (br), **H-4**).

^{13}C NMR (100 MHz, $CDCl_3$): 173.0 (**C-12**), 172.3 (**C-5**), 53.4 (**C-1**), 53.0 (**C-8**), 51.6 (**C-14**), 51.4 (**C-3**), 50.2 (MeOH), 49.3 (**C-10**), 37.2 (**C-7**), 33.9, (**C-4**), 32.7 (**C-11**).

^{1}H T_1 NMR: (MeOH) 3.66 (1.677), 3.26 (0.433), 2.82 (0.274), 2.76 (0.459), 2.62 (0.240), 2.54 (0.377), 2.43 (0.694), 2.36 (0.341).

^{1}H T_1 NMR: ($CDCl_3$) 3.66 (1.449), 3.26 (0.354), 2.76 (0.377), 2.54 (0.297), 2.43 (0.579), 2.36 (0.295).

1.0-[EDA]-8-Amine

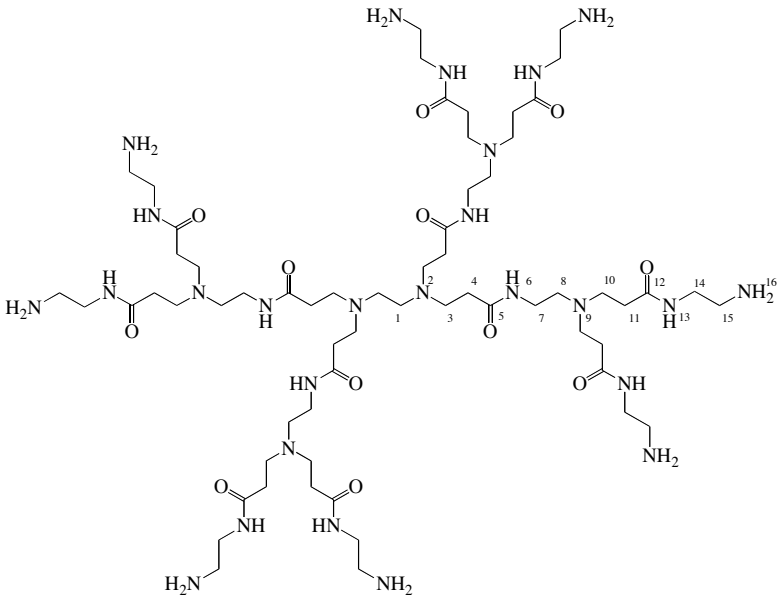

$C_{62}H_{128}N_{26}O_{12}$

RMM = 1429.86

0.5-[EDA]-8-Ester (1.13 g; 0.937 mmol)

EDA (62.6 mL; 937 mmol)

Duration of stirring: 5 days at 5ºC

Purification: Azeotropic distillation

Product: Viscous orange oil (1.56g; 102%, product contaminated with solvent)

^{1}H NMR: (300 MHz, D_2O) 3.31 (MeOH), 3.21 (2H, t, J = 6.3, **H-7/14**), 2.79 (2H, t, J = 7.0, **H-3/10**), 2.69 (2H, t, J = 6.3, **H-8/15**), 2.59 (1H, t, J = 7.1, **H-1/8**), 2.39 (2H, t, J = 7.2, **H-4/11**).

^{13}C NMR (75M Hz, D_2O): 175.7 (**C-12**), 175.2 (**C-5**), 51.9 (**C-8**), 50.7 (**C-1**), 49.7 (**C-3/10**), 49.5 (MeOH), 42.1 (**C-14**), 40.4 (**C-15**), 37.4 (**C-7**), 33.5 (**C-11**), 33.1 (**C-4**).

1.5-[EDA]-16-Ester (40)

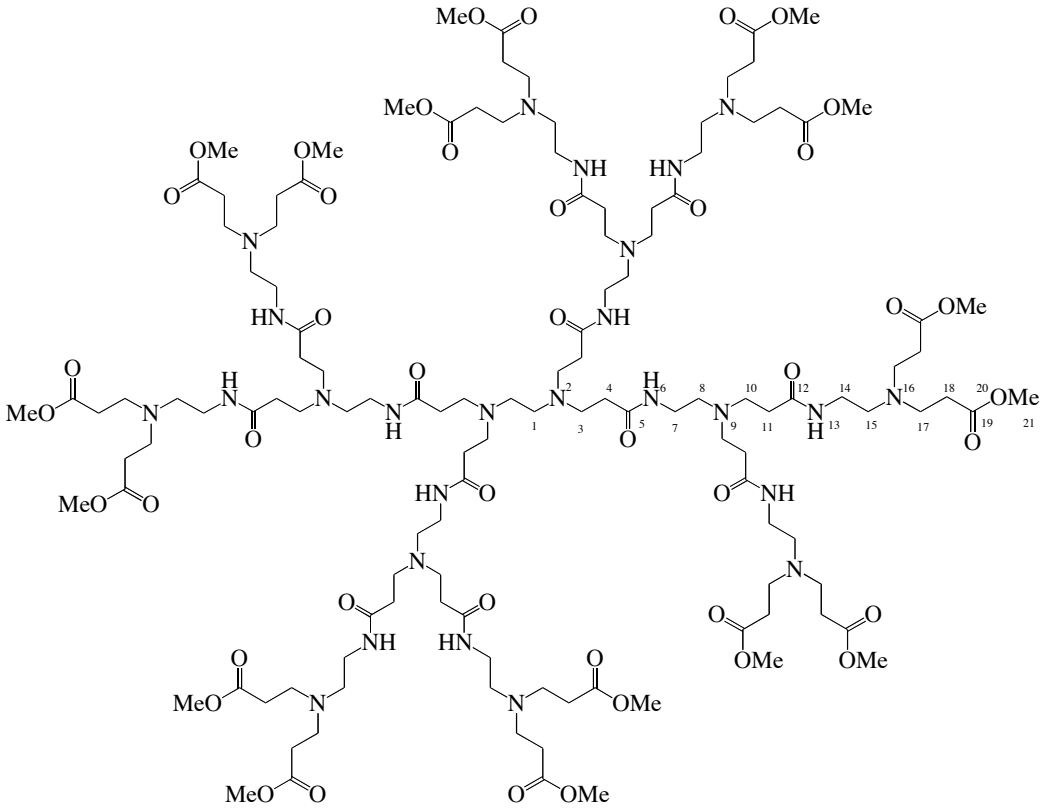

$C_{126}H_{224}N_{26}O_{44}$

RMM = 2807.29

1.0-[EDA]-8-Amine (1.56 g; 1.09 mmol)

Methyl acrylate (2.04 mL; 22.7 mmol)

Duration of stirring: 8 days at room temperature

Purification: Column chromatography (R_f: 0.13, 25% MeOH in DCM, Silica 60)

Product: Viscous yellow oil (1.97 g; 64%)

MS/ES$^+$ (m/z): 937.0 (100% $[M + 3H]^{3+}$), 944.4 (90% $[M + 2H + Na]^{3+}$), 951.7 (40% $[M + H + 2Na]^{3+}$), 1405.2 (30% $[M + 2H]^{2+}$), 1416.2 (20% $[M + H + Na]^{2+}$).

^{1}H NMR (300 MHz, $CDCl_3$): 3.66 (10H, s, **H-21**), 3.43 (MeOH), 3.24 (5H, q (br), **H-7/14**), 2.78 (t, **H-3/10**), 2.73 (t (br), **H-17**), 2.54 (t (br), **H-8**), 2.52 (t (br), **H-15**), 2.40 (8H, t (br), **H-18**), 2.33 (6H, t (br), **H-4/11**).

^{13}C NMR (75 MHz, $CDCl_3$): 173.0 (**C19**), 172.4 (**C-5/12**), 52.9 (**C-15**), 52.4 (**C-8**), 51.6 (**C-21**), 50.5 (MeOH), 50.0 (**C-3/10**), 49.2 (**C-17**), 37.8 (**C-7**), 37.2 (**C-14**), 33.7 (**C-4/11**), 32.3 (**C-18**).

^{1}H T_1 NMR (MeOH): 3.67 (1.584), 3.26 (0.402), 2.77 (0.412), 2.56 (0.352), 2.47 (0.615), 2.39 (0.350).

^{1}H T_1 NMR ($CDCl_3$): 3.66 (1.297), 3.24 (0.340), 2.78 (0.362), 2.54 (0.315), 2.40 (0.513), 2.33 (0.323).

2.0-[EDA]-16-Amine

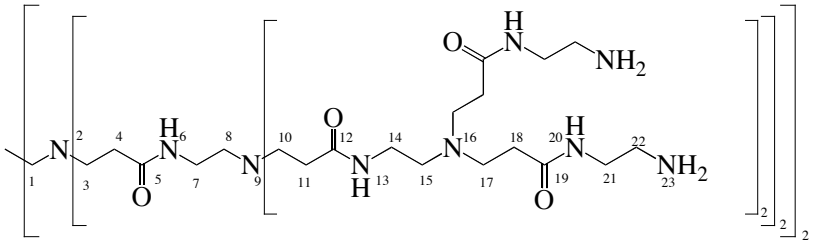

$C_{142}H_{288}N_{58}O_{28}$

RMM = 3256.22

1.5-[EDA]-16-Ester (1.43 g; 0.509 mmol)

EDA (95 mL; 1430 mmol)

Duration of stirring: 14 days at 5ºC

Purification: Azeotropic distillation

Product: Viscous orange oil (1.64 g; 99%)

^{1}H NMR (400 MHz, D_2O): 3.31 (MeOH), 3.26 (t, J = 6.8, **H-7/14**), 3.21 (t, J = 6.4, **H-21**), 2.78 (2H, t, J = 6.4, **H-10/17**), 2.69 (1H, t, J = 6.0, **H-22**), 2.59 (1H, t (br), **H-8/15**), 2.38 (2H, t (br), **H-11/18**).

^{13}C-NMR: (100 MHz, D_2O) 175.7 (**C-19**), 175.2 (**C-12**), 175.0 (**C-5**), 51.9 (**C-8/15**), 49.7 (**C-10/17**), 49.5 (MeOH), 42.2 (**C-21**), 40.4 (**C-22**), 37.4 (**C-7/14**), 33.5 (**C-18**), 33.4 (**C-11**), 33.3 (**C-4**).

2.5-[EDA]-32-Ester

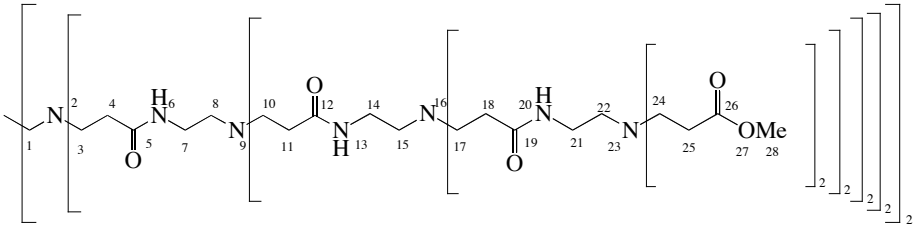

$C_{270}H_{480}N_{58}O_{92}$

RMM = 6011.08

2.0-[EDA]-16-Amine (1.06 g; 0.33 mmol)

Methyl acrylate (1.87 mL; 20.8 mmol)

Duration of stirring: 6 days at room temperature

Purification: Azeotropic distillation

Product: Viscous yellow oil (1.96 g; 101%, product contaminated with solvent)

MS/ES$^+$ (m/z): 1002.7 (40% $[M + 6H]^{6+}$), 1203.4 (30% $[M + 5H]^{5+}$), gives mass of 6011.3 ± 2.8

^{1}H NMR: (400 MHz, $CDCl_3$) 3.63 (13H, s, **H-28**), 3.43 (MeOH), 3.23 (q (br), **H-7/14/21**), 2.77 (t (br), **H-10/17**), 2.73 (t (br), **H-24**), 2.55 (t (br), **H-8/15**), 2.51 (t (br), **H-22**), 2.40 (10H, t (br), **H-25**), 2.32 (t (br), **H-11/18**).

^{13}C NMR: (100 MHz, $CDCl_3$) 173.0 (**C-26**), 172.4 (**C-12**), 172.4(**C-19**), 52.9 (**C-22**), 52.5 (**C-15**), 52.4 (**C-8**), 51.6 (**C-28**), 50.5 (MeOH), 50.0 (**C-3/10**), 49.8 (**C-17**), 49.2 (**C-24**), 37.5 (**C-7/14**), 37.2 (**C-21**), 33.8 (**C-11/18**), 32.6 (**C-25**).

^{1}H T_1 NMR: (MeOD) 3.66 (1.578), 2.77 (0.434), 2.46 (0.632).

^{1}H T_1 NMR: 3.63 (1.358), 3.23 (0.524), 2.73 (0.405), 2.55 (0.355), 2.40 (0.543), (CDCl$_3$) 2.32 (0.378).

3.0-[EDA]-32-Amine

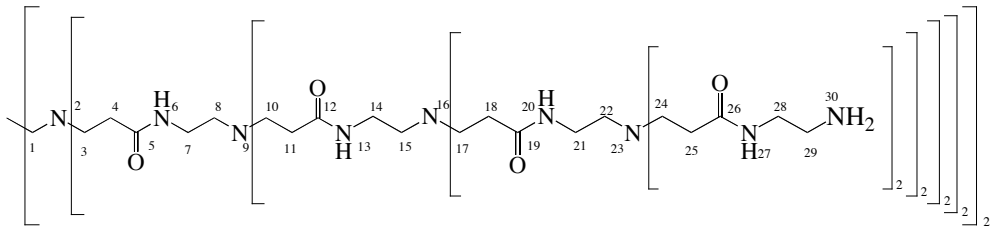

$C_{302}H_{608}N_{122}O_{60}$

RMM = 6908.92

2.5-[EDA]-16-Ester (1.41 g; 0.231 mmol)

EDA (155 mL; 2314 mmol)

Duration of stirring: 14 days at 5ºC

Purification: Azeotropic distillation and dialysis in deionised water

Product: Viscous orange oil (1.71 g; 107%, product contaminated with solvent)

^{1}H NMR: (400 MHz, D_2O) 3.31 (MeOH), 3.25 (t (br), **H-7/14/21**), 3.21 (t (br), **H-28**), 2.78 (t (br), **H-10/17/24**), 2.70 (t (br), **H-29**), 2.59 (t (br), **H-8/15/22**), 2.39 (t (br), **H-11/18/25**).

^{13}C NMR: (100 MHz, D_2O) 175.6 (**C-26**), 175.2 (**C-19**), 175.1 (**C-12**), 175.0 (**C-5**), 51.9 (**C8/15/22**), 49.7 (**C10/17/24**), 49.5 (MeOH), 42.1 (**C28**), 40.4 (**C29**), 37.4 (**C7/14/21**), 33.5 (**C25**), 33.4 (**C11/18/25**).

3.5-[EDA]-64-Ester

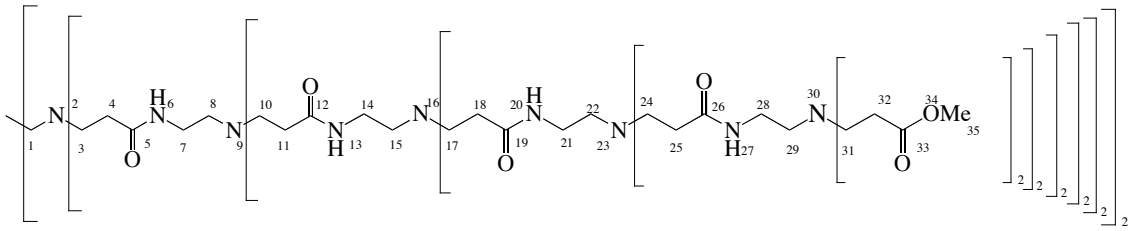

$C_{558}H_{992}N_{122}O_{188}$

RMM = 12418.64

3.0-[EDA]-32-Amine (1.08 g; 0.156 mmol)

Methyl acrylate (1.80 mL; 20.0 mmol)

Duration of stirring: 7 days at room temperature

Purification: Azeotropic distillation

Product: Viscous orange oil (1.89 g; 97%)

^{1}H NMR: (400 MHz, $CDCl_3$) 3.63 (13H, s, **H-35**), 3.42 (MeOH), 3.23 (9.2H, q (br), **H-14/21/28**), 2.77 (t (br), **H-10/17/24**), 2.72 (t (br), **H-31**), 2.54 (t (br), **H-15/22**), 2.51 (t (br), **H-29**), 2.40 (10H, t (br), **H-32**), 2.32 (13H, t (br), **H-11/18/25**).

^{13}C-NMR: (100 MHz, $CDCl_3$) 173.0 (**C-33**), 172.5 (**C-12/19**), 172.4 (**C-26**), 52.8 (**C-29**), 52.4 (**C-8/15/22**), 51.6 (**C-35**), 50.5 (MeOH), 49.9 (**C-3/10**), 49.8 (**C-17/24**), 49.2 (**C-31**), 37.5 (**C-7/14/21**), 37.2 (**C-28**), 33.7 (**C-11/18/25**), 32.6 (**C-32**).

4.0-[EDA]-64-Amine

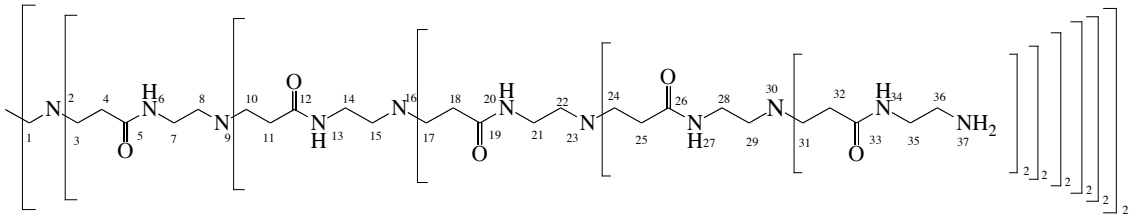

$C_{622}H_{1248}N_{250}O_{124}$

RMM = 14214.33

3.5-[EDA]-32-Ester (0.94 g; 0.0757 mmol)

EDA (222 mL; 3319 mmol)

Duration of stirring: 23 days at 5ºC

Purification: Azeotropic distillation and dialysis in deionised water

Product: Viscous orange oil (0.812g; 75%)

^{1}H-NMR (400 MHz, D_2O): 3.31 (MeOH), 3.26 (t (br), **H-14/21/28**), 3.21 (t, (br), **H-35**), 2.78 (t (br), **H-17/24/31**), 2.70 (t (br), **H-36**), 2.59 (t (br), **H-15/22/29**), 2.39 (t (br), **H-18/25/32**).

^{13}C-NMR (100 MHz, D_2O): 175.6 (**C-33**), 175.1 (**C-26**), 52.0 (**C-15/22/29**), 49.7 (**C-17/24/31**), 49.5 (MeOH), 42.1 (**C-35**), 40.4 (**C-36**), 37.4 (**C-14/21/28**), 33.5 (**C-32**), 33.4 (**C-11/18/25**).

FTIR ν_{max} (cm^{-1}) (thin film): 3271 (s (br), N-H stretch), 3079 (m, N-H amide stretch), 2937 (m, C-H aliphatic stretch), 2871 (m, C-H aliphatic stretch), 1633 (s (br), C=O amide stretch), 1541 (s (br), C-C stretch).

Combustion analysis:	Theoretical	C 52.56%, H 8.85%, N 24.64%
	Found	C 47.16%, H 8.04%, N 21.06%

-0.5-[Phloroglucinol]-3-Ester (113)

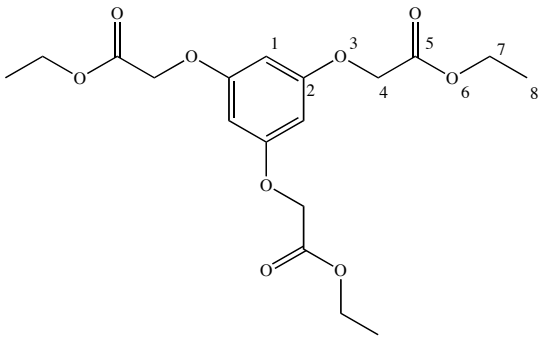

$C_{18}H_{24}O_9$

RMM = 384.38

Anhydrous potassium fluoride (5.90 g; 101.5 mmol), acetonitrile (20 mL) and ethyl bromoacetate (2.75 mL; 24.8 mmol) were mixed and degassed with nitrogen for 30 minutes at reflux with stirring. After slight cooling, 1,3,5-trihydroxybenzene (1.00 g; 7.93 mmol) was added portionwise. The reaction was then allowed to stir at reflux under nitrogen for 72 hours to give a white precipitate.

The cool mixture was filtered and the residue was washed with ethyl acetate (2 x 10 mL). The combined filtrates were reduced *in vacuo* and the resulting oil was taken up in DCM (20 mL). After washing with aqueous sodium hydroxide (2M, 2 x 20 mL), the organic phases were combined and dried over sodium sulphate. The solution was reduced and ethanol (10 mL) added. The oil was then scratched repeatedly to yield white crystals (0.950 g; 31%).

MP: 61 – 62ºC (lit. 65 – 66ºC)

MS/ES$^+$ (m/z): 407.2 (100% $[M + Na]^+$), 791.4 (40% $[2M + Na]^+$).

^{1}H NMR (300MHz, $CDCl_3$): 6.14 (1H, s, **H-1**), 4.55 (2H, s, **H-4**), 4.27 (2H, q, J = 7.1, **H-7**), 1.49 (s (br)), 1.30 (3H, t, J = 7.1, **H-8**).

^{13}C NMR: (75MHz, $CDCl_3$) 168.5 (**C-5**), 159.7 (**C-2**), 95.3 (**C-1**), 65.4 (**C-4**), 61.4 (**C-7**), 14.1 (**C-8**).

^{1}H T_1 NMR: (MeOD) 6.14 (2.327), 4.55 (1.091), 4.27 (2.639), 1.30 (2.611).

^{1}H T_1 NMR: ($CDCl_3$) 6.14 (1.882), 4.55 (0.850), 4.27 (2.210), 1.30 (2.118).

FTIR ν_{max} (cm^{-1}): (solid state) 2936 (m, C-H stretch), 1746 (s, C=O ester stretch), 1603 (s, C-O stretch).

Combustion analysis:	Theoretical	C 56.25%, H 6.29%,
	Found	C 56.16%, H 6.32%

Procedure followed from, and is consistent with, literature.[350,351]

0-[Phloroglucinol]-3-Amine (114)

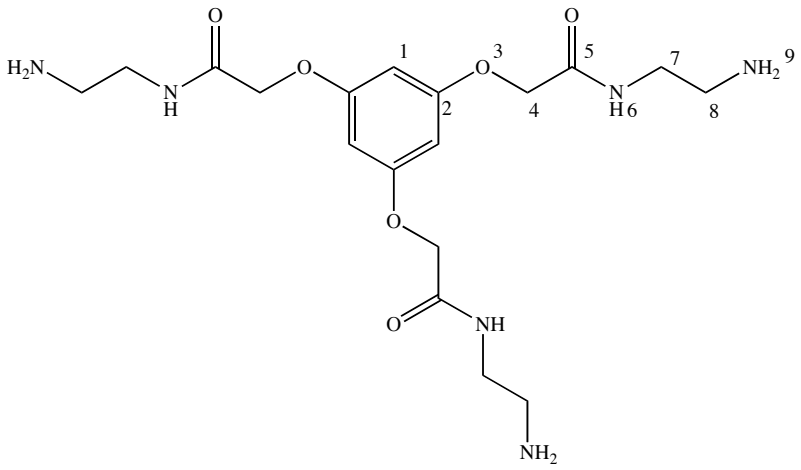

$C_{18}H_{30}N_6O_6$

RMM = 426.47

A solution of -0.5-[phloroglucinol]-3-Ester (0.5 g, 1.3 mmol) in diethyl ether (40 mL) was added to EDA (14.6 mL; 217.9 mmol) in diethyl ether (10 mL) and stirred for 5 days under dry conditions to give a white solid.

After removal of solvent and excess reagent *in vacuo*, a white powder remained (0.360 g; 65%).

MP: 146 - 148ºC (lit. 142 – 144ºC)

^{1}H NMR (300 MHz, D_2O): 6.24 (1H, s, **H-1**), 4.54 (2H, s, **H-4**), 3.31 (2H, t, J = 6.2, **H-7**), 2.72 (2H, t, J = 6.2, **H-8**).

^{13}C NMR (75 MHz, D_2O): 171.2 (**C-5**), 159.2 (**C-2**), 95.5 (**C-1**), 66.8 (**C-4**), 41.3 (**C-7**), 39.8 (**C- 8**).

^{1}H T_1 NMR (MeOD): 6.24 (1.491), 4.54 (0.594), 3.31 (0.842), 2.72 (1.027).

^{1}H T_1 NMR (D_2O): 6.24 (1.261), 4.54 (0.466), 3.31 (0.740), 2.72 (0.862).

FTIR ν_{max} (cm^{-1}) (solid state): 3294 (m, N-H stretch), 2943 (m, C-H stretch), 1682 (s, C=O amide stretch).

Combustion analysis	Theoretical	C 50.69%, H 7.09%, N 19.70%
	Found	C 48.80%, H 6.85%, N 18.76%

Data is consistent with literature.[350,351]

0.5-[Phloroglucinol]-6-Ester

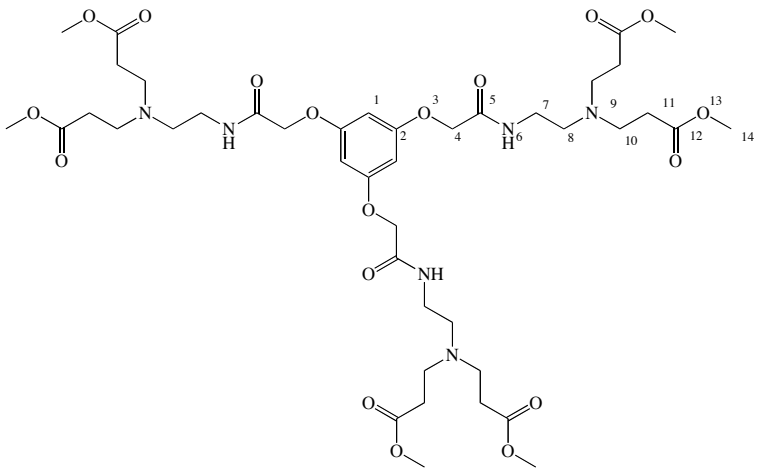

$C_{42}H_{66}N_6O_{18}$

RMM = 943.01

0-[Phloroglucinol]-3-Amine (0.200 g; 0.469 mmol)

Methyl acrylate (0.35 mL; 3.94 mmol)

Duration of stirring: 6 days at room temperature

Purification: Column chromatography (R_f: 0.69, 15% MeOH in DCM, silica 60)

Product: Viscous yellow oil (0.36 g; 81%)

MS/ES$^+$ (m/z): 472.6 (40% $[M + 2H]^{2+}$), 483.5 (80% $[M + H + Na]^{2+}$), 494.5 (90% $[M + 2Na]^{2+}$), 943.8 (40% $[M + H]^+$), 965.9 (100% $[M + Na]^+$).

^{1}H NMR (300 MHz, $CDCl_3$): 6.31 (1H, s, **H-1**), 4.46 (2H, s, **H-4**), 3.69 (s), 3.64 (6H, s, **H-14**), 3.43 (2H, s (br), **H-7**), 2.77 (4H, s (br), **H-10**), 2.60 (2H, s (br), **H-8**), 2.45 (4H, s (br), **H-11**).

^{13}C NMR (75 MHz, $CDCl_3$): 159.5 (**C-2**), 95.6 (**C-1**), 67.5 (**C-4**), 52.9 (**C-8**), 51.7 (**C-14**), 49.2 (**C- 10**).

^{1}H T_1 NMR: 6.38 (1.154), 4.51 (0.475), 3.63 (1.660), 3.37 (0.466), 2.75 (0.487),
(MeOD) 2.58 (0.407), 2.44 (0.723).

^{1}H T_1 NMR: 7.10 (0.688), 6.31 (1.093), 4.45 (0.457), 3.64 (1.603), 3.43 (0.408),
($CDCl_3$) 2.76 (0.441), 2.60 (0.362), 2.42 (0.653).

1.0-[Phloroglucinol]-6-Amine

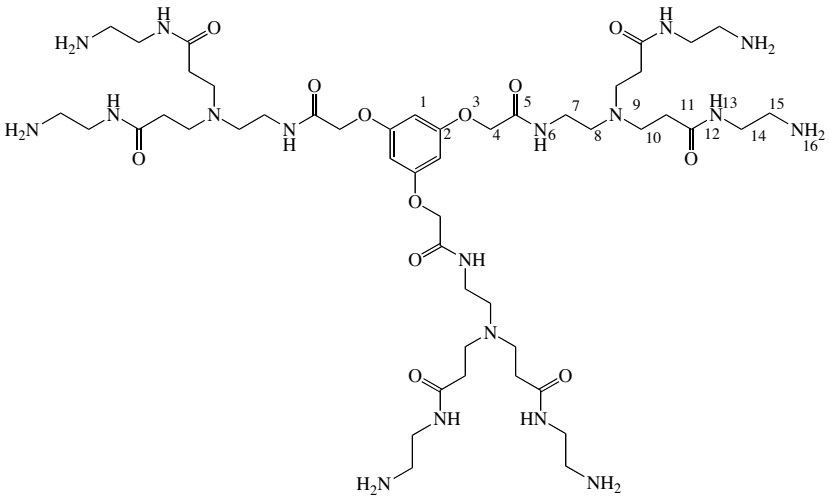

$C_{48}H_{90}N_{18}O_{12}$

RMM = 1111.35

0.5-[Phloroglucinol]-6-Ester (0.365 g: 0.382 mmol)

EDA (19.1 mL; 286.5 mmol)

Duration of stirring: 5 days at 5ºC

Purification: Azeotropic distillation

Product: Viscous orange oil (0.541 g; 127%, product contaminated with solvent)

^{1}H NMR: 6.25 (1H, s, **H-1**), 4.55 (2H, s, **H-4**), 3.31 (MeOH), 3.18 (4H, t, J = 6.3,
(300 MHz, D_2O) **H-7/14**), 2.75 (4H, t, J = 7.1, **H-10**), 2.68 (4H, t, J = 6.3, **H-15**), 2.59
(3H, t (br), **H-8**), 2.33 (4H, t, J = 7.2, **H-4/11**).

^{13}C NMR: (75 MHz, D_2O) 175.7 (**C-12**), 171.2 (**C-5**), 159.9 (**C-2**), 96.1 (**C-1**), 67.4 (**C-4**), 51.9 (**C-8**), 49.7 (**C-10**), 49.5 (MeOH), 42.3 (**C-14**), 40.4 (**C-15**), 37.2 (**C-7**), 33.6 (**C-11**).

1.5-[Phloroglucinol]-12-Ester

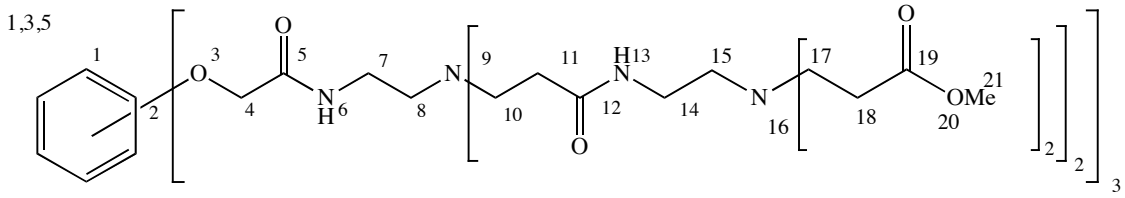

$C_{96}H_{162}N_{18}O_{36}$

RMM = 2144.43

1.0-[Phloroglucinol]-6-Amine (0.541 g; 0.486 mmol)

Methyl acrylate (0.68 mL; 7.58 mmol)

Duration of stirring: 12 days at room temperature

Purification: Column chromatography (R_f: 0.68, 19% MeOH in DCM, silica 60)

Product: Viscous yellow oil (0.423 g; 40%)

MS/ES$^+$ (m/z): 537.0 (60% $[M + 4H]^{4+}$), 715.7 (100% $[M + 3H]^{3+}$), 723.1 (30% $[M + 2H + Na]^{3+}$), 1073.3 (30% $[M + 2H]^{2+}$).

^{1}H NMR: (300 MHz, $CDCl_3$) 6.25 (1H, s, **H-1**), 4.45 (2H, s, **H-4**), 3.66 (14H, s, **H-21**), 3.47 (MeOH), 3.26 (4H, q (br), **H-7/14**), 2.79 (s (br)), 2.74 (11H, t, J = 6.6, **H-10/17**), 2.52 (5H, t, J = 5.8, **H-8/15**), 2.42 (14H, t, J = 6.4, **H-11/18**).

^{13}C NMR: (75 MHz, $CDCl_3$) 173.0 (**C-12/19**), 159.3 (**C-2**), 67.5 (**C-4**), 52.9 (**C-15**), 52.8 (**C-8**), 51.6 (**C-21**), 50.7 (MeOH), 49.9 (**C-10**), 49.2 (**C-17**), 38.4 (**C-7**), 37.2 (**C-14**), 33.4 (**C-11**), 32.7 (**C-18**).

^{1}H T_1 NMR: (MeOD) 6.37 (0.813), 4.55 (0.382), 3.67 (1.446), 3.27 (0.417), 2.79 (0.408), 2.53 (0.441), 2.48 (0.569).

^{1}H T_1 NMR: 4.47 (0.370), 3.66 (1.197), 3.29 (0.0.344), 2.75 (0.364), 2.56 (0.308), 2.44 (0.488).
$(CDCl_3)$

2.0-[Phloroglucinol]-12-Amine

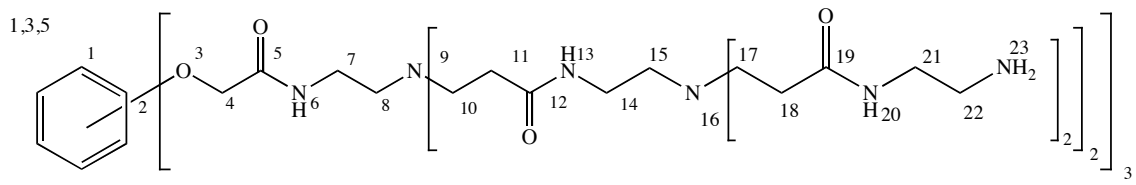

$C_{108}H_{210}N_{42}O_{24}$

RMM = 2481.12

1.5-[Phloroglucinol]-12-Ester (0.300 g, 0.140 mmol)

EDA (16.8 mL; 251.8 mmol)

Duration of stirring: 5 days at 5ºC

Purification: Azeotropic distillation

Product: Viscous orange oil (0.510 g; 140%, product contaminated with solvent)

^{1}H NMR: 6.24 (1H, s, **H-1**), 4.52 (2H, s, **H-4**), 3.31 (MeOH), 3.23 (t (br), **H-7/14**), 3.19 (11H, t, J = 6.3, **H-21**), 2.75 (17H, t, J = 6.9, **H-10/17**), 2.67 (11H, t, J = 6.1, **H-22**), 2.64 (3H, t (br)), 2.56 (5H, t, J = 6.8, **H-8/15**), 2.36 (15H, t, J = 7.0, **H-11/18**).
$(400\ MHz, D_2O)$

^{13}C NMR: 175.4 (**C-19**), 175.1 (**C-12**), 96.0 (**C-1**), 67.2 (**C-4**), 51.9 (**C-15**), 51.8 (**C-8**), 49.7 (**C-10/17**), 49.5 (MeOH), 42.7 (EDA), 42.3 (**C-21**), 40.4 (**C-22**), 37.4 (**C-7/14**), 33.5 (**C-11**), 33.5 (**C-18**).
$(100\ MHz, D_2O)$

2.5-[Phloroglucinol]-24-Ester

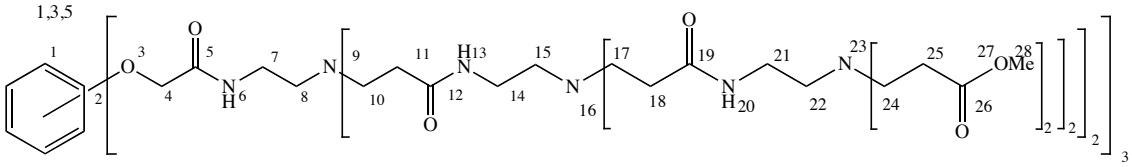

$C_{204}H_{354}N_{42}O_{72}$

RMM = 4547.26

2.0-[Phloroglucinol]-12-Amine (0.510 g; 0.206 mmol)

Methyl acrylate (0.9 mL; 9.87 mmol)

Duration of stirring: 6 days at room temperature

Purification: Azeotropic distillation

Product: Viscous orange oil (0.720 g; 77%).

^{1}H NMR (400 MHz, $CDCl_3$): 7.11 (4H, s (br)), 6.23 (1H, s, **H-1**), 4.44 (3H, s, **H-4**), 3.65 (38H, s, **H-28**), 3.46 (MeOH), 3.25 (19H, q, **H-7/14/21**), 2.81 (s (br), **H-10/17**), 2.74 (t, J = 6.7, **H-24**), 2.53 (t, J = 6.7, **H-8/15/22**), 2.41 (t, J = 6.6,**H-25**), 2.36 (s (br), **H-11/18**).

^{13}C NMR (100 MHz, $CDCl_3$): 173.0 (**C-26**), 172.9 (**C-5**), 172.4 (**C-12**), 172.3 (**C-19**), 67.4 (**C-4**), 52.9 (**C-22**), 52.5 (**C-8**), 52.5 (**C-15**), 52.2 (**C-28**), 50.7 (MeOH), 49.8 (**C-10**), 49.8 (**C-17**), 49.3 (**C-24**), 37.2 (**C-7/14/21**), 33.6 (**C-11/18**), 32.6 (**C-25**).

3.0-[Phloroglucinol]-24-Amine

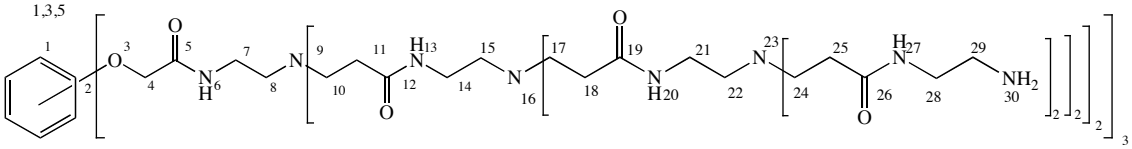

$C_{228}H_{450}N_{90}O_{48}$

RMM = 5220.65

2.5-[Phloroglucinol]-12-Ester (0.500 g: 0.11 mmol)

EDA (31 mL; 462 mmol)

Duration of stirring: 7 days at 5ºC

Purification: Azeotropic distillation and dialysis in deionised water

Product: Viscous orange oil (0.646 g; 111%, product contaminated with solvent)

^{1}H NMR: (400 MHz, D_2O) 6.29 (1H, s, **H-1**), 4.54 (2H, s, **H-4**), 3.31 (MeOH), 3.24 (t (br), **H-7/14/21**), 3.21 (t (br), **H-28**), 2.77 (t (br), **H-10/17/24**), 2.70 (t (br), **H-29**), 2.57 (12H, t (br), **H-8/15/22**), 2.38 (26H, t (br), **H-11/18/25**).

^{13}C NMR: (100 MHz, D_2O) 175.2 (**C-26**), 174.7 (**C-12/19**), 51.5 (**C-8/15/22**), 49.7 (**C-10/17/24**), 49.5 (MeOH), 42.1 ((br) **C-28**), 40.4 (**C-29**), 37.4 (**C-7/14/21**), 33.5 (**C-25**), 33.4 (**C-11/18**).

3.5-[Phloroglucinol]-48-Ester

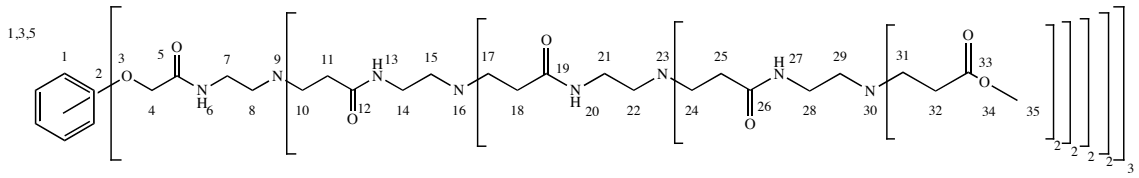

$C_{420}H_{738}N_{90}O_{144}$

RMM = 9352.94

3.0-[Phloroglucinol]-24-Amine (0.647 g; 0.123 mmol)

Methyl acrylate (1.1 mL; 11.8 mmol)

Duration of stirring: 7 days at room temperature

Purification: Azeotropic distillation

Product: Viscous orange oil (0.773 g; 70%)

^{1}H NMR (400 MHz, $CDCl_3$): 7.13 (s (br)), 6.22 (1H, s, **H-1**), 4.43 (2H, s, **H-4**), 3.65 (26H, s, **H-35**), 3.46 (MeOH), 3.25 (q (br), **H-14/21/28**), 2.80 (s (br), **H-10/17/24**), 2.74 (t, J = 6.5, **H-31**), 2.59 (s (br), **H-8/15/22**), 2.53 (t, J = 5.8, **H-29**), 2.42 (t, J = 6.7, **H-32**), 2.36 (s (br), **H-11/18/25**).

^{13}C NMR (100 MHz, $CDCl_3$): 173.0 (**C-33**), 172.5 (**C-26**), 172.4 (**C-12/19**), 52.9 (**C-29**), 52.5 (**C-8/15/22**), 51.6 (**C-35**), 50.7 (MeOH), 50.0 (**C-10**), 49.9 (**C-17/24**), 49.3 (**C-31**), 37.5 (**C-7/14/21**), 37.3 (**C-28**), 33.7 (**C-11/18/25**), 32.7 (**C-32**).

4.0-[Phloroglucinol]-48-Amine

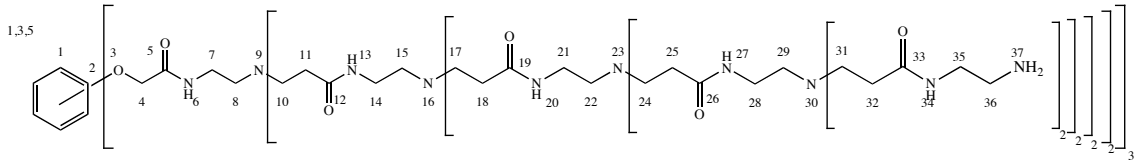

$C_{468}H_{930}N_{186}O_{96}$

RMM = 10699.70

3.5-[Phloroglucinol]-24-Ester (0.631 g; 0.067 mmol)

EDA (140 mL; 2082 mmol)

Duration of stirring: 14 days at 5ºC

Purification: Azeotropic distillation and dialysis in deionised water

Product: Viscous orange oil (0.498 g; 69%)

^{1}H NMR: (400 MHz, D_2O) 6.29 (1H, s, **H-1**), 4.54 (2H, s, **H-4**), 3.31 (MeOH), 3.21 (43H, m (br), **H-21/28/35**), 2.78 (t (br), **H-17/24/31**), 2.70 (t (br), **H-36**), 2.59 (t (br), **H-15/22/29**), 2.39 (d (br), **H-18/25/32**).

^{13}C NMR: (100 MHz, D_2O) 175.6 (**C-33**), 175.2 (**C-26**), 175.1 (**C-19**), 51.9 (**C-15/22/29**), 49.7 (**C-17/24/31**), 49.5 (MeOH), 47.8, 45.1, 42.1 (**C-35**), 40.4 (**C-36**), 39.2, 37.9, 37.4 (**C-14/21/28**), 36.1, 33.5 (**C-25/32**), 33.4 (**C-11/18**).

-0.5-[Ammonia]-3-Ester

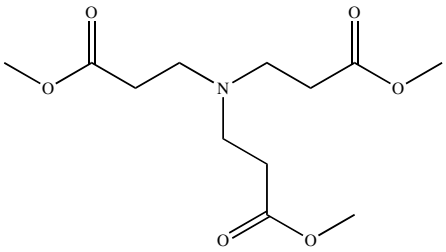

$C_{12}H_{21}NO_6$

RMM = 275.30

Sample prepared by Dr P. Walker and used with permission.

^1H T_1 NMR: 3.66 (3.219), 2.75 (1.311), 2.45 (1.813).
(MeOD)

^1H T_1 NMR: 3.64 (2.384), 2.74 (0.970, 2.42 (1.354).
($CDCl_3$)

0-[Ammona]-3-Amine

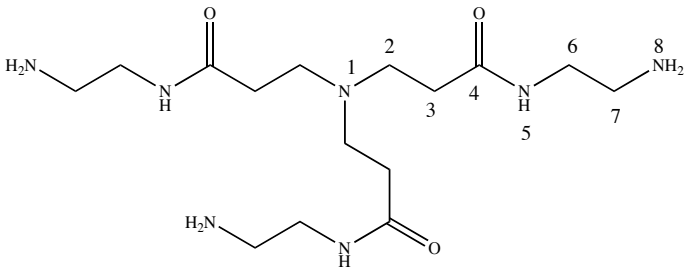

$C_{15}H_{33}N_7O_3$

RMM = 349.47

-0.5-[Ammonia]-3-Amine (1.42 g; 5.16 mmol)

EDA (51.8 mL; 775 mmol)

Duration of stirring: 5 days at room temperature

Purification: Azeotropic distillation

Product: Viscous yellow oil (2.67 g; 144%, product contaminated with solvent)

^{1}H NMR (400 MHz, MeOD): 3.35 (MeOH), 3.32 (6H, t, J = 6.3, **H-6**), 2.76 (t, J = 6.8, **H-2**), 2.72 (t, J = 6.3, **H-7**), 2.36 (6H, t, J = 6.8, **H-3**).

^{13}C NMR (100 MHz, MeOD): 175.3 (**C-4**), 50.6 (**C-2**), 49.9 (MeOH), 43.0 (**C-6**), 42.0 (**C-7**), 34.6 (**C-3**).

^{1}H T_1 NMR (MeOD): 3.24 (0.979), 2.75 (0.398), 2.72 (1.071), 2.36 (0.513).

^{1}H T_1 NMR (D_2O): 3.16 (0.895), 2.68 (0.348), 2.64 (0.992), 2.34 (0.441).

0.5-[Ammonia]-6-Ester (115)

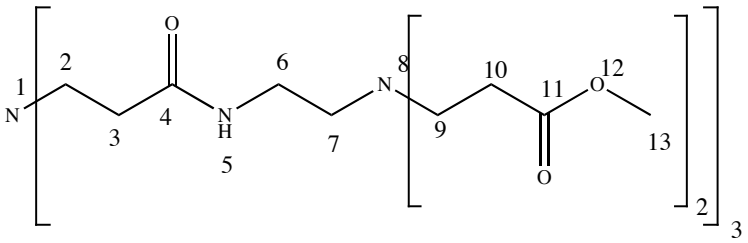

$C_{39}H_{69}N_7O_{15}$

RMM = 876.01

0-[Ammonia]-3-Amine (1.418 g; 3.952 mmol)

Methyl acrylate (6.0 mL; 66.4 mmol)

Duration of stirring: 3 days at room temperature

Purification: Column chromatography (R_f: 0.37, 10% MeOH in DCM, silica 60)

Product: Viscous yellow oil (1.148 g; 33%)

MS/ES$^+$ (m/z): 439.0 (75% $[M + 2H]^{2+}$), 450.0 (75% $[M + H + Na]^{2+}$), 461.0 (20% $[M + 2Na]^{2+}$), 876.7 (80% $[M + H]^+$), 898.7 (100% $[M + Na]^+$).

^{1}H NMR (300 MHz, $CDCl_3$): 6.97 (3H, t (br), **H-5**), 5.29 (DCM), 3.66 (18H, s, **H-13**), 3.27 (6H, q, J = 5.8, **H-6**), 2.79 (t (br), **H-2**), 2.74 (t, J = 6.6, **H-9**), 2.52 (6H, t, J = 5.9, **H-7**), 2.41 (t, J = 6.6, **H-10**), 2.37 (t (br), **H-3**).

^{13}C NMR (75 MHz, $CDCl_3$): 173.0 (**C-11**), 172.0 (**C-4**), 53.4 (DCM), 53.0 (**C-7**), 51.6 (**C-13**), 49.2 (**C-2/9**), 37.1 (**C-6**), 33.5 (**C-3**), 32.7 (**C-10**).

^{1}H T_1 NMR (MeOD): 3.67 (1.938), 3.26 (0.501), 2.81 (0.327), 2.77 (0.526), 2.56 (0.437), 2.48 (0.800), 2.39 (0.402).

^{1}H T_1 NMR ($CDCl_3$): 6.97 (0.550), 3.67 (1.893), 3.26 (0.388), 2.80 (0.291), 2.74 (0.432), 2.52 (0.348), 2.41 (0.634), 2.37 (0.343).

1.0-[Ammona]-6-Amine

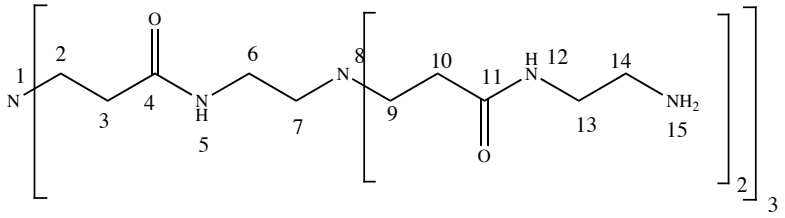

$C_{45}H_{93}N_{19}O_9$

RMM = 1044.35

0.5-[Ammonia]-3-Amine (1.012 g; 1.15 mmol)

EDA (28 mL; 416 mmol)

Duration of stirring: 5 days at room temperature

Purification: Azeotropic distillation

Product: Viscous yellow oil (1.285 g; 107%, product contaminated with solvent)

^{1}H NMR: (400 MHz, MeOD) 3.35 (MeOH), 3.35 (3H, t, J = 6.3, **H-6/13**), 2.79 (3H, t, J = 6.6, **H-2/9**), 2.73 (2H, t, J = 6.4, **H-14**), 2.58 (1H, t, J = 6.5, **H-7**), 2.36 (3H, t, J = 6.8, **H-3**).

^{13}C NMR: (100 MHz, MeOD) 175.2 (**C-11**), 174.8 (**C-4**), 53.5 (**C-7**), 51.2 (**C-9**), 50.6 (**C-2**), 49.9 (MeOH), 43.1 (**C-13**), 42.1 (**C-14**), 38.7 (**C-6**), 34.9 (**C-10**), 34.6 (**C-3**).

1.5-[Ammonia]-12-Ester

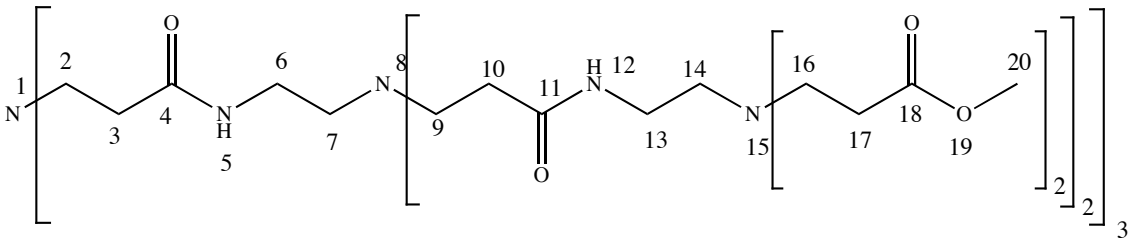

$C_{93}H_{165}N_{19}O_{33}$

RMM = 2077.43

0-[Ammonia]-3-Amine (0.859 g; 0.823 mmol)

Methyl acrylate (2.7 mL; 29.6 mmol)

Duration of stirring: 3 days at room temperature

Purification: Azeotropic distillation

Product: Viscous yellow oil (0.827 g; 48%)

MS/ES^{+} (m/z): 1061.9 (100% $[M + 2Na]^{2+}$).

^{1}H NMR: (400 MHz, $CDCl_3$) 7.61 (3H, t (br), **H-5**), 7.01 (5H, t (br), **H-12**), 3.65 (36H, s, **H-20**), 3.26 (18H, q, J = 5.5, **H-6/13**), 2.79 (t (br), **H-2/9**), 2.74 (t, J = 6.7,

H-16), 2.56 (t (br), **H-7**), 2.53 (t, J = 5.9, **H-14**) 2.41 (25H, t, J = 6.8, **H-17**), 2.34 (t (br), **H-3/10**).

^{13}C NMR (400 MHz, $CDCl_3$): 173.0 (**C-18**), 172.3 (**C-4/11**), 52.9 (**C-14**), 52.5 (**C-7**), 51.6 (**C-20**), 50.6 (MeOH), 49.9 (**C-2/9**), 49.2 (**C-16**), 37.5 (**C-6**), 37.2 (**C-13**), 33.8 (**C-10**), 33.4 (**C-3**), 32.7 (**C-17**).

^{1}H T_1 NMR (MeOD): 3.67 (1.585), 3.26 (0.410), 2.83 (0.292), 2.77 (0.426), 2.61 (0.294), 2.56 (0.359), 2.47 (0.640), 2.39 (0.343).

^{1}H T_1 NMR ($CDCl_3$): 7.08 (0.424), 3.64 (1.292), 3.25 (0.318), 2.77 (0.303), 2.73 (0.340), 2.53 (0.295), 2.50 (0.293), 2.41 (0.487), 2.35 (0.299).

0.5-[PAMAM]-2-Ester Dendron (117)

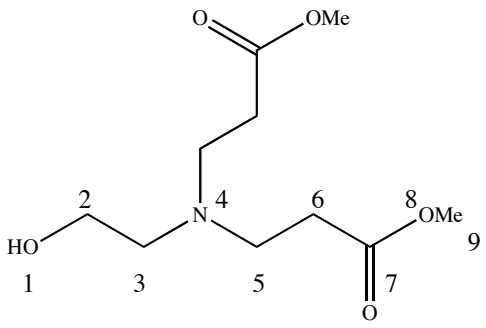

$C_{10}H_{19}NO_5$

RMM = 233.26

Ethanolamine (2 mL; 32.7 mmol)

Methyl acrylate (12 mL; 131 mmol)

Duration of stirring: 4 days at room temperature

Purification: Azeotropic distillation

Product: Colourless oil (8.62 g; 109%, product contaminated with solvent)

MS/ES$^+$ (m/z): 234.2 (100% $[M + H]^+$), 256.3 (20% $[M + Na]^+$).

^{1}H NMR: (300 MHz, $CDCl_3$) 3.67 (6H, s, **H-9**), 3.58 (2H, t(br), **H-2**), 2.80 (4H, t, J = 6.7, **H-5**), 2.60 (2H, t, J = 5.1, **H-3**), 2.47 (4H, t, J = 6.7, **H-6**).

^{13}C NMR: (75 MHz, $CDCl_3$) 172.9 (**C-7**), 59.0 (**C-2**), 56.1 (**C-3**), 51.6 (**C-9**), 49.2 (**C-5**), 32.5 (**C-6**).

^{1}H T_1 NMR: ($CDCl_3$) 3.66 (3.037), 3.56 (1.313), 2.77 (1.270), 2.57 (1.177), 2.44 (1.614).

Data is consistent with literature.[351]

1.0-[PAMAM]-2-Amine Dendron (118)

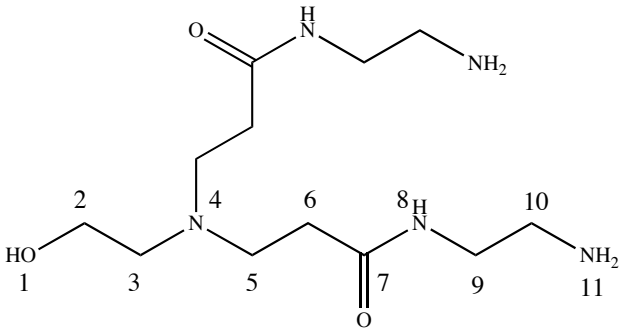

$C_{12}H_{27}N_5O_3$

RMM = 289.38

0.5-[PAMAM]-2-Ester (2.34 g; 10.0 mmol)

EDA (57 mL; 857 mmol)

Duration of stirirng: 5 days at 5ºC

Purification: Azeotropic distillation

Product: Yellow oil (3.43 g; 118%, product contaminated with solvent)

MS/ES^{+} $_{(m/z)}$: 312.4 (30% $[M + Na]^{+}$).

^{1}H NMR (300 MHz, D_2O): 3.63 (2H, t, J = 6.1, **H-2**), 3.31 (MeOH), 3.20 (4H, t, J = 6.2, **H-9**), 2.79 (4H, t, J = 7.1, **H-5**), 2.67 (4H, t, J = 6.3, **H-10**), 2.62 (3H, t, J = 6.1, **H-3**), 2.40 (4H, t, J = 7.1, **H-6**).

^{13}C NMR (75 MHz, D_2O): 175.9 (**C-7**), 59.3 (**C-2**), 54.9 (**C-3**), 49.9 (**C-5**), 49.5 (MeOH), 42.3 (**C-9**), 40.4 (**C-10**), 33.4 (**C-6**).

Data is consistent with literature.[351]

1.5-[PAMAM]-4-Ester Dendron

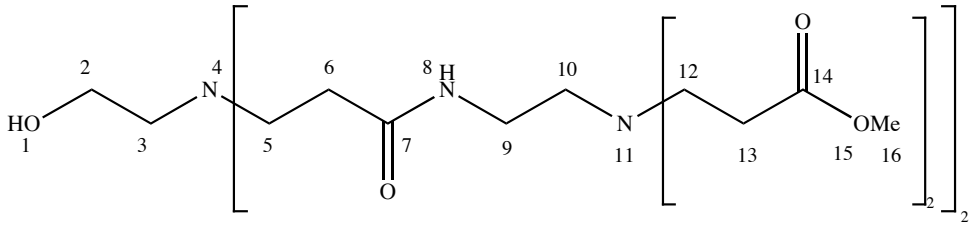

$C_{28}H_{51}N_5O_{11}$

RMM = 633.73

1.0-[PAMAM]-2-Amine (3.43 g; 11.87 mmol)

Methyl acrylate (5.6 mL; 61.7 mmol)

Duration of stirring: 5 days at room temperature

Purification: Column chromatography (R_f: 0.41, 10% MeOH in DCM, silica 60)

Product: Pale yellow oil (4.60 g; 61%)

MS/ES^{+} $_{(m/z)}$: 318.0 (60% $[M + 2H]^{2+}$), 634.4 (100% $[M + H]^{+}$).

^{1}H NMR: (300 MHz, $CDCl_3$) 3.66 (18H, s, **H-16**), 3.60 (2H, t (br), **H-2**), 3.46 (MeOH), 3.28 (6H, q, J = 5.8, **H-9**), 2.82 (6H, t (br), **H-5**), 2.74 (12H, t, J = 6.7, **H-12**), 2.62 (3H, s (br), **H-3**), 2.53 (6H, t, J = 5.6, **H-10**), 2.42 (17H, t, J = 6.6, **H-6/13**).

^{13}C NMR: (75 MHz, $CDCl_3$) 173.0 (**C-14**), 172.2 (**C-7**), 59.3 (**C-2**), 55.7 (**C-3**), 52.9 (**C-10**), 51.6 (**C-16**), 50.0 (**C-5**), 49.2 (**C-12**), 37.1 (**C-9**), 33.7 (**C-6**), 32.6 (**C-13**).

Data is consistent with literature.[351]

2.0-[PAMAM]-4-Amine Dendron

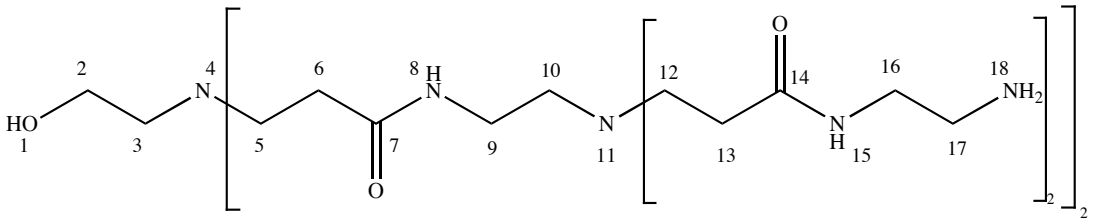

$C_{32}H_{67}N_{13}O_7$

RMM = 745.97

1.5-[PAMAM]-2-Ester (2.0 g, 3.16 mmol)

EDA (51 mL, 758 mmol)

Duration of stirring: 5 days at 5ºC

Purification: Azeotropic distillation

Product: Yellow oil (3.33 g; 133%, product contaminated with solvent)

MS/ES^{+} (m/z): 249.2 (60% $[M + 3H]^{3+}$), 374.1 (100% $[M + 2H]^{2+}$).

^{1}H NMR: (300 MHz, D_2O) 3.63 (1H, t, J = 6.0, **H-2**), 3.31 (MeOH), 3.24 (8H, t, J = 6.2, **H-9/16**), 2.79 (t (br), **H-5/12**), 2.74 (t, J = 6.2, **H-10/17**), 2.60 (5H, q (br), **H-3/6**), 2.42 (8H, t (br), **H-13**).

^{13}C NMR: (75 MHz, D_2O) 175.7 (**C-14**), 175.4 (**C-7**), 59.4 (**C-2**), 54.9 (**C-3**), 51.9 (**C-10**), 49.9 (**C-5**), 49.7 (**C-12**), 49.5 (MeOH), 41.7 (**C-16**), 40.4 (**C-17**), 37.4 (**C-9**), 33.5 (**C-13**), 33.3 (**C-6**).

Data is consistent with literature.[351]

2.5-[PAMAM]-4-Ester Dendron

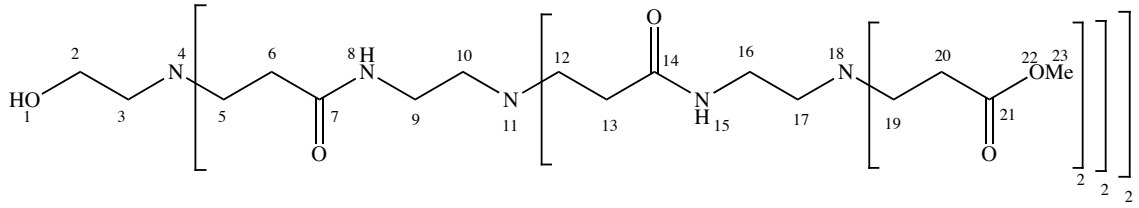

$C_{64}H_{115}N_{13}O_{23}$

RMM = 1434.68

Methyl acrylate (6.4 mL, 71.4 mmol)

2-[PAMAM]-4-Amine (3.33 g, 4.46 mmol)

Duration of stirring: 5 days at room temperature

Purification: Column chromatography failed; reclaimed from silica phase

Product: Pale yellow oil (2.52 g; 39%)

^{1}H NMR: (400 MHz, $CDCl_3$) 7.00 (1H, t, J = 5.1, **H-15**), 3.64 (2H, s, **H-23**), 3.25 (1H, q (br), **H-9/16**), 2.77 (t, J = 6.7, **H-5/12**), 2.72 (t, J = 6.6, **H-19**), 2.56 (t (br), **H-10**), 2.51 (t, J = 5.9 Hz, **H-17**), 2.40 (6H, t, J = 6.6, **H-20**), 2.34 (t, J = 6.8, **H-6/13**).

^{13}C NMR: (100 MHz, $CDCl_3$) 172.9 (**C-21**), 172.4 (**C-7**), 172.3 (**C-14**), 59.4 (**C-2**), 55.7 (**C-3**), 53.4 (DCM), 52.9 (**C-17**), 52.5 (**C-10**), 51.6 (**C-23**), 50.1 (**C-5**), 49.9 (**C-12**), 49.2 (**C-19**), 37.3 (**C-9**), 37.2 (**C-16**), 33.8 (**C-6/13**), 32.6 (**C-20**).

Data is consistent with literature.[351]

General Procedure for the Acetylation of 1.0-[EDA]-8-Amine

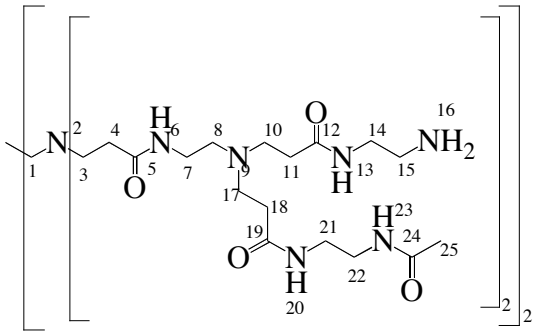

Acetic anhydride was added dropwise to a stirred solution of 1.0-[EDA]-8-amine and triethylamine in dry methanol (4 mL). After 24 hours the solvent was removed *in vacuo* to give an orange oil.

Procedure adapted from literature.[360,376]

25% Acetylated (119)

1.0-[EDA]-8-Amine (0.100 mg; 0.070 mmol)
Acetic anhydride (0.013 mL; 0.140 mmol)
Triethylamine (0.021 mL; 0.154 mmol)
Product: Viscous orange oil (0.083 g)
Calculated surface coverage: 3 groups by ^{1}H NMR

^{1}H-NMR (300MHz, D_2O): 3.38 (9H, t (br)), 3.31 (MeOH), 3.26 (22H, s (br), **H-14/21/22**), 2.96 (9H, t (br)), 2.77 (23H, t (br), **H-10/15/17**), 2.58 (12H, s (br), **H-1/8**), 2.40 (24H, m (br), **H-4/11**), 1.94 (8H, s, **H-25**), 1.87 (5H, TEA).

50% Acetylated (120)

1.0-[EDA]-8-Amine (0.100 mg; 0.070 mmol)
Acetic anhydride (0.026 mL; 0.280 mmol)
Triethylamine (0.043 mL; 0.308 mmol)
Product: Viscous orange oil (0.090 g)
Calculated surface coverage: 5 groups by ^{1}H NMR

^{1}H-NMR (300MHz, D_2O): 3.47 (5H, t (br)), 3.31 (MeOH), 3.26 (23H, s (br), **H-14/21/22**), 3.11 (5H, t (br)), 2.98 (6H, t (br)), 2.89 (21H, (br), **H-10/15/17**), 2.73 (10H, (br), **H-1/8**), 2.44 (24H, m (br), **H-4/11**), 1.94 (13H, s, **H-25**), 1.87 (6H, TEA).

75% Acetylated (121)

1.0-[EDA]-8-Amine (0.100 mg; 0.070 mmol)

Acetic anhydride (0.040 mL; 0.420 mmol)
Triethylamine (0.064 mL; 0.462 mmol)
Product: Viscous orange oil (0.095 g)
Calculated surface coverage: 7 groups by ^{1}H NMR

^{1}H-NMR (300MHz, D_2O): 3.47 (2H, t (br)), 3.35 (br), 3.31 (MeOH), 3.26 (29H, s (br), **H-14/21/22**), 3.11 (2H, t (br)), 3.01 (7H, q (br)), 2.94 (20H, t (br), **H-10/15/17**), 2.78 (8H, (br), **H-1/8**), 2.40 (24H, m (br), **H-4/11**), 1.94 (18H, s, **H-25**), 1.87 (4H, TEA).

100% Acetylated (122)

1.0-[EDA]-8-Amine (0.050 mg; 0.035 mmol)
Acetic anhydride (0.032 mL; 0.336 mmol)
Triethylamine (0.052 mL; 0.370 mmol)
Product: Viscous orange oil (0.029 g)
Calculated surface coverage: 9 groups by ^{1}H NMR

^{1}H-NMR (300MHz, D_2O): 3.45 (9H, t (br)), 3.31 (MeOH), 3.26 (32H, s (br)), 3.14 (26H, m (br)), 2.99 (12H, t (br)), 2.56 (24H, t (br)), 1.94 (19H, s, **H-25**), 1.87 (7H, TEA).

General Procedure for the Acetylation of 4.0-[EDA]-64-Amine

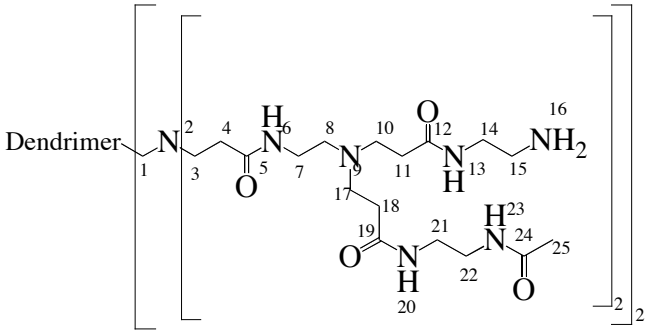

Acetic anhydride was added dropwise to a stirred solution of 4.0-[EDA]-64-amine and triethylamine in dry methanol (4 mL). After 72 hours the solvent was removed *in vacuo* to give an orange oil. The oil was then dialysed in deionised water for 7 days. The resulting oil was then azeotropically distilled in MeOH/toluene to give product as a viscous orange oil. ^{13}C NMR showed incomplete dialysis, so this step was repeated.

Procedure adapted from published data to give consistent results.[234]

25% Acetylation (127)

4.0-[EDA]-64-Amine (0.100 g; 0.00704 mmol)
Acetic anhydride (0.011 mL; 0.113 mmol)
Triethylamine (0.017 mL; 0.124 mmol)
Product: Viscous orange oil (0.087 g)
Calculated surface coverage: 16 groups (25%) by ^{1}H NMR

^{1}H-NMR (400MHz, D_2O): 3.31 (MeOH), 3.26 (21H, s, **H-14/21/22**), 2.77 (d, **H-10/15/17**), 2.66 (t), 2.58 (10H, s (br), **H-1/8**), 2.38 (20H, s (br), **H-4/11**), 1.94 (4H, s, **H-25**).

^{13}C-NMR (100MHz, D_2O): 175.7 (**C-12**), 175.6 (**C-5**), 175.2 (internal carbonyl), 174.7 (**C-24**), 51.9 (**C-8**), 49.7 (**C-3/10/17**), 49.5 (MeOH), 47.8 (G4 defect), 45.1 (G4

defect), 41.3 (**C-14**), 40.3 (**C-15**), 39.3 (**C-21**), 39.2 (**C-22**), 37.9, 37.4 (**C-7**), 36.0 (G4 defect), 33.4 (**C-4/11/18**), 22.6 (**C-25**).

50% Acetylation (124)

4.0-[EDA]-64-Amine (0.100 g; 0.00704 mmol)
Acetic anhydride (0.021 mL; 0.225 mmol)
Triethylamine (0.047 mL; 0.338 mmol)
Product: Viscous orange oil (0.076 g)
Calculated surface coverage: 34 groups (53%) by ^{1}H NMR

^{1}H-NMR (400MHz, D_2O): 3.40 (2H, s (br)), 3.31 (MeOH), 3.25 (22H, s, **H-14/21/22**), 2.99 (2H, s (br)), 2.77 (19H, s (br), **H-10/15/17**), 2.58 (10H, s (br), **H-1/8**), 2.37 (20H, s (br), **H-4/11**), 1.93 (8H, s, **H-25**).

^{13}C-NMR (100MHz, D_2O): 175.5 (**C-12**), 175.1 (**C-5**), 174.7 (**C-24**), 51.9 (**C-8**), 49.7 (**C-3/10/17**), 49.5 (MeOH), 40.0, 39.3 (**C-21**), 39.2 (**C-22**), 37.9, 37.4 (**C-7**), 33.3 (**C-4/11/18**), 22.6 (**C-25**).

75% Acetylation (125)

4.0-[EDA]-64-Amine (0.100 g; 0.070 mmol)
Acetic anhydride (0.032 mL; 0.333 mmol)
Triethylamine (0.071 mL; 0.507 mmol)
Product: Viscous orange oil (0.095 g)
Calculated surface coverage: 40 groups (63%) by ^{1}H NMR

^{1}H-NMR (300MHz, D_2O): 3.40 (2H, s (br)), 3.31 (MeOH), 3.25 (21H, s, **H-14/21/22**), 3.00 (2H, s (br)), 2.77 (18H, s (br), **H-10/15/17**), 2.58 (10H, s (br), **H-1/8**), 2.37 (19H, s (br), **H-4/11**), 2.07 (1H, d (br)), 1.93 (9H, s, **H-25**).

^{13}C-NMR (75MHz, D_2O): 175.5 (**C-12**), 175.1 (**C-5**), 174.7 (**C-24**), 51.9 (**C-8**), 49.7 (**C-3/10/17**), 49.5 (MeOH), 39.9, 39.3 (**C-21**), 39.2 (**C-22**), 37.8, 37.4 (**C-7**), 33.3

(**C-4/11/18**), 22.6 (**C-25**).

75% Acetylation (128)

4.0-[EDA]-64-Amine (0.250 g; 0.0176 mmol)
Acetic anhydride (0.080 mL; 0.844 mmol)
Triethylamine (0.129 mL; 0.929 mmol)
Product: Viscous orange oil (0.242 g)
Calculated surface coverage: 47 groups (74%) by ^{1}H NMR

^{1}H-NMR (400MHz, D_2O): 3.31 (MeOH), 3.25 (24H, s, **H-14/21/22**), 2.77 (18H, s (br), **H-10/15/17**), 2.58 (10H, s (br), **H-1/8**), 2.37 (19H, s (br), **H-4/11**), 2.07 (d), 1.93 (11H, s, **H-25**).

^{13}C-NMR (100MHz, D_2O): 175.6 (**C-12**), 175.1 (**C-5**), 174.7 (**C-24**), 51.9 (**C-8**), 49.7 (**C-3/10/17**), 49.5 (MeOH), 44.9 (G4 defect), 39.3 (**C-21**), 39.2 (**C-22**), 38.7, 37.9, 37.4 (**C-7**), 33.3 (**C-4/11/18**), 22.6 (**C-25**).

75% Acetylation-d_3 (130)

4.0-[EDA]-64-Amine (0.150 mg; 0.0106 mmol)
Acetic anhydride-d_6 (0.048 mL; 0.509 mmol)
Triethylamine (0.077 mL; 0.557 mmol)
Product: Viscous orange oil (0.136 g)
Calculated surface coverage: 50 groups (78%) by inverse-gated decoupled ^{13}C NMR

^{13}C NMR (inverse-gated decoupled, MeOD): Dendrimer carbonyl 174.7 (124C), acetyl carbonyl 173.5 (50C).

100% Acetylation (126)

4.0-[EDA]-64-Amine (0.050 mg; 0.0035 mmol)

Acetic anhydride (0.028 mL; 0.293 mmol)
Triethylamine (0.061 mL; 0.439 mmol)
Product: Viscous orange oil (0.029 g)
Calculated surface coverage: 46 groups (72%) by ^{1}H NMR

^{1}H-NMR (300MHz, D_2O): 3.31 (MeOH), 3.25 (23H, s (br), **H-14/21/22**), 2.77 (17H, t (br), **H-10/15/17**), 2.58 (10H, t (br), **H-1/8**), 2.37 (19H, t (br), **H-4/11**), 2.07 (1H, d (br)), 1.93 (10H, s, **H-25**).

^{13}C-NMR (75MHz, D_2O): 175.5 (**C-12**), 175.1 (**C-5**), 174.7 (**C-24**), 51.9 (**C-8**), 49.7 (**C-3/10/17**), 49.5 (MeOH), 39.3 (**C-21**), 39.2 (**C-22**), 37.9, 37.4 (**C-7**), 33.3 (**C-4/11/18**), 22.6 (**C-25**).

100% Acetylation (129)

4.0-[EDA]-64-Amine (0.090 mg; 0.00633 mmol)
Acetic anhydride (0.058 mL; 0.608 mmol)
Triethylamine (0.104 mL; 0.743 mmol)
Product: Viscous orange oil (0.082 g)
Calculated surface coverage: 54 groups (84%) by ^{1}H NMR

^{1}H-NMR (400MHz, D_2O): 3.31 (MeOH), 3.25 (27H, s (br), **H-14/21/22**), 2.77 (20H, t (br), **H-10/15/17**), 2.58 (10H, t (br), **H-1/8**), 2.37 (21H, t (br), **H-4/11**), 2.07 (2H, d), 1.93 (14H, s, **H-25**), 1.40 (2 H, s).

^{13}C-NMR (100MHz, D_2O): 175.5 (**C-12**), 175.1 (**C-5**), 175.0 (internal carbonyl), 174.7 (**C-24**), 51.9 (**C-8**), 49.7 (**C-3/10/17**), 49.5 (MeOH), 45.1 (G4 defect), 39.3

(**C-21**), 39.2 (**C-22**), 37.9, 37.4 (**C-7**), 35.3, 34.6, 33.3 (**C-4/11/18**), 28.2, 22.6 (**C-25**).

5-[EDA]-60-Amine-1-FITC-67-acetylated (131)

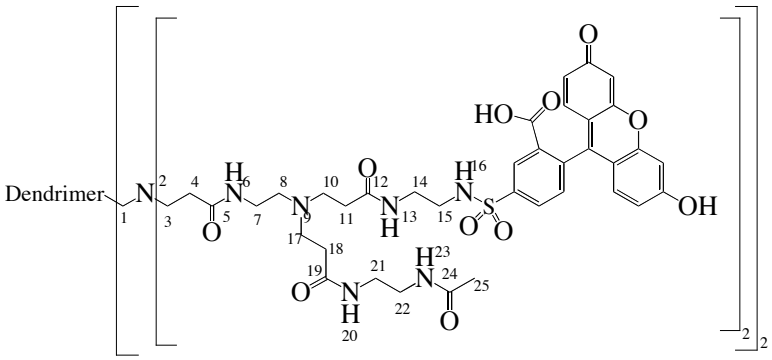

Acetic anhydride (0.00964 mL; 0.0102 mmol) was added dropwise to a stirred solution of 5-[EDA]-127-Amine-1-FITC (0.046 g; 0.0016 mmol) and triethylamine (4 drops) in dry methanol (4 mL). After 18 hours the solvent was removed *in vacuo* to give an orange oil. The oil was then dialysed against deionised water for 3 days. The resulting oil was then azeotropically distilled in MeOH/toluene to give product as a viscous orange oil (0.0342 g).

^{1}H-NMR: (400MHz, MeOD) 3.35 (MeOH), 3.28 (s (br), **H-14/21/22**), 2.79 (147H, t (br), **H-10/15/17**), 2.58 (100H, s (br), **H-1/8**), 2.36 (171H, s (br), **H-4/11**), 2.12 (40H, d (br)), 1.95 (68H, s, **H-25**).

^{13}C-NMR: (100MHz, MeOD) 175.2 (**C-12**), 174.7 (**C-5**), 173.5 (**C-24**), 53.5, 51.1 (**C-8**), 49.9 (MeOH), 40.2 (**C-14**), 40.1 (**C-15**), 38.6 (**C-21/22**) 34.7 (**C-4/11/18**), 22.9 (**C-25**).

Calculated surface coverage: 67 groups (52%) by ^{1}H NMR

No literature reference was found.

Preparation of Poly(ethylene glycol) Derivatives

α-Methyl-ω-bromopoly(ethylene glycol) (134)

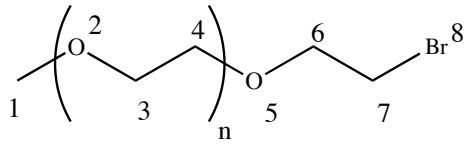

av. RMM = 613 (n = 5 to 16)

Monomethyl PEG (550) (10.0 g; 18.2 mmol) was dissolved in DCM (40 mL) and cooled over ice. Phosphorus tribromide (0.85 mL; 9.08 mmol) was added dropwise and the reaction mixture was allowed to stir for 1 hr at 0ºC before being warmed to RT and then stirred for a further 2 hrs giving a brown solution.

Ice was added to the reaction (with external cooling) to quench unreacted PBr_3 and the product extracted into DCM (3 x 40 mL). The organics were combined, dried over Na_2SO_4 and the solvent removed *in vacuo* to give product as a colourless oil (9.19 g; 82%).

MS/ES$^+$ (m/z): 559.3 (100%, n = 9, $[M + Na]^+$), n = 5 to 16. Bromine splitting observed.

^{1}H NMR (300 MHz, $CDCl_3$): 3.79 (6H, t, J = 6.3, **H-6**), 3.63 (s), 3.62 (s, **H-3/4**), 3.53 (d, J = 3.5), 3.52 (d, J = 3.5), 3.45 (4H, t, J = 6.4, **H-7**), 3.36 (7H, s, **H-1**).

^{13}C NMR (75 MHz, $CDCl_3$): 71.9 (Me-O-**C**H_2-), 71.1 (**C-6**), 70.5 (**C-3/4**), 64.7, 59.0 (**C-1**), 30.3 (**C-7**).

FTIR ν_{max} (cm^{-1}) (thin film): 2966 (s, C-H aliphatic stretch), 1456 (m, C-C stretch), 1093 (s, C-O stretch), 653 (w, C-Br stretch).

Procedure adapted from literature.

α-Methyl-ω-phthalimidopoly(ethylene glycol) (135)

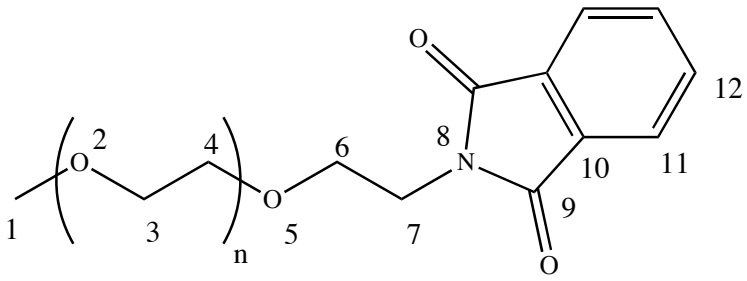

av. RMM = 679 (n = 5 to 16)

Potassium phthalimide (6.23 g; 33.6 mmol) was added portionwise to a solution of α-methyl-ω-bromopoly(ethylene glycol) (10.31 g; 16.82 mmol) in dry methanol (80 mL) and the mixture was stirred at 85ºC for 22 hrs to give a pale yellow solution with white solid.

The methanol was removed *in vacuo* and the resulting oil partitioned between water (40 mL) and DCM (40 mL). The organic phase was collected and the aqueous layer was washed a further two times with DCM (2 x 40 mL). The organics were combined and the DCM removed *in vacuo*. The resulting white oil was partitioned between water (40 mL) and ethyl acetate (40 mL). The organic phase was collected and the aqueous layer was washed a further two times with ethyl acetate (2 x 40 mL). The organics were combined, dried over Na_2SO_4 and the solvent removed *in vacuo* to give product as a white oily solid (2.32 g; 20%).

MS/ES$^+$ (m/z): 624.3 (100%, n = 9, $[M + Na]^+$), n = 5 to 16.

^{1}H NMR (300 MHz, DMSO): 11.33 (phthalimide), 7.86 (d, J = 3.3, **H-11/12**), 7.83 (phthalimide), 4.04 (trace ethyl acetate), 3.75 (4H, t, J = 5.5, **H-7**), 3.62 (4H, t, J = 6.3, **H-6**), 3.50 (s, **H-3/4**), 3.46 (s), 3.41 (s), 3.23 (5H, s, **H-1**), 3.03 (MeOH), 1.98 (trace ethyl acetate), 1.17 (trace ethyl acetate).

^{13}C NMR (75 MHz, DMSO): 169.1 (phthalimide), 167.7 (**C-9**), 134.3 (**C-12**), 134.2 (phthalimide), 132.5 (phthalimide), 131.4 (**C-10**), 122.9 (**C-11**), 122.8 (phthalimide), 71.2 (Me-O-**C**H_2-), 69.5 (**C-3/4**), 66.8 (**C-6**), 57.9 (**C-1**), 37.0 (**C-7**).

FTIR ν_{max} (cm^{-1}) (solid state): 3287 (m, N-H amide stretch), 3059 (m, [Ar] C-H stretch), 2869 (s, C-H aliphatic stretch), 1709 (s, C=O amide stretch), 1465 (m, C-C stretch), 1088 (s, C-O stretch),.

Preparation adapted from literature.[372] No literature reference was found.

α-Methyl-ω-aminopoly(ethylene glycol) (136)

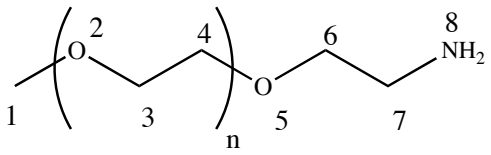

av. RMM = 549 (n = 5 to 16)

Hydrazine monohydrate (0.31 mL; 6.4 mmol) was added to a stirred solution of α-methyl-ω-phthalimidopoly(ethylene glycol) (2.20 g; 3.20 mmol) in methanol (50 mL) and the mixture was allowed to reflux for 72 hrs giving a lime green solution.
The reaction mixture was allowed to cool before the solvent was removed *in vacuo* to give a pale oil. This was dissolved in basic water (40 mL, pH 11, NaOH) and product was extracted with DCM (3 x 50 mL). The organics were combined, dried over Na_2SO_4 and the solvent removed *in vacuo* to give product as a colourless oil (0.78 g; 44%).

MS/ES$^+$ (m/z): 472.3 (100%, n = 9, $[M + H]^+$), n = 5 to 16.

^{1}H NMR (400 MHz, $CDCl_3$): 3.64 (s), 3.63 (s, **H-3/4**), 3.54 (d, J = 5.1), 3.52 (d, J = 4.7), 3.49 (t, J = 5.2, **H-6**), 3.36 (3H, s, **H-1**), 2.85 (2H, t, J = 5.1, **H-7**), 1.50 (2H, s (br), **H-8**).

^{13}C NMR (100 MHz, $CDCl_3$): 73.4 (**C-6**), 71.9 (Me-O-**C**H_2-), 70.5 (**C-3/4**), 70.3 (Me-O-CH_2-**C**H_2-), 59.0 (**C-1**), 41.8 (**C-7**).

FTIR ν_{max} (cm^{-1}) (thin film): 2864 (s (br), C-H aliphatic and N-H amine stretch), 1465 (w, C-C stretch), 1095 (s, C-O stretch).

Preparation adapted from literature.[372]

α-Methyl-ω-isothiocyanatopoly(ethylene glycol) (137)

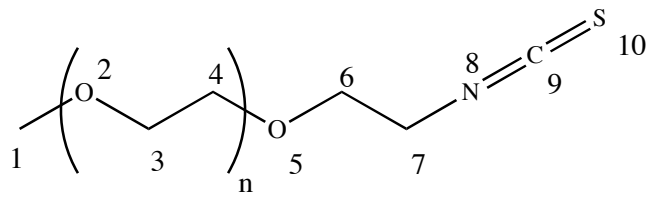

av. RMM = 591 (n = 5 to 16)

Thiophosgene (0.093 mL; 1.2 mmol) and sodium carbonate (0.25 g; 2.4 mmol) were suspended in stirred chloroform (30 mL) under nitrogen over an ice bath. A solution of α-methyl-ω-aminopoly(ethylene glycol) (0.23 g; 0.42 mmol) in chloroform (10 mL) was added dropwise over 1hr before being warmed to RT and stirred for a further 72 hrs.

The chloroform was removed *in vacuo* and the crude product re-dissolved in fresh chloroform (20 mL). The Na_2CO_3 was removed by centrifugation, the chloroform was decanted and solvent was removed *in vacuo* to give product as a yellow oil (0.27 g; 76%).

MS/ES$^+$ (m/z): 536.2 (100%, n = 9, $[M + Na]^+$), n = 5 to 16.

^{1}H NMR (400 MHz, $CDCl_3$): 3.37 (m), 3.64 (s, **H-3/4**), 3.55 (d, J = 4.7), 3.54 (d, J = 4.4), 3.37 (s, **H-1**), 1.78 (s).

^{13}C NMR (100 MHz, $CDCl_3$): 71.9 (Me-O-**C**H_2-), 70.8 (**C-6**), 70.6 (**C-3/4**), 69.3 (Me-O-CH_2-**C**H_2-), 59.0 (**C-1**), 45.2 (**C-7**), 33.0. No C=S signal observed.

FTIR ν_{max} (cm^{-1}) (thin film): 2867 (s (br), C-H aliphatic stretch), 2116 (m, N=C=S stretch), 1453 (w, C-C stretch), 1094 (s, C-O stretch).

No literature reference was found.

4-[EDA]-41-Amine-23-PEG (138)

A solution of α-methyl-ω-isothiocyanatopoly(ethylene glycol) (0.0856 g; 0.143 mmol) in 1,4-dioxane (0.5 mL) was added dropwise to a stirred solution of triethylamine (4 drops) and 4-[EDA]-64-Amine (0.1268 g, 0.00892 mmol) in water (5 mL). The resulting mixture was stirred for 18 hrs.

This solution was purified by dialysis against water for 5 days. The oil obtained was then azeotropically distilled in MeOH/toluene to give product as a viscous orange oil (0.1540 g).

Combustion analysis: C 48.70%, H 7.88%, N 13.69%, S 3.01. N:S ratio suggests 23 PEG groups present.

No literature reference was found.

4-[EDA]-46-Amine-18-PEG (139)

A solution of α-methyl-ω-isothiocyanatopoly(ethylene glycol) (0.1016 g; 0.169 mmol) in 1,4-dioxane (1 mL) was added dropwise to a stirred solution of triethylamine (4 drops) and 4-[EDA]-64-Amine (0.1504 g, 0.0106 mmol) in water (5 mL). The resulting mixture was stirred for 18 hrs.
This solution was purified by dialysis against water for 5 days. The oil obtained was then azeotropically distilled in MeOH/toluene to give product as a viscous orange oil (0.1648 g).

Combustion analysis: C 50.37%, H 8.45%, N 15.07%, S 2.37. N:S ratio suggests 18 PEG groups present.

No literature reference was found.

5-[EDA]-102-Amine-26-PEG (140)

Sample prepared by Dr P. Walker and used with permission.

Combustion analysis: C 51.00%, H 8.47%, N 14.82%, S 1.72. N:S ratio suggests 26 PEG groups present.

No literature reference was found.

5-[EDA]-103-Amine-25-PEG (141)

A solution of α-methyl-ω-isothiocyanatopoly(ethylene glycol) (0.0425 g; 0.071 mmol) in 1,4-dioxane (1 mL) was added dropwise to a stirred solution of triethylamine (4

drops) and 5-[EDA]-128-Amine (0.064 g, 0.002 mmol) in water (5 mL). The resulting mixture was stirred for 18 hrs.

This solution was purified by dialysis against water for 5 days. The oil obtained was then azeotropically distilled in MeOH/toluene to give product as a viscous orange oil (0.030 g).

Combustion analysis: C 49.42%, H 8.13%, N 16.38%, S 1.88. N:S ratio suggests 25 PEG groups present.

No literature reference was found.

5-[EDA]-70-Amine-1-FITC-1-57-PEG (142)

A solution of α-methyl-ω-isothiocyanatopoly(ethylene glycol) (0.062 g; 0.105 mmol) in DMSO (5 mL) was added dropwise to a stirred solution of triethylamine (4 drops) and 5-[EDA]-127-Amine-1-FITC (0.0473 g; 0.00164 mmol) in DMSO (15 mL). The resulting mixture was then stirred for 18 hrs.

The solution obtained was purified by dialysis against water for 3 days. The resulting oil was then azeotropically distilled in MeOH/toluene to give product as a viscous orange oil (0.075 g).

FTIR ν_{max} (cm^{-1}) (thin film): 3271 (s (br), O-H stretch), 2870 (s (br), C-H aliphatic and N-H amine stretch), 1641 (s, C=O amide stretch), 1099 (s, C-O and C=S stretch).

Combustion analysis: C 49.76%, H 8.49%, N 12.81%, S 3.38. N:S ratio suggests 58 sulphur atoms present, therefore 1 FITC and 57 PEG chains.

No literature reference was found.

Preparation of Fluorescent Samples

5-(Dimethylamino)-N-propylnaphthalene-1-sulphonamide (144)

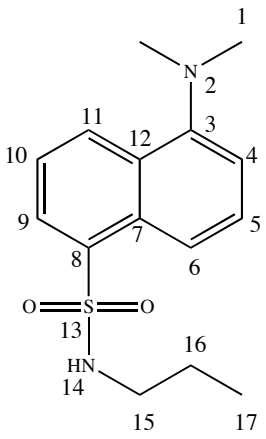

$C_{15}H_{20}N_2O_2S$

RMM = 292.40

1-Propylamine (0.035 mL; 0.41 mmol) was added dropwise to a stirred solution of dansyl chloride (0.100 g; 0.37 mmol) and triethylamine (0.057 mL; 0.41 mmol) in dry DCM (15 mL). The reaction was allowed to reflux under nitrogen for 1 hour, giving a solution colour change from yellow to green.

The solvent was removed and fresh DCM (10 mL) was added. The solution was then washed with sodium bicarbonate (2M, 20 mL) and water (20 mL). The organic phase was dried ($MgSO_4$) and the solvent removed *in vacuo*. The crude material was purified by column chromatography (R_f: 0.19, DCM, silica 60) to give product as a green oil (0.070 g, 65%).

MS/ES$^+$ (m/z): 293.2 (30% $[M + H]^+$), 315.2 (50% $[M + Na]^+$), 607.4 (100% $[2M + Na]^+$).

MS/ES$^+$ (m/z): 291.2 (100% $[M-H]^-$).

^{1}H-NMR (400MHz, $CDCl_3$): 8.54 (1H, d, J = 8.5, **H-11**), 8.29 (1H, d, J = 8.6, **H-6**), 8.25 (1H, dd, J = 7.3, 1.2, **H-9**), 7.54 (2H, m, **H-5/10**), 7.19 (1H, d, J = 7.5, **H-4**), 4.58 (1H, t (br), **H-14**), 2.89 (6H, s, **H-1**), 2.86 (2H, q, J = 6.8, **H-15**), 1.57 (1H, s), 1.41 (2H, sx, J = 7.2, **H-16**), 0.78 (3H, t, J = 7.4, **H-17**).

^{13}C-NMR (100MHz, $CDCl_3$): 152.0 (**C-3**), 134.8 (**C-8**), 130.4 (**C-6**,**10** or **11**), 130.0 (**C-7/12**), 129.6 (**C-6**,**10** or **11**), 128.3 (**C-6**,**10** or **11**), 123.2 (**C-9**), 118.7 (**C-5**), 115.1 (**C-4**), 45.4 (**C-1**), 45.1 (**C-15**), 23.0 (**C-16**), 11.0 (**C-17**).

Procedure adapted from literature.[267] Product consistent with literature.[1]

4-[EDA]-60-Amine-4-Dansyl

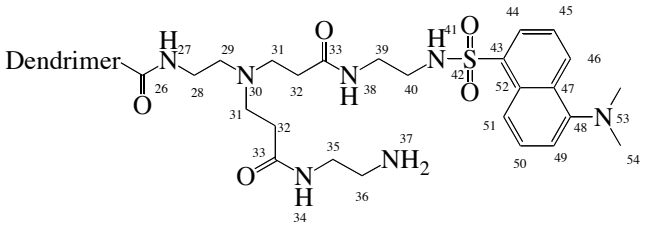

(numbering started at 26 to allow for easy comparison to 4.0-[EDA]-64-Amine)

An aqueous solution (20 mL) of dansyl chloride (0.0076 g; 0.028 mmol) was added dropwise to a stirred solution of 4.0-[EDA]-64-amine (0.100 g; 0.007 mmol) in methanol/water (10/10 mL) over 40 minutes. The pH value of the reaction was kept between 10 and 12 by the addition of NaOH (20 wt%). The reaction was then heated to 35ºC and stirred for 2.5 hrs, before removing the solvents *in vacuo*.

The resulting orange oil/orange solid was dialysed in methanol for 3 days, followed by water for 4 days. The product was the azeotroped (MeOH/toluene) to give a viscous orange oil (0.0715 g, 68%).

^{1}H-NMR (400MHz, D_2O): 8.41-7.25 (4H, dansyl), 4.72 (H_2O), 3.31 (MeOH), 3.26 (s (br), **H-28/35**), 2.77 (36H, s (br), **H-31/36**), 2.57 (10H, s (br), **H-29**), 2.37 (23H, s (br), **H-32**), 1.88 (s (br)), 1.28(1H, d).

^{13}C-NMR (100MHz, D_2O): 175.8 (**C-33**), 175.5 (**C-26**), 175.2 (**C-12/19**), 165.1, 151.7 (**C-48**), 135.2 (**C-43**), [130.7, 129.7, 129.3 (dansyl)], 126.5 (dansyl quarternary), [124.6, 119.8, 116.4 (dansyl)], 69.1, 51.9 (**C-29**), 49.6 (**C-31**), 49.5 (MeOH), 47.8 (G4 defect), 45.7 (**C-54**), 45.0 (G4 defect), 42.4 (**C-40**), 41.0 (**C-35**), 40.6, 40.3 (**C-36**), 39.3, 39.1, 37.4 (**C-28**), 35.9 (G4 defect), 35.1 (**C-39**), 33.4 (**C-32**).

Procedure adapted from literature.[267]

4-[EDA]-63-Amine-1-FITC (145)

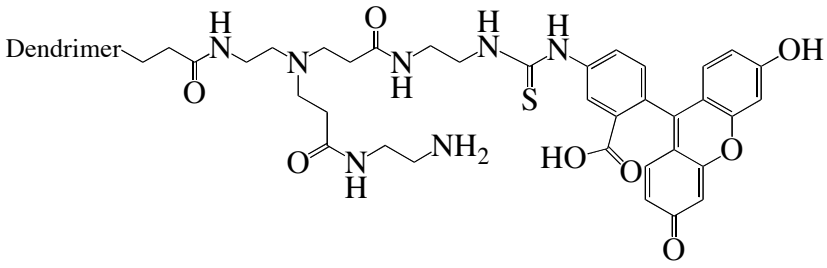

Fluorescein isothiocyanate (0.061 g; 0.0157 mmol) was added portionwise to a stirred solution of 4-[EDA]-64-Amine (0.1113 g; 0.00783 mmol) in DMSO (10 mL). After 18 hrs the reaction was dialysed against water for 24 hrs then MeOH for 48 hrs. The product was then concentrated *in vacuo* to give a viscous orange oil (0.0726 g).

FTIR ν_{max} (cm^{-1}) (thin film): 3273 (s (br), N-H stretch), 3077 (m, N-H amide stretch), 2943 (m, C-H aliphatic stretch), 2849 (m, C-H aliphatic stretch), 1647 (s (br), C=O amide stretch), 1556 (s (br), C-C stretch).

Combustion analysis: C 48.07%, H 7.64%, N 19.92%, S 0.10. N:S ratio suggests only 1 FITC group present.

Procedure adapted from literature.[435]

4-[EDA]-44-Amine-18-PEG-2-FITC (146)

Fluoroscein isothiocyanate (0.0033 g; 0.0084 mmol) was added portionwise to a stirred solution of 4-[EDA]-46-Amine-18-PEG (0.100 g; 0.00420 mmol) in DMSO (7 mL). After 18 hrs the reaction was dialysed against water for 3 days then MeOH for 2 days. The product was concentrated *in vacuo* to give a viscous orange oil (0.0924 g).

FTIR ν_{max} (cm^{-1}) (thin film): 3290 (s (br), N-H stretch), 3078 (m, N-H amide stretch), 2872 (m, C-H aliphatic stretch), 1652 (s (br), C=O amide stretch), 1557 (s (br), C-C stretch), 1103 (s, C-O ether stretch).

Combustion analysis: C 50.14%, H 8.34%, N 14.18%, S 2.48. N:S ratio suggests 20 sulphur atoms present, therefore 2 FITC and 18 PEG chains.

No literature reference was found.

5-[EDA]-126-Amine-2-FITC (147)

Fluorescein isothiocyanate (0.0028 g; 0.00584 mmol) was added portionwise to a stirred solution of 5-[EDA]-128-Amine (0.0421 g; 0.00146 mmol) in DMSO. After 18 hrs the reaction was dialysed against water for 24 hrs then MeOH for 48 hrs. The product was concentrated *in vacuo* to give an orange oil (0.0376 g).

Combustion analysis: C 46.78%, H 7.19%, N 19.07%, S 2.30. N:S ratio suggests 23 FITC groups.

Procedure adapted from literature.[435]

5-[EDA]-127-Amine-1-FITC (132)

Fluorescein isothiocyanate (0.0045g; 0.0116 mmol) was dissolved in DMSO (15 mL) and added dropwise to a solution of 5-[EDA]-128-amine (0.167 g; 0.00578 mmol) in DMSO (15 mL), and the reaction mixture was stirred overnight at room temperature. The resulting solution was purified by dialysis against water for 3 days. The product was azeotropically distilled (MeOH/toluene) to give a bright orange viscous oil (0.1528 g).

Combustion analysis: C 48.95%, H 8.19%, N 20.41%, S 0.1. N:S ratio suggests 1 FITC group present.

Procedure adapted from literature.[435]

5-[EDA]-100-Amine-25-PEG-3-FITC (148)

Fluoroscein isothiocyanate (0.009 g; 0.002 mmol) was added portionwise to a stirred solution of 5-[EDA]-103-Amine-25-PEG (0.032 g; 0.001 mmol) in DMSO (3 mL). After 18 hrs the reaction was dialysed against water for 3 days then MeOH for 2 days. The product was concentrated *in vacuo* to give a viscous orange oil (0.034 g).

Combustion analysis: C 49.50%, H 7.47%, N 16.25%, S 2.08. N:S ratio suggests 25 PEG groups present.

No literature reference was found.

Preparation of Histidine Molecules for Surface Attachment

tert-Butyl 2-aminoethylcarbamate (Boc-EDA, 150)

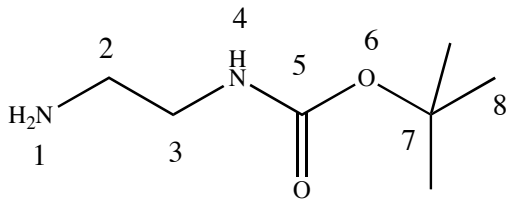

$C_7H_{16}N_2O_2$

RMM = 160.22

A solution of di-tert-butyl dicarbonate (3.27 g; 15 mmol) in DCM (5 mL) was added dropwise over 20 minutes to a stirred solution of ethylenediamine (2 mL; 30 mmol) in DCM (40 mL).

After 2 hrs the resulting solid was removed by filtration and was then washed with DCM. The solvent was removed from the filtrate *in vacuo* to give a colourless oil. Water (20 mL) was added which resulted in the precipitation of a white solid which was removed by filtration. The filtrate was saturated with K_2CO_3 and extracted with diethyl ether (3 x 20 mL), dried over $MgSO_4$ and reduced *in vacuo* to give product as a colourless oil (1.902 g; 79%).

MS/ES$^+$ (m/z): 161.2 (60% $[M + H]^+$).

^{1}H-NMR (400MHz, $CDCl_3$): 4.90 (1H, s (br), **H-4**), 3.52 (2H, q, J = 5.6, **H-3**), 2.78 (2H, t, J = 6.0, **H-2**), 1.43 (9H, s, **H-8**).

^{13}C-NMR (100MHz, $CDCl_3$): 156.2 (**C-5**), 79.2 (**C-7**), 43.4 (**C-3**), 41.9 (**C-2**), 31.2, 28.4 (**C-8**).

Procedure adapted from, and is consistent with, literature.[408,436]

(*S*)-Trityl 4-(2-(*tert*-butoxycarbonylamino)-3-(2-(*tert*-butoxycarbonylamino)ethylamino)-3-oxopropyl)-1*H*-imidazole-1-carboxylate (Boc-His(Trt)-EDA-Boc, 151)

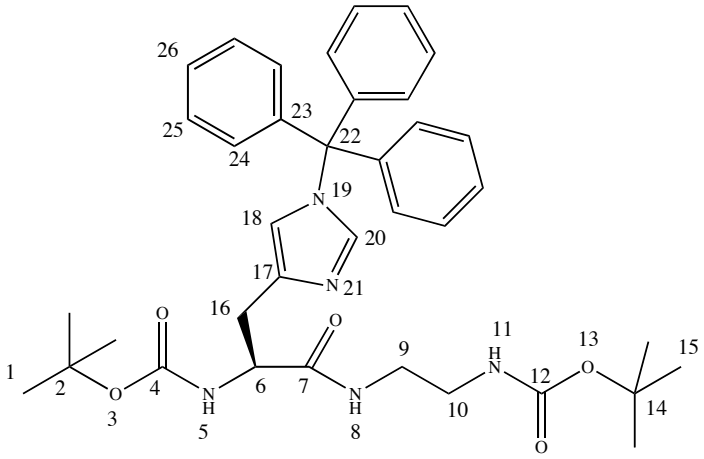

$C_{37}H_{45}N_5O_5$

RMM = 639.79

A solution containing Boc-Hist(Trt)-OH (0.100 g; 0.201 mmol), EDC (0.042 g; 0.221 mmol), HOBt•H_2O (0.034 g; 0.221 mmol) and DIPEA (0.077 mL; 0.442 mmol) in DMF/water (5/1 mL) was made at 0ºC and stirred for 20 minutes. To this was added dropwise a solution of *tert*-butyl 2-aminoethylcarbamate (0.030 g; 0.190 mmol) in DMF (1 mL) and the reaction mixture was stirred for 45 minutes at 0ºC, then at RT for 64 hours.

The solvent was removed *in vacuo* to give a white solid which was dissolved in DCM (15 mL). This solution was then washed with water (2 x 15 mL), HCl (5%, 2 x 15 mL), water (15 mL), sat. $NaHCO_3$ (2 x 15 mL), water (15 mL) and brine (20 mL). The organic phase was dried over Na_2SO_4, and reduced under vacuum to yield product as a pale cream solid. This was further purified by column chromatography (R_f: 0.15, 4% methanol in DCM, silica 60) to give product as a white solid (0.051 g; 42%).

MP: 72 - 74ºC

MS/ES^+ (m/z): 243 (100%), 640 (10% $[M + H]^+$).

^{1}H-NMR (400MHz, $CDCl_3$): 7.39 (1H, s, **H-20**), 7.32 (9H, dd, J = 3.1, 3.1, **H-24/26**), 7.10 (6H, m, **H-25**), 6.89 (1H, s (br), **H-8**), 6.66 (1H, s, **H-18**), 6.13 (1H, s (br), **H-5**), 5.58 (1H, s (br), **H-11**), 4.30 (1H, s (br), **H-6**), 3.38 (1H, s (br), **H-9**), 3.22 (3H, s (br), **H-9/10**), 3.07 (1H, dd, J = 14.8, 4.3, **H-16**), 2.95 (s, DMF), 2.91 (1H, dd, J = 14.8, 6.4, **H-16**), 1.76 (1H, s (br)), 1.43 (9H, s, **H-15**), 1.35 (9H, s, **H-1**).

^{13}C-NMR (100MHz, $CDCl_3$): 172.0 (**C-7**), 156.2 (**C-4**), 155.7 (**C-12**), 142.3 (**C-23**), 138.6 (**C-20**), 136.7 (**C-17**), 129.7 (**C-25**), 128.1 (**C-24/26**), 119.8 (**C-18**), 79.8 (**C-2**), 79.1 (**C-14**), 75.3 (**C-22**), 54.8 (**C-6**), 40.0 (**C-9/10**), 30.5 (**C-16**), 28.4 (**C-1/15**).

No literature reference was found.

Boc-His(Trt)-EDA-Boc (151) 2nd attempt

Procedure: as Boc-His(Trt)-EDA-Boc
Boc-Hist(Trt)-OH (0.100 g; 0.201 mmol)
EDC (0.042 g; 0.221 mmol)
HOBt•H_2O (0.034 g; 0.221 mmol)
DIPEA (0.077 mL; 0.442 mmol)
Boc-EDA (0.030 g; 0.190 mmol)
DCM (6 mL)
Purification: Column chromatography (R_f: 0.22, 5% methanol in DCM, silica 60)
Product: White solid (0.093 g; 76%)

MP: 78 - 82ºC

MS/ES^+ (m/z): 130 (100%), 640 (10% $[M + H]^+$).

HRMS (ES^+): $C_{37}H_{45}N_5NaO_5$ Expected (m/z): 662.3313, Found: 662.3324.

^{1}H-NMR (300MHz, $CDCl_3$): 7.39 (1H, d, J = 1.2, **H-20**), 7.33 (9H, dd, J = 3.1, 3.1, **H-24/26**), 7.10 (6H, m, **H-25**), 6.90 (1H, s (br), **H-8**), 6.65 (1H, s, **H-18**), 6.13 (1H, s (br), **H-5**), 5.59 (1H, s (br), **H-11**), 5.30 (DCM), 4.30 (1H, q (br), **H-6**), 3.38 (1H, s (br), **H-9**), 3.22 (3H, s (br), **H-9/10**), 3.08 (1H, dd, J = 14.8, 4.4, **H-16**), 2.91 (1H, dd, J = 14.8, 6.4, **H-16**), 1.76 (1H, s (br)), 1.43 (9H, s, **H-15**), 1.35 (9H, s, **H-1**).

FTIR ν_{max} (cm^{-1}) (solid state): 3312 (m (br), N-H amide stretch), 2975 (m, C-H aliphatic stretch), 1683 (s (br), C=O carbamate stretch).

Combustion analysis:	Theoretical	C 69.46%, H 7.09%, N 10.94%
	Found	C 69.18%, H 6.96%, N 11.10%

No literature reference was found.

Boc-His(Trt)-EDA-Boc (151) 3rd attempt

Procedure: as Boc-His(Trt)-EDA-Boc
Boc-Hist(Trt)-OH (0.100 g; 0.201 mmol)
HBTU (0.084 g; 0.221 mmol)
HOBt•H_2O (0.034 g; 0.221 mmol)
DIPEA (0.077 mL; 0.442 mmol)
Boc-EDA (0.030 g; 0.190 mmol)
DMF (6 mL)
Purification: Column chromatography (R_f: 0.65, 10% methanol in DCM, silica 60)
Product: White solid (0.101 g; 84%)

MP: 71 - 75ºC

MS/ES^+ (m/z): 130 (80%), 157 (80%), 314 (80%), 640 (100% $[M + H]^+$), 662 (30% $[M + Na]^+$).

^{1}H-NMR (400MHz, $CDCl_3$): 7.39 (1H, s, **H-20**), 7.33 (9H, dd, J = 3.1, 3.1, **H-24/26**), 7.10 (6H, m, **H-25**), 6.89 (1H, s (br), **H-8**), 6.65 (1H, s, **H-18**), 6.13 (1H, s (br), **H-5**), 5.59 (1H, s (br), **H-11**), 4.30 (1H, s (br), **H-6**), 3.38 (1H, s (br), **H-9**), 3.22 (3H, s (br), **H-9/10**), 3.07 (1H, dd, J = 14.8, 4.3, **H-16**), 2.95 (s, DMF), 2.91 (dd, J = 14.8, 6.4, **H-16**), 2.88 (s, DMF), 2.80 (1H, s, $C(O)(N(C\mathbf{H}_3)_2)_2$), 1.82 (1H, s (br)), 1.43 (9H, s, **H-15**), 1.35 (9H, s, **H-1**).

No literature reference was found.

Boc-His(Trt)-EDA-Boc (151) 4th attempt

Procedure: as Boc-His(Trt)-EDA-Boc
Boc-Hist(Trt)-OH (0.100 g; 0.201 mmol)
HBTU (0.084 g; 0.221 mmol)
HOBt•H_2O (0.034 g; 0.221 mmol)
DIPEA (0.077 mL; 0.442 mmol)
Boc-EDA (0.035 g; 0.221 mmol)
DCM (6 mL)
Purification: Column chromatography (R_f: 0.33, 5% methanol in DCM, silica 60)
Product: White solid (0.089 g; 69%)

MP: 75 – 77ºC

MS/ES$^+$ (m/z): 640 (100% $[M + H]^+$), 662 (10% $[M + Na]^+$).

^{1}H-NMR (400MHz, $CDCl_3$): 7.39 (1H, s, **H-20**), 7.33 (9H, dd, J = 3.1, 3.1, **H-24/26**), 7.10 (6H, m, **H-25**), 6.89 (01H, s (br), **H-8**), 6.65 (1H, s, **H-18**), 6.12 (1H, s (br), **H-5**), 5.59 (1H, s (br), **H-11**), 4.30 (1H, s (br), **H-6**), 3.38 (1H, s (br), **H-9**), 3.22 (3H, s (br), **H-9/10**), 3.07 (1H, dd, J = 14.8, 4.2, **H-16**), 2.95 (s, DMF), 2.91 (dd, J = 14.9, 6.4, **H-16**), 2.88 (s, DMF), 1.74 (1H, s (br)), 1.43 (9H, s, **H-15**), 1.35 (9H, s, **H-1**).

No literature reference was found.

(*S*)-*tert*-Butyl 4-(2-(*tert*-butoxycarbonylamino)-3-(2-(*tert*-butoxycarbonylamino)ethylamino)-3-oxopropyl)-1*H*-imidazole-1-carboxylate (Boc-His(Boc)-EDA-Boc, 152)

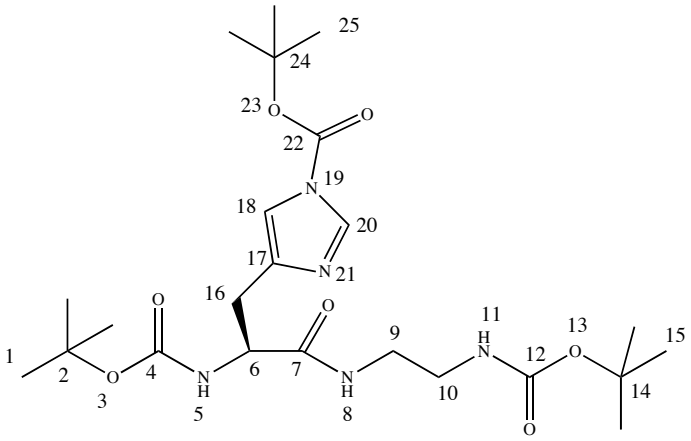

$C_{23}H_{39}N_5O_7$

RMM = 497.59

A solution containing Boc-Hist(Boc)-OH (0.100 g; 0.186 mmol), EDC (0.039 g; 0.205 mmol), HOBt•H_2O (0.031 g; 0.205 mmol) and DIPEA (0.11 mL; 0.615 mmol) in DMF (5 mL) was prepared at 0ºC and stirred for 20 minutes. To this was added dropwise a solution of *tert*-butyl 2-aminoethylcarbamate (0.028 g; 0.176 mmol) in DMF (1 mL) and the reaction mixture stirred for 45 minutes at 0ºC, then at RT for 18 hours to give a colourless solution and white solid.

The solvents were removed and the resulting material was dissolved in DCM (6 mL), any residual solid being collected by filtration. The filtrate was then washed with water

(2 x 15 mL), HCl (5%, 2 x 15 mL), sat. $NaHCO_3$ (2 x 15 mL), and water (15 mL). The organic phase was dried over Na_2SO_4, and reduced under vacuum to yield product as a white solid. This was further purified by column chromatography (R_f: 0.28, 5% methanol in DCM, silica 60) to give product as a white solid (0.045 g; 52%).

MP: 60 - 62ºC

MS/ES$^+$ (m/z): 498 (20% $[M + H]^+$), 520 (100% $[M + Na]^+$), 1018 (30% $[2M + Na]^+$).

^{1}H-NMR (400MHz, $CDCl_3$): 8.02 (1H, s, **H-20**), 7.18 (1H, s, **H-18**), 6.87 (1H, s (br), **H-8**), 5.91 (1H, s (br), **H-5**), 5.46 (1H, s (br), **H-11**), 5.29 (DCM), 4.35 (1H, q (br), **H-6**), 3.35 (1H, s (br), **H-9**), 3.24 (3H, s (br), **H-9/10**), 3.09 (1 H, dd, J = 14.9, 4.9, **H-16**), 2.95 (DMF), 2.95 (1H, dd, J = 14.8, 5.9, **H-16**), 2.88 (DMF), 1.83 (1H, s), 1.60 (9H, s, **H-25**), 1.44 (s, **H-15**), 1.44 (s, **H-1**).

^{13}C-NMR (100MHz, $CDCl_3$): 171.7 (**C-7**), 156.2 (**C-4**), 155.6 (**C-12**), 146.8 (**C-22**), 138.9 (**C-17**), 136.9 (**C-20**), 114.9 (**C-18**), 85.7 (**C-24**), 80.1 (**C-2**), 79.3 (**C-14**), 77.2, 54.3 (**C-6**), 40.0 (**C-9/10**), 30.3 (**C-16**), 28.4 (**C-15**), 28.3 (**C-1**), 27.9 (**C-25**).

No literature reference was found.

Boc-His(Boc)-EDA-Boc (152) 2nd attempt

Procedure: as Boc-His(Boc)-EDA-Boc
Boc-Hist(Boc)-OH (0.100 g; 0.186 mmol)
EDC (0.039 g; 0.205 mmol)
HOBt•H_2O (0.031 g; 0.205 mmol)
DIPEA (0.11 mL; 0.615 mmol)
Boc-EDA (0.028 g; 0.176 mmol)
DCM (6 mL)
Purification: Column chromatography (R_f: 0.28, 5% methanol in DCM, silica 60)
Product: White solid (0.066 g; 75%)

MP: 61 - 62ºC

MS/ES$^+$ (m/z): 498 (10% $[M + H]^+$), 520 (100% $[M + Na]^+$), 1018 (50% $[2M + Na]^+$).

HRMS (ES^+): $C_{23}H_{39}N_5NaO_7$ Expected (m/z): 520.2742, Found: 520.2736.

^{1}H-NMR (400MHz, $CDCl_3$): 8.02 (1H, s, **H-20**), 7.18 (1H, s, **H-18**), 6.89 (1H, s (br), **H-8**), 5.91 (1H, s (br), **H-5**), 5.47 (1H, s (br), **H-11**), 5.29 (DCM), 4.35 (1H, q (br), **H-6**), 3.35 (1H, s (br), **H-9**), 3.24 (3H, s (br), **H-9/10**), 3.08 (1H, dd, J = 14.9, 4.9, **H-16**), 2.94 (1H, dd, J = 14.9, 5.9, **H-16**), 1.59 (9H, s, **H-25**), 1.44 (s, **H-15**), 1.43 (s, **H-1**).

FTIR ν_{max} (cm^{-1}) (solid state): 3292 (m (br), N-H amide stretch), 2977 (m, C-H aliphatic stretch), 1755 (s, C=O amide stretch), 1693 (s, C=O carbamate stretch), 1659 (s, C=O carbamate stretch).

Combustion analysis:	Theoretical	C 55.52%, H 7.90%, N 14.07%
	Found	C 55.76%, H 7.66%, N 13.40%

No literature reference was found.

Boc-His(Boc)-EDA-Boc (152) 3rd attempt

Procedure: as Boc-His(Boc)-EDA-Boc
Boc-Hist(Boc)-OH (0.100 g; 0.186 mmol)
HBTU (0.078 g; 0.205 mmol)
HOBt•H_2O (0.031 g; 0.205 mmol)
DIPEA (0.11 mL; 0.615 mmol)
Boc-EDA (0.028 g; 0.176 mmol)
DMF (6 mL)
Purification: Column chromatography (R_f: 0.21, 5% methanol in DCM, silica 60)
Product: Yellow solid (impure) (0.053 g; 61%)

MP: 45 - 47ºC

MS/ES$^+$ (m/z): 498 (10% $[M + H]^+$), 520 (100% $[M + Na]^+$), 1018 (20% $[2M + Na]^+$).

^{1}H-NMR (300MHz, $CDCl_3$): 8.02 (1H, s, **H-20**), 7.69 (dd, J = 5.7, 3.3, trace HOBt), 7.51 (dd, J = 5.7, 3.3, trace HOBt), 7.18 (1H, s, **H-18**), 6.89 (1H, s (br), **H-8**), 5.91 (1H, s (br), **H-5**), 5.48 (1H, s(br), **H-11**), 5.29 (DCM), 4.34 (1H, q (br), **H-6**), 4.21 (1H, t, J = 5.7), 3.35 (1H, s (br), **H-9**), 3.24 (3H, s (br), **H-9/10**), 3.08 (1H, dd, J = 14.7, 4.9, **H-16**), 2.95 (1H, dd, J = 14.5, 5.9, **H-16**), 2.94 (DMF), 2.87 (DMF), 2.79 (1H, s, $C(O)(N(C\mathbf{H}_3)_2)_2$), 1.59 (9H, s, **H-25**), 1.44 (s, **H-15**), 1.43 (s, **H-1**).

No literature reference was found.

Boc-His(Boc)-EDA-Boc (152) 4th attempt

Procedure: as Boc-His(Boc)-EDA-Boc
Boc-Hist(Boc)-OH (0.100 g; 0.186 mmol)
HBTU (0.078 g; 0.205 mmol)
HOBt•H_2O (0.031 g; 0.205 mmol)
DIPEA (0.11 mL; 0.615 mmol)
Boc-EDA (0.028 g; 0.176 mmol)
DCM (6 mL)
Purification: Column chromatography (R_f: 0.24, 5% methanol in DCM, silica 60)
Product: White solid (0.041 g; 48%)

MP: 60 - 62ºC

MS/ES$^+$ (m/z): 498 (10%, $[M + H]^+$), 520 (100% $[M + Na]^+$), 1018 (50% $[2M + Na]^+$).

^{1}H-NMR (300MHz, $CDCl_3$): 8.02 (1H, s, **H-20**), 7.18 (1H, s, **H-18**), 6.87 (1H, s (br), **H-8**), 5.91 (1H, s (br), **H-5**), 5.48 (1H, s (br), **H-11**), 5.29 (DCM), 4.35 (1H, q (br), **H-6**), 3.35 (1H, s (br), **H-9**), 3.24 (3H, s (br), **H-9/10**), 3.09 (1H, dd, J = 14.9, 4.9, **H-16**), 2.95 (1H, dd, J = 14.9, 5.9, **H-16**), 2.79 (1H, s, $C(O)(N(C\mathbf{H}_3)_2)_2$), 1.87 (1H, s), 1.59 (9H, s, **H-25**), 1.44 (s, **H-15**), 1.43 (s, **H-1**).

No literature reference was found.

Preparation of Dendrimers with a Histidine Surface

4.0-[EDA]-64-(Boc-His(Boc)) (153)

A solution containing Boc-His(Boc)-OH (0.302 g; 0.562 mmol), HBTU (0.298 g; 0.786 mmol), HOBt•H_2O (0.120 g; 0.786 mmol) and DIPEA (0.32 mL; 1.887 mmol) in DMF/DCM (10/2 mL) was made at 0ºC and stirred for 20 minutes. To this was added dropwise a solution of 4.0-[EDA]-64-Amine (0.083 g; 0.0058 mmol) in DMF (2 mL) and the reaction stirred for 40 minutes at 0ºC, and then at RT for 64 hours. The solution turned from yellow to brown over the first 5 hours, and a precipitate formed after a further 13 hours. The solvent was removed *in vacuo* to give a brown oil/solid. Chloroform was added to partially dissolve the mixture and this was dialysed against chloroform for 1 day, which resulted in no change. Ethanol was added which gave a brown solution and a brown oil/solid. These were separated by centrifugation. The solution was reduced *in vacuo* to give a brown oil, NMR data shows that no dendrimer is present but that the coupling by-product (1,1,3,3-tetramethylurea) is. The NMR spectrum of the solid material is inconclusive as this is only partially soluble in DMSO-d_6.

4.0-[EDA]-59-Amine-5-(Boc-His(Boc)) (154)

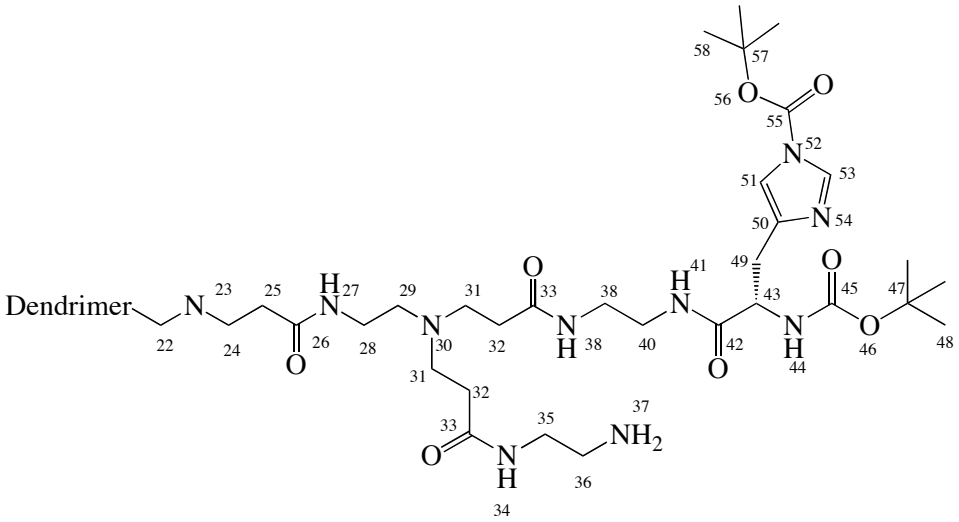

(numbering started at 26 to allow for easy comparison to 4.0-[EDA]-64-Amine)

A solution containing Boc-His(Boc)-OH dicyclohexylamine salt (0.0132 g; 0.247 mmol), HBTU (0.0131 g; 0.0345 mmol), HOBt•H_2O (0.0053 g; 0.0345 mmol) and DIPEA (0.014 mL; 0.0828 mmol) in DMF (5 mL) was made at 0ºC and stirred for 20 minutes. To this was added dropwise a solution of 4-[EDA]-64-Amine (0.0438 g; 0.0031 mmol) in DMF/water (5/2 mL) and the reaction mixture stirred for 40 minutes at 0ºC, then at RT for 18 hours.

The solvents were removed and the resulting yellow oil was dissolved in methanol and the solution dialysed for 1 day against water followed by 3 days against methanol. The product was then reduced to give an orange oil (0.0478 g). Calculated surface coverage: 5 groups by ^{1}H NMR.

^{1}H-NMR (400MHz, MeOD): 8.10 (1H, s(br), **H-53**), 7.68 (s (br)), 7.62 (s (br)), 7.27 (1H, s (br)), 6.88 (1H, s (br), **H-51**), 3.35 (MeOH), 3.26 (s (br), **H-14/21/28/35**), 2.97 (2H, s (br), **H-36**), 2.89 (s (br)), 2.78 (s (br), **H-17/24/31**), 2.57 (10H, s (br), **H-15/22/29**), 2.37 (21H, s (br), **H-18/25/32**), 1.60 (1H, s (br)), 1.38 (7H, s (br), **H-48/58**).

^{13}C-NMR: (100MHz, MeOD) 175.5 (C=O), 175.1 (C=O), 174.6 (C=O), 164.2, 157.6 (**C-45**), 136.4 (**C-50**), 125.2, 125.0, 118.9 (**C-51**), 112.6, 80.7 (**C-57**), 56.4 (**C-43**), 53.5 (**C-15/22/29**), 51.1 (**C-17/24/31**), 41.7, 41.2, 40.2 (**C-39/40**), 38.7 (**C-14/21/28**), 34.9 (**C-18/25/32**), 31.0 (**C-49**), 28.8 (**C-48/49**), 28.2.

No literature reference was found.

4.0-[EDA]-55-Amine-9-(Boc-His(Boc)) (155)

Procedure: as 4.0-[EDA]-56-Amine-8-(Boc-His(Boc))
Boc-His(Boc)-OH dicyclohexylamine salt (0.0299 g; 0.0558 mmol)
HBTU (0.0296 g; 0.0782 mmol)
HOBt•H_2O (0.0120 g; 0.0782 mmol)
DIPEA (0.033 mL; 0.188 mmol)
4-[EDA]-64-Amine (0.0496 g; 0.00349 mmol)
DMF/water (10/2 mL)
Product: viscous orange oil (0.0586 g)
Calculated surface coverage: 9 groups by ^{1}H NMR

^{1}H-NMR: (400MHz, MeOD) 8.10 (1H, s (br), **H-53**), 7.68 (s (br)), 7.63 (s (br)), 7.27 (1H, s (br)), 6.88 (1H, s (br), **H-51**), 3.42 (4H, s (br)), 3.35 (MeOH), 3.26 (s (br), **H-14/21/28/35**), 2.98 (7H, s (br), **H-36**), 2.78 (18H, s (br), **H-17/24/31**), 2.57 (10H, s (br), **H-15/22/29**), 2.37 (18H, s (br), **H-18/25/32**), 1.60 (1H, s (br)), 1.38 (12H, s (br), **H-48/58**).

^{13}C NMR (inverse-gated decoupled, MeOD): 175.8 (C=O), 175.1 (C=O), 174.8 (C=O), 164.3, 163.3, 158.5 (4C, **C-45**), 157.7, 144.6 (**C-55**), 136.4 (**C-50**), 134.8 (**C-53**), 128.9, 125.3, 118.9 (10C, **C-51**), 112.6, 80.7 (**C-57**), 80.2 (**C-47**), 56.5 (**C-43**), 53.4 (**C-15/22/29**), 51.1 (**C-17/24/31**), 46.0, 41.4, 40.1 (**C-39/40**), 38.6 (**C-14/21/28**), 34.7 (100C, **C-18/25/32**), 31.0 (7C, **C-49**), 28.8 (41C, **C-48/49**).

No literature reference was found.

4.0-[EDA]-53-Amine-11-(Boc-His(Boc)) (156)

Procedure: as 4.0-[EDA]-56-Amine-8-(Boc-His(Boc))
Boc-His(Boc)-OH dicyclohexylamine salt (0.0301 g; 0.0561 mmol),
HBTU (0.0298 g; 0.0785 mmol),
HOBt•H_2O (0.0120 g; 0.0782 mmol)
DIPEA (0.033 mL; 0.188 mmol)
4-[EDA]-64-Amine (0.0498 g; 0.00350 mmol)
DMSO (10 mL)
Product: viscous orange oil (0.0332 g)
Calculated surface coverage: 11 groups by ^{1}H NMR

^{1}H-NMR (400MHz, MeOD): 8.11 (1H, s (br), **H-53**), 7.62 (1H, s (br)), 7.30 (1H, s (br)), 6.88 (1H, s (br), **H-51**), 4.26 (2H, s (br)), 3.35 (MeOH), 3.27 (s (br), **H-14/21/28/35**), 3.00 (s (br), **H-36**), 2.89 (s (br)), 2.79 (s (br), **H-17/24/31**), 2.59 (10H, s (br), **H-15/22/29**), 2.37 (21H, s (br), **H-18/25/32**), 1.61 (3H, s (br)), 1.38 (16H, s (br), **H-48/58**).

^{13}C-NMR (400MHz, MeOD): 175.4 (C=O), 175.1 (C=O), 174.6 (C=O), 164.1, 157.5 (**C-45**), 148.1, 138.2, 136.4 (**C-50**), 118.4 (**C-51**), 116.2, 87.2, 80.7 (**C-57**), 56.4 (**C-43**), 53.5 (**C-15/22/29**), 51.1 (**C-17/24/31**), 49.9, 41.7, 41.0, 40.2 (**C-39/40**), 40.0, 38.7 (**C-14/21/28**), 34.8 (**C-18/25/32**), 31.0 (**C-49**), 28.8 (**C-48/49**), 28.2.

FTIR ν_{max} (cm^{-1}) (thin film): 3291 (s (br), N-H stretch), 3080 (m, N-H amide stretch), 2942 (m, C-H aliphatic stretch), 2842 (m, C-H aliphatic stretch), 1646 (s (br), C=O amide stretch), 1541 (s (br), C-C stretch).

No literature reference was found.

4.0-[EDA]-56-Amine-8-(Cbz-His) (159)

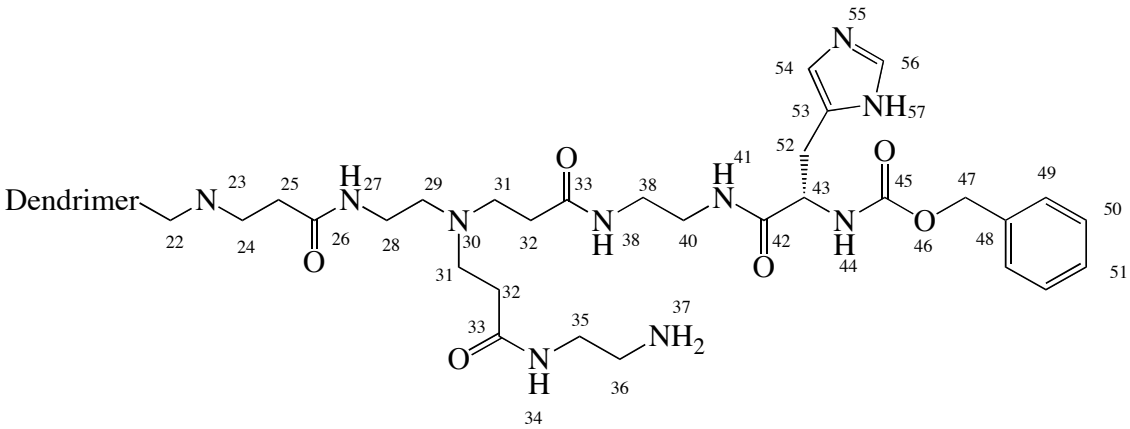

(numbering started at 26 to allow for easy comparison to 4.0-[EDA]-64-Amine)

Procedure: as 4.0-[EDA]-56-Amine-8-(Boc-His(Boc))

Cbz-His-OH (0.0179 g; 0.0619 mmol),

HBTU (0.0329 g; 0.0867 mmol),

HOBt•H_2O (0.0133 g; 0.0867 mmol)

DIPEA (0.022 mL; 0.124 mmol)

4-[EDA]-64-Amine (0.110 g; 7.70 μmol)

DMF/water (25/3 mL)

Product: viscous orange oil (0.0849 g)

Calculated surface coverage: 7 groups by ^{1}H NMR

^{1}H-NMR (400MHz, MeOD): 8.10 (s), 7.68 (m), 7.32 (m), 7.27 (m), 4.82 (MeOH), 3.35 (MeOH), 3.23 (s (br)), 2.99 (5H, s (br)), 2.79 (22H, s (br)), 2.58 (10H, s (br)), 2.37 (24H, s (br)), 1.32 (3H, m).

^{13}C-NMR (400MHz, MeOD): 175.2 (C=O), 174.7 (C=O), 164.2, 164.0, 128.9 (Cbz), 128.8(Cbz), 125.1(Cbz), 124.9(Cbz), 118.8 (**C-54**), 112.6, 53.5 (**C-15/22/29**), 51.2 (**C-17/24/31**), 49.9, 46.4, 41.9, 40.3 (**C-39/40**), 40.0, 38.7 (**C-14/21/28**), 34.8 (**C-18/25/32**), 21.8.

No literature reference was found.

4.0-[EDA]-56-Amine-8-Histidine (160)

Palladium on carbon (0.015 g) was added to a stirred solution of 4.0-[EDA]-56-Amine-8-(CBZ-His) (0.0849 g) in dry ethanol (20 mL). The reaction flask was repeatedly (x 3) flushed with nitrogen and then purged under vacuum. Once under vacuum, a balloon containing hydrogen was connected to the flask and the reaction mixture was stirred under hydrogen for 2 days.

The palladium on carbon was removed by filtration and the filtrate dialysed against methanol for 5 days. The product was reduced to give a viscous orange oil (0.0465 g).

^{1}H-NMR (400MHz, D_2O): 8.10 (6H, s), 7.97 (2H, s), 7.79 (3H, s), 7.68 (4H, s), 7.40 (s (br)), 7.32 (s, br)), 6.95 (2H, s), 3.37, 3.32, 2.97, 2.82, 2.63, 2.43, 1.35 (10H, d, J = 6.9).

^{13}C-NMR (400MHz, D_2O): 174.9 (C=O), 51.6 (**C-17/24/31**), 49.4, 40.0, 37.1, 33.1. All broad.

FTIR ν_{max} (cm^{-1}) (thin film): 3272 (s (br), N-H stretch), 3078 (m, N-H amide stretch), 2942 (m, C-H aliphatic stretch), 2844 (m, C-H aliphatic stretch), 1633 (s (br), C=O amide stretch), 1548 (s (br), C-C stretch).

No literature reference was found.

tert-Butyl 2-(((9*H*-fluoren-9-yl)methoxy)carbonylamino)ethylcarbamate (Boc-EDA-Fmoc, 161)

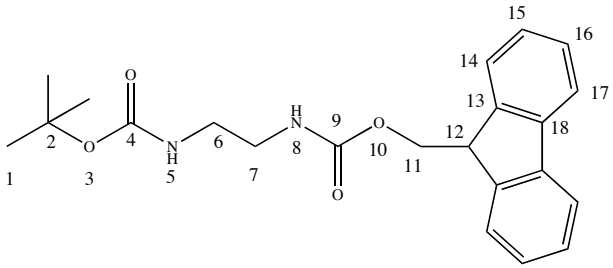

$C_{22}H_{26}N_2O_4$

RMM = 382.46

tert-Butyl 2-aminoethylcarbamate (1.891 g; 11.8 mol) was dissolved in water (15 mL) and the pH of the solution adjusted to 9 – 9.5 using 1M NaOH. A solution of Fmoc-O-succinamide (3.982 g; 11.8 mol) in acetonitrile (25 mL) was added to the stirred solution in one portion and this was then left for 1 hr.

The resulting precipitate was collected by filtration, washing with water the acetonitrile. The product was then dissolved in chloroform (8 mL) and azeotropically distilled with methanol/toluene. Product was obtained as a white powder was dried in a desicator for 48 hrs (3.206 g; 71%).

MP: 135 – 137 ºC (lit. 155 – 156ºC)

MS/ES$^+$ (m/z): 405 (100% $[M + Na]^+$), 787 (70% $[2M + Na]^+$).

^{1}H-NMR (300MHz, $CDCl_3$): 7.76 (2H, d, J = 7.5, **H-17**), 7.59 (2H, d, J = 7.4, **H-14**), 7.40 (2H, t, J = 7.4, **H-16**), 7.31 (2H, t, J = 7.3, **H-15**), 5.20 (1H, s (br), **H-8**), 4.80 (1H, s (br), **H-5**), 4.41 (2H, d, J = 9.7, **H-11**), 4.21 (1H, t, J = 6.7, **H-12**), 3.28 (4H, s (br), **H-6/7**), 1.45 (9H, s, **H-1**).

^{13}C-NMR (75MHz, $CDCl_3$): 156.7 (**C-9**), 156.4 (**C-4**), 143.9 (**C-13**), 141.3 (**C-18**), 127.7 (**C-16**), 127.0 (**C-15**), 125.0 (**C-14**), 119.9 (**C-17**), 79.7 (**C-2**), 66.7 (**C-11**), 47.3 (**C-12**), 41.6 (**C-6**), 40.5 (**C-7**), 28.4 (**C-1**).

Procedure adapted from, and is mostly consistent with, literature.[408]

(9*H*-Fluoren-9-yl)methyl 2-aminoethylcarbamate hydrochloride (Fmoc-EDA•HCl, 162)

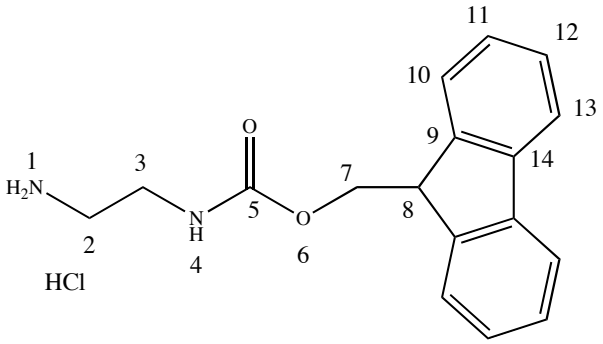

$C_{17}H_{19}ClN_2O_2$

RMM = 318.89

tert-Butyl 2-(((9*H*-fluoren-9-yl)methoxy)carbonylamino)ethylcarbamate (1.305 g; 3.42 mmol) was added to methanol/conc HCl (1:1, 40 mL). The mixture was stirred at reflux for 18 hrs under nitrogen. The reaction was allowed to cool, upon which a white solid formed.

The solvents were removed *in vacuo* and the solid was collected by filtration, and washed with water. The product was the crystallised from hot methanol and diethyl ether to give white needles (1.0142 g; 93%).

MP: 123 – 125ºC (no lit. mp found)

MS/ES$^+$ (m/z): 283 (100% $[M - HCl + H]^+$).

^{1}H-NMR: (300MHz, DMSO) 8.10 (3H, s, **H-1**), 7.89 (2H, d, J = 7.4, **H-13**), 7.70 (2H, d, J = 7.4, **H-10**), 7.50 (1H, t, J = 5.3, **H-4**), 7.41 (2H, t, J = 7.1, **H-12**), 7.33 (2H, t, J = 8.1, **H-11**), 4.33 (2H, d, J = 6.8, **H-7**), 4.22 (1H, t, J = 6.4, **H-8**), 3.26 (2H, dt, J = 6.4, 6.0, **H-3**), 2.84 (2H, t, J = 6.3, **H-2**).

^{13}C-NMR: (75MHz, DMSO) 156.2 (**C-5**), 143.7 (**C-9**), 140.6 (**C-14**), 127.5 (**C-12**), 127.0 (**C-11**), 125.1 (**C-10**), 120.0 (**C-13**), 65.5 (**C-7**), 46.6 (**C-8**), 38.5 (**C-2**), 38.0 (**C-3**).

FTIR ν_{max} (cm^{-1}): 3379 (s (br), N-H amide stretch), 2927 (m, (br) C-H aliphatic stretch), (solid state) 1690 (s, C=O carbamate stretch).

Combustion:	Theoretical	C 64.05%, H 6.01%, N 8.78%
analysis	Found	C 60.31%, H 6.38%, N 8.40%

Procedure adapted from, and is consistent with, literature.[408,409]

(*S*)-*tert*-Butyl 4-(3-(2-(((9*H*-fluoren-9-yl)methoxy)carbonylamino)ethylamino)-2-(*tert*-butoxycarbonylamino)-3-oxopropyl)-1*H*-imidazole-1-carboxylate (Boc-His(Boc)-EDA-Fmoc, 163)

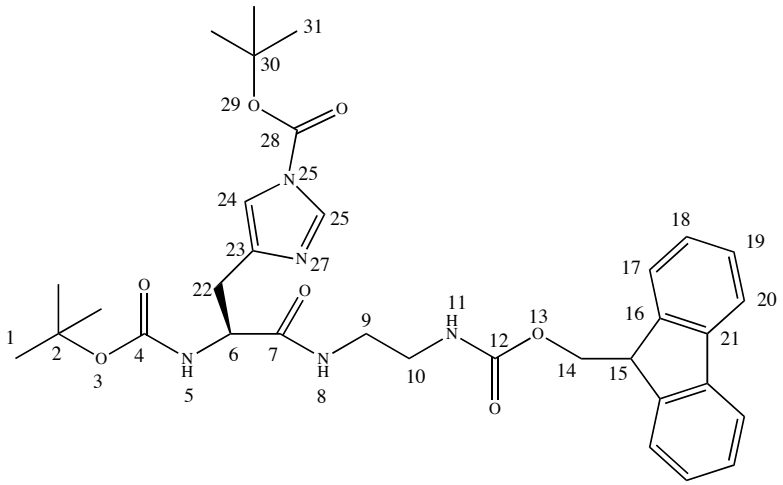

$C_{33}H_{41}N_5O_7$

RMM = 619.71

A solution containing Boc-Hist(Boc)-OH dicyclohexylamine salt (0.250 g; 0.503 mmol), HBTU (0.210 g; 0.708 mmol), HOBt•H_2O (0.854 g; 0.708 mmol) and DIPEA (0.288 mL; 1.658 mmol) in DCM (12 mL) was prepared at 0ºC and stirred for 45 minutes. To this was added dropwise a solution of (9*H*-fluoren-9-yl)methyl 2-aminoethylcarbamate hydrochloride (0.156 g; 0.490 mmol) in DCM (3 mL) and the reaction stirred for 20 minutes at 0ºC, then at RT for 18 hours.

The solvent was removed *in vacuo* to give a white solid. DCM (15 mL) was added and the resulting solution was then washed with water (2 x 15 mL), HCl (5%, 2 x 15 mL), water (15 mL), sat. $NaHCO_3$ (2 x 15 mL), water (15 mL) and brine (20 mL). The

organic phase was reduced *in vacuo* and the resulting colourless oil was dissolved in methanol (4 mL). A white precipitate formed upon addition of water that was collected by filtration and then partitioned between DCM (15 mL) and water (15 mL). The organic phase was washed with water (15 mL) and brine (15 mL), dried over Na_2SO_4, and reduced under vacuum to give crude product as an off-white solid. The product was further purified by column chromatography (R_f: 0.27, 5% methanol in DCM, silica 60) to give product as a white solid (0.257 g; 89%).

MP: 99 – 100ºC

MS/ES$^+$ (m/z): 620 (20% $[M + H]^+$), 642 (100% $[M + Na]^+$).

^{1}H-NMR (300MHz, $CDCl_3$): 7.92 (1H, s, **H-25**), 7.77 (2H, d, J = 7.5, **H-20**), 7.58 (2H, d (br), J = 7.4, **H-17**), 7.37 (2H, t, J = 5.9, **H-19**), 7.29 (t, J = 7.3, **H-18**), 7.17 (1H, s, **H-24**), 6.67 (1H, s, **H-8**), 6.05 (1H, s, **H-11**), 5.90 (1H, s, **H-5**), 5.30 (DCM), 4.39 (3H, q (br), **H-6/14**), 4.21 (1H, t, J = 6.8, **H-15**), 3.30 (4H, s (br), **H-9/10**), 3.08 (1H, dd, J = 14.9, 4.7, **H-22**), 2.99 (1H, dd, J = 14.9, 6.1, **H-22**), 2.80 (3H, s, C(O)(N(C**H**$_3$)$_2$)), 1.72 (1H, s), 1.55 (9H, s, **H-31**), 1.46 (9H, s, **H-1**).

^{13}C-NMR (75MHz, $CDCl_3$): 171.8 (**C-7**), 156.6 (**C-4**), 155.6 (**C-12**), 143.9 (**C-16**), 141.3 (**C-21**), 138.6 (**C-25**), 136.9 (**C-23**), 127.6 (**C-19**), 127.0 (**C-18**), 125.2 (**C-17**), 119.9 (**C-20**), 115.0 (**C-24**), 85.8 (**C-30**), 66.5 (**C-14**), 54.1 (**C-6**), 53.4 (DCM), 52.4, 47.4, 40.3 (**C-9**), 39.7 (**C-10**), 38.6 (C(O)(N(**C**H$_3$)$_2$)), 30.4 (**C-22**), 28.3 (**C-31**), 27.8 (**C-1**).

FTIR ν_{max} (cm^{-1}) (solid state): 3304 (m (br), N-H amide stretch), 2976 (m, C-H aliphatic stretch), 2930 (m, C-H aliphatic stretch) 1754 (s, C=O amide stretch), 1694 (s, C=O carbamate stretch), 1659 (s, C=O carbamate stretch).

Combustion analysis:	Theoretical	C 63.96%, H 6.67%, N 11.30%
	Found	C 63.20%, H 6.78%, N 11.28%

No literature reference was found.

Boc-His(Boc)-EDA-Fmoc (163) 2nd attempt

Procedure: as Boc-His(Boc)-EDA-Fmoc

Boc-Hist(Boc)-OH (0.108 g; 0.201 mmol)

EDCI (0.042 g; 0.221 mmol)

HOBt•H_2O (0.034 g; 0.221 mmol)

DIPEA (0.12 mL; 0.663 mmol)

Fmoc-EDA•HCl (0.0637 g; 0.200 mmol)

DCM (6 mL)

Purification: Column chromatography (R_f: 0.33, 5% methanol in DCM, silica 60)

Product: White solid (0.0117 g; 9%)

MS/ES^+ $_{(m/z)}$: 642.1 (100% $[M + Na]^+$).

^1H and ^{13}C-NMR show product heavily contaminated with HOBt.

Preparation of Click-Histidine related Dendrimer Attachments

tert-Butyl 2-aminopropylcarbamate (171)

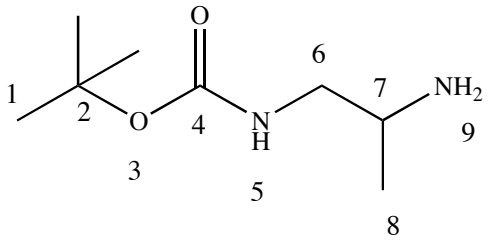

$C_8H_{18}N_2O_2$

RMM = 174.24

A solution of di-tert-butyl dicarbonate (3.84 g; 17.6 mmol) in dry DCM (30 mL) was added dropwise over 40 minutes to a stirred solution of 1,2-diaminopropane (2.25 mL; 26.4 mmol) in dry DCM (170 mL).

After 4 hrs the resulting solid was removed by filtration and washed with DCM. The solvent was removed from the filtrate *in vacuo* to give a colourless oil. Water (20 mL) was added which resulted in the precipitation of a white solid which was removed by filtration. The filtrate was saturated with K_2CO_3 and extracted with diethyl ehter (3 x 20 mL). The combined extracts were dried over $MgSO_4$ and reduced *in vacuo* to give product as a colourless oil (1.35 g; 44%).

MS/ES$^+$ (m/z): 175.3 (100% $[M + H]^+$), 197.3 (20% $[M + Na)^+$).

^{1}H-NMR (400MHz, $CDCl_3$): 4.92 (1H, s (br), **H-5**), 3.11 (1H, m, **H-7**), 2.99 (1H, m, **H-6**), 2.86 (1H, m, **H-6**), 2.72 (trace regio-isomer), 2.60 (trace regio-isomer), 1.43 (9H, s, **H-1**), 1.10 (trace regio-isomer), 1.05 (3H, d, J = 6.3, **H-8**).

^{13}C-NMR (100MHz, $CDCl_3$): 156.2 (**C-4**), 79.1 (**C-2**), 48.5 (**C-6**), 46.9 (**C-7**), 28.4 (**C-1**), 21.5 (**C-8**).

Procedure adapted from, and is consistent with, literature.[407]

tert-Butyl 2-(N,N-di(prop-2-ynyl))aminopropylcarbamate (172)

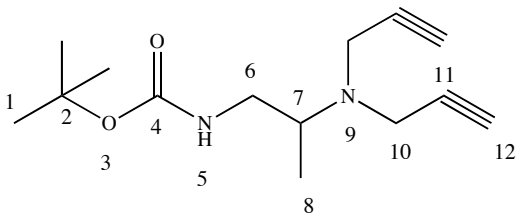

$C_{14}H_{22}N_2O_2$

RMM = 250.34

Propargyl chloride (0.64 mL; 8.90 mmol) was added to a stirred solution of sodium iodide (1.459 g; 7.727 mmol) in dry acetone (10 mL) and the mixture was allowed to stir for 1 hr. K_2CO_3 (0.672 g; 4.870 mmol) was added to the mixture, followed by *tert*-butyl 2-aminopropylcarbamat**e** (0.705 g; 4.052 mmol) in dry acetone (10 mL).
After stirring for 72 hrs the solvent was removed and the resulting solid partitioned between DCM and water (20 mL each). The organic phase was then washed with water

(20 mL), sat. $NaHCO_3$ (2 x 20 mL) and brine (20 mL). The DCM was dried over $MgSO_4$ and reduced to give a brown oil. The crude product was purified by column chromatography (R_f: 0.18, 15% ethyl acetate in petrol (40/60), silica 60) to give product as a colourless oil (0.308 g, 30%)

MS/ES^+ (m/z): 251.2 (40% $[M + H]^+$), 273.2 (100% $[M + Na]^+$).

HRMS (ES^+): $C_{14}H_{23}N_2O_2$ Expected (m/z): 251.1754, Found: 251.1754.

^{1}H-NMR (400 MHz, $CDCl_3$): 4.96 (1H, s (br), **H-5**), 3.43 (4H, s, **H-10**), 3.22 (1H, s (br), **H-7**), 3.07 1H, dd, J = 7.5, 4.2, **H-6**), 3.03 (1H, m, **H-6**), 2.22 (2H, t, J = 2.4, **H-12**), 1.44 (9H, s, **H-1**), 1.11 (3H, d, J = 6.4, **H-8**).

^{13}C-NMR (100 MHz, $CDCl_3$): 156.0 (**C-4**), 80.0 (**C-11**), 79.1 (**C-2**), 72.8 (**C-12**), 55.9 (**C-7**), 43.5 (**C-6**), 38.9 (**C-10**), 28.4 (**C-1**), 13.9 (**C-8**).

FTIR ν_{max} (cm^{-1}) (thin film): 3422, 3294 (s, C≡C-H stretch), 2975 (m, C-H aliphatic stretch), 2931, 2100 (m, C-H aliphatic stretch), 1699 (s, C=O stretch).

No literature reference was found.

N',N'-di(prop-2-ynyl)propane-1,2-diamine salt with trifluoroacetic acid (173)

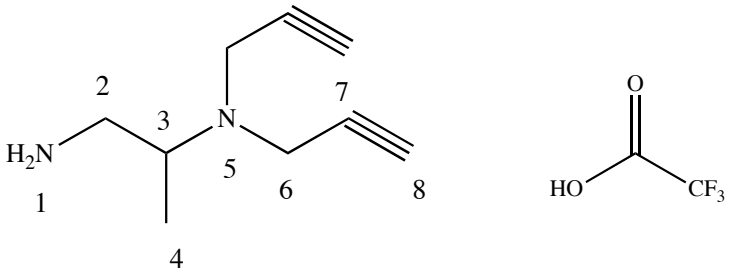

$C_{11}H_{15}F_3N_2O_2$

RMM = 264.25

A solution of *tert*-butyl 2-(diprop-2-ynylamino)propylcarbamate (0.105 g; 0.420 mmol) in dry DCM (2 mL) was added dropwise to a stirred solution of TFA (4 mL) and dry DCM (2 mL).

After 2 hrs the solvents were removed to give a brown oil. MeOH (10 mL) was added and then removed to help remove any residual TFA, and the residue was then dried under high vacuum to give a colourless oil/white solid (0.150 g, quantitative).

MS/ES$^+$ (m/z): 134.1 (100% [M - CH_2CCH – TFA + Na]$^+$), 151.1 (80% [M – TFA + H]$^+$).

^{1}H-NMR (300MHz, MeOD): 3.57 (4H, s **H-6**), 3.27 (m, **H-3**), 3.02 (1H, dd, J = 13.1, 10.1, **H-2**), 2.89 (1H, dd, J =13.1, 4.6, **H-2**), 2.67 (2H, s, **H-8**), 1.35 (1H, m (br)), 1.21 (3H, d, J = 6.6, **H-4**), 0.94 (1H, m)

^{13}C-NMR (75MHz, MeOD): 80.5 (**C-7**), 74.9 (**C-8**), 56.2 (**C-3**), 43.1 (**C-2**), 39.8 (**C-6**), 12.7 (**C-4**).

No literature reference was found.

1-Isothiocyanato-2-(N,N-di(prop-2-ynyl))aminopropane (174)

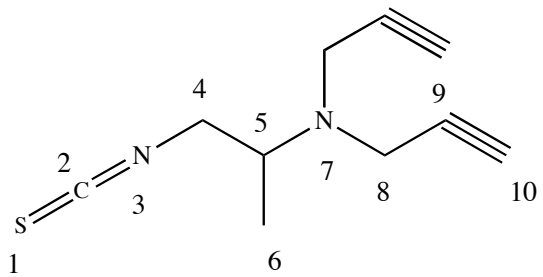

$C_{10}H_{12}N_2S$

RMM = 192.28

N',N'-di(prop-2-ynyl)propane-1,2-diamine hydrochloride (0.083 g; 0.314 mmol) in chloroform (4 mL) was added dropwise to a stirred solution of thiophosgene (0.09 mL;

1.136 mmol) and sodium carbonate (0.241 g; 2.272 mmol) in chloroform (11 mL) at 0ºC. The mixture was allowed to warm to RT and stirred for 64 hrs.
The solvent was removed under reduced pressure and the resulting solid/oil resuspended in fresh chloroform. The solid was then removed by filtration and the solvent removed *in vacuo* to give product as a pale brown oil (0.058 g; 96%).

MS/ES$^+$ (m/z): 130.1 (80%), 193.1 (40% $[M + H]^+$), 247.1 (40% $[N + Na]^+$), 269.1 (100%). (N is the methanol derivative which occurs due to the MS being run in MeOH)

^{1}H-NMR (300MHz, $CDCl_3$): 3.67 (1H, dd, J = 14.5, 5.2, **H-4**), 3.56 (d, J = 2.4, **H-8**), 3.55 (dd, **H-4**), 3.47 (m), 3.19 (2H, m, **H-5**), 2.26 (2H, t, J = 2.4, **H-10**), 1.27 (3H, d, J = 6.7, **H-6**), 1.16 (1H, d, J = 6.4), 0.92 (1H, t, J = 7.5).

^{13}C-NMR (75MHz, $CDCl_3$): 79.4 (**C-9**), 73.3 (**C-10**), 56.3 (S/M), 54.7 (**C-5**), 48.6 (**C-4**), 42.4 (S/M), 39.5 (**C-8**), 39.2 (S/M), 15.4 (**C-**), 13.1 (S/M). No C=S signal was observed.

FTIR ν_{max} (cm^{-1}) (thin film): 3292 (s, C≡C-H stretch), 2934 (m, C-H aliphatic stretch), 2100 (s (br) N=C=S stretch), 1720 (s, C=O stretch), 640 (s, C-H (sp) bend stretch).

No literature reference was found.

4-[EDA]-36-Amine-18-PEG-20-alkyne (175)

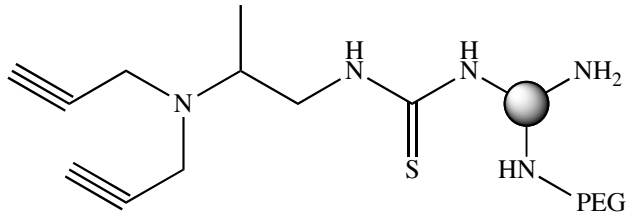

1-Isothiocyanato-2-(N,N-di(prop-2-ynyl))aminopropane (0.0115 g; 0.0601 mmol) in dry DCM (5 mL) was added dropwise to a stirred solution of 4-[EDA]-46-Amine-18-PEG

(0.0939g; 3.75 μmol) in dry DCM (15 mL) at 0ºC over 30 min and the reaction mixture allowed to stir for 16 hrs.

The reaction mixture was then dialysed against methanol/DCM (4 L, 1:1) for 2 days. The solvent was removed and the resulting oil was then azeotropically distilled in MeOH/toluene to give product as a viscous orange oil (0.1232 g).

^{1}H-NMR (400MHz, $CDCl_3$): 7.67 (1H, m, trace toluene), 7.49 (1H, m, trace toluene), 5.27 (DCM), 4.18 (1H, t), 3.61 (s (br), PEG-C**H**$_2$), 3.51 (d (br), CH≡C-C**H**$_2$-), 3.34 (s, PEG-C**H**$_3$), 2.70 (s (br), PAMAM), 2.49 (s (br), PAMAM), 2.32 (s (br), PAMAM), 1.65 (q), 1.38 (m, -CH_2-CH(C**H**$_3$)-N-), 1.29 (s (br)), 1.11 (m), 0.86 (t), 0.03 (1H, s).

^{13}C-NMR (100MHz, $CDCl_3$): 172.9, 167.6, 132.4 (trace toluene), 130.8 (trace toluene), 128.7 (trace toluene), 125.9 (trace toluene), 71.8 (CH≡**C**-CH_2-), 70.4 (PEG-**C**H_2-), 68.1 (**C**H≡C-CH_2-), 58.9 (PEG-**C**H_3), 53.4, 38.7, 30.3, 28.8, 23.7, 22.9, 13.9 (-CH_2-CH(**C**H_3)-N-), 10.9, 0.9. Unassigned peaks are due to PAMAM dendrimer.

FTIR ν_{max} (cm^{-1}) (thin film): 3272 (s (br), N-H stretch), 3078 (m, N-H amide stretch), 2871 (m, C-H aliphatic stretch), 1638 (s (br), C=O amide stretch), 1540 (s (br), C-C stretch), 1093 (s, C-O stretch).

Combustion analysis: C 50.21%, H 8.60%, N 12.51%, S, 2.80%. N:S ratio shows 28 sulphur atoms, 18 of which are known to come from the PEG, therefore 10 are due to the alkyne group coupling.

No literature reference was found.

(*S*)-*tert*-Butyl 4-(2-(*tert*-butoxycarbonylamino)-3-(3-chloropropylamino)-3-oxopropyl)-1*H*-imidazole-1-carboxylate (Boc-His(Boc)-propylchloride, 167)

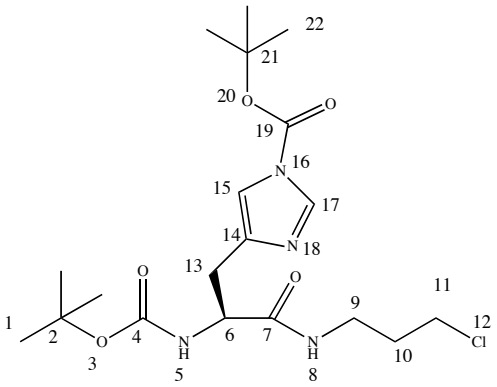

$C_{19}H_{31}ClN_4O_5$

RMM = 431.02

A solution containing Boc-Hist(Boc)-OH (0.250 g; 0.503 mmol), HBTU (0.210 g; 0.708 mmol), HOBt•H_2O (0.085 g; 0.708 mmol) and DIPEA (0.29 mL; 1.658 mmol) in DCM (15 mL) was prepared at 0ºC and stirred for 20 minutes. To this was added dropwise a solution of 3-chloropropylamine•HCl (0.064 g; 0.490 mmol) in DCM (1 mL) and the reaction mixture stirred for 45 minutes at 0ºC, then at RT for 64 hours to give a very pale yellow solution.

The reaction mixture was then washed with water (2 x 15 mL), 1M HCl (5%, 2 x 15 mL), sat. $NaHCO_3$ (2 x 15 mL), and water (15 mL). The organic phase was dried over Na_2SO_4, and reduced under vacuum to yield crude product as a colourless oil. The product was further purified by column chromatography (R_f: 0.26, 5% methanol in DCM, silica 60) to give a white solid foam (0.178 g, 84%).

MP: 43 - 45ºC

MS/ES$^+$ (m/z): 431.3 (30% $[M + H]^+$), 453.2 (100% $[M + Na]^+$), 455.2 (40%), 883.7 (70% $[2M + Na]^+$). Chlorine splitting observed.

HRMS (ES$^+$): $C_{19}H_{32}ClN_4O_5$ Expected (m/z): 431.2056, Found: 431.2065.

^{1}H-NMR: (400MHz, $CDCl_3$) 7.96 (1H, s, **H-17**), 7.13 (1H, s, **H-15**), 6.90 (1H, s (br), **H-8**), 6.13 (1H, d, J = 7.2, **H-5**), 5.27 (DCM), 4.36 (1H, q (br), **H-6**), 3.39 (2H, m (br), **H-11**), 3.31 (2H, q, J = 6.1, **H-9**), 3.04 (1H, dd (br), **H-13**), 2.89 (1H, dd, J = 14.7, 5.7, **H-13**), 1.85 (2H, qn, J = 6.6, **H-10**), 1.56 (9H, s, **H-22**), 1.40 (9H, s, **H-1**).

^{13}C-NMR: (100MHz, $CDCl_3$) 171.7 (**C-7**), 155.5 (**C-4**), 146.7 (**C-19**), 139.1 (**C-14**), 136.6 (**C-17**), 114.7 (**C-15**), 85.6 (**C-21**), 79.9 (**C-2**), 54.2 (**C-6**), 53.3 (DCM), 42.0 (**C-11**), 36.6 (**C-9**), 31.9 (**C-10**), 30.1 (**C-13**), 28.2 (**C-22**), 27.7 (**C-11**).

No literature reference was found.

(*S*)-*tert*-Butyl 4-(2-(*tert*-butoxycarbonylamino)-3-(3-bromopropylamino)-3-oxopropyl)-1*H*-imidazole-1-carboxylate (Boc-His(Boc)-propylbromide, 176)

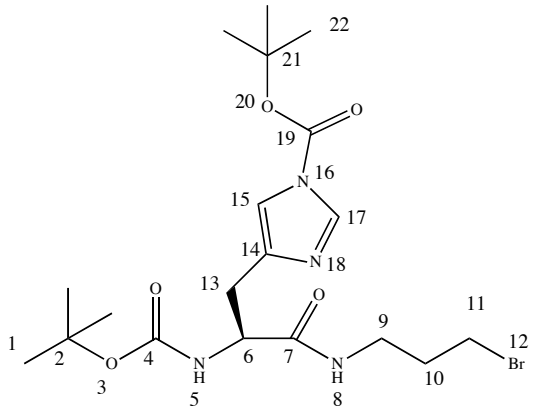

$C_{19}H_{31}BrN_4O_5$

RMM = 475.38

Procedure: as (Boc-His(Boc)-propylchloride)

Boc-Hist(Trt)-OH (0.250 g; 0.503 mmol)

HBTU (0.229 g; 0.603 mmol)

DIPEA (0.32 mL; 1.809 mmol)

Bromopropylamine•HBr (0.105 g; 0.479 mmol)

DCM (18 mL)

Purification: Column chromatography (R_f: 0.51, 5% methanol in diethyl ether, silica 60)

Product: Colourless glass (0.102 g; 43%)

MP: 40 – 42ºC

MS/ES$^+$ (m/z): 475.1 (10% $[M + H]^+$), 497.1 (40% $[M + Na]^+$), 973.3 (100% $[2M + Na]^+$). Bromine splitting observed.

HRMS (ES^+): $C_{19}H_{32}BrN_4O_5$ Expected (m/z): 475.1551, Found: 475.1540.

^{1}H-NMR (400MHz, $CDCl_3$): 8.01 (1H, s, **H-17**), 7.17 (1H, s, **H-15**), 6.88 (1H, s (br), **H-8**), 6.14 (1H, d, J = 7.2, **H-5**), 4.38 (1H, q (br), **H-6**), 3.48 (MeOH), 3.33 (m (br), **H-11**), 3.28 (q (br), **H-9**), 3.10 (1H, dd (br), **H-13**), 2.90 (1H, dd, J = 14.8, 5.9, **H-13**), 1.97 (2H, qn (br), **H-10**), 1.60 (9 H, s, **H-22**), 1.44 (9H, s, **H-1**).

^{13}C-NMR (100MHz, $CDCl_3$): 171.6 (**C-7**), 155.7 (**C-4**), 146.8 (**C-19**), 139.2 (**C-14**), 136.7 (**C-17**), 114.8 (**C-15**), 85.8 (**C-21**), 80.2 (**C-2**), 54.3 (**C-6**), 37.7 (**C-9**), 32.1 (**C-10**), 30.5 (**C-11**), 30.1 (**C-13**), 28.3 (**C-22**), 27.9 (**C-1**).

FTIR ν_{max} (cm^{-1}) (solid state): 3276 (m (br), N-H amide stretch), 2977 (m, C-H aliphatic stretch), 1753 (s, C=O amide stretch), 1706 (s, C=O carbamate stretch), 1658 (s, C=O carbamate stretch).

No literature reference was found.

(*S*)-*tert*-Butyl 4-(2-(*tert*-butoxycarbonylamino)-3-(3-azidopropylamino)-3-oxopropyl)-1*H*-imidazole-1-carboxylate (Boc-His(Boc)-propylazide, 178)

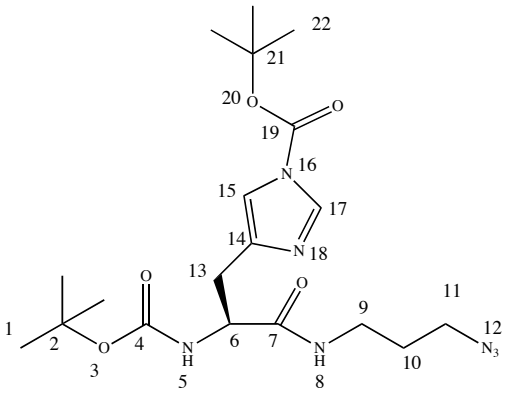

$C_{19}H_{31}N_7O_5$

RMM = 437.50

A solution containing (*S*)-*tert*-Butyl 4-(2-(*tert*-butoxycarbonylamino)-3-(3-bromopropylamino)-3-oxopropyl)-1*H*-imidazole-1-carboxylate (0.072 g; 0.151 mmol) in dry DMF (8 mL) had a solution of sodium azide (0.030 g; 0.454 mmol) in dry DMF (2 mL) added to it dropwise. The reaction mixture was stirred at 60ºC under nitrogen. After 40 hr the pale cream solution was partitioned between DCM/water (20 mL each), the water being washed with DCM (2 x 20 mL). The organic phases were combined, dried over Na_2SO_4, and reduced *in vacuo* to yield crude product as a colourless oil. The product was further purified by column chromatography (R_f: 0.58, 5% methanol in diethyl ether, silica 60) to give a colourless glass (0.0213 g; 32%).

MS/ES$^+$ (m/z): 438.2 (30% $[M + H]^+$), 460.1 (100% $[M + Na]^+$), 897.5 (80% $[2M + Na]^+$).

HRMS (ES$^+$): $C_{19}H_{31}N_7NaO_5$ Expected (m/z): 460.2279, Found: 460.2279.

^{1}H-NMR (300MHz, $CDCl_3$): 8.00 (1H, s, **H-17**), 7.17 (1H, s, **H-15**), 6.90 (1H, s (br), **H-8**), 6.13 (1H, d, J = 7.2, **H-5**), 5.29 (DCM), 4.38 (1H, q (br), **H-6**), 3.28 (2H, dt, J = 6.6, **H-9**), 3.22 (2H, t, J = 5.9, **H-11**), 3.09 (1H, dd, J = 14.7, 5.3, **H-13**), 2.91 (1H, dd, J = 14.7, 5.3, **H-13**), 1.73 (2H, qn, J = 6.7, **H-10**), 1.59 (9H, s, **H-22**), 1.43 (9H, s, **H-1**).

^{13}C-NMR: (75MHz, $CDCl_3$) 171.5 (**C-7**), 155.7 (**C-4**), 146.8 (**C-19**), 139.2 (**C-14**), 136.6 (**C-17**), 114.8 (**C-15**), 85.7 (**C-21**), 80.0 (**C-2**), 54.3 (**C-6**), 48.9, 36.7 (**C-9**), 32.3 (**C-11**), 30.1 (**C-13**), 28.6 (**C-10**), 28.3 (**C-22**), 27.8 (**C-1**).

No literature reference was found.

(*S*)-2-Amino-*N*-(3-azidopropyl)-3-(1*H*-imidazol-5-yl)propanamide di-trifluoroacetic acid (179)

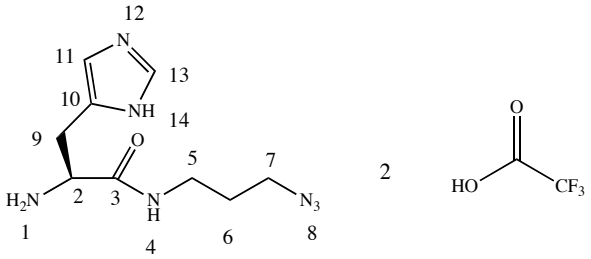

$C_{13}H_{17}F_6N_7O_5$

RMM = 465.31

TFA (2 mL) was added dropwise to a solution of (*S*)-*tert*-Butyl 4-(2-(*tert*-butoxycarbonylamino)-3-(3-azidopropylamino)-3-oxopropyl)-1*H*-imidazole-1-carboxylate (0.0395 g; 0.0904 mmol) in DCM (2 mL) at 0ºC. The reaction was stirred for 18 hrs at RT before the solvent was removed *in vacuo*. The resulting oil was azeotroped with methanol/ether to give a white solid (0.0359 g, 85%).

MS/ES$^+$ (m/z): 238.2 (60% [M -2TFA + H]$^+$), 250.2 (100% [M -2TFA + Na]$^+$).

^{1}H-NMR: (400MHz, DMSO) 8.81 (1H, s, **H-13**), 8.59 (1H, t (br), **H-4**), 7.36 (1H, s, **H-11**), 4.07 (1H, t, J = 6.7, **H-2**), 3.31 (2H, t, J = 6.7, **H-7**), 3.12 (5H, m, **H-5/9**), 1.62 (2H, m, **H-6**).

^{13}C-NMR: (100MHz, DMSO) 167.1 (**C-2**), 134.4 (**C-13**), 127.8 (**C-10**), 117.4 (**C-11**), 51.7 (**C-2**), 48.1 (**C-7**), 36.0 (**C-5**), 28.0 (**C-6**), 26.7 (**C-9**).

No literature reference was found.

(*S*)-2-Amino-*N*-(3-chloropropyl)-3-(1*H*-imidazol-5-yl)propanamide di-trifluoroacetic acid (180)

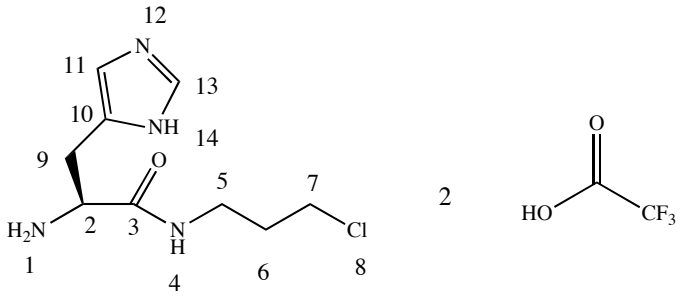

$C_{13}H_{17}ClF_6N_4O_5$

RMM = 458.83

TFA (0.35 mL) was added dropwise to a solution of (*S*)-*tert*-butyl 4-(2-(*tert*-butoxycarbonylamino)-3-(3-chloropropylamino)-3-oxopropyl)-1*H*-imidazole-1-carboxylate (0.100 g; 0.232 mmol) in DCM (2 mL). The reaction mixture was stirred for 2 hrs at RT before the solvent was removed *in vacuo*. The resulting oil was azeotroped with methanol/ether to give a white solid (0.1047 g, 98%). This reaction was performed to trial the removal of the Boc groups, so complete analysis was not obtained.

MP: 38 – 40ºC

MS/ES$^+$ (m/z): 233.1 (100% $[M]^+$).

^{1}H-NMR (400MHz, D_2O): 8.82 (1H, s, **H-13**), 7.42 (1H, s, **H-11**), 4.17 (1H, t, J = 7.0, **H-2**), 3.54 (2H, t, J = 6.4, **H-7**), 3.37 (t, J = 5.8, **H-5**), 3.31 (m), 1.94 (2H, m, **H-6**).

^{13}C-NMR (100MHz, D_2O): 168.7 (**C-2**), 136.0 (**C-13**), 128.8 (**C-10**), 119.4 (**C-11**), 53.6 (**C-2**), 42.9 (**C-7**), 38.2 (**C-5**), 33.1 (**C-6**), 27.9 (**C-9**).

No literature reference was found.

4-[EDA]-36-Amine-18-PEG-20-(triazole-Histidine) (181)

4-[EDA]-38-Amine-18-PEG-16-alkyne (0.1005 g; 3.58 μmol), (*S*)-2-Amino-*N*-(3-azidopropyl)-3-(1*H*-imidazol-5-yl)propanamide (0.0487 g; 0.105 mmol), sodium ascorbate (10 mol%) and copper sulphate pentahydrate (5 mol%) were combined in THF/water (10 mL, 4:1) and allowed to stir for 18 hrs.

The reaction mixture was then dialysed against water for 2 days and methanol for 3 days. The solvent was removed and the resulting oil was then azeotropically distilled in MeOH/toluene to give product as a viscous orange oil (0.0795 g).

^{1}H-NMR (400MHz, MeOD): 8.12 (s), 4.83 (MeOH), 3.64 (s, PEG-C**H**$_2$-), 3.55 (d, J = 5.0, CH≡C-C**H**$_2$-), 3.36 (s, PEG-C**H**$_3$), 3.35 (s), 2.84 (s (br), PAMAM), 2.65 (s (br), PAMAM), 2.41 (s (br), PAMAM), 1.16 (s).

^{13}C-NMR (100MHz, MeOD): 174.6, 73.0 (CH≡**C**-CH$_2$-), 71.6 (PEG-**C**H$_2$-), 59.2 (PEG-**C**H$_3$), 53.6, 51.2, 40.1, 38.5, 34.6. Unassigned peaks are due to PAMAM dendrimer.

Combustion analysis: C 48.69%, H 7.39%, N 14.38%, S, 3.26%. N:S ratio shows 28 sulphur atoms, 18 of which are known to come from the PEG, therefore 10 are due to the alkyne group coupling, so no ‘click’ reaction observed.

No literature reference was found.

Preparation of Azobenzene Molecules to act as a Dendrimer Core

Azobenzene-4,4'-dicarboxylic acid (183)

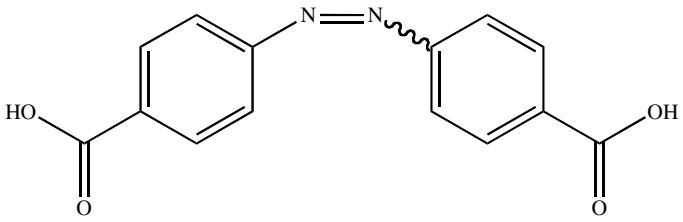

$C_{14}H_{10}N_2O_4$

RMM = 270.24

p-Nitrobenzoic acid (5.00 g; 30 mmol) and sodium hydroxide (13.3 g; 330 mmol) were stirred in water (100 mL) at 50ºC. Glucose (33.0 g; 180 mmol) in water (50 mL) at 50ºC was then added slowly via cannula to give a yellow precipitate followed by the solution turning brown. Air was passed through the reaction mixture to aid the precipitation of an orange solid.

The solid was collected by filtration, dissolved in water (50 mL) and acidified with glacial acetic acid to give a pink precipitate. This was collected by filtration and washed with copious amounts of water (150 mL). The residue was oven dried at 105ºC to give product as a pale brown solid (2.44 g; 60%).

(It was found that the product was insoluble in most organic solvents.)

MP: > 250ºC

Preparation followed from literature (no analytical data found).[251,418,419,428]

Azobenzene-4,4'-dicarboxylic acid (183)

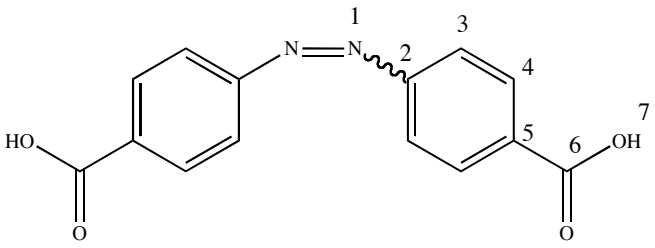

$C_{14}H_{10}N_2O_4$

RMM = 270.24

p-Nitrobenzoic acid (4.00 g; 23.9 mmol) in methanol (40 mL) and sodium hydroxide (9.57 g; 239 mmol) in water (6 mL) were mixed at 70ºC until homogeneous. The mixture was cooled to 40ºC then zinc powder (6.22 g; 95.7 mmol) was added to give a green mixture. This was refluxed for 18 hours to give an orange mixture.

The solids were removed by filtration and the residue was washed with water. The orange filtrate was then acidified to pH 2 with conc. HCl to give pink solid which was collected by filtration. The solid was washed with copious amounts of water before being dried in an oven at 120ºC overnight (2.165 g; 69%).

MP: > 250ºC

^{1}H-NMR (300MHz, DMSO): 12.27 (4H, s (br), **H-7**), 8.47 (4H, s), 8.18 (1H, d, J = 8.8, S/M), 8.02 (1H, d, J = 8.8, S/M), 7.74 (4H, d, J = 8.8, **H-4**) 6.73 (4H, d, J = 8.8, **H-3**).

^{13}C-NMR (300MHz, DMSO): 167.2 (**C-6**), 166.5, 154.1, 153.1 (**C-2**), 133.3, 131.1 (**C-4**), 130.6, 122.7, 119.6 (**C-5**), 110.4 (**C-3**). Unassigned peaks are due to trace starting material.

FTIR ν_{max} (cm^{-1}) (solid state): 3338 (s, O-H carboxylic acid stretch), 3100-2600 (m (br), C-H aromatic and aliphatic stretch), 1652 (s, C=O acid stretch), 1597 (s, N=N stretch).

Preparation followed from literature (no analytical data found).[418,420,421]

4,4'-bis(Chlorocarbonyl)azobenzene (184)

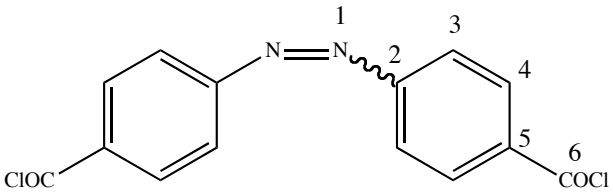

$C_{14}H_8 Cl_2N_2O_2$

RMM = 307.32

Phosphorus pentachloride (0.230 g; 1.10 mmol) in 1,2-dichloroethane (5 mL) was added dropwise to a stirred solution of azobenzene-4,4'-dicarboxylic acid (0.12 g; 0.44 mmol) at 0ºC under nitrogen. The mixture was then refluxed for 2 hours to give a red solution. Red crystals formed on cooling which were collected by filtration. The solid was crystallised from toluene to give red crystals (0.0364 g; 27%).

MP: > 250ºC

^{1}H-NMR: (300MHz, $CDCl_3$) 8.18 (1H, dt, J=8.8, 2.0, **H-4**), 7.93 (1H, dt, J=8.8, 2.0, **H-3**).

^{13}C-NMR: (75MHz, $CDCl_3$) 167.7 (**C-6**), 155.8 (**C-2**), 135.4 (**C-5**), 132.5 (**C-4**), 123.5 (**C-3**).

Procedure followed from, and is consistent with, literature.[418,428]

4,4'-bis(Chlorocarbonyl)azobenzene (184)

Thionyl chloride (0.54 mL; 7.40 mmol) was added dropwise to a solution of azobenzene-4,4'-dicarboxylic acid (0.400 g, 1.48 mmol) in dry DCM (40 mL) and DMF (3 drops). The mixture was then allowed to reflux under nitrogen (the output was bubbled through NaOH solution) for 17 hrs to give a red solution and pale brown precipitate.

The mixture was filtered and the filtrate was reduced *in vacuo* to give a brown/orange solid. This was dissolved in chloroform to give a red solution and orange residue. The mixture was filtered and the filtrate was reduced *in vacuo* to give a red solid. This was dried under high vacuum for 4 hours (0.320 g, 70%).

MP: > 250ºC

^{1}H-NMR (300MHz, $CDCl_3$): 8.31 (1H, dt, J=8.8, 1.9, **H-4**), 8.06 (1H, dt, J=8.8, 1.9, **H-3**), 7.69 (0.02H, dd), 7.54 (0.02H, dd), 1.60 (0.1H, br), 1.31 (0.1H, br), 0.91 (0.1H, q).

^{13}C-NMR (75MHz, $CDCl_3$): 167.7 (**C-6**), 155.8 (**C-2**), 135.4 (**C-5**), 132.5 (**C-4**), 123.5 (**C-3**).

Product is consistent with literature.[418,428]

tert-Butyl-4-aminobenzylcarbamate (188)

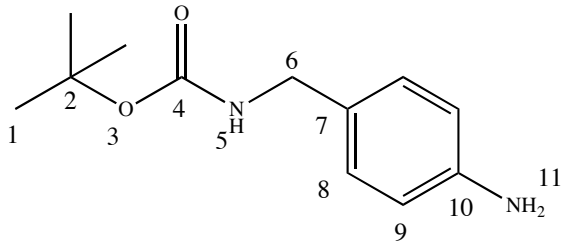

$C_{12}H_{18}N_2O_2$

RMM = 222.29

A solution of di(^{t}butyl)dicarbonate (2.36 g; 10.80 mmol) in THF (8 mL) was added dropwise to a stirred solution of 4-aminobenzylamine (1.11 mL; 9.82 mol) in THF (16 mL). The reaction mixture was stirred for 2 hrs before the solvent was removed under reduced pressure to give an orange oil. The crude product was triturated from a 1:1 mix of diethyl ether/petroleum ether (40/60) to give a pale yellow solid (2.039 g; 93%)

MP: 73 – 74ºC (lit. 73 – 74ºC)

MS/ES^{+} $_{(m/z)}$: 223.2 (100%, $[M + H]^{+}$), 245.2 (40%, $[M + Na]^{+}$).

^{1}H-NMR $_{(400MHz, CDCl_3)}$: 7.06 (1H, d, J = 8.3, **H-8**), 6.63 (1H, dt, J = 8.4, 2., **H-9**), 4.72 (s (br), **H-5**), 4.18 (1H, d, J = 5.4, **H-6**), 3.64 (1H, s, **H-11**), 1.46 (9H, s, **H-1**).

^{13}C-NMR $_{(100MHz, CDCl_3)}$: 155.8 (**C-4**), 145.7 (**C-10**), 128.8 (**C-8**), 115.1 (**C-9**), 79.2 (**C-2**), 44.4 (**C-6**), 28.4 (**C-1**).

Procedure followed from, and is consistent with, literature.[426]

4,4'-bis(4-((tButoxycarbonyl)aminomethyl)phenyl)azobenzamide (189)

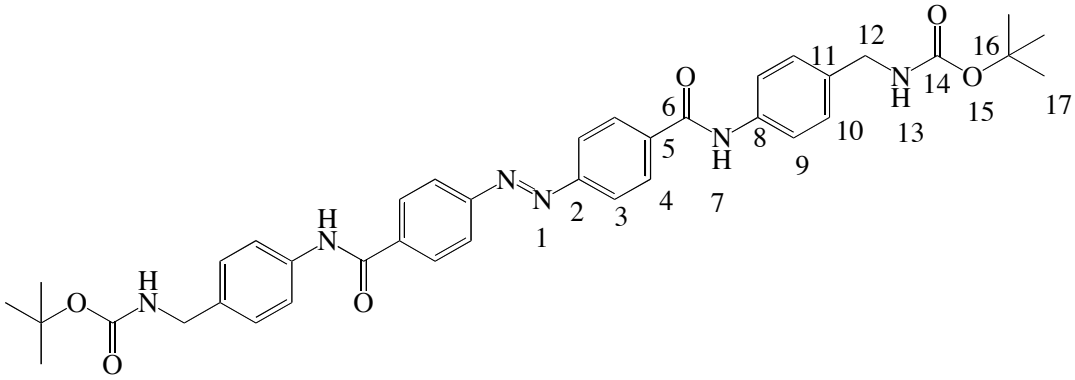

$C_{38}H_{42}N_6O_6$

RMM = 678.79

Crude 4,4'-bis(chlorocarbonyl)azobenzene (0.073 g; 0.240 mmol) in dry DCM (5 mL) was added dropwise to a stirred solution of *tert*-butyl 4-aminobenzylcarbamate (0.117 g; 0.528 mmol) in dry DCM (10 mL).

After 30 minutes an orange precipitate had formed which was collected by filtration. The solid was dissolved in the minimum amount of DMSO and added dropwise to rapidly stirring diethyl ether (200 mL). The orange precipitate was collected by filtration (0.154 g; 95%).

MP: NMR data showed that product still contains DMSO so MP not recorded.

MS/ES$^+$ (m/z): Product not soluble

^{1}H-NMR (400MHz, DMSO): 10.44 (1H, s (br), **H-7**), 8.21(2H, d, J = 8.5, **H-3**), 8.07 (2H, d, J = 8.5, **H-4**), 7.73 (2H, d, J = 8.4, **H-9**), 7.41 (1H, t (br), **H-13**), 7.36 (1H, t (br)), 7.32 (2H, d, J = 8.2, **H-10**), 7.25 (3H, m), 4.12 (4H, d, J = 5.6, **H-12**), 2.54 (DMSO), 1.34 (18H, s, **H-17**).

^{13}C-NMR (100MHz, DMSO): 155.7 (**C-14**), 129.0 (**C-11**), 128.0 (**C-4**), 127.2 (**C-10**), 122.5 (**C-3**), 122.3 (**C-8**), 120.3 (**C-9**), 77.8 (**C-16**), 40.3 (**C-12**), 28.1 (**C-17**).

No literature reference was found.

4,4'-bis(4-Aminomethylphenyl)azobenzamide (190)

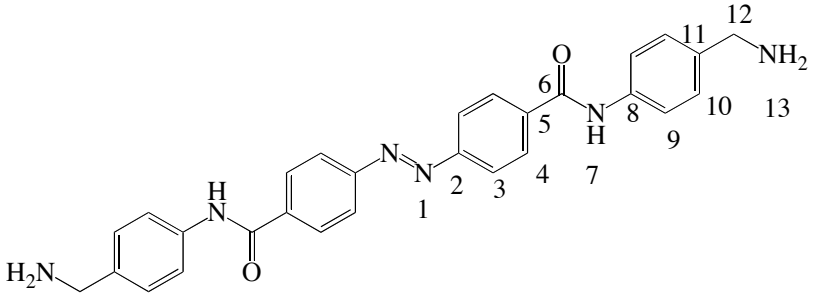

$C_{28}H_{26}N_6O_2$

RMM = 478.55

4,4'-Bis(tert 4-amidobenzylcarbamate)azobenzene (0.050 g; 0.074 mmol) was added portionwise to a stirred solution of TFA (5 mL) in dry DCM (5 mL). This resulted in an orange solution. After 3 hr the solvents were removed to give an orange solid. This solid was found to be very insoluble, it is only partially soluble in hot DMSO. A ^{1}H NMR spectrum gave a very weak signal but did not show the presence of the Boc group.

No literature reference was found.

tert-Butyl 4-(4-nitrobenzamido)benzylcarbamate (191)

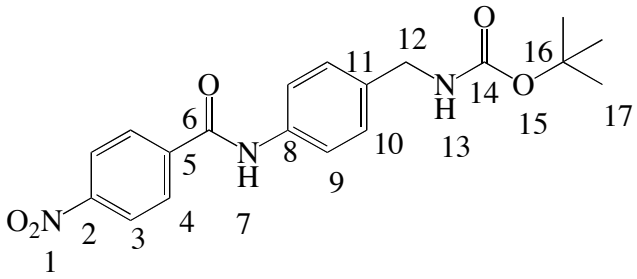

$C_{19}H_{21}N_3O_5$

RMM = 371.39

4-Nitrobenzoyl chloride (0.325 g; 1.64 mmol) in dry DCM (10 mL) was added dropwise to a stirred solution of *tert*-butyl 4-aminobenzylcarbamate (0.430 g; 1.80 mmol) in dry DCM (15 mL) under nitrogen.

After 2 hr an orange precipitate had formed which was collected by filtration. The solid was dissolved in DCM (20 mL) and the solution washed with 2M HCl (2 x 20 mL), sat. $NaHCO_3$ (2 x 20 mL) and water (2 x 20 mL). The organic phase was dried over $MgSO_4$ and reduced to give a yellow solid. This was further purified by column chromatography (R_f: 0.65, 50% petrol 40-60 in ethyl acetate, silica 60) to give product as a yellow solid (0.293 g; 48%).

MP: 186 – 187ºC

MS/ES^- (m/z): 370.3 (100% $[M - H]^-$), 741.6 (30% $[2M - H]^-$).

HRMS (ES^+): $C_{19}H_{25}N_4O_5$ Expected (m/z): 389.1819, Found: 389.1822.

^{1}H-NMR (400MHz, DMSO): 10.53 (1H, s (br), **H-7**), 8.38 (2H, d, J = 8.9, **H-3**), 8.19 (2H, d, J = 8.9, **H-4**), 7.71 (2H, d, J = 8.4, **H-9**), 7.35 (1H, t (br), **H-13**), 7.24 (2H, d, J = 8.5, **H-10**), 4.11 (2H, d, J = 6.1, **H-12**), 1.40 (9H, s, **H-17**).

^{13}C-NMR (100MHz, DMSO): 163.6 (**C-6**), 155.6 (**C-14**), 149.0 (**C-2**), 140.5 (**C-5**), 137.1 (**C-11**), 135.9 (**C-8**), 129.1 (**C-4**), 127.2 (**C-10**), 123.4 (**C-3**), 120.3 (**C-9**), 77.6 (**C-16**), 42.9 (**C-12**), 28.2 (**C-17**).

FTIR ν_{max} (cm^{-1}) (solid state): 3393 (m, N-H amide stretch), 3354 (w, N-H carbamate stretch), 2958 (m, C-H aliphatic stretch), 1681 (s, C=O carbamate stretch), 1651 (s, C=O amide stretch).

No literature reference was found.

4,4'-Bis(4-aminomethylbenzyl)azobenzamide (192)

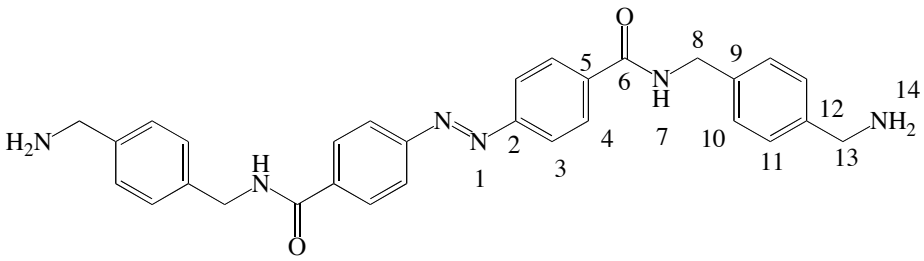

$C_{30}H_{30}N_6O_2$

RMM = 506.61

4,4'-Bis(chlorocarbonyl)azobenzene (0.152 g; 0.496 mmol) in chloroform (10 mL) was added dropwise to a stirred solution of *p*-xylylene diamine (0.270 g; 1.98 mmol) and triethylamine (0.28 mL; 1.98 mmol) in $CHCl_3$ (40 mL) to give an orange solid. After 2 hours, the solvents were removed to give an orange and white solid. The solids were collected but found to be insoluble in all solvents tried.

MP: > 300ºC

No literature reference was found.

Preparation of Azobenzene Molecules to Attach to the Dendrimer Surface

4,4'-Diaminoazobenzene (194)

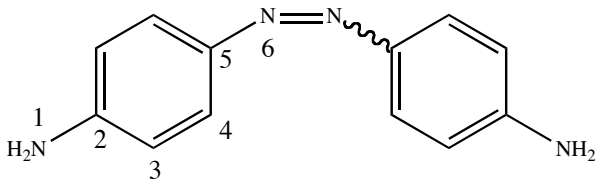

$C_{12}H_{12}N_4$

RMM = 212.25

Manganese (IV) oxide (2.57 g; 29.59 mmol) was added to a stirred solution of 1,4-phenylene diamine (0.5 g; 4.62 mmol) in chloroform (40 mL) and allowed to stir. After 18 hours the resulting black mixture was filtered through celite to give a red filtrate, which was reduced in volume *in vacuo*. Ether was added and the mixture filtered again. The filtrate was purified by column chromatography (R_f: 0.53, 2% MeOH in Ether, silica 60) to give product as a yellow solid (0.0129 g, 2.6%).

MS/ES^- (m/z): 213 (100% $[M + H]^+$), 233 (20% $[M + H]^+$).

^{1}H-NMR (400MHz, $CDCl_3$): 7.74 (1H, dt, J = 8.7, **H-4**), 6.98 (s), 6.73 (1.1H, dt, J = 8.7, **H-3**), 5.00, 4.22 (t), 3.94 (s(br), **H-1**), 3.49 (t), 1.56 (s), 1.44 (s), 1.23 (s), 0.92 (t), 0.07 (s).

^{13}C-NMR (100MHz, $CDCl_3$): 148.5 (**C-2**), 145.8 (**C-5**), 128.8, 125.5, 124.3 (**C-4**), 114.8 (**C-3**), 38.8, 34.2, 30.3, 29.7.

tert-Butyl 4-aminophenylcarbamate (195)

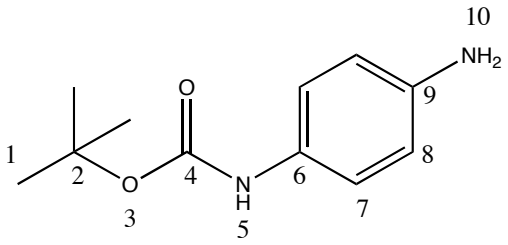

$C_{11}H_{16}N_2O_2$

RMM = 208.26

A solution of di(^{t}butyl)dicarbonate (0.917 g; 4.20 mmol) in DCM (7 mL) was added to a solution of 1,4-phenylene diamine (1.00 g; 9.25 mmol) in DCM (23 mL) and the mixture stirred for 48 hours at RT.

1M HCl (40 mL) was added and the reaction mixture was partitioned. The aqueous layer was basified with 2M NaOH and washed with DCM (3 x 20 mL). The organic phases were combined, dried over $MgSO_4$, and reduced *in vacuo*. The product was purified by column chromatography (R_f: 0.37, 5% MeOH in DCM, silica 60) and then crystallised from hot toluene to give a white crystalline solid (0.781 g; 81%).

MP: 104 – 105ºC (lit. 111 – 113ºC)

^{1}H-NMR (300MHz, $CDCl_3$): 7.12 (2H, d, J = 8.4, **H-7**), 6.63 (2H, dt, J = 8.7, 2.1, **H-8**), 6.25 (1H, s(br), **H-5**), 3.52 (2H, s(br), **H-10**), 1.50 (9H, s, **H-1**).

^{13}C-NMR (75MHz, $CDCl_3$): 153.3 (**C-4**), 142.4 (**C-9**), 129.7 (**C-6**), 120.9 (**C-7**), 115.6 (**C-8**), 80.0 (**C-2**), 28.4 (**C-1**).

FTIR ν_{max} (cm^{-1}) (solid state): 3373 (m, N-H amine stretch), 3299 (w, N-H carbamate stretch), 2988 (m, C-H aliphatic stretch), 1689 (s, C=O carbamate stretch).

Combustion analysis:	Theoretical	C 63.44%, H 7.74%, N 13.45%
	Found	C 63.47%, H 7.97%, N 13.69%

Product is consistent with literature.[437]

(9*H*-Fluoren-9-yl) methyl 4-aminobenzylcarbamate (202)

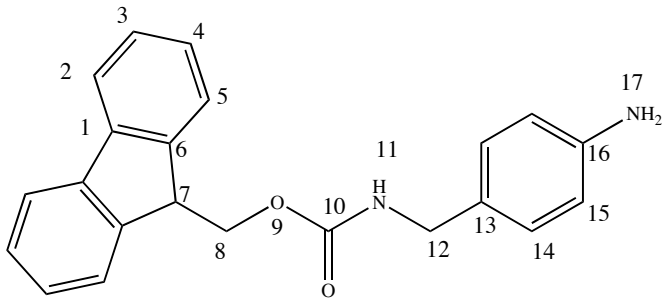

$C_{22}H_{20}N_2O_2$

RMM = 344.41

A solution of Fmoc-OSu (2.00 g; 5.93 mmol) in acetonitrile (15 mL) was added dropwise over 30 minutes to a stirred solution of (4-amino)benzylamine (0.72 g; 5.93 mmol) and triethylamine (0.83 mL; 5.93 mmol) in acetonitrile/DMF (8/0.8 mL). After stirring this mixture for 1 hour, the product was precipitated with water, filtered and washed with a solution of ^{t}butyl methylether/trifluoroethanol (1:1). Residue was crystallised from hot ethanol to give product as a white solid (0.698 g; 34%).

MP: 145 - 146ºC (no lit. mp found)

MS/ES^+ (m/z): 345 (100%, $[M + H]^+$).

^{1}H-NMR (400MHz, $CDCl_3$): 7.77 (2H, d, J = 7.8, **H-2**), 7.60 (2H, d, J = 7.6, **H-5**), 7.41 (2H, t, J = 7.4, **H-3**), 7.32 (2H, t, J = 7.3, **H-4**), 7.06 (1H, d, J = 7.1, **H-14**), 6.64 (2H, d, J = 6.7, **H-15**), 5.29 (1H, s(br), **H-11**), 4.45 (3H, d, J = 6.8, **H-8**), 4.25 (3H, d (br), **H-7**), 3.70 (EtOH), 2.48 (s), 1.24 (t, EtOH).

^{13}C-NMR (100MHz, $CDCl_3$): 156.4 (**C-10**), 145.7 (**C-16**), 143.8 (**C-6**), 141.2 (**C-1**), 128.8 (**C-14**), 128.2 (**C-13**), 127.5 (**C-3**), 126.9 (**C-4**), 124.9 (**C-5**), 119.8 (**C-2**), 115.2 (**C-15**), 66.4 (**C-8**), 58.0 (EtOH), 47.2 (**C-7**), 44.6 (**C-12**), 18.1 (EtOH).

FTIR ν_{max} (cm^{-1}) (solid state): 3423 (s, N-H amine stretch), 3300 (s, N-H amide stretch), 1689 (s, C=O formate stretch), 1622 (s, N-H amine bend), 1516 (s, C=C [Ar] stretch), 1255 (s, C-O stretch),

Procedure followed from, and is consistent with, literature.[438]

4-Nitrosophenylacetic acid (203)

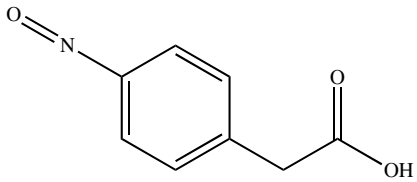

$C_8H_7NO_3$

RMM = 165.15

Ammonium chloride (0.370 g; 6.96 mmol) and zinc powder (0.680 g; 10.43 mmol) were added portionwise to a stirred solution of 4-nitrobenzoic acid (0.700 g; 3.86 mmol) in 2-methoxy ethanol (20 mL) at RT. After 45 minutes, the mixture was cooled to 0ºC and a solution of iron (III) chloride (2.230 g; 13.76 mmol) in ethanol/water (5:1, 25 mL) was added dropwise. The reaction was stirred at 0ºC for 1 hour, then warmed to RT and stirred for a further 30 minutes.

The mixture was extracted with diethyl ether (3 x 30 mL), dried over $MgSO_4$ and it's volume was reduced *in vacuo* to give a yellow/green solid (0.325 g; 51%).

No analytical data was collected as nitroso compounds can rapidly decompose.

Procedure followed from literature.[427,428]

4-((4-(^{t}Butoxycarbonyl)aminomethyl)phenylazo)benzoic acid (204)

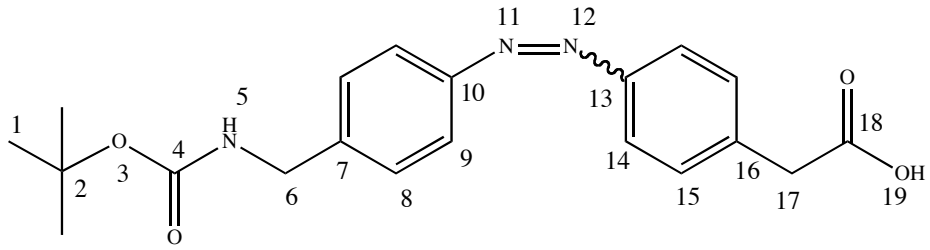

$C_{20}H_{23}N_3O_4$

RMM = 369.42

^{t}Boc-4-aminobenzylcarbamate (0.230 g; 1.39 mmol) was added portionwise to a solution of 4-nitrosophenylacetic acid (0.22 g; 1.0 mmol) in acetic acid (20 mL) and the mixture allowed to stir for 24 hrs at RT.

The solvent was removed *in vacuo* to give orange solid which was dissolved in DCM (20 mL) and washed with water (5 x 20 mL). The organic phase was the dried over $MgSO_4$ and reduced under vacuum. DCM (10 mL) was added to precipitate the product as an orange solid which was collected by filtration (0.030 g; 8%).

MP: 189 – 190ºC (lit. 196 – 198ºC)

MS/ES$^+$ (m/z): 370.2 (100%, $[M + H]^+$), 392.2 (20%, $[M + Na]^+$), 739.5 (20%, $[2M + H]^+$), 761.2 (10%, $[2M + Na]^+$).

MS/ES$^-$ (m/z): 324.3 (100%, $[M - CO_2 - H]^-$), 368.2 (5%, $[M - H]^-$), 737.5 (20%, $[2M - H]^-$).

HRMS (ES$^+$): $C_{20}H_{24}N_3O_4$ Expected (m/z): 370.1761, Found: 370.1764.

^{1}H-NMR (400MHz, DMSO): 7.84 (3H, dd, J = 7.4, 6.0, **H-9/14**), 7.48 (d, J = 8.1, **H-15**), 7.44 (d, J = 8.3, **H-8**), 4.22 (2H, d, J = 4.5, **H-6**), 3.68 (2H, s, **H-17**), 1.41 (9H, s, **H-1**).

^{13}C-NMR (100MHz, DMSO): 155.7 (**C-4**), 150.8 (**C-13**), 150.6 (**C-10**), 143.7 (**C-7**), 138.8 (**C-16**), 130.4 (**C-15**), 127.7 (**C-8**), 122.4 (**C-9**), 122.2 (**C-14**), 77.8 (**C-2**), 43.1 (**C-6**), 40.6 (**C-17**), 28.1 (**C-1**).

FTIR ν_{max} (cm^{-1}) (solid state): 3323 (s, N-H amide stretch), 2974 & 2925 (s, C-H aliphatic stretch), 1695 (s, C=O carboxylic acid stretch), 1677 (C=O formate stretch),1600 (N=N stretch), 1511 (C=C [Ar]), 1245 (C-O carboxylic acid stretch), 1166 (C-O ester stretch).

Combustion:	Theoretical	C 65.03%, H 6.28%, N 11.37%
analysis	Found	C 64.72%, H 6.01%, N 11.18%

Procedure followed from, and is consistent with, literature.[426-428]

4-((4-((9H-fluoren-9-yl)methoxycarbonyl)aminomethyl)phenylazo)benzoic acid (205)

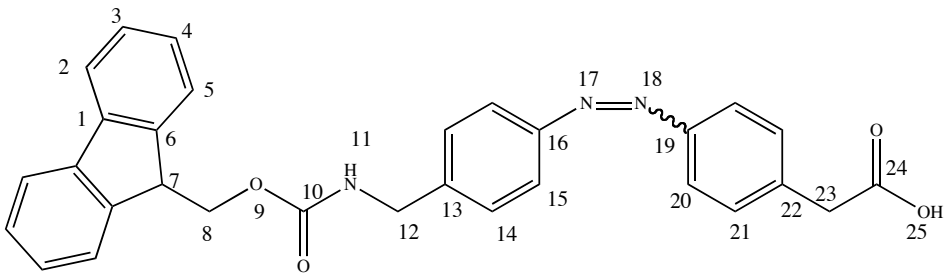

$C_{30}H_{25}N_3O_4$

RMM = 491.54

Fmoc-(4-aminomethyl)benylamine (0.452 g; 1.31 mmol) was added portionwise to a mixture of 4-nitrosophenylacetic acid (0.325 g; 1.97 mmol) in acetic acid (20 mL) and the mixture allowed to stir for 12 hrs at RT.

The solvent was removed *in vacuo* to give crude product as an orange solid. The solid was crystallised twice from hot ethanol then purified by column chromatography (R_f: 0.53, 9% EtOH in DCM, silica 60) to give product as orange solid (0.056 g; 9%).

M.P.: 174 - 176ºC

MS/ES$^+$ (m/z): 492.3 (100%, $[M + H]^+$), 514.3 (30%, $[M + Na]^+$), 530.2 (10%, $[M + K]^+$), 983.6 (20%, $[2M + H]^+$), 1005.6 (10%, $[2M + Na]^+$).

MS/ES$^-$ (m/z): 446.3 (100%, $[M – CO_2 – H]^-$), 490.2 (10%, $[M – H]^-$).

HRMS (ES$^+$): $C_{30}H_{26}N_3O_4$ Expected (m/z): 492.1918, Found: 492.1918.

^{1}H-NMR (400MHz, DMSO): 7.93 (t, J = 6.0), 7.89 (d, J = 7.6, **H-15/20**), 7.84 (d, J = 8.4, **H-2**), 7.71 (2H, d, J = 7.6, **H-5**), 7.48 (d, J = 8.0, **H-14/21**), 7.43 (t (br), J = 4.8, **H-3**), 7.34 (t, J = 7.6, **H-4**), 4.39 (2H, d, J = 6.8, **H-8**), 4.28 (d, J = 6.0, **H-12**), 4.25 (t, J = 6.8, **H-7**), 3.70 (2H, s, **H-23**).

^{13}C-NMR (100MHz, DMSO): 172.1 (**C-24**), 156.2 (**C-10**), 150.8 (**C-19**), 150.6 (**C-16**), 143.7 (**C-6**), 143.3 (**C-13**), 140.6 (**C-1**), 138.7 (**C-22**), 130.4 (**C-21**), 127.8 (**C-14**),

127.5 (**C-3**), 126.9 (**C-4**), 125.0 (**C-5**), 122.4 (**C-15**), 122.3 (**C-20**), 120.0 (**C-2**), 65.2 (**C-8**), 46.8 (**C-7**), 43.3 (**C-12**), 40.5 (**C-23**).

FTIR ν_{max} (cm^{-1}): (solid state) 3300 (s, N-H amide stretch), 1690 (C=O carboxylic acid stretch), 1604 (N=N stretch), 1541 (N-H amide bend), 1450 (C=C [Ar] stretch), 1419 & 1294 (C-O carboxylic acid stretch), 1257 (C-O ester stretch).

Combustion:	Theoretical	C 73.31%, H 5.13%, N 8.54%
analysis	Found	C 72.60%, H 5.18%, N 8.10%

Procedure adapted from literature.[427,428] No literature reference was found.

4-((4-((*tert*-Butoxycarbonyl)amino)phenyl)diazenyl)phenol (206)

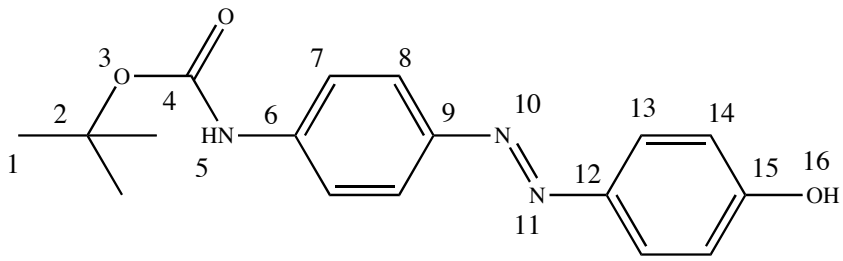

$C_{17}H_{19}N_3O_3$

RMM = 313.36

[t]Butyl 4-aminophenylcarbamate (0.272 g; 1.31 mmol) was added portionwise to a solution of conc. HCl (0.12 mL; 3.93 mmol) in water (10 mL) and the mixture was stirred at <5ºC for 20 min. Sodium nitrite (0.095 g; 1.38 mmol) in water (3 mL) was

added dropwise. After 30 minutes phenol (0.188 g; 2.00 mmol) in 1M NaOH (3 mL) was added resulting in the formation of an orange precipitate.

Diethyl ether (30 mL) was added and the layers were separated, the water being washed with more diethyl ether (2 x 30 mL). The organics were combined, dried over Na_2SO_4 and reduced *in vacuo*. The crude material was purified by column chromatography (R_f: 0.32, 50% petrol 40-60 in diethyl ether) to give product as a light orange solid (0.381 g, 93%).

MP: 197 – 198ºC

MS/ES$^+$ (m/z): 314.2 (10% $[M + H]^+$), 336.2 (20% $[M + Na]^+$), 368.2 (50% $[M + Na + MeOH]^+$).

MS/ES$^-$ (m/z): 312.2 (100% $[M – H]^-$).

HRMS (ES$^+$): $C_{17}H_{20}N_3O_3$ Expected (m/z): 314.1499, Found: 314.1500.

^{1}H-NMR (300MHz, MeOD): 7.78 (d, J = 9.1, **H-7**), 7.77 (d, J = 9.0, **H-8**), 7.55 (2H, dt, J = 9.0, 2.0, **H-13**), 6.90 (2H, dt, J = 8.9, 2.1, **H-14**), 1.54 (9H, s, **H-1**).

^{13}C-NMR (75MHz, MeOD): 161.7 (**C-15**), 155.0 (**C-4**), 149.4 (**C-9**), 147.6 (**C-12**), 143.0 (**C-6**), 125.6 (**C-13**), 124.3 (**C-8**), 119.6 (**C-7**), 116.7 (**C-14**), 81.2 (**C-2**), 28.7 (**C-1**).

FTIR ν_{max} (cm^{-1}) (solid state): 3368 (s, N-H carbamate stretch), 3300 – 2900 (O-H broad stretch), 2985 (m, C-H aliphatic stretch), 1697 (s, C=O carbamate stretch), 1504 (m, N=N azo stretch).

Combustion analysis:	Theoretical	C 65.16%, H 6.11%, N 13.40%
	Found	C 65.36%, H 6.17%, N 13.37%

Procedure adapted from literature.[432] No literature reference was found.

4-((4-Acetamidophenyl)diazenyl)phenol (207)

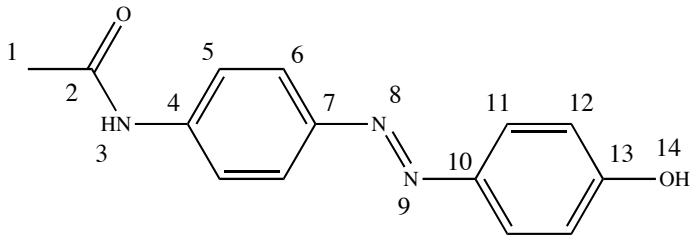

$C_{14}H_{13}N_3O_2$

RMM = 255.28

4'-Aminoacetanilide (1.00 g; 6.66 mmol) was added portion-wise to a solution of conc. HCl (0.6 mL) in water (10 mL) and stirred at <5ºC for 20 min. Sodium nitrite (0.476 g; 6.90 mmol) in water (3 mL) was added dropwise. After 30 minutes phenol (0.59 mL; 6.66 mmol) in 1M NaOH (2.5 mL) was added resulting in an orange precipitate which was collected by filtration and dried in a desicator over night. The crude material was purified by column chromatography (R_f: 0.32, 2% MeOH in diethyl ether, silica 60) to give product as an orange solid (0.432 g, 25%).

MP: 192 – 194ºC (no lit. mp found)

MS/ES$^+$ (m/z): 256.2 (10% $[M + H]^+$), 278.2 (40% $[M + Na]^+$), 310.1 (100% $[M + Na + MeOH]^+$), 533.2 (60% $[2M + Na]^+$).

MS/ES$^-$ (m/z): 254.1 (100% $[M - H]^-$).

HRMS (ES$^+$): $C_{14}H_{14}N_3O_2$ Expected (m/z): 256.1081, Found: 256.1082.

^{1}H-NMR (300MHz, MeOD): 7.81 (d, J = 8.8, **H-6**), 7.79 (d, J = 8.6, **H-5**), 7.71 (2H, d, J = 8.9, **H-11**), 6.91 (2H, dt, J = 8.9, 3.0, **H-12**), 2.16 (3H, s, **H-1**).

^{13}C-NMR (75MHz, MeOD): 171.8 (**C-2**), 161.9 (**C-13**), 150.3 (**C-7**), 147.5 (**C-10**), 142.0 (**C-4**), 125.8 (**C-11**), 124.2 (**C-6**), 121.1 (**C-5**), 116.7 (**C-12**), 24.0 (**C-1**).

FTIR ν_{max} (cm^{-1}): 3388 (w, N-H carbamate stretch), 3300 – 2900 (O-H broad stretch), (solid state) 1673 (m, C=O carbamate stretch), 1501 (N=N azo stretch).

Combustion:	Theoretical	C 65.87%, H 5.13%, N 16.45%
analysis	Found	C 64.62%, H 5.52%, N 16.06%

Procedure followed from, and is consistent with, literature.[432]

2-(4-(4-(Acetamidophenyl)diazenyl)phenoxy)acetic acid (208)

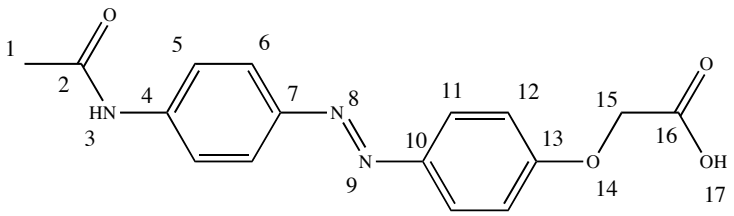

$C_{16}H_{15}N_3O_4$

RMM = 313.31

4-Hydroxyazobenzene-4'-acetamide (0.050 g; 0.196 mmol) was dissolved in dry DMF (15 mL). To this solution was added Cs_2CO_3 (0.319 g; 0.980 mmol) portionwise and allowed to stir for 30 minutes resulting in a solution colour change from yellow to red.

Ethyl bromoacetate (0.02 mL; 0.196 mmol) in dry DMF (5 mL) was then added dropwise followed by portionwise addition of sodium iodide (0.029 g; 0.196 mmol). The reaction was warmed to 100ºC and allowed to stir for 18 hr.

The solvent was removed *in vacuo* and the resulting solid partitioned between ether and water (30 mL each). It was observed that a solid formed at the organic/aqueous interface, so this was collected by filtration before the mixture separated. The organic phase was reduced and found to be the same product as the solid by TLC. The organics and the solid were combined and recrystalised from MeOH/petrol 40-60 to give an orange solid (0.019 g, 31%).

MP: 229 – 233ºC

MS/ES^{+} (m/z): 368.2 (100% $[M + Na + MeOH]^{+}$).

MS/ES^{-} (m/z): 254.2 (100%), 312.2 (40% $[M - H]^{-}$).

^{1}H-NMR (300MHz, MeOD): 7.87 (dt, J = 9.2, 2.1, **H-5**), 7.84 (dt, J = 9.1, 2.1, **H-6**), 7.73 (2H, dt, J = 9.0, 2.0, **H-11**), 7.08 (2H, dt, J = 9.1, 2.1, **H-12**), 4.71 (2H, s, H), 3.35 (MeOH), 2.16 (2.9H, s, **H-14**).

FTIR ν_{max} (cm^{-1}) (solid state): 2921 (w, C-H aliphatic stretch), 1601 (w, C=O carboxylic acid stretch), 1500 (w, N=N stretch).

No literature reference was found.

(9*H*-fluoren-9-yl)methyl-3-chloropropylcarbamate (209)

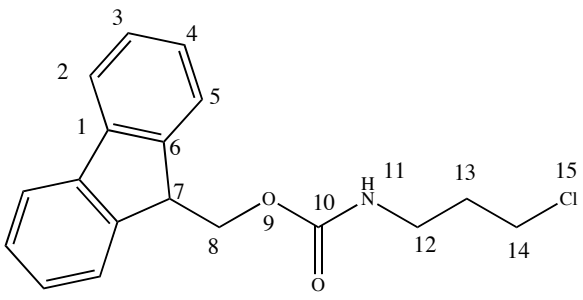

$C_{18}H_{18}ClNO_2$

RMM = 315.89

Triethylamine (0.54 mL; 3.85 mmol) was added to a stirred suspension of 3-chloropropylamine hydrochloride (0.500 g; 3.85 mmol) in acetonitrile/water (10/2 mL). Once dissolved, fmoc-O-succinamide (1.297 g; 3.85 mmol) in acetonitrile (15 mL) was added drop-wise and the reaction mixture stirred for 18 hrs.

The solvent was removed *in vacuo* to give a yellow solid. This was dissolved in DCM (20 mL) and washed with water (20 mL), 1M HCl (20 mL), sat. $NaHCO_3$ (20 mL) and water (20 mL). The organic phase was dried and concentrated *in vacuo* to give crude product as a yellow solid which was purified by column chromatography (R_f: 0.66, 3% MeOH in DCM, silica 60) to give product as a white solid (1.024 g, 84%).

MP: 106 – 107ºC

MS/ES^+ (m/z): 316.1 (10% $[M + H]^+$), 338.1 (100% $[M + Na]^+$). Chlorine isotope splitting observed.

HRMS (ES^+): $C_{18}H_{18}ClNNaO_2$ Expected (m/z): 338.0918, Found: 338.0912.

^{1}H-NMR (400MHz, MeOD): 7.77 (2H, d, J = 7.5, **H-2**), 7.59 (2H, d, J = 7.5, **H-5**), 7.41 (2H, t, J = 7.4, **H-3**), 7.32 (2H, t, J = 7.4, **H-4**), 4.89 (s (br), **H-11**), 4.44 (2H, d, J = 6.4, **H-8**), 4.22 (1H, t, J = 6.5, **H-7**), 3.57 (2H, t, J = 11.9, **H-14**), 3.36 (2H, d, J = 6.1, **H-12**), 1.99 (2 H, t (br), J = 5.8, **H-13**).

^{13}C-NMR (100MHz, MeOD): 156.4 (**C-10**), 143.9 (**C-6**), 141.3 (**C-1**), 127.7 (**C-3**), 127.0 (**C-4**), 124.9 (**C-5**), 120.0 (**C-2**), 65.6 (**C-8**), 47.3 (**C-7**), 42.2 (**C-14**), 38.3 (**C-12**), 32.4 (**C-13**).

FTIR ν_{max} (cm^{-1}) (solid state): 3339 (s, N-H carbamate stretch), 3065 (w, C-H [Ar] stretch), 2952 (m, C-H aliphatic stretch), 1692 (s, C=O carbamate stretch).

Combustion analysis:	Theoretical	C 68.46%, H 5.74%, N 4.43%
	Found	C 68.53%, H 5.91%, N 4.48%

No literature reference was found.

(9*H*-fluoren-9-yl)methyl-3-bromopropylcarbamate (210)

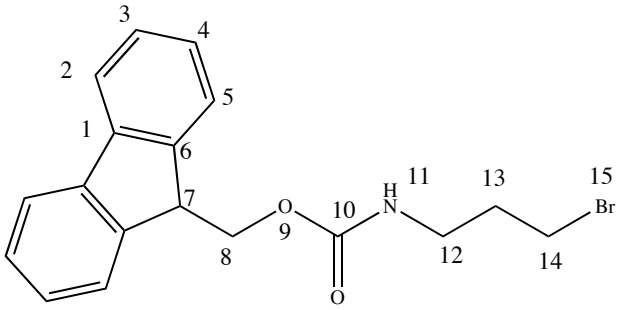

$C_{18}H_{18}BrNO_2$

RMM = 360.25

Method: as for (9 *H*-fluoren-9-yl)methyl-3-chloropropylcarbamate

3-Bromopropylamine hydrobromide (0.500 g; 2.284 mmol)

Fmoc-O-succinamide (0.770 g; 2.284 mmol)

Triethylamine (0.35 mL; 2.500 mmol)

Purification: Column chromatography (R_f: 0.74, 2% MeOH in DCM, silica 60), recrystalised from DCM/petrol

Product: White crystals (0.561 g; 68%).

MP: 86 – 88ºC (no lit. mp found)

MS/ES$^+$ (m/z): 382.1 (100% $[M + Na]^+$), 384.1 (100% $[M + Na]^+$). Br isotope splitting observed.

HRMS (ES$^+$): $C_{18}H_{18}BrNNaO_2$ (^{79}Br) Expected (m/z): 382.0413, Found: 382.0406.

^{1}H-NMR (400MHz, $CDCl_3$): 7.78 (2H, d, J = 7.5, **H-2**), 7.59 (2H, d, J = 7.5, **H-5**), 7.41 (2H, t, J = 7.4, **H-3**), 7.32 (2H, t, J = 7.4, **H-4**), 4.89 (1H, s (br), **H-11**), 4.44 (2H, d (br), **H-8**), 4.22 (1H, d, J = 6.5, **H-7**), 3.42 (2H, s (br), **H-14**), 3.35 (2H, s (br), **H-12**), 2.01 (2H, t (br), J = 5.8, **H-13**).

^{13}C-NMR: (100MHz, $CDCl_3$)	156.4 (**C-10**), 143.9 (**C-6**), 141.3 (**C-1**), 127.7 (**C-3**), 127.0 (**C-4**), 124.9 (**C-5**), 120.0 (**C-2**), 65.5 (**C-8**), 47.3 (**C-7**), 39.4 (**C-12**), 32.4 (**C-13**), 30.8 (**C-14**).	
FTIR ν_{max} (cm^{-1}): (solid state)	3338 (s, N-H carbamate stretch), 3065 (w, C-H [Ar] stretch), 2952 (m, C-H aliphatic stretch), 1692 (s, C=O carbamate stretch).	
Combustion: analysis	Theoretical	C 60.01%, H 5.04%, N 3.89%
	Found	C 59.99%, H 5.23%, N 3.91%

Product is consistent with literature.[439]

(9*H*-fluoren-9-yl)methyl 2-(2-bromoacetamido)ethylcarbamate (211)

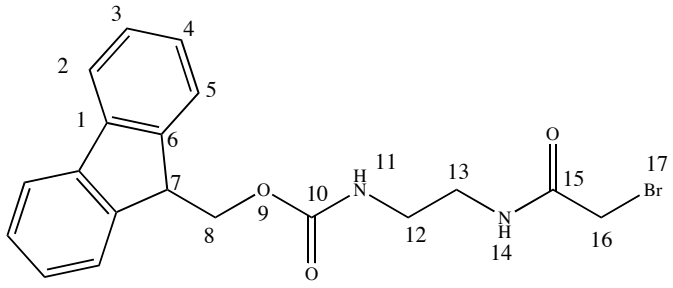

$C_{19}H_{19}BrN_2O_3$

RMM = 403.27

Fmoc-EDA•HCl (0.052 g; 0.164 mmol) was dissolved in MeOH (5 mL) and an excess of $NaHCO_3$ was added. After stirring for 30 minutes, the solvent was removed and the amine extracted into DCM (20 mL).

The free amine (0.030 g; 0.11 mmol) in dry DCM (10 mL) was added dropwise over 1 hr to a stirred solution of bromo acetylbromide (0.009 mL; 0.11 mmol) and triethylamine (0.028 mL; 0.20 mmol) in dry DCM (10 mL).

After 18 hrs the solvent was removed. The resulting solid was then dissolved in DCM (20 mL) and washed with water (2 x 20 mL), 2M HCl (2 x 20 mL), sat. $NaHCO_3$ (2 x 20 mL) and water (20 mL). The organic phase was dried over $MgSO_4$ and reduced to give white solid. This was purified by column chromatography (R_f: 0.46, 2% MeCN in diethyl ether, silica 60) to give product as a white solid (0.024 g; 55%).

MP: 178 – 180ºC

MS/ES$^+$ (m/z): 425.2 (100% $[M + Na]^+$), 427.2 (100% $[M + Na]^+$). Br splitting observed.

^{1}H-NMR (300MHz, DMSO): 7.89 (2H, d, J = 7.3, **H-2**), 7.68 (2H, d, J = 7.3, **H-5**), 7.41 (t, J = 7.4, **H-3**), 7.32 (t, J = 7.3, **H-4**), 5.74 (DCM), 4.31 (2H, d, J = 6.8, **H-8**), 4.21 (1H, t, J = 6.7, **H-7**), 3.83 (3H, s, **H-16**), 3.12 (d (br), J = 5.6, **H-13**), 3.06 (d (br), J = 6.7, **H-12**), 1.35 (1H, s).

^{13}C-NMR (75MHz, DMSO): 144.0 (**C-6**), 140.6 (**C-1**), 127.5 (**C-3**), 127.0 (**C-4**), 125.1 (**C-5**), 120.0 (**C-2**), 65.3 (**C-8**), 54.8 (DCM), 46.6 (**C-7**), 39.2 (**C-12**), 38.9 (**C-13**), 29.4 (**C-16**).

No literature reference was found.

Benzyl 4-aminobenzylcarbamate (213)

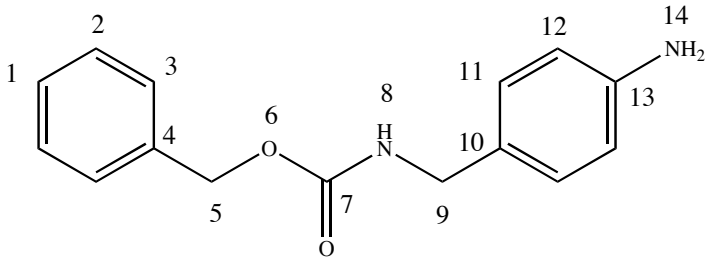

$C_{15}H_{16}N_2O_2$

RMM = 256.30

Benzyl chloroformate (0.84 mL; 5.86 mmol) in dry DCM (20 mL) was added drop-wise over 30 min to a solution of 4-aminobenzylamine (0.93 mL; 8.20 mmol) and triethylamine (5 drops) in dry DCM (40 mL) at 0 ºC. The reaction was stirred at 0 ºC for 1 hr before being warmed to room temperature and stirred for a further 2 hrs.

The reaction mixture was washed with 2M HCl (3 x 30 mL). The acidic aqueous phase was then neutralised with $NaHCO_3$ and extracted with DCM (3 x 40 mL). The combined organic extracts were dried over Na_2CO_3, filtered, and reduced *in vacuo* to give an orange oil. The product was further purified by column chromatography (R_f: 0.62, 10% MeOH in DCM, silica 60) to give product as an orange oil (0.7173 g; 48%).

MS/ES$^+$ (m/z): 257.1 (75% $[M + H]^+$), 279.1 (70% $[M + Na]^+$), 303.2 (75%), 513.2 (100% $[2M + H]^+$), 535.2 (95% $[2M + Na]^+$).

^{1}H NMR (400 MHz, $CDCl_3$): 7.36 (5H, m, **H-1/2/3**), 7.08 (2H, d, J = 8.0, **H-11**), 6.64 (2H, dt, J = 8.4, 1.9, **H-12**), 5.13 (2H, s, **H-5**), 4.26 (2H, d, J = 5.7, **H-9**), 3.62 (2H, s (br), **H-14**).

^{13}C NMR (100 MHz, $CDCl_3$): 156.3 (**C-7**), 145.8 (**C-13**), 136.6 (**C-10**), 128.9 (**C-2**), 128.5 (**C-11**), 128.0 (**C-1/3**), 115.1 (**C-12**), 66.7 (**C-5**), 44.8 (**C-9**).

Product is consistent with literature (and references therein).[440]

4-((4-((Benzyloxycarbonyl)aminomethyl)phenyl)diazenyl)phenol (214)

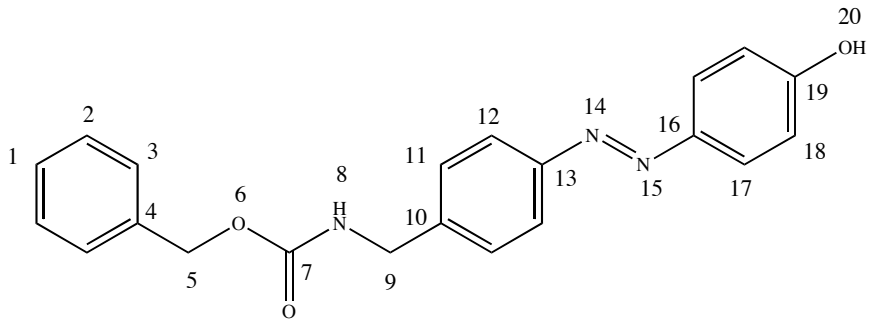

$C_{21}H_{19}N_3O_3$

RMM = 361.40

Conc. HCl (0.25 mL; 8.33 mmol) was added to a suspension of Benzyl 4-aminobenzylcarbamate (0.7173 g; 2.80 mmol) in water (5 mL) and allowed to stir at 0 ºC. After 10 min, sodium nitrite (0.200 g; 2.90 mmol) was added portionwise resulting in an orange suspension. After 40 min, phenol (0.263 g; 2.80 mmol) in 1M NaOH (3 mL) was added dropwise and the resulting orange/red suspension was stirred for 30 min at 0 ºC followed by 1 hr at room temperature. Diethyl ether (20 mL) was added and the phases were separated. The aqueous phase was washed a further 2 times with diethyl ether (30 mL). The organics were combined, dried over Na_2CO_3 and reduced *in vacuo* to give crude product as a red solid. The product was further purified by column chromatography (R_f: 0.37, 40% ethyl acetate in petrol 40-60, silica 60) to give product as a red solid (0.4026 g; 40%).

MP: 131 – 132ºC

MS/ES$^+$ (m/z): 133 (100%), 384.1 (60% $[M + H]^+$).

HRMS (ES$^+$): $C_{21}H_{20}N_3O_3$ Expected (m/z): 362.1499, Found: 362.1497.

^{1}H NMR (400 MHz, $CDCl_3$): 10.27 (1H, s), 7.91 (1H, t, J = 6.0, **H-8**), 7.79 (d, J = 8.7, **H-17**), 7.78 (d, J = 8.1, **H-12**), 7.43 (2H, d, J = 8.2, **H-11**), 7.37 (5H, m, **H-1/2/3**), 6.94 (2H, d, J = 8.9, **H-18**), 5.07 (2H, s, **H-5**), 4.30 (2H, d, J = 8.9, **H-9**).

^{13}C NMR (100 MHz, $CDCl_3$): 160.7 (**C-19**), 156.3 (**C-7**), 151.0 (**C-13**), 145.1 (**C-16**), 142.2 (**C-10**), 137.0 (**C-4**), 128.3 (**C-2**), 127.7 (**C-1/3**), 127.7 (**C-11**), 124.7 (**C-17**), 122.0 (**C-12**), 115.8 (**C-18**), 65.4 (**C-5**), 43.5 (**C-9**).

FTIR ν_{max} (cm^{-1}): (solid state) 3423 (br, O-H stretch), 3312 (s, N-H amide stretch), 3033 (s, [Ar] C-H stretch), 2943 (m, C-H stretch), 1685 (s, C=O formate stretch), 1595 (s, N=N stretch).

Combustion:	Theoretical	C 69.79%, H 5.30%, N 11.62%
analysis	Found	C 69.84%, H 5.33%, N 11.58%

No literature reference was found.

Ethyl 2-(4-((4-((benzyloxycarbonyl)aminomethyl)phenyl)diazenyl)phenoxy)acetate (215)

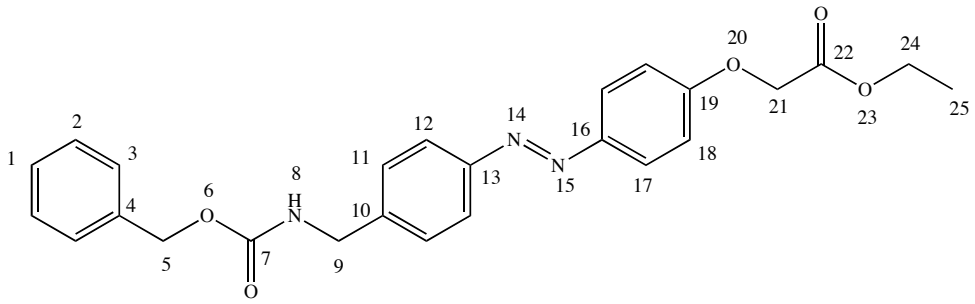

$C_{25}H_{25}N_3O_5$

RMM = 447.49

Potassium carbonate (0.479 g; 3.47 mmol) was added to a solution of 4-((4-((Benzyloxycarbonyl)aminomethyl)phenyl)diazenyl)phenol (0.200 g; 0.554 mmol) in dry acetone (30 mL) and stirred at 30ºC to aid dissolution. Ethyl bromoacetate (0.12 mL; 1.09 mmol) was added dropwise followed by sodium iodide (0.083 g; 0.554 mmol) in dry acetone (3 mL) and the reaction mixture was allowed to reflux for 16 hrs.

The solvent was removed and the resulting solid extracted into diethyl ether (3 x 40 mL) from water (40 mL). The organics were combined, dried over Na_2CO_3 and reduced *in vacuo* to give product as an orange solid (0.1288 g; 52%).

MP: 114 – 116ºC

MS/ES$^+$ (m/z): 470.1 (100% [M + H]$^+$), 694.1 (40% [3M + 2Na]$^+$), 917.4 (40% [2M + Na]$^+$).

HRMS (ES$^+$): $C_{25}H_{26}N_3O_5$ Expected (m/z): 448.1867, Found: 448.1878.

^{1}H NMR (400 MHz, DMSO): 7.92 (t (br), **H-8**), 7.88 (d, J = 8.9, **H-17**), 7.82 (2H, d, J = 8.3, **H-12**), 7.45 (2H, d, J = 8.3, **H-11**), 7.37 (5H, m, **H-1/2/3**), 7.13 (2H, d, J = 9.0, **H-18**), 5.07 (2H, s, **H-5**), 4.92 (2H, s, **H-21**), 4.30 (2H, d, J = 6.1, **H-9**), 4.18 (2H, q, J = 7.1, **H-24**), 1.23 (3H, t, J = 7.1, **H-25**).

^{13}C NMR (100 MHz, DMSO): 168.3 (**C-22**), 160.1 (**C-19**), 156.3 (**C-7**), 150.9 (**C-13**), 146.5 (**C-16**), 142.7 (**C-10**), 137.0 (**C-4**), 128.3 (**C-2**), 127.8 (**C-1/3**), 127.7 (**C-11**), 124.3 (**C-17**), 122.2 (**C-12**), 115.1 (**C-18**), 65.4 (**C-5**), 64.8 (**C-21**), 60.7 (**C-24**), 43.5 (**C-9**), 13.9 (**C-25**).

FTIR ν_{max} (cm^{-1}) (solid state): 3297 (s, N-H amide stretch), 3033 (s, [Ar] C-H stretch), 2914 (m, C-H stretch), 1770 (s, C=O ester stretch), 1686 (s, C=O formate stretch), 1602 (m, N=N stretch).

Combustion analysis		
	Theoretical	C 67.10%, H 5.63%, N 9.39%
	Found	C 66.34%, H 5.63%, N 9.25%

No literature reference was found.

2-(4-((4-((Benzyloxycarbonyl)aminomethyl)phenyl)diazenyl)phenoxy)acetic acid (216)

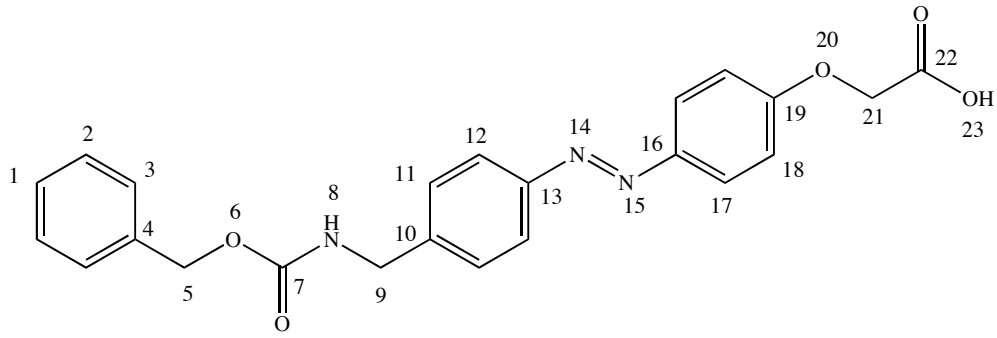

$C_{23}H_{21}N_3O_5$

RMM = 419.43

Ethyl 2-(4-((4-((benzyloxycarbonyl)aminomethyl)phenyl)diazenyl)phenoxy)acetate (0.100 g; 0.224 mmol) was dissolved in ethanol (40 mL) and aqueous sodium hydroxide (15 mL; 0.037 M) was added. The solution was then stirred at RT for 16 hrs. The mixture was acidified (conc. HCl) before the solvents were removed *in vacuo*. The solid was extracted into diethyl ether (3 x 300 mL) from water (50 mL). The organics were combined, dried over Na_2CO_3 and reduced *in vacuo* to give product as a yellow solid (0.0909 g; > 99%).

MP: 202 – 203ºC

MS/ES$^-$ (m/z): 418.1 (100% $[M - H]^-$).

HRMS (ES^+): $C_{23}H_{22}N_3O_5$ Expected (m/z): 420.1554, Found: 420.1558.

^{1}H NMR (400 MHz, DMSO): 13.10 (1H, s, **H-23**), 7.93 (t, J = 5.5, **H-8**), 7.88 (d, J = 8.9, **H-17**), 7.82 (2H, d, J = 8.1, **H-12**), 7.45 (2H, d, J = 8.1, **H-11**), 7.37 (5H, m, **H-1/2/3**), 7.12 (2H, d, J = 8.9, **H-18**), 5.07 (2H, s, **H-5**), 4.81 (2H, s, **H-21**), 4.30 (2H, d, J = 6.0, **H-9**).

^{13}C NMR (100 MHz, DMSO): 169.7 (**C-22**), 160.3 (**C-19**), 156.3 (**C-7**), 150.9 (**C-13**), 146.3 (**C-16**), 142.7 (**C-10**), 137.0 (**C-4**), 128.3 (**C-2**), 127.8 (**C-1/3**), 127.7 (**C-11**),

124.3 (**C-17**), 122.2 (**C-12**), 115.0 (**C-18**), 65.4 (**C-5**), 64.7 (**C-21**), 43.5 (**C-9**).

FTIR ν_{max} (cm^{-1}): (solid state) 3314 (s, N-H amide stretch), 3100-2600 (w (br), O-H stretch), 3034 (w, [Ar] C-H stretch), 2924 (w, C-H stretch), 1706 (s, C=O acid stretch), 1685 (s, C=O formate stretch), 1603 (m, N=N stretch).

No literature reference was found.

2-(4-((4-((Benzyloxycarbonyl)aminomethyl)phenyl)diazenyl)phenoxy)acetyl chloride (217)

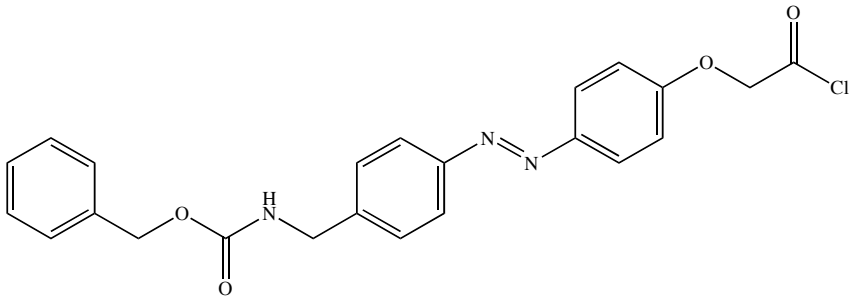

$C_{23}H_{20}ClN_3O_4$

RMM = 437.88

2-(4-((4-((Benzyloxycarbonyl)aminomethyl)phenyl)diazenyl)phenoxy)acetic acid (0.043 g; 0.104 mmol) was added portion wise to stirred thionyl chloride (5 mL; 68.5 mmol) and allowed to reflux under nitrogen for 18 hrs.

The excess thionyl chloride was removed under reduced pressure and the resulting solid dried under high vacuum to give a dark red solid (assumed quantitative conversion and the product was used immediately without further purification (0.043 g).

MP: 79 – 83ºC

No literature reference was found.

4-[EDA]-51-Amine-13-(Cbz-Azo)-x-Acetate-y-(Ethyl thiourea) (218)

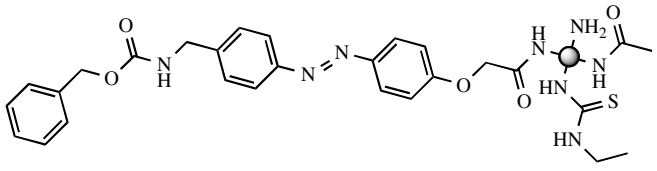

2-(4-((4-((Benzyloxycarbonyl)aminomethyl)phenyl)diazenyl)phenoxy)acetyl chloride (0.043 g; 98.2 μmol) in DMSO (5 mL) was added dropwise to a stirred solution of 4.0-[EDA]-64-Amine (0.100 g; 7.04 μmmol) and triethylamine (15 drops) in DMSO (10 mL) resulting in a 'polymer like' precipitate.

The precipitate was removed by decanting away the solvent (the solid is henceforth known as **218a** whilst the supernatant is **218b**). The solid was found to be insoluble in bench solvents, so DMSO (10 mL) and an excess of acetic anhydride (1 mL) was added and the mixture was allowed to stir for 64 hrs resulting in some dissolution. 2M HCl (40 mL) was added which dissolved the remaining solid over 4 days and then the mixture dialysed against 1M HCL (4 L) for 2 days and then against water (4L) for 3 days to give product as an orange viscous oil. The product was dissolved in water (10 mL) and an excess ethyl isothiocyanate (0.1 mL) was added. The mixture was then dialysed against water (4 L) for a further 3 days (0.0428 g).

The decanted solution (**218b**) had an excess of acetic anhydride (1 mL) added to it and was stirred for 64 hrs. The mixture was dialysed against water (4 L) for 1 day and then against methanol (4 L) for 4 days to give product as an orange viscous oil. The product was dissolved in water (10 mL) and excess ethyl isothiocyanate (0.1 mL) was added. The mixture was then dialysed against methanol (4 L) for a further 3 days (0.0268 g).

218a

^{1}H-NMR (400MHZ, D_2O): 3.63 (s (br)), 3.43 (s (br)), 3.32 (MeOH), 3.24 (q, J = 7.3), 3.07 (25H, s (br), PAMAM), 2.75 (DMSO), 2.57 (44H, s (br), PAMAM), 2.13 (10H, d (br)), 2.00 (10H, s, acetyl), 1.31 (6H, t, J = 7.4), 1.17 (13H, d (br)). Calculated acetyl surface coverage: 19 groups (29%). Calculated ethyl urea surface coverage: 35 groups (55%).

Combustion analysis: C 45.92%, H 7.88%, N 14.86%, S 4.90% N:S ratio suggests 36 sulphur groups present.

218b

^{1}H-NMR (400MHZ, MeOD): 7.51 (1H, m), 7.29 (1H, m), 3.35 (MeOH), 3.28 (s, PAMAM), 2.80 (11H, s (br), PAMAM), 2.66 (DMSO and PAMAM), 2.36 (13H, s (br), PAMAM), 2.12 (4H, d (br)), 1.94 (6H, s, acetyl), 1.29 (2H, s). Calculated acetyl surface coverage: 34 groups (53%). Calculated ethyl urea surface coverage: 13 groups (20%).

FTIR ν_{max} (cm^{-1}) (thin film): 3285 (s (br), N-H stretch), 3080 (m, N-H amide stretch), 2936 (m, C-H aliphatic stretch), 2849 (m, C-H aliphatic stretch), 1647 (s (br), C=O amide stretch), 1556 (s (br), C-C stretch).

No literature reference was found.

4-[EDA]-51-Amine-13-Azo-x-Acetate-y-(Ethyl thiourea) (219)

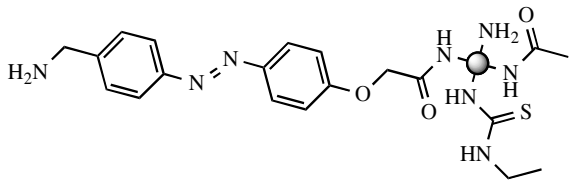

Palladium on carbon (0.005 g) was added to a stirred solution of 4-[EDA]-51-amine-13-(CBZ-Azo)-x-Acetate-y-(Ethyl thiourea) (**218a**) (0.0268 g) in dry ethanol (20 mL). The reaction flask was repeatedly (x 3) flushed with nitrogen then purged under vacuum. Once under vacuum, a balloon containing hydrogen was connected to the flask and the reaction mixture was stirred under hydrogen for 2 days.

The palladium on carbon was removed by filtration and the filtrate was dialysed against methanol for 5 days. The product was reduced to give a viscous orange oil (0.0037 g).

^{1}H-NMR (400MHz, MeOD): 8.10 (1H, s), 3.35 (MeOH), 3.28 S (br), PAMAM), 2.79 (17H, s (br), PAMAM), 2.58 (10H, s (br), PAMAM), 2.36 (20H, s (br), PAMAM), 2.13 (7H, d (br)), 1.94 (10H, s, acetyl), 1.29 (4H, s). Calculated acetyl surface coverage: 40 groups (63%).

No literature reference was found.

4.0-[EDA]-32-Amine-32-Azobenzene (220)

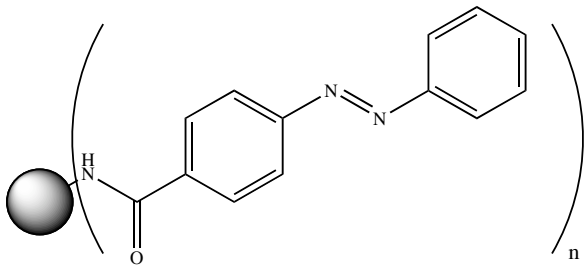

A solution of 4-(phenylazo)benzoyl chloride (0.070 g; 0.286 mmol) in DMSO (2 mL) was added dropwise to a stirred solution of 4.0-[EDA]-64-Amine (0.127 g; 8.90 μmol) and triethylamine (0.06 mL; 0.429 mmol) in DMSO (8 mL). The reaction was warmed to 35ºC and stirred for 64 hrs.

The reaction mixture was then purified by dialysis against water (1 day) followed by 5% water in methanol (2 days). The solvents were removed and the product was further purified by azeotropic distillation to give a viscous orange oil (0.101 g).

^{1}H-NMR (400MHz, MeOD): 8.06 – 6.81 (7H, m, azobenzene), 3.34 (MeOH), 3.23 (s (br), PAMAM), 2.75 (22H, s (br), PAMAM), 2.54 (10H, s (br), PAMAM), 2.34 (23H, s (br), PAMAM). Calculated surface coverage: 10 groups (15%).

^{13}C-NMR (100MHz, MeOD): 175.3, 174.7, 164.2, 132.6 (azo), 131.3 (azo), 130.4 (azo), 124.0 (azo), 123.3 (azo), 120.8 (azo), 53.5, 51.2, 49.9 (MeOH), 41.9, 40.0, 38.7, 34.8, 33.7. Unassigned peaks are due to the PAMAM dendrimer.

Procedure adapted from literature.[257]

References

1 Brown, T. A., *Genomes*, 2nd ed., **2002**, John Wiley & Sons: New York.

2 Kornberg, A.; Baker, T. A., *DNA Replication*, **2005**, W. H. Freeman and Company: New York.

3 Sober, H. A., *Handbook of Biochemistry: Selected Data for Molecular Biology*, 2nd ed., **1970**, Rubber Co.: Cleveland.

4 Watson, J.; Crick, F., *Nature*, **1953**, *171*, 738.

5 Brooker, R. J., *Genetics: Analysis and Principles*, 2nd ed., **2008**, McGraw-Hill: New York.

6 Redon, C.; Pilch, D.; Rogakou, E.; Sedelnikova, O.; Newrock, K.; Bonner, W., *Curr. Opin. Genet. Dev.*, **2002**, *12*, 162.

7 Hood, L.; Galas, D., *Nature*, **2003**, *421*, 444.

8 Wheeler, R., Image Used with Permision.

9 Zhou, Y.; Gerchman, S.; Ramakrishnan, V.; Travers, A.; Muyldermans, S., *Nature*, **1998**, *395*, 402.

10 Travers, A., *Trends Biochem. Sci.*, **1999**, *24*, 4.

11 Wolffe, A.; Bouvet, P.; Dasso, M.; Dimitrov, S.; Hayes, J.; Nightingale, K.; Pruss, D.; Ura, K., *Faseb J.*, **1995**, *9*, 1388.

12 Pennisi, E., *Science*, **1996**, *274*, 503.

13 Esfand, R.; Tomalia, D., *Drug Discov. Today*, **2001**, *6*, 427.

14 Jenuwein, T.; Allis, C., *Science*, **2001**, *293*, 1074.

15 Ito, T., *Curr. Top. Microbiol.*, **2003**, *274*, 1.

16 Pennisi, E., *Science*, **1997**, *275*, 155.

17 Owen, D.; Ornaghi, P.; Yang, J.; Lowe, N.; Evans, P.; Ballario, P.; Neuhaus, D.; Filetici, P.; Travers, A., *Embo J.*, **2000**, *19*, 6141.

18 Zeng, L.; Zhou, M., *Febs Lett.*, **2002**, *513*, 124.

19 Taunton, J.; Hassig, C.; Schreiber, S., *Science*, **1996**, *272*, 408.

20 Berzelius, J. J., *Jahresberchte*, **1933**, *12*, 63.

21 Wisniak, J., *Chem. Educator*, **2000**, *5*, 343.

22 Berzelius, J. J., *Annalen*, **1830**, *19*, 305

23 Simon, E., *Liebigs Ann. Chem.*, **1839**, *31*, 265.

24 Lourenço, A.-V., *Adv. Chem. Phys.*, **1963**, *3*, 257.

25 Lourenço, A.-V., *Compt. Rend.*, **1860**, *51*, 365.

26 Young, R. J.; Lovell, P. A., *Introduction to Polymers*, **1991**, CRC Press: New York.

27 Worden, E., *Nitrocellulose Industry: A Compendium of the History, Chemistry, Manufacture, and Commercial Uses*, **1911**, Van Nostrand: New York.

28 Grafflin, W. M.; Ott, E.; Spurlin, M. H., *Cellulose and Cellulose Derivatives, Part 1*, 2nd ed., **1954**, Interscience: New York.

29 Williams, C., *J. Chem. Soc.*, **1862**, 110.

30 Hancock, T., *The Origin and Progress of the Caoutchouc or India-Rubber Manufacture in England*, **1857**, Charles Macintosh and Co,: London.

31 Goodyear, C., *US Patent RE1,084*, **1844**.

32 Baekeland, L., *Ind. Eng. Chem.*, **1913**, *5*, 506.

33 Wolf, H., *Rubber: A Story of Glory and Greed*, **1936**, Covici & Friede: New York.

34 Herbert, V.; Bisio, A., *Synthetic Rubber: A Project That Had to Succeed*, **1983**, Greenwood Press: Westport, Connecticut.

35 Mülhaupt, R., *Angew. Chem. Int. Edit.*, **2004**, *43*, 1054.

36 Feldman, S. D.; Tauber, A. I., *B. Hist. Med.*, **1997**, *71*, 623.

37 Staudinger, H., *Trans. Faraday Soc.*, **1933**, 18.

38 Staudinger, H., *B. Deut. Chem. Ges.*, **1920**, *53*, 1073.

39 Staudinger, H., *Trans. Faraday Soc.*, **1936**, *32*, 323.

40 Meisel, I., *Macromol. Chem. Phys.*, **2003**, *204*, 199.

41 Spaner, C. *Sales Specification - Neoprene, DuPont Performance Elastomers* **2009**.

42 Carothers, W.; Mark, H.; Whitby, G., *Collected Papers of Wallace Hume Carothers on High Polymeric Substances*, **1940**, Wiley-Interscience: New York.

43 Carothers, W.; Arvin, J., *J. Am. Chem. Soc.*, **1929**, *31*, 2560.

44 Carothers, W.; Natta, F., *J. Am. Chem. Soc.*, **1930**, *52*, 314.

45 Carothers, W.; Dorough, G., *J. Am. Chem. Soc.*, **1930**, *52*, 711.

46 Carothers, W.; Arvin, J.; Dorough, G., *J. Am. Chem. Soc.*, **1930**, *52*, 3292.

47 Carothers, W.; Hill, J.; Kirby, J., *J. Am. Chem. Soc.*, **1930**, *52*, 5270.

48 Carothers, W.; Berchet, G., *J. Am. Chem. Soc.*, **1930**, *52*, 5289.

49 Ziegler, K.; Holzkamp, E.; Breil, H.; Martin, H., *Angew. Chem.*, **1955**, *67*, 541.

50 Natta, G.; Pino, P.; Corradini, P.; Danusso, F.; Mantica, E.; Mazzanti, G.; Moraglio, G., *J. Am. Chem. Soc.*, **1955**, *77*, 1708.

51 Bawn, C., *Nature*, **1979**, *280*, 707.

52 Flory, P. J., *Principles of Polymer Chemistry*, **1953**, Cornell University Press: New York.

53 Flory, P. J., *J. Chem. Phys.*, **1941**, *9*, 660.

54 Huggins, M. L., *J. Chem. Phys.*, **1941**, *9*, 440.

55 Hill, T. L., *An Introduction to Statistical Thermodynamics*, **1986**, Dover Publications: New York.

56 Manesiotis, P.; Borrelli, C.; Aureliano, C. S. A.; Svensson, C.; Sellergren, B., *J. Mater. Chem.*, **2009**, *19*, 6185.

57 Stevens, M. P., *Polymer Chemistry: An Introduction*, **1999**, Oxford University Press: New York.

58 Miller, M. L., *The Structure of Polymers*, 2nd ed., **1966**, Reinhold Publishing Corporation: New York.

59 Schildknecht, C. E., *Polymer Processes: Chemical Technology of Plastics, Resins, Rubbers, Adhesives and Fibers*, **1956**, Interscience Publications Ltd: London.

60 Cowie, J. M. G., *Polymers: Chemistry and Physics of Modern Materials*, **1974**, Intext Educational Publishers: New York.

61 Nicholson, J. W., *The Chemistry of Polymers*, **1997**, The Royal Society of Chemistry: Cambridge.

62 Carothers, W., *J. Am. Chem. Soc.*, **1929**, *51*, 2548.

63 Mita, I.; Stepto, R.; Suter, U., *Pure Appl. Chem.*, **1994**, *66*, 2483.

64 Carothers, W., *US Patent 2,130,523*, **1938**.

65 Carothers, W., *US Patent 2,130,948*, **1938**.

66 Carothers, W., *US Patent 2,130,947*, **1938**.

67 Parsons, A. F., *An Introduction to Free Radical Chemistry*, **2000**, University Press: Cambridge.

68 Rhodes, S. K.; Lambeth, R. H.; Gonzales, J.; Moore, J. S.; Lewis, J. A., *Langmuir*, **2009**, *25*, 6787.

69 Liang, Y.-H.; Wang, C.-C.; Chen, C.-Y., *J. Power Sources*, **2008**, *176*, 340.

70 Du, N.; Song, J.; Robertson, G. P.; Pinnau, I.; Guiver, M. D., *Macromol. Rapid Comm.*, **2008**, *29*, 783.

71 Kudo, H.; Shigematsu, K.; Milani, K.; Nishikubo, T.; Kasuga, N. C.; Uekusa, H.; Ohashi, Y., *Macromolecules*, **2008**, *41*, 2030.

72 Gibson, H.; Hamilton, L.; Yamaguchi, N., *Polym Advan Technol*, **2000**, *11*, 791.

73 Stoddart, J. F., *Chem. Soc. Rev.*, **2009**, *38*, 1802.

74 Takata, T.; Kihara, N.; Furusho, Y., *Adv. Polym. Sci.*, **2004**, *171*, 1.

75 Stoddart, J. F., *Chem. Soc. Rev.*, **2009**, *38*, 1521.

76 Watanabe, N.; Ikari, Y.; Kihara, N.; Takata, T., *Macromolecules*, **2004**, *37*, 6663.

77 Tomalia, D.; Baker, H.; Dewald, J.; Hall, M.; Kallos, G.; Martin, S.; Roeck, J.; Ryder, J.; Smith, P., *Polym. J.*, **1985**, *17*, 117.

78 Klajnert, B.; Bryszewska, M., *Acta Biochim. Pol.*, **2001**, *48*, 199.

79 Fréchet, J. M. J., *Proc. Natl. Acad. Sci. USA*, **2002**, *99*, 4782.

80 Helms, B.; Mynar, J. L.; Hawker, C. J.; Fréchet, J. M. J., *J. Am. Chem. Soc.*, **2004**, *126*, 15020.

81 Newkome, G.; Shreiner, C., *Polymer*, **2008**, *49*, 1.

82 Vert, M., *Biodegradable Polymers and Plastics*, **1992**, Redwood Press Ltd: Melksham, Wiltshire.

83 Le Bras, M., *Fire Retardancy of Polymers: The Use of Intumescence*, **1998**, European Meeting on Fire Retardancy of Polymeric Materials: University of Lille.

84 Flick, E. W., *Plastics Additives: An Industrial Guide*, **1986**, Noyes: Park Ridge, New Jersey.

85 Lutz, J. T., *Thermoplastic Polymer Additives*, **1988**, Dekker: New York.

86 Stevens, M., *J. Chem. Educ.*, **1993**, *70*, 444.

87 Štěpek, J.; Daoust, H., *Additives for Plastics*, **1983**, Springer-Verlag: New York.

88 Ibert, M., *Industrial Plasticizers*, **1963**, Macmillan: New York.

89 Sears, J. K.; Darby, J. R., *The Technology of Plasticizers*, **1982**, Wiley-Interscience: New York.

90 Buhleier, E.; Wehner, W.; Vogtle, F., *Synthesis-Stuttgart*, **1978**, 155.

91 Flory, P.; Rehner Jr, J., *J. Chem. Phys.*, **1943**, *11*, 512.

92 Flory, P., *J. Am. Chem. Soc.*, **1952**, *74*, 2718.

93 Stockmayer, W., *J. Chem. Phys.*, **1944**, *12*, 125.

94 Gordon, M.; Malcolm, G., *Proc. R. Soc. London Ser. A Mat.*, **1966**, *295*, 29.

95 Dusek, K., *Makromol. Chem.*, **1979**, 35.

96 Graessley, W., *Macromolecules*, **1975**, *8*, 186.

97 Graessley, W., *Macromolecules*, **1975**, *8*, 865.

98 Good, I., *Proc. R. Soc. London Ser. A Mat.*, **1963**, *272*, 54.

99 Fréchet, J. M. J.; Tomalia, D. A., *Dendrimers and Other Dendritic Polymers*, **2001**, Wiley: New York.

100 Tomalia, D. A.; Naylor, A. M.; Goddard, W. A., *Angew. Chem. Int. Edit.*, **1990**, *29*, 138.

101 Denkewalter, R.; Kolc, J.; Lukasavage, W., *US Patent 4,289,872*, **1981**.

102 Aharoni, S.; Crosby, C.; Walsh, E., *Macromolecules*, **1982**, *15*, 1093.

103 Degennes, P.; Hervet, H., *J. Phys. Lett.-Paris*, **1983**, *44*, 351.

104 Tomalia, D.; Baker, H.; Dewald, J.; Hall, M.; Kallos, G.; Martin, S.; Roeck, J.; Ryder, J.; Smith, P., *Macromolecules*, **1986**, *19*, 2466.

105 Tomalia, D.; Dewald, J., *US Patent 4,507,466*, **1985**.

106 Tomalia, D.; Dewald, J., *US Patent 4,558,120*, **1985**.

107 Tomalia, D.; Dewald, J., *US Patent 4,568,737*, **1986**.

108 Tomalia, D.; Dewald, J., *US Patent 4,587,329*, **1986**.

109 Tomalia, D.; Dewald, J., *US Patent 4,631,337*, **1986**.

110 Tomalia, D.; Wilson, L., *US Patent 4,713,975*, **1987**.

111 Tomalia, D., *US Patent 4,737,550*, **1988**.

112 Tomalia, D.; Stahlbush, J., *US Patent 4,857,599*, **1989**.

113 Killat, G.; Tomalia, D., *US Patent 4,871,779*, **1989**.

114 Moors, R.; Vogtle, F., *Chem. Ber.-Recl.*, **1993**, *126*, 2133.

115 Newkome, G.; Yao, Z.; Baker, G.; Gupta, V., *J. Org. Chem.*, **1985**, *50*, 2003.

116 Newkome, G.; Yao, Z.; Baker, G.; Gupta, V.; Russo, P.; Saunders, M., *J. Am. Chem. Soc.*, **1986**, *108*, 849.

117 Newkome, G.; Baker, G.; Saunders, M.; Russo, P.; Gupta, V.; Yao, Z.; Miller, J.; Bouillion, K., *J. Chem. Soc. Chem. Comm.*, **1986**, 752.

118 Hallé, F.; Oldeman, R. A. A.; Tomlinson, P. B., *Tropical Trees and Forests: An Architectural Analysis*, **1978**, Springer: Verlag, Berlin.

119 Fréchet, J. M. J.; Jiang, Y.; Hawker, C. J.; Philippides, A. E., *Proc. IUPAC Int. Symp. Marcromol. Seoul*, **1989**, 19.

120 Frechet, J.; Hawker, C.; Philippides, A., *US Patent 5,041,516*, **1991**.

121 Hawker, C.; Frechet, J., *J. Chem. Soc. Chem. Comm.*, **1990**, 1010.

122 Hawker, C.; Frechet, J., *J. Am. Chem. Soc.*, **1990**, *112*, 7638.

123 Turro, N.; Barton, J.; Tomalia, D., *Acc. Chem. Res.*, **1991**, *24*, 332.

124 Hawker, C.; Frechet, J., *Macromolecules*, **1990**, *23*, 4726.

125 Wooley, K.; Hawker, C.; Frechet, J., *J. Chem. Soc. Perk. T. 1*, **1991**, 1059.

126 Wooley, K.; Hawker, C.; Frechet, J., *J. Am. Chem. Soc.*, **1991**, *113*, 4252.

127 Hawker, C. J.; Wooley, K. L.; Lee, R.; Fréchet, J. M. J., *Polym. Mat. Sci. Eng.*, **1991**, *64*, 73.

128 Hawker, C.; Frechet, J., *Polymer*, **1992**, *33*, 1507.

129 Hawker, C.; Frechet, J., *J. Am. Chem. Soc.*, **1992**, *114*, 8405.

130 Uhrich, K.; Boegeman, S.; Frechet, J.; Turner, S., *Polym. Bull.*, **1991**, *25*, 551.

131 Tomalia, D.; Hedstrand, D.; Ferritto, M., *Macromolecules*, **1991**, *24*, 1435.

132 Gauthier, M.; Moller, M., *Macromolecules*, **1991**, *24*, 4548.

133 Gauthier, M., *J. Polym. Sci. Pol. Chem.*, **2007**, *45*, 3803.

134 Teertstra, S.; Gauthier, M., *Prog. Polym. Sci.*, **2004**, *29*, 277.

135 Shu, L.; Schafer, T.; Schluter, A., *Macromolecules*, **2000**, *33*, 4321.

136 Carlmark, A.; Hawker, C.; Hult, A.; Malkoch, M., *Chem. Soc. Rev.*, **2009**, *38*, 352.

137 Zhang, A.; Shu, L.; Bo, Z.; Schluter, A., *Macromol. Chem. Physic.*, **2003**, *204*, 328.

138 Paul, D.; Miyake, H.; Shinoda, S.; Tsukube, H., *Chem. Eur. J.*, **2006**, *12*, 1328.

139 Kudo, H.; Inoue, H.; Inagaki, T.; Nishikubo, T., *Macromolecules*, **2009**, *42*, 1051.

140 Deschenaux, R.; Donnio, B.; Guillon, D., *New J. Chem.*, **2007**, *31*, 1064.

141 Langereis, S.; Dirksen, A.; Hackeng, T. M.; Van Genderen, M. H. P.; Meijer, E. W., *New J. Chem.*, **2007**, *31*, 1152.

142 Debrabandervandenberg, E.; Meijer, E., *Angew. Chem. Int. Edit.*, **1993**, *32*, 1308.

143 Mansfield, M., *Macromolecules*, **1993**, *26*, 3811.

144 Miller, T.; Neenan, T., *Chem. Mater.*, **1990**, *2*, 346.

145 Miller, T.; Neenan, T.; Zayas, R.; Bair, H., *J. Am. Chem. Soc.*, **1992**, *114*, 1018.

146 Matthews, O.; Shipway, A.; Stoddart, J., *Prog. Polym. Sci.*, **1998**, *23*, 1.

147 Uhrich, K.; Frechet, J., *J. Chem. Soc. Perk. T. 1*, **1992**, 1623.

148 Rengan, K.; Engel, R., *J. Chem. Soc. Perk. T. 1*, **1991**, 987.

149 Miller, T.; Neenan, T.; Kwock, E.; Stein, S., *J. Am. Chem. Soc.*, **1993**, *115*, 356.

150 Feast, W.; Stainton, N., *J. Mater. Chem.*, **1994**, *4*, 1159.

151 Kawaguchi, T.; Walker, K.; Wilkins, C.; Moore, J., *J. Am. Chem. Soc.*, **1995**, *117*, 2159.

152 Rebov, E. A.; Muzafarov, A. M.; Papkov, V. S.; Zhdanov, A. A., *Dokl. Akad. Nauk. SSSR*, **1990**, *309*, 376.

153 Seyferth, D.; Son, D.; Rheingold, A.; Ostrander, R., *Organometallics*, **1994**, *13*, 2682.

154 Launay, N.; Caminade, A.; Majoral, J., *J. Am. Chem. Soc.*, **1995**, *117*, 3282.

155 Twyman, L.; Beezer, A.; Mitchell, J., *Tetrahedron Lett.*, **1994**, *35*, 4423.

156 Nagasaki, T.; Ukon, M.; Arimori, S.; Shinkai, S., *J. Chem. Soc. Chem. Comm.*, **1992**, 608.

157 Zhang, W.; Xie, J.; Shi, W., *Eur. Polym. J.*, **2007**, *43*, 2387.

158 Achar, S.; Puddephatt, R., *Organometallics*, **1995**, *14*, 1681.

159 Campagna, S.; Denti, G.; Serroni, S.; Juris, A.; Venturi, M.; Ricevuto, V.; Balzani, V., *Chem.-Eur. J.*, **1995**, *1*, 211.

160 Balzani, V.; Juris, A.; Venturi, M.; Campagna, S.; Serroni, S., *Chem. Rev.*, **1996**, *96*, 759.

161 Bielinska, A. U.; Kukowska-Latallo, J. F.; Baker, J. R., *Biochim. Biophys. Acta*, **1997**, *1353*, 180.

162 Tang, M. X.; Redemann, C. T.; Szoka, F. C., *Bioconjugate Chem.*, **1996**, *7*, 703.

163 Roberts, J. C.; Bhalgat, M. K.; Zera, R. T., *J. Biomed. Mater. Res.*, **1996**, *30*, 53.

164 Newkome, G.; Baker, G.; Arai, S.; Saunders, M.; Russo, P.; Theriot, K.; Moorefield, C.; Rogers, L.; Miller, J.; Lieux, T.; Murray, M.; Phillips, B.; Pascal, L., *J. Am. Chem. Soc.*, **1990**, *112*, 8458.

165 Majoros, I. N. J.; Williams, C. R.; Tomalia, D. A.; Baker, J. R., *Macromolecules*, **2008**, *41*, 8372.

166 Galliot, C.; Larre, C.; Caminade, A.; Majoral, J., *Science*, **1997**, *277*, 1981.

167 Elizarov, A.; Chang, T.; Chiu, S.; Stoddart, J., *Org. Lett.*, **2002**, *4*, 3565.

168 Wendland, M.; Zimmerman, S., *J. Am. Chem. Soc.*, **1999**, *121*, 1389.

169 Kolb, H.; Finn, M.; Sharpless, K., *Angew. Chem. Int. Edit.*, **2001**, *40*, 2004.

170 Kolb, H. C.; Sharpless, K. B., *Drug Discov. Today*, **2003**, *8*, 1128.

171 Wu, P.; Feldman, A.; Nugent, A.; Hawker, C.; Scheel, A.; Voit, B.; Pyun, J.; Frechet, J.; Sharpless, K.; Fokin, V., *Angew. Chem. Int. Edit.*, **2004**, *43*, 3928.

172 Malkoch, M.; Schleicher, K.; Drockenmuller, E.; Hawker, C.; Russell, T.; Wu, P.; Fokin, V., *Macromolecules*, **2005**, *38*, 3663.

173 Lee, J.; Kim, B.; Kim, J.; Shin, W.; Jin, S., *Bull. Korean Chem. Soc.*, **2005**, *26*, 1790.

174 Lee, J. W.; Kim, J. H.; Kim, H. J.; Han, S. C.; Kim, J. H.; Shin, W. S.; Jin, S.-H., *Bioconjugate Chem.*, **2007**, *18*, 579.

175 Lee, J. W.; Kim, J. H.; Han, S. C.; Kim, W. R.; Kim, B.-K.; Kim, J. H.; Huh, D.-S.; Shin, W. S.; Jin, S.-H., *Macromol. Symp.*, **2007**, *249-250*, 357.

176 Lee, J. W.; Kim, B.-K.; Kim, J. H.; Shin, W. S.; Jin, S.-H., *J. Org. Chem.*, **2006**, *71*, 4988.

177 Wang, G.; Luo, X.; Liu, C.; Huang, J., *J. Polym. Sci. A*, **2008**, *46*, 2154.

178 Naylor, A.; Goddard, W.; Kiefer, G.; Tomalia, D., *J. Am. Chem. Soc.*, **1989**, *111*, 2339.

179 Maiti, P.; Cagin, T.; Wang, G.; Goddard, W., *Macromolecules*, **2004**, *37*, 6236.

180 Maciejewski, M., *J. Macromol. Sci. Chem.*, **1982**, *A17*, 689.

181 Richards, F., *Annu. Rev. Biophys. Bio.*, **1977**, *6*, 151.

182 Tomalia, D.; Hall, M.; Hedstrand, D., *J. Am. Chem. Soc.*, **1987**, *109*, 1601.

183 Maiti, P.; Cagin, T.; Lin, S.; Goddard, W., *Macromolecules*, **2005**, *38*, 979.

184 Prosa, T.; Bauer, B.; Amis, E.; Tomalia, D.; Scherrenberg, R., *J. Polym. Sci., Part B*, **1997**, *35*, 2913.

185 Rathgeber, S.; Monkenbusch, M.; Kreitschmann, M.; Urban, V.; Brulet, A., *J. Chem. Phys.*, **2002**, *117*, 4047.

186 Topp, A.; Bauer, B.; Tomalia, D.; Amis, E., *Macromolecules*, **1999**, *32*, 7232.

187 Meltzer, A.; Tirrell, D.; Jones, A.; Inglefield, P.; Tomalia, D. A.; Hedstrand, D. M., *Macromolecules*, **1992**, *25*, 4541.

188 Meltzer, A.; Tirrell, D.; Jones, A.; Inglefield, P., *Macromolecules*, **1992**, *25*, 4549.

189 Van-Quynh, A.; Filip, D.; Cruz, C.; Sebastiao, P.; Ribeiro, A.; Rueff, J.; Marcos, M.; Serrano, J., *Eur. Phys. J. E.*, **2005**, *18*, 149.

190 Topp, A.; Bauer, B.; Klimash, J.; Spindler, R., *Macromolecules*, **1999**, *32*, 7226.

191 Malveau, C.; Baille, W.; Zhu, X.; Ford, W., *J. Polym. Sci., Part B*, **2003**, *41*, 2969.

192 Bakshi, M. S.; Sood, R.; Ranganathan, R.; Shin, P., *Colloid Polym. Sci.*, **2005**, *284*, 58.

193 Moreno, K.; Simanek, E., *Macromolecules*, **2008**, *41*, 4108.

194 Rathgeber, S.; Monkenbusch, M.; Hedrick, J. L.; Trollså S, M.; Gast, A. P., *J. Chem. Phys.*, **2006**, *125*, 204908.

195 Rosenfeldt, S.; Dingenouts, N.; Pötschke, D.; Ballauff, M., *J. Lumin.*, **2005**, *111*, 225.

196 Chen, W.; Porcar, L.; Liu, Y.; Butler, P.; Magid, L., *Macromolecules*, **2007**, *40*, 5887.

197 Lescanec, R.; Muthukumar, M., *Macromolecules*, **1990**, *23*, 2280.

198 Naylor, A. M.; Goddard Iii, W. A., *Polym. Prepr.*, **1988**, *29*, 215.

199 Lee, H.; Baker, J.; Larson, R., *J. Phys. Chem. B*, **2006**, *110*, 4014.

200 Lin, S.; Maiti, P.; Goddard, W., *J. Phys. Chem. B*, **2005**, *109*, 8663.

201 Lyulin, A.; Davies, G.; Adolf, D., *Macromolecules*, **2000**, *33*, 6899.

202 Lyulin, S.; Darinskii, A.; Lyulin, A.; Michels, M., *Macromolecules*, **2004**, *37*, 4676.

203 Gunatillake, P.; Odian, G.; Tomalia, D., *Macromolecules*, **1988**, *21*, 1556.

204 Kim, Y.; Webster, O., *Abstr. Pap. Am. Chem. Soc.*, **1988**, *196*, 104.

205 Kim, Y.; Webster, O., *J. Am. Chem. Soc.*, **1990**, *112*, 4592.

206 He, Y.; Wang, X.; Zhou, Q., *Synthetic Met.*, **2003**, *132*, 245.

207 Ding, L.; Zhang, L.; Han, H.; Huang, W.; Song, C.; Xie, M.; Zhang, Y., *Macromolecules*, **2009**, *42*, 5036.

208 Mathias, L.; Carothers, T., *J. Am. Chem. Soc.*, **1991**, *113*, 4043.

209 Hawker, C.; Wooley, K.; Lee, R.; Frechet, J., *Abstr. Pap. Am. Chem. Soc.*, **1991**, *201*, 41.

210 Uhrich, K.; Hawker, C.; Frechet, J.; Turner, S., *Abstr. Pap. Am. Chem. Soc.*, **1991**, *201*, 137.

211 Hawker, C.; Lee, R.; Frechet, J., *J. Am. Chem. Soc.*, **1991**, *113*, 4583.

212 Tomalia, D.; Kirchhoff, P., *US Patent 4,694,064*, **1987**.

213 Yin, R.; Zhu, Y.; Tomalia, D.; Ibuki, H., *J. Am. Chem. Soc.*, **1998**, *120*, 2678.

214 Frauenrath, H., *Prog. Polym. Sci.*, **2005**, *30*, 325.

215 Schluter, A.; Rabe, J., *Angew. Chem. Int. Edit.*, **2000**, *39*, 864.

216 Alonso, B.; Gonzalez, B.; Garcia, B.; Ramirez-Oliva, E.; Zamora, M.; Casado, C.; Cuadrado, I., *J. Organomet. Chem.*, **2001**, *637*, 642.

217 Schluter, A.; Bothe, H.; Gosau, J., *Makromol. Chem.*, **1991**, *192*, 2497.

218 Karakaya, B.; Claussen, W.; Gessler, K.; Saenger, W.; Schluter, A., *J. Am. Chem. Soc.*, **1997**, *119*, 3296.

219 Karakaya, B.; Claussen, W.; Schafer, A.; Lehmann, A.; Schluter, A., *Acta Polym.*, **1996**, *47*, 79.

220 Kaneko, T.; Horie, T.; Asano, M.; Aoki, T.; Oikawa, E., *Macromolecules*, **1997**, *30*, 3118.

221 Tomalia, D., *Sci. Am.*, **1995**, *272*, 62.

222 Tomalia, D., *Adv. Mater.*, **1994**, *6*, 529.

223 Tomalia, D., *High Perform. Polym.*, **2001**, *13*, 1.

224 Khopade, A.; Mohwald, H., *Macromol. Rapid Comm.*, **2005**, *26*, 445.

225 Mcelhanon, J.; Mcgrath, D., *J. Am. Chem. Soc.*, **1998**, *120*, 1647.

226 Pollak, K.; Leon, J.; Frechet, J.; Maskus, M.; Abruna, H., *Chem. Mater.*, **1998**, *10*, 30.

227 Vogtle, F.; Gestermann, S.; Hesse, R.; Schwierz, H.; Windisch, B., *Prog. Polym. Sci.*, **2000**, *25*, 987.

228 Worner, C.; Mulhaupt, R., *Angew. Chem. Int. Edit.*, **1993**, *32*, 1306.

229 Moszner, N.; Volkel, T.; Rheinberger, V., *Macromol. Chem. Physic.*, **1996**, *197*, 621.

230 Gebbink, R.; Bosman, A.; Feiters, M.; Meijer, E.; Nolte, R., *Chem.-Eur. J.*, **1999**, *5*, 65.

231 Stevelmans, S.; Vanhest, J.; Jansen, J.; Vanboxtel, D.; Vandenberg, E.; Meijer, E., *J. Am. Chem. Soc.*, **1996**, *118*, 7398.

232 Baars, M.; Froehling, P.; Meijer, E., *Chem. Commun.*, **1997**, 1959.

233 Valerio, C.; Fillaut, J.; Ruiz, J.; Guittard, J.; Blais, J.; Astruc, D., *J. Am. Chem. Soc.*, **1997**, *119*, 2588.

234 Majoros, I.; Keszler, B.; Woehler, S.; Bull, T.; Baker, J., *Macromolecules*, **2003**, *36*, 5526.

235 Killops, K. L.; Campos, L. M.; Hawker, C. J., *J. Am. Chem. Soc.*, **2008**, *130*, 5062.

236 Kim, R.; Manna, M.; Hutchins, S.; Griffin, P.; Yates, N.; Bernick, A.; Chapman, K., *Proc. Natl. Acad. Sci. USA*, **1996**, *93*, 10012.

237 James, T.; Shinmori, H.; Takeuchi, M.; Shinkai, S., *Chem. Commun.*, **1996**, 705.

238 Wooley, K.; Hawker, C.; Frechet, J., *J. Am. Chem. Soc.*, **1993**, *115*, 11496.

239 Hawker, C.; Wooley, K.; Frechet, J., *J. Chem. Soc. Perk. T. 1*, **1993**, 1287.

240 Moore, J.; Xu, Z., *Macromolecules*, **1991**, *24*, 5893.

241 Xu, Z.; Moore, J., *Angew. Chem. Int. Edit.*, **1993**, *32*, 1354.

242 Devadoss, C.; Bharathi, P.; Moore, J., *J. Am. Chem. Soc.*, **1996**, *118*, 9635.

243 Xu, Z.; Moore, J., *Acta Polym.*, **1994**, *45*, 83.

244 Issberner, J.; Vogtle, F.; Decola, L.; Balzani, V., *Chem.-Eur. J.*, **1997**, *3*, 706.

245 Plevoets, M.; Vogtle, F.; De Cola, L.; Balzani, V., *New J. Chem.*, **1999**, *23*, 63.

246 Tomoyose, Y.; Jiang, D.; Jin, R.; Aida, T.; Yamashita, T.; Horie, K.; Yashima, E.; Okamoto, Y., *Macromolecules*, **1996**, *29*, 5236.

247 Hawker, C.; Frechet, J., *J. Am. Chem. Soc.*, **1990**, *112*, 7638.

248 Diederich, F.; Felber, B., *Proc. Natl. Acad. Sci. USA*, **2002**, *99*, 4778.

249 Newkome, G.; Lin, X.; Young, J., *Synlett*, **1992**, 53.

250 Dirksen, A., *CR. Chim.*, **2003**, *6*, 873.

251 Ghosh, S.; Banthia, A.; Chen, Z., *Tetrahedron*, **2005**, *61*, 2889.

252 Jiang, D.; Aida, T., *Nature*, **1997**, *388*, 454.

253 Liao, L.-X.; Stellacci, F.; Mcgrath, D. V., *J. Am. Chem. Soc.*, **2004**, *126*, 2181.

254 Zollinger, H., *Color Chemistry: Synthesis, Properties and Applications of Organic Dyes*, **1987**, VCH: Weinheim.

255 Schenning, A.; Elissen-Roman, C.; Weener, J.; Baars, M.; Van Der Gaast, S.; Meijer, E., *J. Am. Chem. Soc.*, **1998**, *120*, 8199.

256 Mekelburger, H.; Rissanen, K.; Vogtle, F., *Chem. Ber.-Recl.*, **1993**, *126*, 1161.

257 Archut, A.; Vogtle, F.; De Cola, L.; Azzellini, G.; Balzani, V.; Ramanujam, P.; Berg, R., *Chem.-Eur. J.*, **1998**, *4*, 699.

258 Li, S.; Mcgrath, D., *J. Am. Chem. Soc.*, **2000**, *122*, 6495.

259 Junge, D.; Mcgrath, D., *J. Am. Chem. Soc.*, **1999**, *121*, 4912.

260 Junge, D.; Mcgrath, D., *Chem. Commun.*, **1997**, 857.

261 Ghosh, S.; Banthia, A., *Tetrahedron Lett.*, **2001**, *42*, 501.

262 Grabchev, I.; Chovelon, J.; Bojinov, V.; Ivanova, G., *Tetrahedron*, **2003**, *59*, 9591.

263 Vogtle, F.; Gestermann, S.; Kauffmann, C.; Ceroni, P.; Vicinelli, V.; De Cola, L.; Balzani, V., *J. Am. Chem. Soc.*, **1999**, *121*, 12161.

264 Vogtle, F.; Gestermann, S.; Kauffmann, C.; Ceroni, P.; Vicinelli, V.; Balzani, V., *J. Am. Chem. Soc.*, **2000**, *122*, 10398.

265 Balzani, V.; Ceroni, P.; Gestermann, S.; Gorka, M.; Kauffmann, C.; Vogtle, F., *Tetrahedron*, **2002**, *58*, 629.

266 Grabchev, I.; Bojinov, V.; Chovelon, J., *Polymer*, **2003**, *44*, 4421.

267 Wang, B.-B.; Zhang, X.; Jia, X.-R.; Li, Z.-C.; Ji, Y.; Yang, L.; Wei, Y., *J. Am. Chem. Soc.*, **2004**, *126*, 15180.

268 Hong, S.; Bielinska, A.; Mecke, A.; Keszler, B.; Beals, J.; Shi, X.; Balogh, L.; Orr, B.; Baker, J.; Holl, M., *Bioconjugate Chem.*, **2004**, *15*, 774.

269 Thomas, T.; Myaing, M.; Ye, J.; Candido, K.; Kotlyar, A.; Beals, J.; Cao, P.; Keszler, B.; Patri, A.; Norris, T.; Baker, J., *Biophys. J.*, **2004**, *86*, 3959.

270 Ottaviani, M.; Cossu, E.; Turro, N.; Tomalia, D., *J. Am. Chem. Soc.*, **1995**, *117*, 4387.

271 Jansen, J.; De Brabander-Van Den Berg, E.; Meijer, E., *Science*, **1994**, *266*, 1226.

272 Jansen, J.; Janssen, R.; Debrabandervandenberg, E.; Meijer, E., *Adv. Mater.*, **1995**, *7*, 561.

273 Jansen, J.; Meijer, E.; Debrabandervandenberg, E., *J. Am. Chem. Soc.*, **1995**, *117*, 4417.

274 Liu, M.; Fréchet, J., *Pharm. Sci. Technol. Today.*, **1999**, *2*, 393.

275 Paramonov, S. E.; Bachelder, E. M.; Beaudette, T. T.; Standley, S. M.; Lee, C. C.; Dashe, J.; Fréchet, J. M. J., *Bioconjugate Chem.*, **2008**, *19*, 911.

276 Pistolis, G.; Malliaris, A.; Tsiourvas, D.; Paleos, C., *Chem.-Eur. J.*, **1999**, *5*, 1440.

277 Archut, A.; Azzellini, G.; Balzani, V.; De Cola, L.; Vogtle, F., *J. Am. Chem. Soc.*, **1998**, *120*, 12187.

278 Smith, D.; Hirst, A.; Love, C.; Hardy, J.; Brignell, S.; Huang, B., *Prog. Polym. Sci.*, **2005**, *30*, 220.

279 Huck, W.; Hulst, R.; Timmerman, P.; Vanveggel, F.; Reinhoudt, D., *Angew. Chem. Int. Edit.*, **1997**, *36*, 1006.

280 Huck, W.; Prins, L.; Fokkens, R.; Nibbering, N.; Van Veggel, F.; Reinhoudt, D., *J. Am. Chem. Soc.*, **1998**, *120*, 6240.

281 Suarez, M.; Lehn, J.; Zimmerman, S.; Skoulios, A.; Heinrich, B., *J. Am. Chem. Soc.*, **1998**, *120*, 9526.

282 Zimmerman, S.; Zeng, F.; Reichert, D.; Kolotuchin, S., *Science*, **1996**, *271*, 1095.

283 Zeng, F.; Zimmerman, S., *Chem. Rev.*, **1997**, *97*, 1681.

284 Percec, V.; Johansson, G.; Ungar, G.; Zhou, J., *J. Am. Chem. Soc.*, **1996**, *118*, 9855.

285 Yevlampieva, N.; Beljaev, N.; Lavrenko, P.; Deschenaux, R., *Mol. Cryst. Liq. Cryst.*, **2009**, *506*, 34.

286 Frein, S.; Camerel, F.; Ziessel, R.; Barberá, J.; Deschenaux, R., *Chem. Mater.*, **2009**, *21*, 3950.

287 Jones, J. W.; Bryant, W. S.; Bosman, A. W.; Janssen, R. A. J.; Meijer, E. W.; Gibson, H. W., *J. Org. Chem.*, **2003**, *68*, 2385.

288 Dykes, G.; Smith, D.; Seeley, G., *Angew. Chem. Int. Edit.*, **2002**, *41*, 3254.

289 Dykes, G.; Smith, D., *Tetrahedron*, **2003**, *59*, 3999.

290 Gillies, E.; Frechet, J., *J. Org. Chem.*, **2004**, *69*, 46.

291 Lee, J.; Ko, Y.; Park, S.; Yamaguchi, K.; Kim, K., *Angew. Chem. Int. Edit.*, **2001**, *40*, 746.

292 Kim, D.; Kim, E.; Kim, J.; Park, K. M.; Baek, K.; Jung, M.; Ko, Y. H.; Sung, W.; Kim, H. S.; Suh, J. H.; Park, C. G.; Na, O. S.; Lee, D.-K.; Lee, K. E.; Han, S. S.; Kim, K., *Angew. Chem.*, **2007**, *119*, 3541.

293 Pittelkow, M.; Brock-Nannestad, T.; Moth-Poulsen, K.; Christensen, J. B., *Chem. Commun.*, **2008**, 2358.

294 Mathews, B. T.; Beezer, A. E.; Snowden, M. J.; Hardy, M. J.; Mitchell, J. C., *New J. Chem.*, **2001**, *25*, 807.

295 Brunner, H., *J. Organomet. Chem.*, **1995**, *500*, 39.

296 Bolm, C.; Derrien, N.; Seger, A., *Synlett*, **1996**, 387.

297 Matyjaszewski, K.; Shigemoto, T.; Frechet, J.; Leduc, M., *Macromolecules*, **1996**, *29*, 4167.

298 Villoslada, R.; Alonso, B.; Casado, C. M.; Garcia-Armada, P.; Losada, J., *Organometallics*, **2009**, *28*, 727.

299 Kim, Y.; Klutz, A. M.; Jacobson, K. A., *Bioconjugate Chem.*, **2008**, *19*, 1660.

300 Liu, S.; Maheshwari, R.; Kiick, K. L., *Macromolecules*, **2009**, *42*, 3.

301 Gillies, E.; Frechet, J., *Drug Discov. Today*, **2005**, *10*, 35.

302 Svenson, S., *Eur. J. Pharm. Biopharm.*, **2009**, *71*, 445.

303 Unal, B.; Hedden, R. C., *Polymer*, **2009**, *50*, 905.

304 Hirst, A. R.; Smith, D. K.; Feiters, M. C.; Geurts, H. P. M., *Langmuir*, **2004**, *20*, 7070.

305 Hirst, A. R.; Smith, D. K.; Feiters, M. C.; Geurts, H. P. M., *Chem. Eur. J.*, **2004**, *10*, 5901.

306 Ji, Y.; Kuang, G.-C.; Jia, X.-R.; Chen, E.-Q.; Wang, B.-B.; Li, W.-S.; Wei, Y.; Lei, J., *Chem. Commun.*, **2007**, 4233.

307 Jiang, D.; Aida, T., *Chem. Commun.*, **1996**, 1523.

308 Hudde, T.; Rayner, S.; Comer, R.; Weber, M.; Isaacs, J.; Waldmann, H.; Larkin, D.; George, A., *Gene. Ther.*, **1999**, *6*, 939.

309 Eichman, J.; Bielinska, A.; Kukowska-Latallo, J.; Baker, J., *Pharm. Sci. Technol. Today.*, **2000**, *3*, 232.

310 Weyermann, P.; Gisselbrecht, J.; Boudon, C.; Diederich, F.; Gross, M., *Angew. Chem. Int. Edit.*, **1999**, *38*, 3215.

311 Brothers, H.; Piehler, L.; Tomalia, D., *J. Chromatogr. A*, **1998**, *814*, 233.

312 Hecht, S.; Frechet, J., *Angew. Chem. Int. Edit.*, **2001**, *40*, 74.

313 Singh, P.; Moll, F.; Lin, S.; Ferzli, C.; Yu, K.; Koski, R.; Saul, R.; Cronin, P., *Clin. Chem.*, **1994**, *40*, 1845.

314 Singh, P.; Lin, S.; Moll, F.; Yu, K.; Ferzli, C.; Saul, R.; Diamond, S., *Abstr. Pap. Am. Chem. Soc.*, **1994**, *207*, 127.

315 Singh, P., *Bioconjugate Chem.*, **1998**, *9*, 54.

316 Tomalia, D.; Berry, V.; Hall, M.; Hedstrand, D., *Macromolecules*, **1987**, *20*, 1164.

317 Watkins, D.; Sayed-Sweet, Y.; Klimash, J.; Turro, N.; Tomalia, D. A., *Langmuir*, **1997**, *13*, 3136.

318 Gopidas, K.; Leheny, A.; Caminati, G.; Turro, N.; Tomalia, D., *J. Am. Chem. Soc.*, **1991**, *113*, 7335.

319 Darbre, T.; Reymond, J.-L., *Acc. Chem. Res.*, **2006**, *39*, 925.

320 Svenson, S.; Chauhan, A. S., *Nanomedicine-Uk*, **2008**, *3*, 679.

321 Waengler, C.; Moldenhauer, G.; Eisenhut, M.; Haberkorn, U.; Mier, W., *Bioconjugate Chem.*, **2008**, *19*, 813.

322 Habicher, T.; Diederich, F., *Helv. Chim. Acta*, **1997**, *82*, 1066.

323 Liu, L.; Breslow, R., *J. Am. Chem. Soc.*, **2003**, *125*, 12110.

324 Crespo, L.; Sanclimens, G.; Pons, M.; Giralt, E.; Royo, M.; Albericio, F., *Chem. Rev.*, **2005**, *105*, 1663.

325 Haensler, J.; Szoka, F., *Bioconjugate Chem.*, **1993**, *4*, 372.

326 Jevprasesphant, R.; Penny, J.; Jalal, R.; Attwood, D.; Mckeown, N.; D'emanuele, A., *Int. J. Pharm.*, **2003**, *252*, 263.

327 Kukowskalatallo, J.; Bielinska, A.; Johnson, J.; Spindler, R.; Tomalia, D.; Baker, J., *Proc. Natl. Acad. Sci. USA*, **1996**, *93*, 4897.

328 Huang, R.-Q.; Qu, Y.-H.; Ke, W.-L.; Zhu, J.-H.; Pei, Y.-Y.; Jiang, C., *Faseb J.*, **2007**, *21*, 1117.

329 Bielinska, A.; Kukowska-Latallo, J. F.; Johnson, J.; Tomalia, D. A.; Baker, J. R., *Nucleic Acids Res.*, **1996**, *24*, 2176.

330 Fant, K.; Esbjörner, E. K.; Lincoln, P.; Nordén, B., *Biochemistry*, **2008**, *47*, 1732.

331 Kostiainen, M. A.; Smith, D. K.; Ikkala, O., *Angew. Chem. Int. Edit.*, **2007**, *46*, 7600.

332 James, T.; Sandanayake, K.; Shinkai, S., *Nature*, **1995**, *374*, 345.

333 Mark, S.; Sandhyarani, N.; Zhu, C.; Campagnolo, C.; Batt, C., *Langmuir*, **2004**, *20*, 6808.

334 Yoon, H.; Hong, M.; Kim, H., *Anal. Biochem.*, **2000**, *282*, 121.

335 Alonso, B.; Armada, P.; Losada, J.; Cuadrado, I.; Gonzalez, B.; Casado, C., *Biosens. Bioelectron.*, **2004**, *19*, 1617.

336 Klajnert, B.; Bryszewska, M., *Cell. Mol. Biol. Lett.*, **2002**, *7*, 288.

337 Trinchi, A.; Muster, T., *Supramol. Chem.*, **2007**, *19*, 431.

338 Klajnert, B.; Bryszewska, M., *Bioelectrochemistry*, **2002**, *55*, 33.

339 Ibey, B.; Beier, H.; Rounds, R.; Cote, G.; Yadavalli, V.; Pishko, M., *Anal. Chem.*, **2005**, *77*, 7039.

340 Waengler, C.; Moldenhauer, G.; Saffrich, R.; Knapp, E.-M.; Beijer, B.; Schnoelzer, M.; Waengler, B.; Eisenhut, M.; Haberkorn, U.; Mier, W., *Chem.-Eur. J.*, **2008**, *14*, 8116.

341 *European Commission Grant Application - Synthetic analogues of cell nuclei - NeoNuclei project*; Contract No 12967 (NEST) **2005**.

342 Twyman, L.; King, A.; Burnett, J.; Martin, I., *Tetrahedron Lett.*, **2004**, *45*, 433.

343 Tomalia, D.; Swanson, D., *US Patent App. 10/568,481*, **2004**.

344 Müller, R.; Laschober, C.; Szymanski, W.; Allmaier, G., *Macromolecules*, **2007**, *40*, 5599.

345 Giordanengo, R.; Mazarin, M.; Wu, J.; Peng, L.; Charles, L., *Int. J. Mass spectrom.*, **2007**, *266*, 62.

346 He, M.; Mcluckey, S. A., *Rapid Commun. Mass Spectrom.*, **2004**, *18*, 960.

347 Peterson, J.; Ebber, A.; Allikmaa, V.; Lopp, M., *Proc. Est. Acad. Sci.*, **2001**, *50*, 156.

348 Vincent, T. J.-C.; Dolé, R.; Lange, C. M., *Rapid Commun. Mass Spectrom.*, **2008**, *22*, 363.

349 Meltzer, A.; Tirrell, D.; Jones, A.; Engelfield, P.; Downing, D.; Tomalia, D., *Abstr. Pap. Am. Chem. Soc.*, **1989**, *197*, 38.

350 Amabilino, D., PhD Thesis, University of Southampton, 1991.

351 Lu, J.; Zeng, Q.-D.; Wang, C.; Zheng, Q.-Y.; Wan, L.; Bai, C., *J. Mater. Chem.*, **2002**, *12*, 2856.

352 Breitmaier, E.; Spohn, K.; Berger, S., *Angew. Chem. Int. Edit.*, **1975**, *14*, 144.

353 Levy, G., *Acc Chem Res*, **1973**, *6*, 161.

354 Naylor, A.; Goddard, W., *Abstr. Pap. Am. Chem. Soc.*, **1988**, *195*, 112.

355 Balakrishnan, P.; Harruna, I.; Polk, M., *Macromolecules*, **1988**, *21*, 1538.

356 Bielinska, A. U.; Chen, C.; Johnson, J.; Baker, J. R., *Bioconjugate Chem.*, **1999**, *10*, 843.

357 Lee, J. H.; Lim, Y.-B.; Choi, J. S.; Lee, Y.; Kim, T.-I.; Kim, H. J.; Yoon, J. K.; Kim, K.; Park, J.-S., *Bioconjugate Chem.*, **2003**, *14*, 1214.

358 Luo, D.; Haverstick, K.; Belcheva, N.; Han, E., *Macromolecules*, **2002**, *35*, 3456.

359 Mintzer, M.; Simanek, E.; Nano, A., *Chem. Rev.*, **2008**, *109*, 259.

360 Choi, Y.; Mecke, A.; Orr, B.; Holl, M.; Baker Jr, J., *Nano Lett.*, **2004**, *4*, 391.

361 Lee, C. C.; Mackay, J. A.; Fréchet, J. M. J.; Szoka, F. C., *Nat. Biotechnol.*, **2005**, *23*, 1517.

362 Lee, J.; Kim, B.; Kim, H.; Han, S.; Shin, W.; Jin, S., *Macromolecules*, **2006**, *39*, 2418.

363 Bodnar, I.; Silva, A.; Deitcher, R.; Weisman, N.; Kim, Y.; Wagner, N., *J. Polym. Sci., Part B*, **2000**, *38*, 857.

364 Wang, W.; Xiong, W.; Wan, J.; Sun, X.; Xu, H.; Yang, X., *Nanotechnology*, **2009**, *20*, 105103.

365 Bai, S.; Ahsan, F., *Pharm. Res.-Dord*, **2009**, *26*, 539.

366 Calabretta, M. K.; Kumar, A.; Mcdermott, A. M.; Cai, C., *Biomacromolecules*, **2007**, *8*, 1807.

367 Chandrasekar, D.; Sistla, R.; Ahmad, F. J.; Khar, R. K.; Diwan, P. V., *J. Biomed. Mater. Res. A*, **2007**, *82A*, 92.

368 Gajbhiye, V.; Kumar, P. V.; Tekade, R. K.; Jain, N. K., *Eur. J. Med. Chem.*, **2009**, *44*, 1155.

369 Kojima, C.; Kono, K.; Maruyama, K.; Takagishi, T., *Bioconjugate Chem.*, **2000**, *11*, 910.

370 Kim, Y.; Hechler, B.; Klutz, A.; Gachet, C.; Jacobson, K., *Bioconjugate Chem.*, **2008**, *19*, 406.

371 Wade, L. G., *Organic Chemistry*, 6th ed., **2006**, Pearson Prentice Hall: Upper Saddle River, New Jersey.

372 Gibson, M.; Bradshaw, R., *Angew. Chem. Int. Edit.*, **1968**, *7*, 919.

373 Vermeulen, M.; Zwanenburg, B.; Chittenden, G.; Verhagen, H., *Eur. J. Med. Chem.*, **2003**, *38*, 729.

374 Ceroni, P.; Laghi, I.; Maestri, M.; Balzani, V.; Gestermann, S.; Gorka, M.; Vogtle, F., *New J. Chem.*, **2002**, *26*, 66.

375 Jin, L.; Liu, H.; Yang, W.; Wang, C.; Yu, K., *J. Polym. Sci. Pol. Chem.*, **2008**, *46*, 2948.

376 Majoros, I. J.; Thomas, T. P.; Mehta, C. B.; Baker, J. R., *J. Med. Chem.*, **2005**, *48*, 5892.

377 Fant, K. *Thesis for the Degree of Licentiate of Engineering*, Chalmers University of Technology, Gothenbuurg, Sweden, **2008**.

378 Chen, W.; Turro, N.; Tomalia, D., *Langmuir*, **2000**, *16*, 15.

379 Mcghee, J.; Hippel, P., *J. Mol. Biol.*, **1974**, *86*, 469.

380 Ghosh, P.; Wells, C.; Numata, Y.; Read, R.; Armstrong, S., *Curr. Ther. Res. Clin. E.*, **1993**, *54*, 703.

381 Conner, S.; Schmid, S., *Nature*, **2003**, *422*, 37.

382 Fuchs, S.; Kapp, T.; Otto, H.; Schöneberg, T.; Franke, P.; Gust, R.; Schlüter, A. D., *Chem. Eur. J.*, **2004**, *10*, 1167.

383 Chandler, D., *Nature*, **2005**, *437*, 640.

384 Mecke, A.; Majoros, I.; Patri, A.; Baker, J.; Holl, M.; Orr, B., *Langmuir*, **2005**, *21*, 10348.

385 Kuo, J.; Jan, M.; Chu, H., *J. Pharm. Pharmacol.*, **2005**, *57*, 489.

386 Parimi, S.; Barnes, T. J.; Prestidge, C. A., *Langmuir*, **2008**, *24*, 13532.

387 Lee, H.; Larson, R. G., *J. Phys. Chem. B*, **2008**, *112*, 12279.

388 Lee, H.; Larson, R. G., *J. Phys. Chem. B*, **2006**, *110*, 18204.

389 Lee, H.; Larson, R. G., *J. Phys. Chem. B*, **2008**, *112*, 7778.

390 Lee, H.; Larson, R., *Molecules*, **2009**, *14*, 423.

391 Kelly, C. V.; Leroueil, P. R.; Nett, E. K.; Wereszczynski, J. M.; Baker, J. R.; Orr, B. G.; Holl, M. M. B.; Andricioaei, I., *J. Phys. Chem. B*, **2008**, *112*, 9337.

392 Kelly, C. V.; Leroueil, P. R.; Orr, B. G.; Holl, M. M. B.; Andricioaei, I., *J. Phys. Chem. B*, **2008**, *112*, 9346.

393 Hess, B.; Kutzner, C.; Van Der Spoel, D.; Lindahl, E., *J. Chem. Theory Comput.*, **2008**, *4*, 435.

394 Atkins, P.; De Paula, J., *Physical Chemistry*, 7th ed., **2002**, Oxford University Press: Oxford.

395 Chen, W.; Tomalia, D.; Thomas, J., *Macromolecules*, **2000**, *33*, 9169.

396 Kostiainen, M.; Hardy, J.; Smith, D., *Angewandte Chemie International Edition*, **2005**, *44*, 2556.

397 Tack, F.; Bakker, A.; Maes, S.; Dekeyser, N.; Bruining, M.; Elissen-Roman, C.; Janicot, M.; Brewster, M.; Janssen, H. M.; De Waal, B. F. M.; Fransen, P. M.; Lou, X.; Meijer, E. W., *J. Drug. Target.*, **2006**, *14*, 69.

398 Obata, Y.; Suzuki, D.; Takeoka, S., *Bioconjugate Chem.*, **2008**.

399 Harrison, S. C., *J. Cell Biol.*, **2008**, *183*, 177.

400 Casolaro, M.; Ito, Y.; Ishii, T.; Bottari, S.; Samperi, F.; Mendichi, R., *Express Polym. Lett.*, **2008**, *2*, 165.

401 Okada, A.; Miura, T.; Takeuchi, H., *Biochemistry*, **2001**, *40*, 6053.

402 Claydon, T.; Boyett, M.; Sivaprasadarao, A.; Ishii, K.; Owen, J.; O'beirne, H.; Leach, R.; Komukai, K.; Orchard, C., *J. Physiol-London*, **2000**, *526*, 253.

403 Arbely, E.; Rutherford, T. J.; Sharpe, T. D.; Ferguson, N.; Fersht, A. R., *J. Mol. Biol.*, **2009**, *387*, 986.

404 Iwaki, M.; Yakovlev, G.; Hirst, J.; Osyczka, A.; Dutton, P.; Marshall, D.; Rich, P., *Biochemistry*, **2005**, *44*, 4230.

405 Hass, M. A. S.; Hansen, D. F.; Christensen, H. E. M.; Led, J. J.; Kay, L. E., *J. Am. Chem. Soc.*, **2008**, *130*, 8460.

406 Delort, E.; Nguyen-Trung, N.-Q.; Darbre, T.; Reymond, J.-L., *J. Org. Chem.*, **2006**, *71*, 4468.

407 Pittelkow, M.; Christensen, J., *Org. Lett.*, **2005**, *7*, 1295.

408 Boeijen, A.; Van Ameijde, J.; Liskamp, R., *J. Org. Chem.*, **2001**, *66*, 8454.

409 Myllymäki, V.; Lindvall, M.; Koskinen, A., *Tetrahedron*, **2001**, *57*, 4629.

410 El-Agnaf, O.; Goodwin, H.; Sheridan, J.; Frears, E.; Austen, B., *Protein Peptide Lett.*, **2000**, *7*, 1.

411 Ast, T.; Heine, N.; Germeroth, L.; Schneider-Mergener, J.; Wenschuh, H., *Tetrahedron Lett.*, **1999**, *40*, 4317.

412 Wade, J.; Mathieu, M.; Macris, M.; Tregear, G., *Lett. Pept. Sci.*, **2000**, *7*, 107.

413 Kruijtzer, J.; Lefeber, D.; Liskamp, R., *Tetrahedron Lett.*, **1997**, *38*, 5335.

414 Englund, E.; Gopi, H.; Appella, D., *Org. Lett.*, **2004**, *6*, 213.

415 Ninomiya, K.; Shioiri, T.; Yamada, S., *Tetrahedron*, **1974**, *30*, 2151.

416 Denholm, A.; George, M.; Hailes, H.; Tiffin, P., *J. Chem. Soc., Perkin Trans. 1*, **1995**, 541.

417 Ginisty, M.; Roy, M.; Charette, A., *J. Org. Chem.*, **2008**, *73*, 2542.

418 Ameerunisha, S.; Zacharias, P., *J. Chem. Soc. Perk. T. 2*, **1995**, 1679.

419 Galbraith, H.; Degering, E.; Hitch, E., *J. Am. Chem. Soc.*, **1951**, *73*, 1323.

420 Shinkai, S.; Nakaji, T.; Ogawa, T.; Shigematsu, K.; Manabe, O., *J. Am. Chem. Soc.*, **1981**, *103*, 111.

421 Pipoosananakaton, B.; Sukwattanasinitt, M.; Jaiboon, N.; Chaichit, N.; Tuntulani, T., *Bull. Korean Chem. Soc.*, **2000**, *21*, 867.

422 Pratt, E.; Mcgovern, T., *J. Org. Chem.*, **1964**, *29*, 1540.

423 Bhatnagar, I.; George, M., *J. Org. Chem.*, **1968**, *33*, 2407.

424 Daidone, G., *Eur. J. Med. Chem.*, **2004**, *39*, 219.

425 Frank, H., *J. Histochem. Cytochem.*, **1990**, *38*, 1295.

426 Juodaityte, J., *J. Biotechnol.*, **2004**, *112*, 127.

427 Dong, S.-L.; Löweneck, M.; Schrader, T. E.; Schreier, W. J.; Zinth, W.; Moroder, L.; Renner, C., *Chem. Eur. J.*, **2006**, *12*, 1114.

428 Aemissegger, A.; Kräutler, V.; Van Gunsteren, W. F.; Hilvert, D., *J. Am. Chem. Soc.*, **2005**, *127*, 2929.

429 Ghosh, S.; Banthia, A., *J. Polym. Sci. Pol. Chem.*, **2001**, *39*, 4182.

430 Auernheimer, J.; Dahmen, C.; Hersel, U.; Bausch, A.; Kessler, H., *J. Am. Chem. Soc.*, **2005**, *127*, 16107.

431 Pohner, C.; Hilbrig, F.; Jerome, V.; Freitag, R., *Biotechnol. Progr.*, **2006**, *22*, 1170.

432 Cisnetti, F.; Ballardini, R.; Credi, A.; Gandolfi, M. T.; Masiero, S.; Negri, F.; Pieraccini, S.; Spada, G. P., *Chem. Eur. J.*, **2004**, *10*, 2011.

433 Wang, B.; Zhang, X.; Yang, L.; Jia, X.; Ji, Y.; Li, W., *Polym. Bull.*, **2006**, *56*, 63.

434 Puntoriero, F.; Ceroni, P.; Balzani, V.; Bergamini, G.; Vögtle, F., *J. Am. Chem. Soc.*, **2007**, *129*, 10714.

435 Majoros, I.; Myc, A.; Thomas, T.; Mehta, C.; Baker, J., *Biomacromolecules*, **2006**, *7*, 572.

436 Saari, W. S.; Schwering, J. E.; Lyle, P. A.; Smith, S. J.; Engelhardt, E. L., *J. Med. Chem.*, **1990**, *33*, 97.

437 Rao, B.; Venkateswarlu, T.; Rao, P.; Divi, M., *Org. Prep. Proced. Int.*, **2001**, *33*, 621.

438 Behrendt, R.; Schenk, M.; Musiol, H. J.; Moroder, L., *J. Pept. Sci.*, **1999**, *5*, 519.

439 Sawada, H.; Zenkoh, T.; Setoi, H.; Tanaka, H., *European Patent W09641795*, **1996**.

440 Tanoury, G.; Wilkinson, H.; Hett, R.; Senanayake, C.; Wald, S., *Abstr Pap Am Chem*, **2000**, *219*, 32.

441 Levitt, M. H., *Spin Dynamics: Basics of Nuclear Magnetic Resonance*, **2008**, John Wiley & Sons Ltd: Chichester, UK.

442 Marrink, S. J.; Risselada, H. J.; Yefimov, S.; Tieleman, D. P.; De Vries, A. H., *J. Phys. Chem. B*, **2007**, *111*, 7812.

443 Berendsen, H.; Postma, J.; Vangunsteren, W.; Dinola, A.; Haak, J., *J. Chem. Phys.*, **1984**, *81*, 3684.

444 Essmann, U.; Perera, L.; Berkowitz, M.; Darden, T.; Lee, H.; Pedersen, L., *J. Chem. Phys.*, **1995**, *103*, 8577.

Appendix I NMR Relaxation Mechanisms

The nuclear spin equilibrium, which is characterised by the equilibrium magnetisation M_0, and transverse magnetisation ($M_y = 0$), are regenerated by recovery processes after a pulse of radio frequency. These relaxation processes of the nuclear spins are shown in the rotating coordinate system *x*, *y*, *z*, and are outlined below.

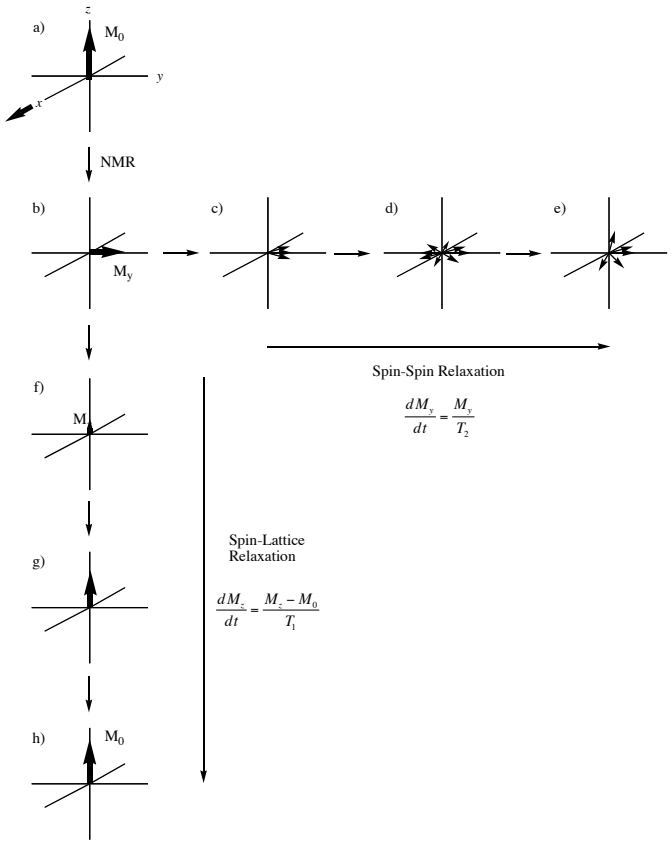

***Figure 107**. Relaxation processes in NMR.*

A1 Spin-Spin Relaxation

This is a decay of the *transverse* magnetisation induced by an NMR experiment as shown in **Figure 107** (b-e) and is assumed to occur continuously as a single exponential. Regardless as to whether their Boltzmann distribution over the magnetic energy levels has been re-established, the precessing magnetic vectors lose their phase

coherence and adopt a regular distribution over the precession cone. This process is observed as an exponential decay of the nuclear induction current (free induction decay, FID) with time constant T_2. The spin-spin relaxation time, T_2, is the time after which the nuclear induction current has dropped to 1/e of its original value.

A2 Spin-Lattice Relaxation

During this relaxation the nuclear spins return from an excited to a stable state (**Figure 107** (b-h)), i.e. the Boltzmann spin distribution returns to the equilibrium value M_0 from M_z, the magnetisation along the *z* axis. The spin-lattice relaxation is assumed to be a continuous process, increasing in the *longitudinal* magnetisation M_z to the equilibrium value with a time constant T_1, the spin-lattice relaxation time. T_1 is defined as the time after which M_z has risen to 1/e of the equilibrium value M_0. This relaxation involves the release of energy from the excited nuclei to neighbouring molecules, the lattice.

Spin-spin and spin-lattice relaxations can occur at different rates for a given nucleus. Macromolecules in solution or solid state, for example, have a slower spin-lattice relaxation than spin-spin relaxation (so that $T_1 > T_2$). In this case, redistribution of the magnetic vectors over the precession cone and transverse magnetisation has dropped to zero before the Boltzmann distribution of the spins is reached, thus restoring equilibrium. For small and medium sized molecules in the liquid or dissolved state, the relaxation processes often occur at a similar rate so that T_1 is approximately equal to T_2. Because the equilibrium magnetisation $M_z = M_0$ cannot be reached by a certain number of spins before the transverse magnetisation M_y has fallen to zero ($M_0 = M_y + M_z$), spin-lattice relaxation can proceed slowed but never faster than spin-spin relaxation.

A2.1 Mechanisms of Spin-Lattice Relaxation

The excited nuclei transfer their excitation energy to the environment *via* interactions of their magnetic vectors with fluctuating local fields that have sufficient strength and a fluctuation frequency of the order of the Larmor frequency of the nuclear spin type. The atomic and electronic environment of a nucleus in a molecule and molecular motion determine which of the four potential mechanisms (shown below) most contribute to the spin-lattice relaxation, though all affect the T_1.

$$\frac{1}{T_1} = \frac{1}{T_{1(DD)}} + \frac{1}{T_{1(SR)}} + \frac{1}{T_{1(SC)}} + \frac{1}{T_{1(CSA)}} + \ldots \qquad \textbf{Equation 4}$$

A2.1.1 Relaxation by Internuclear Dipole-Dipole Interaction (DD Mechanism)

A local magnetic field is generated by each nuclear spin. When two nuclei are linked by a bond then each nucleus (e.g. ^{1}H and ^{13}C) will experience the local field as well as the external field H_0. Rapid molecular motion in liquids means fast rotations of C-H bonds for dissolved organic molecules, so the orientation of ^{1}H and ^{13}C nuclei is constantly changing relative to H_0. Fluctuating local fields are generated by this constantly imposed magnetic reorientation of the nuclear spins, which contributes to the relaxation of the nuclei. This mechanism is particularly important for hydrogen-containing molecules owing to its high natural abundance.

Unpaired electrons generate much stronger fluctuating local fields than the nuclear spins owing to their considerably greater magnetic moment. As a result of this, relaxation is dominated by electron spin-nucleus dipole-dipole interactions in the presence of unpaired electrons (these are analogous to internuclear dipole-dipole interactions). Smaller T_1 values are therefore observed for parmagnetic compounds. The same is true when paramagnetic contaminants, such as oxygen, are present so it is important to remove them for accurate T_1 information to be obtained.

A2.1.2 Relaxation Resulting from Chemical Shift Anisotropy (CSA Mechanism)

Magnetic shielding of a nucleus arising from the surrounding electrons can be anisotropic. The contribution of the CSA mechanism is observed by a correlation between T_1 values and the square of the applied magnetic field strength H_0.

A2.1.3 Relaxation by Scalar Coupling (SC Mechanism)

The spins of two proximate nuclei in a molecule undergo coupling, i.e. their signals become split, but only when the lifetime of these nuclei in their magnetic energy levels

is sufficiently large (scalar coupling). If one nucleus relaxes faster than the other, no signal splitting is observed. However, this relaxation generates fluctuating fields that can contribute to the relaxation of nearby nuclei. It should be noted that quadrupole nuclei having $I \geq 1$ relax so fast that they can accelerate the relaxation of neighbouring nuclei. The contribution of the SC mechanism can be observed by a frequency and temperature dependence of T_1, which can be large if the coupling nuclei precess with similar Larmor frequencies.

A2.1.4 Relaxation by Spin Rotation (SR Mechanism)

If a molecule rotates then the magnetic vectors of the bonding electron spin will also rotate, giving rise to fluctuating local fields. These fields can contribute to spin-lattice relaxation of the nuclei of the rotating molecule. The same is true for molecular segments such as alkyl groups. This mechanism plays an important role in small symmetrical molecules, or in large molecules that have small segments (e.g. methyl groups).

Information on NMR relaxation mechanisms taken from published literature.[352,353,441]

Appendix II Molecular Dynamic Simulation Details

The coarse-grained (CG) model of the PAMAM dendrimer used is an extended form by Lee *et al.*[388] of the CG lipid force field, MARTINI, developed by Marrink *et al.*[442] This represents different chemical moieties in the dendrimer molecule as separate beads (**Figure 108**) which are distinguished by their charge type [polar (P), nonpolar (N), apolar (C) and charged (Q)] and hydrogen bonding capability. This enables the nodes and branches of the dendrimer architecture to be distinguished. A node is represented by N_0, as a nonpolar unit with no hydrogen bonding capabilities; a branch is represented by N_{da} as a nonpolar unit with hydrogen bond donors and acceptors. In this study, charged dendrimers were terminated with Q_d beads, whilst dendrimers terminated with polar beads (P) were simulated to represent other surface functionality. Harmonic bonding and angle potentials were used to connect these beads to give the coarse-grained dendrimer (**Figure 108**).

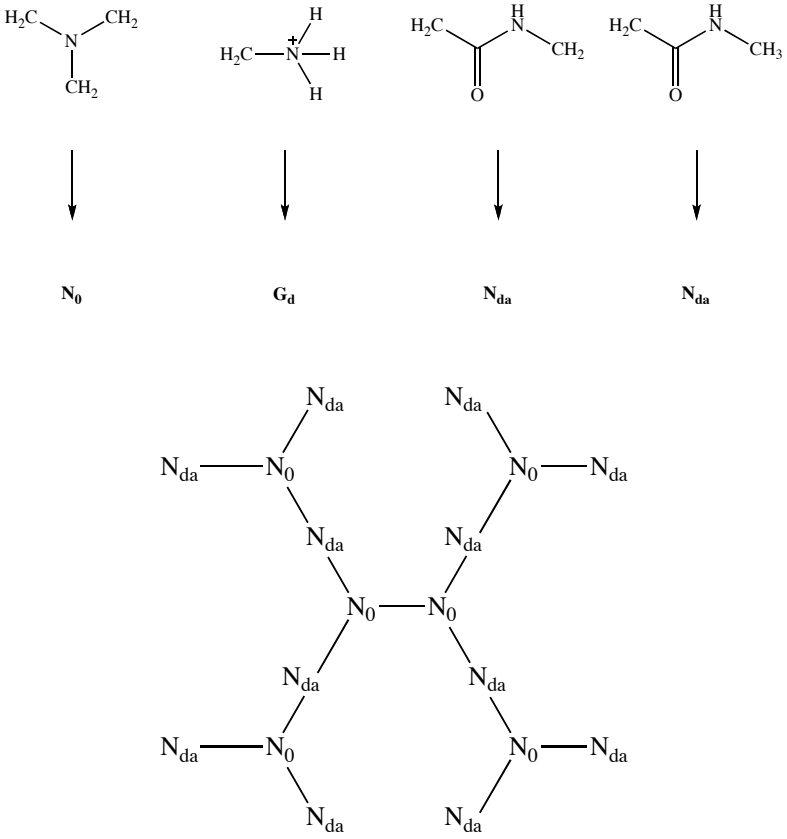

Figure 108. *Coarse-grained chemical components of PAMAM dendrimer.*

CG lipids are represented with four methylene groups encapsulated into each tail bead, with the head groups represented by two beads, one for phosphate and one for choline. Four real water molecules are represented by a single water bead. The MARTINI CG force field was used for the dendrimers, lipids, water and ions.[442] All simulations were performed using GROMACS simulation package.[393]

Each simulation system comprised of four 4th generation dendrimers in a lipid patch containing 1024 POPC or POPE/POPG molecules. The system was solvated with ~29000 CG water molecules in a periodic box of size 18.5 × 18.5 × 14.5 nm^3. The temperature was maintained at 323K by applying the Berendsen thermostat[443] in an NPT ensemble. A time step of 40 fs and a total duration of 100 ns was used. A cut off of 1.2 nm was used for van der Waals interactions, to which a standard shift function was applied to smoothly shift the Lennard Jones potential to zero between 0.9 and 1.2 nm. Electrostatic interactions were modelled with a particle mesh Ewald summation which enables long-ranged interactions to be taken into account.[444]